The impact of a human cytomegalovirus subviral particle vaccine on the host cell proteome and on virus replication

Dissertation submitted for the achievement of the academic degree

“Doctor rerum naturalium”
(Dr.rer.nat.)

At the department of Biology of
the Johannes Gutenberg-University
in Mainz

Inessa Penner

Born on 3rd of August 1986
in Usun-Agatsch (Kazakhstan)

Mainz, 2021

Dean Department of Biology:

1.Referee:

2.Referee:

Day of the oral examination: 02. August 2021

Statutory declaration

I, Inessa Penner, declare that I have authored this dissertation independently, that I have not used other than the declared sources / resources, and that I have explicitly marked all material which has been quoted either literally or by content from the used sources.

……. ……..
Date Signature

"Absence of evidence is not evidence of absence"

Summary

The development of a vaccine against the human cytomegalovirus (HCMV), suitable to prevent congenital disease in neonates and to reduce morbidity and mortality in immunocompromised patients has been ranked as a top-priority medical goal. Non-infectious HCMV particles, termed Dense Bodies (DBs) are a promising platform to develop such a vaccine. The particles are a unique product of cytomegalovirus infected cells and are concomitantly released with infectious virions. Purified DBs are highly immunogenic in laboratory animals, as they elicit both neutralizing antibodies as well as antiviral T lymphocytes. A DB-based vaccine has, however, not yet been tested in humans. In preparation of clinical studies, this project was designed to investigate the molecular interactions of DBs with different target cells and to study the impact of DBs on HCMV replication.

Proteomic analyses were performed on different culture cells, like fibroblasts or endothelial cells that were exposed to DBs. A striking result of this was that exposure of cells to DBs resulted in the upregulation of an array of interferon (IFN) regulated genes (IRGs), likely leading to the establishment of an antiviral state in these cells. The inhibition of the IFN JAK/STAT signalling cascade during DB incubation demonstrated that upregulation of IRGs like MX1, IFIT3 and ISG15 was dependent on type I IFN signalling. Another remarkable finding was that DBs also promoted the upregulation of components of the major histocompatibility complex (MHC) antigen presentation pathways and connected cellular processes, namely ubiquitination and autophagy. This adds significantly to our understanding about the particular feature of DBs to efficiently induce antiviral CD4- and CD8- T lymphocytes in the absence of viral gene expression. Besides this, proteins involved in other biological processes like cell-cycle regulation and chromosome organisation were upregulated in fibroblasts and endothelial cells, but also in haematopoietic cells like monocytes and dendritic cells (DCs), showing the complex pattern of cellular protein regulation following DB-exposure.

As a DB-vaccine would be applied to millions of individuals, part of whom would be latently infected, a second prompting question was, if these particles would support or restrict HCMV replication. Enhancement of viral replication would be an adverse function of these particles that likely would prevent vaccine licensing. Exposure of fibroblasts to DBs however indeed reduced HCMV progeny production. The effect was most prominent when the cells were “primed” by DBs prior to infection. This fosters the hypothesis that DBs are produced by cells as an antiviral mechanism, similar to IFNs that induce an antiviral state in neighbouring cells and thus protects them against subsequent HCMV infection. This work provides the basis to further test this hypothesis.

Zusammenfassung

Die Entwicklung eines Impfstoffs gegen das humane Cytomegalovirus (HCMV) ist von hoher medizinischer Relevanz. Im Vordergrund stehen dabei die Prävention der kongenitalen HCMV-Infektion und die Reduktion der HCMV-bedingten Krankheitslast bei immunsupprimierten Patienten. Nicht-infektiöse HCMV-Partikel, so genannte Dense Bodies (DBs) sind eine vielversprechende Plattform zur Entwicklung eines solchen Impfstoffs. Die Partikel werden von infizierten Zellen gebildet und zusammen mit infektiösen Virionen freigesetzt. Gereinigte DBs erwiesen sich im Tierversuch als hoch immunogen, sie waren geeignet sowohl neutralisierende Antikörper als auch antivirale T-Lymphozyten zu induzieren. Ein DB-basierter Impfstoff wurde jedoch noch nicht am Menschen getestet. In Vorbereitung auf klinische Studien wurden in diesem Projekt die molekularen Interaktionen von DBs mit verschiedenen Zielzellen untersucht. In einem weiteren Schritt wurde der Einfluss von DBs auf die HCMV Vermehrung analysiert.

Mit Hilfe der Massenspektrometrie wurden in einem ersten Schritt DB-induzierte Veränderungen am Proteom von unterschiedlichen Zellkulturen, wie Fibroblastenkulturen oder Endothelzellkulturen analysiert. Ein spannendes Ergebnis war, dass die DB-Exposition zur deutlichen Steigerung der Expression von Interferon-(IFN)-regulierten Genen (IRGs) führte. Die Expression von IRGs ist ein zellulärer Abwehrmechanismus gegen Virusinfektion. Die Ergebnisse legen daher nahe, dass DBs zur Etablierung eines antiviralen Zustands in den Zellen führen. Die Hemmung der IFN-JAK/STAT-Signalkaskade während der DB-Inkubation hemmte auch die Induktion der IRGs MX1, IFIT3 und ISG15. Dies zeigte, dass die DB-vermittelte IRG-Induktion über die Typ-I-IFN-abhängige Signaltransduktion vermittelt wird. Ein weiterer bemerkenswerter Befund war, dass DBs Komponenten der MHC Klasse I und MHC Klasse II vermittelten Antigenpräsentation, sowie Proteine der Ubiquitin-vermittelten Proteindegradation und der Autophagie induzierten. Diese Befunde tragen wesentlich zu unserem Verständnis der außergewöhnlichen, immunogenen Eigenschaften von DBs bei, die antivirale CD4- und CD8-T-Lymphozyten in Abwesenheit viraler Genexpression effizient zu induzieren. Daneben fanden sich Proteine der Zellzyklusregulation und der Chromosomenorganisation in Fibroblasten und Endothelzellen, aber auch in hämatopoetischen Zellen wie Monozyten und dendritischen Zellen verstärkt exprimiert. Diese Analysen zeigten somit ein bemerkenswert komplexes Muster der zellulären Proteinregulation nach DB-Exposition auf.

Da ein DB-Impfstoff prospektiv Millionen von Menschen appliziert wird, von denen ein Teil latent HCMV-infiziert ist, war eine zweite Fragestellung, ob diese Partikel die HCMV-Vermehrung unterstützen oder reprimieren würden. Eine Verstärkung der viralen Replikation wäre eine nachteilige Funktion dieser Partikel, die wahrscheinlich die Zulassung des Impfstoffs behindern würde. Die Exposition von Fibroblasten gegenüber DBs reduzierte jedoch

tatsächlich die Produktion von HCMV Tochterviren. Der Effekt war am deutlichsten, wenn die Zellen vor der Infektion mit DBs vor-inkubiert wurden. Dies unterstützt unsere Hypothese, dass DBs von Zellen als antiviraler Mechanismus produziert werden um, ähnlich wie IFN, einen antiviralen Zustand in benachbarten Zellen zu induzieren und sie so vor einer nachfolgenden HCMV-Infektion zu schützen. Diese Arbeit bietet die Grundlage, um diese Hypothese weiter zu testen.

Zusammengefasst unterstreichen die Ergebnisse dieser Studie die potenziellen antiviralen Funktionen von DBs. Sie beschreiben wichtige Mechanismen zur Wirkung dieser Partikel und liefern damit maßgebliche Argumente für die Beantragung erster klinischer Studien mit einem DB-Impfstoff.

List of abbreviations

7-AAD	7-Aminoactinomycin
AEC	3-Amino-9-Ethylcarbazole
AIDS	Acquired Immune Deficiency Syndrome
APC	Antigen-Presenting Cell
BAC	Bacterial Artificial Chromosome
BCA	Bicinchoninic Acid
BSA	Bovine Serum Albumin
cCMV	Congenital Cytomegalovirus
CD	Cluster of Differentiation
CME	Clathrin-Mediated Endocytosis
CPE	Cytopathic Effect
CRS	Cytosolic RNA Sensor
CTL	Cytotoxic T Lymphocyte
DAPI	4′,6-Diamidino-2-Phenylindole
DBs	Dense Bodies
DC	Dendritic Cell
ddH2O	double distilled water
DMF	Dimethylformamide
DMSO	Dimethyl Sulfoxide
DNA	Deoxyribonucleic Acid
dNTP	Deoxynucleotide Triphosphate
DOX	Doxycycline
d.p.a	days post application
d.p.i	days post infection
dsDNA	double-stranded DNA
dsRNA	double-stranded RNA
EC	Endothelial Cell
Em	Emission
EPC	Epithelial Cell
ER	Endoplasmic Reticulum
Ex	Excitation
Exp	Exponential
Exp.	Experiment
FACS	Fluorescence-Activated Cell Sorter
FBS	Foetal Bovine Serum

Fig.	Figure
GAPDH	Glyceraldehyde 3-Phosphate Dehydrogenase
GAVI	Global Alliance for Vaccines and Immunization
GFP	Green Fluorescent Protein
gH	glycoprotein H
GO	Gene Ontology
GTP	Guanosine Triphosphate
HCMV	Human Cytomegalovirus
hDaxx	Death Domain Associated Protein
HEC-LTT	Human Endothelial Cell-Large T antigen and Telomerase
HFF	Human Foreskin Fibroblasts
HHV-5	Human Herpes Virus 5
HLA	Human Leukocyte Antigen
h.p.a	hours post application
h.p.i	hours post infection
HPLC	High Performance Liquid Chromatography
HRP	Horseradish peroxidase
hTERT	human telomerase catalytic subunit
HUVEC	Human Umbilical Vein Endothelial Cells
iDC	immature Dendritic Cell
IE	Immediate Early
IF	Immunofluorescence
IFI16	Interferon Gamma Inducible Protein 16
IFIT1	Interferon Induced Protein with Tetratricopeptide Repeats 1
IFN	Interferon
IFNAR	Interferon-alpha/beta Receptor
IKBα	Nuclear factor of kappa light polypeptide gene enhancer in B-cells inhibitor alpha
IKK	IkB Kinase
IRF	Interferon Regulatory Factor
IRG	Interferon Regulated Gene
IRSE	Interferon Responsive Sequence Element
ISG15	Interferon Stimulated Gene 15
ISGF3	Interferon Stimulated Gene Factor 3
JAK	Januskinase
LC3B	Microtubule Associated Protein 1 Light Chain 3 Beta
LGP2	Laboratory of Genetics and Physiology 2

LICOR	Lightning Correlation
LPS	Lipopolysaccharide
MAVS	Mitochondrial Antiviral Aignalling
MDA5	Melanoma Differentiation-Associated Protein 5
mDC	myeloid Dendritic Cell
MHC	Major Histocompatibility Complex
MIEP	Major Immediate Early Promoter
m.o.i.	multiplicity of infection
mRNA	messenger-RNA
MS	Mass Spectrometry
MX1	Interferon induced GTP-binding protein MX1
MYD88	Myeloid Differentiation primary response 88
NAb	Neutralizing Antibody
ND10	Nuclear Domain 10
NF-kB	Nuclear Factor kappa light chain enhancer of activated B-cells
NIEP	Non-infectious Enveloped Particle
Nrp2	Neuropilin-2
NTC	Non Template Control
OR14I1	Olfactory Receptor 14I1
PAGE	Polyacrylamide Gel Electrophoresis
PAMP	Pathogen-Associated Molecular Patterns
PBMC	Peripheral Blood Mononuclear Cell
PBS	Phosphate Buffered Saline
PC	Pentameric Complex
PC-	Pentameric Complex Negative
PC+	Pentameric Complex Positive
PCR	Polymerase Chain Reaction
PDGFR-α	Platelet Derived Growth Factor Receptor-alpha
PF	Primer Forward
pIRS	Internal Repeated Sequence
PML	Promyelocytic Leukemia
PMNL	Polymorphonuclear Leukocytes
pp65	phosphoprotein 65
PPI	Protein-Protein Interaction
PR	Primer Reverse
PRR	Pattern Recognition Receptor
pTRS	Terminal Repeated Sequence

PVDF	Polyvinylidene Fluoride
qPCR	Real Time quantitative Polymerase Chain Reaction
R1	Technical Replicate 1
RF	Restriction Factor
RIG-I	Retinoic acid Inducible Gene-I
RLR	RIG-I-like receptors
RNA	Ribonucleic acid
ROX	X-Rhodamin
RV	Reconstituted Virus
SDS	Sodium Dodecyl Sulfate
SNHL	Sensorineural Hearing Loss
Sp100	Speckled 100 kDa
STAT	Signal Transducer and Activator of Transcription
STEM	Scanning Transmission Electron Microscope
STING	Stimulator of Interferon Genes
STRING	Search Tool for the Retrieval of Interacting Genes
TANK	TRAF Family Member Associated NFKB Activator
TAP	Antigen Peptide Transporter
TAPBP	Tapasin
Taq	*Thermus aquaticus*
TBK1	TANK Binding Kinase 1
TC	Trimeric Complex
TEM	Transmission Electron Microscopy
TLR	Toll-Like Receptor
TNF	Tumor Necrosis Factor
TRAF	TNF Associated Factor
TYK2	Tyrosine Kinase 2
UL	Unique Long
UniProtKB	Universal Protein Knowledge Base
UV	Ultraviolet
vAC	virion Assembly Compartment
VPL	Virus Like Particles

Units

°C	Degree Celsius
bp	base pair
Da	Dalton

g	gram
h	hour
L	Litre
M	Molar (mol/l)
m	meter
min	minute
pH	pondus Hydrogenii
rpm	revolutions per minute
sec	second
U	Units
V	volt

Prefixes

k	kilo
m	mini
µ	micro
n	nano

Table of contents

SUMMARY I

ZUSAMMENFASSUNG II

LIST OF ABBREVIATIONS IV

1. INTRODUCTION 1

1.1 Human Cytomegalovirus 1
1.1.1 Epidemiology 2
1.1.2 HCMV pathogenesis 2
1.1.3 HCMV cell tropism 3
1.1.4 Dense Bodies 4

1.2 Interferon (IFN) signalling 6

2 MATERIALS AND METHODS 10

2.1. Materials 10
2.1.1 Devices 10
2.1.2 Consumables 12
2.1.3 Chemicals and reagents 15
2.1.4 Solutions, buffers, and media 17
2.1.5 Commercial kits 20
2.1.6 Antibiotics 20
2.1.7 Cytokines 20
2.1.8 Inhibitors 21
2.1.9 Antibodies 21
2.1.10 Oligonucleotides for qPCR 23
2.1.11 HEC-LTT cell line 23
2.1.12 Viruses 23
2.1.13 Software and online tools 24

2.2 Methods 25
2.2.1 Cell culture 25
2.2.2 Virus cultivation and propagation 28
2.2.3 Infection of HFF cells with virus supernatant for gradient purification of DBs in presence of Letermovir 31
2.2.4 Gradient purification of Dense Bodies 31
2.2.5 Determination of protein concentration 32
2.2.6 UV- inactivation of DBs 32
2.2.7 Exposure of HFFs and ECS cells to DBs 33
2.2.8 Growth kinetics 33
2.2.9 Infectivity assay via IE1 staining 34
2.2.10 Immunofluorescence analysis of the inhibition of dynamin- dependent endocytosis using Dynasore 35

2.2.11 Cell lysates ... 36
2.2.12 Sodium dodecyl sulfate polyacrylamide gel electrophoresis (SDS-PAGE) and immunoblot analysis ... 36
2.2.13 FACS analysis ... 36
2.2.14 Mass spectrometry-based proteomics ... 37
2.2.15 Statistical analysis ... 40

3 RESULTS ... 41

3.1 Effects of HCMV- DBs on the proteome of different cell types ... 41
3.1.1 Impact of DBs on the cellular proteome of HFFs ... 42
3.1.2 Validation of proteome analysis of HFFs ... 51
3.1.3 Impact of DBs on the cellular proteome of ECs ... 59
3.1.4 Validation of proteomic results of endothelial cells in immunoblot analysis ... 66
3.1.5 Impact of DBs on the cellular proteome of monocytes ... 70
3.1.6 Impact of DBs on the cellular proteome of immature dendritic cells (iDCs) ... 76

3.2 Involvement of the JAK/STAT signalling pathway in DBs-induced IRGs upregulation. ... 81

3.3 Endocytosis as optional pathway for the uptake of DBs into HFFs and ECs ... 84
3.3.1 Inhibition of dynamin-dependent endocytosis delayed the uptake of DBs into HFFs ... 84
3.3.2 Entry of DBs into ECs was diminished after inhibition of dynamin-dependent endocytosis ... 87

3.4 Impact of DBs on infected HFFs ... 89
3.4.1 DBs abrogate the downregulation of IRG-expression at late stages of HCMV infection ... 89
3.4.2 Impact of DBs on HCMV infection ... 91
3.4.3 Cytopathic effects (CPE) were accelerated in infected fibroblasts co-treated, or pre-treated with DBs compared to infected cells ... 98
3.4.4 Early apoptosis is increased in infected HFFs exposed to DBs ... 99

3.5 Effect of DBs on autophagy ... 102
3.5.1 Effects of DBs on autophagy in HFFs ... 102
3.5.2 Effects of DBs on autophagy in endothelial cells ... 109

4. DISCUSSION ... 112

4.1 Effect of DBs on the proteome of HFFs, ECs, monocytes and iDCs ... 112

4.2 Upregulation of the major histocompatibility complex (MHC) class I and II antigen presentation pathways in response to DBs ... 114

4.3 Impact of DBs on autophagy ... 115

4.4 Activation of apoptosis of HCMV infected HFFs by DBs ... 115

4.5 The ND10 antiviral restriction factor (RF) is not targeted by DBs ... 116

4.6 Interference of DBs with virus infection ... 116

4.7 Effect of Dynamin inhibition on DBs internalization ... 118

4.8 Conclusion and future directions ... 119

REFERENCES **120**

APPENDIX **129**

ACKNOWLEDGEMENTS **156**

1. Introduction

The current pandemic has highlighted the importance of vaccines to prevent and control life- threatening diseases. Vaccines have made it possible to eradicate smallpox, to eliminate polio and to reduce the threat of diseases such as measles, mumps, or rabies (World Health Organization, 2021). Since the year 2000 alone, immunization programs prevented up to 14 million deaths worldwide (Global Alliance for Vaccines and Immunization (GAVI). Annual Progress Report, 2019).

Considering the large frequency of congenital infection and the morbidity and mortality associated with human cytomegalovirus (HCMV) in immunocompromised individuals, it is not surprising that HCMV is on the top priority list for vaccine development since postulated in 1999 by the Institute of Medicine and emphasized as a priority by the National Vaccine Program Office (Institute of Medicine. 2000. Vaccines for the 21st Century: A Tool for Decisionmaking. Washington, DC: The National Academies Press. https://doi.org/10.17226/5501; [1]. Although a number of vaccine candidates are under investigation, including recombinant protein, live attenuated, DNA-based, mRNA-based, virus-like particles (VLPs) and others, there is currently no approved vaccine for the prevention of HCMV infection [2, 3].

1.1 Human Cytomegalovirus

HCMV, officially known as HHV-5 (Human Herpesvirus 5), is the largest of the nine known human herpesviruses with a genome at 236 kbp in size [4]. A morphological characteristic of HCMV infection is the formation of giant cells, which was eponymous for this pathogen [5, 6]. The increase in cellular volume results from a DNA-containing intranuclear inclusion body and one or more intra-cytoplasmic inclusion bodies. Because of the resemblance of a real owl's eyes shape, these cells were also named "owl´s eye cells" and serve as a histological sign of HCMV disease [5, 6]. Cytomegaloviruses are highly species specific. HCMV infects only humans and primary infection results in the establishment of lifelong latency within the host, from which it may be reactivated by a number of stimuli [7, 8].

1.1.1 Epidemiology

HCMV is one of the most ubiquitous human pathogens worldwide. Depending on the socioeconomic background of the country, the estimated seroprevalence of HCMV in the human population ranges from 56% to 95% [9]. Transmission of HCMV occurs both, horizontally and vertically. Horizontal transmission is mediated by a range of body fluids such as urine, saliva, tears, genital secretions, blood transfusion or organ transplants. HCMV can also be vertically transmitted from the mother to the foetus through the placenta, during birth, or postnatally through the breast milk, causing congenital HCMV (cCMV) [3].

1.1.2 HCMV pathogenesis

HCMV pathogenesis and clinical manifestations of infection depend on the host's immune status. Primary or reactivated HCMV infection in healthy individuals is usually asymptomatic or may be accompanied by the development of relapsing symptoms such as fever, swollen glands, fatigue, and a sore throat [3, 10, 11]. Occasionally HCMV can cause mononucleosis or hepatitis in immunocompetent patients [3, 10, 11]. In patients with compromised immune defence functions, especially in recipients of solid organ or hematopoietic stem cell transplants, HCMV may lead to severe disease conditions, such as pneumonia, hepatitis or colitis. In some cases, HCMV may be the cause of transplant rejection and graft-versus-host disease [3]. Co- infection with HCMV of individuals with acquired immune deficiency syndrome (AIDS) is associated with common clinical manifestations like retinitis, esophagitis and colitis or severe HCMV disease [3, 12, 13].

Thousands of babies are born each year with cCMV infection (Centers for Disease Control Prevention, April 2020). It is the most common viral infection acquired in utero and is associated with severe clinical sequelae in the foetus and the new-born. Primary HCMV infection of the mother during pregnancy has an estimated 30–35% risk of in-utero transmission to the foetus [14]. At birth, most of the infected babies are asymptomatic, while 10-15% present with clinical signs or may develop permanent sequelae later on [14]. Symptoms of the disease include microcephaly, retinitis, intrauterine growth restriction, rash, jaundice, pneumonitis [14-16]. cCMV in addition is the leading, nonhereditary cause of sensorineural hearing loss (SNHL) in children and an important cause of neurodevelopmental delay [17, 18]. In the most severe case, cCMV may lead to pregnancy loss.

1.1.3 HCMV cell tropism

In the human host, HCMV can spread to many tissues due to its extremely broad cell tropism. In vivo, the list of HCMV susceptible cell types is long and includes epithelial cells (EPCs), endothelial cells (ECs), fibroblasts, and smooth muscle cells [19-22]. Several cell types, e.g., monocytes or polymorphonuclear leukocytes (PMNLs) do not support productive HCMV replication but can transport the virus passively through the body [23-27]. Furthermore, CD34+ bone marrow monocyte precursor cells represent a crucial reservoir of latent HCMV, a risk that has to be considered during organ or tissue transplantations [28, 29]. EPCs, Ecs, and fibroblasts are the major targets of HCMV infection in vivo [20]. Especially fibroblasts are permissive for productive infection of HCMV and the most common cell line used in laboratories for HCMV passaging. Following extensive propagation in cell culture fibroblasts, the tropism of clinical HCMV isolates for certain cell types gets lost [30-32]. Genetic analysis of clinical isolates and laboratory strains of HCMV revealed that some genes in laboratory-adapted strains have been lost due to spontaneous mutations in the gene locus UL131-UL130-UL128 (UL128L) during propagation in fibroblasts [30, 31]. It became evident that UL128L was essential for EPC, EC, and DC tropism [33-35].

HCMV entry into host cells is a complex process involving interactions between different viral envelope glycoprotein complexes and host cell surface receptors [29, 36]. The complex HCMV genome encodes at least 25 glycoproteins [36-38]. While the pentameric complex (PC), comprising the glycoproteins gH/gL assembled with the UL128L locus, is indispensable for infection of EPCs, Ecs and leukocytes, the trimeric complex (TC) of gH/gL/gO is required for infection of all cell types [29]. In 2016, platelet-derived growth factor-α (PDGFR-α) was identified as the cellular receptor recognized by the TC. The PDGFR-α – TC interaction mediates the viral entry into fibroblasts [39, 40]. Two years later, the cellular receptor neuropilin-2 (Nrp2) was found to interact with the PC. Nrp2-interaction is used by the virus for entry into epithelial and endothelial cells via low pH-dependent endocytosis [41, 42]. Additional receptors reported for epithelial cell entry include cluster of differentiation 147 (CD147, also known as basigin), cluster of differentiation 46 (CD46), and the olfactory receptor family 14 subfamily I member 1 (OR14I1) [42-46].

1.1.4 Dense Bodies

During lytic HCMV infection, three virus-related particles are formed and released by infected cells into the cytoplasm [47]. The infectious virion is composed of an icosahedral capsid, containing the viral double-stranded DNA (dsDNA) genome, a tegument or matrix layer attached to it, and an envelope. Non-infectious enveloped particles (NIEPs) look very similar but lack viral genomes. They are released in only small amounts. Lastly, subviral Dense Bodies (DBs), which are enveloped electron-dense structure and morphologically distinct from virions are also released. Compared to virions and NIEPs, DBs vary in size ranging from 250 nm to 600 nm. DBs lack a capsid and an infectious viral DNA and are therefore non-infectious and non-replicating [47-51]. The electron-dense core of DBs is predominantly composed of a tegument layer of structural proteins, of which the phosphoprotein 65 (pp65) is the most abundant. This core is surrounded by a lipid bilayer envelope from which viral glycoproteins protrude [37, 38, 52]. The envelope shows a protein composition similar to that of infectious virions. Using transmission electron microscopy (TEM), Grefte et al., demonstrated that DBs are also formed in vivo. They found DBs in HCMV-infected circulating cytomegalic cells from patients thus refuting the presumption that DBs might be a cell culture artefact [53]. It was shown that proteins as well as different types of RNAs of viral and cellular origin are incorporated into virions and DBs which then can be delivered into cells [38, 54].

DBs and virions share viral antigens that are major targets of the host immune response [37, 38, 55]. Several studies have investigated the ability of DBs to elicit humoral and cellular immune responses against HCMV, thereby considering them as a vaccine candidate [55-59]. The production of neutralizing antibodies (NAbs) by the host is considered as an indication of protective immunity and vaccine success. NAbs recognize epitopes of the glycoproteins in the HCMV envelope and inhibit viral entry into host cells [60, 61]. The identification of the PC as major determinant of HCMV cell tropism paved the way for studies that uncovered the PC as key target for NAbs [62-65]. An effective vaccine should induce broad NAbs and balanced $CD4^+$ and $CD8^+$ T cell responses, ideally comparable to those seen in naturally infected individuals. [2, 66]. In preclinical studies, DB-inoculation into mice and rabbits induced consistent NAb titres [57, 59]. Furthermore, DB immunization of transgenic mice expressing the human HLA-A2 induced significant anti-HCMV cytotoxic T lymphocytes (CTLs) and T-helper cell responses in absence of any adjuvants [55, 57, 58, 67]. Subsequent studies showed that DBs could be modified to mediate introduction of additional antigens into the major histocompatibility complex (MHC) class I presentation pathway and enhance the immune response [68, 69].

The crucial antigen-presenting cells (APCs) for the induction of T-cell responses are DCs and macrophages [70, 71]. The uptake of antigens by DCs, trafficking of the DCs to the lymph

nodes and triggering of DC maturation, are key steps in the generation of potent immune responses [72]. Indeed, iDCs could efficiently take up antigen from DBs [73]. Furthermore, DBs induced the activation and maturation of iDCs [73].

All initial studies addressing the immunogenicity of DBs were performed with purified DBs derived from laboratory HCMV strains. Since laboratory HCMV strains do not contain the PC, our group restored the PC in a Towne-based HCMV strain, hereafter referred as RV-Towne-repΔGFP [59]. Sera from mice and rabbits that had been immunized with PC-positive DBs showed a higher neutralization capacity against HCMV infection in different cell types than sera from animals that received PC-negative DBs [59]. Although the DB vaccine has not yet entered clinical trials, methods to scale up the purification process and to adapt this process to safety requirements have been published [74, 75]. Based on these properties, DBs are suitable for HCMV vaccine development.

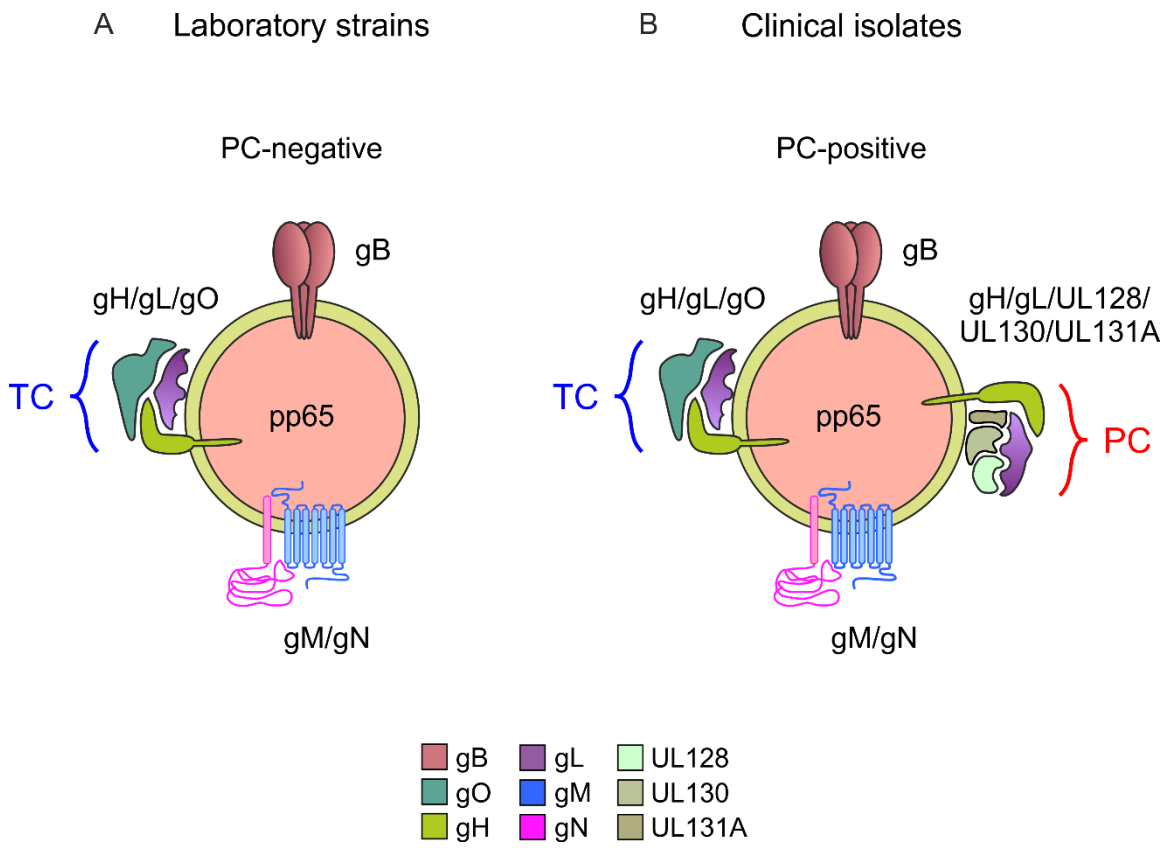

Fig.1: Schematic of DBs derived from HCMV laboratory strains and clinical isolates. The DBs tegument layer, mainly composed of pp65, is enclosed by an envelope studded with glycoprotein complexes critical for viral entry into different cell types. (A) Laboratory strain derived DBs express the trimeric complex (TC), comprising gH/gL/gO on the surface. (B) DBs derived from clinical isolates harbour both, the TC and the pentameric complex (PC) consisting of gH/

gL/pUL128/pUL130/pUL131A on the surface. gB, glycoprotein B; gM/gN complex, consisting of glycoproteins M and N; pp65, phosphoprotein 65. Figure modified by Sauer C., dissertation 2013.

1.2 Interferon (IFN) signalling

The establishment of a rapidly induced antiviral defence is crucial to restrict viral infection. The immediate secretion of IFNs is a key effector mechanism in that sense. Secretion of IFNs leads to a plethora of downstream effects like the induction of a large number of IFN-regulated genes (IRGs), which exert broad antiviral effects [76, 77].
Immediately after virus entry into the host cell, intracellular sensors, known as pattern recognition receptors (PRRs) detect pathogen-associated molecular patterns (PAMPs) of the invading pathogen and activate an innate immune response to eliminate the pathogen [78]. In mammalian cells, two classes of PRRs can be distinguished: the membrane bound PRRs, that include Toll-like receptors (TLRs), and the cytosolic PRRs, that include cytosolic RNA sensors (CRS), cytosolic DNA sensors (CDS), and sensors of the inflammasome pathway [78].

The recognition of pathogen-derived nucleic acids by CRS or CDS is a potent trigger of IFN induction (Fig. 2A.). The exact regulatory mechanism of CDS to stimulate transcription of IFNs is still unclear, but most of them seem to activate the IFN response via the key adaptor protein stimulator of interferon genes (STING). Upon stimulation by a DNA ligand, activated STING translocates from the endoplasmic reticulum (ER) to the perinuclear-Golgi region where it interacts with tumor necrosis factor receptor-associated factor (TRAF) family member associated NF-kappa B activator (TANK)-binding-kinase-I (TBK1) or IkB kinase (IKK) [79] . Following STING phosphorylation by TBK1, it recruits interferon regulatory factor 3 (IRF3), which is also phosphorylated by TBK1. Phosphorylated IRF3 dimerizes and enters the nucleus, where it stimulates the transcriptional expression of type I IFNs (Fig. 2A). In parallel, IkBα phosphorylation by IKK results in the translocation of nuclear factor kappa-light-chain-enhancer of activated B-cells (NF-κB) to the nucleus and in the corresponding transcriptional expression of inflammatory cytokines (Fig. 2A) [79, 80].

Retinoic acid-inducible gene I (RIG-I)-like receptors (RLRs) sense RNA in the cytosol [81]. This family of cytoplasmic PRRs encompasses three members: RIG-I, melanoma differentiation-associated protein 5 (MDA5) and laboratory of genetics and physiology 2 (LGP2). Using virus infection models, it has been demonstrated that RIG-I and MDA5 are essential for antiviral defence and type I IFN induction by RNA-sensing. LGP2 is believed to regulate RIG-I and MDA5 [81]. RIG-I and MDA5 recognize different types of RNA, but use a common RLR

signalling pathway (Fig. 2B) [81]. RNA binding by RIG-I or MDA5 results in the attachment of unanchored lysine-63 (K63)-linked polyubiquitin chains to the receptors, which promotes their homotetramerization and stabilization (not shown for simplicity). Following activation, RIG-I or MDA5 interact with mitochondrial antiviral signalling (MAVS) adaptor protein on the mitochondrial membrane. MAVS associates with multiple adaptor proteins including tumor necrosis factors (TNF) receptor-associated factor-2 (TRAF-2) and TRAF-6 which recruit TRAF-3 and TANK (not shown for simplicity) to trigger the activation of TBK1 and IKKε. TBK1 and IKKε phosphorylate IRF3 and IRF7 which then homodimerize and translocate to the nucleus to promote the expression of type I and type III IFNs (Fig. 2.B) [81].

Released type I IFNs (IFNα/β) bind to the cognate IFNα/β receptor (IFNAR), which is expressed on most cell types and which activates a signalling cascade through the canonical Janus kinase and signal transducer and activator of transcription (JAK/STAT) pathway (Fig. 2C) [82]. Engagement of the receptor subunits IFNAR1 and IFNR2 activate the tyrosine kinases JAK1 and tyrosine kinase 2 (Tyk2), which subsequently phosphorylate and activate signal transducer and activator of transcription (STAT) 1 and 2 proteins. Activated STAT proteins heterodimerize and recruit the IFN-regulatory factor 9 (IRF9) to form the IFN-stimulated gene factor 3 (ISGF3) complex. The ISGF3 transcription factor translocates into the nucleus and induces the expression of IRGs, which exert anti-viral effects (Fig. 2.C) [79].
Regarding HCMV infection, several TLRs, CRS and CDS have been described to recognize HCMV´s PAMPs [80]. One study, performed by Compton et al, identified TLR2 as a cellular sensor that mediated innate immune responses to HCMV DBs [83].

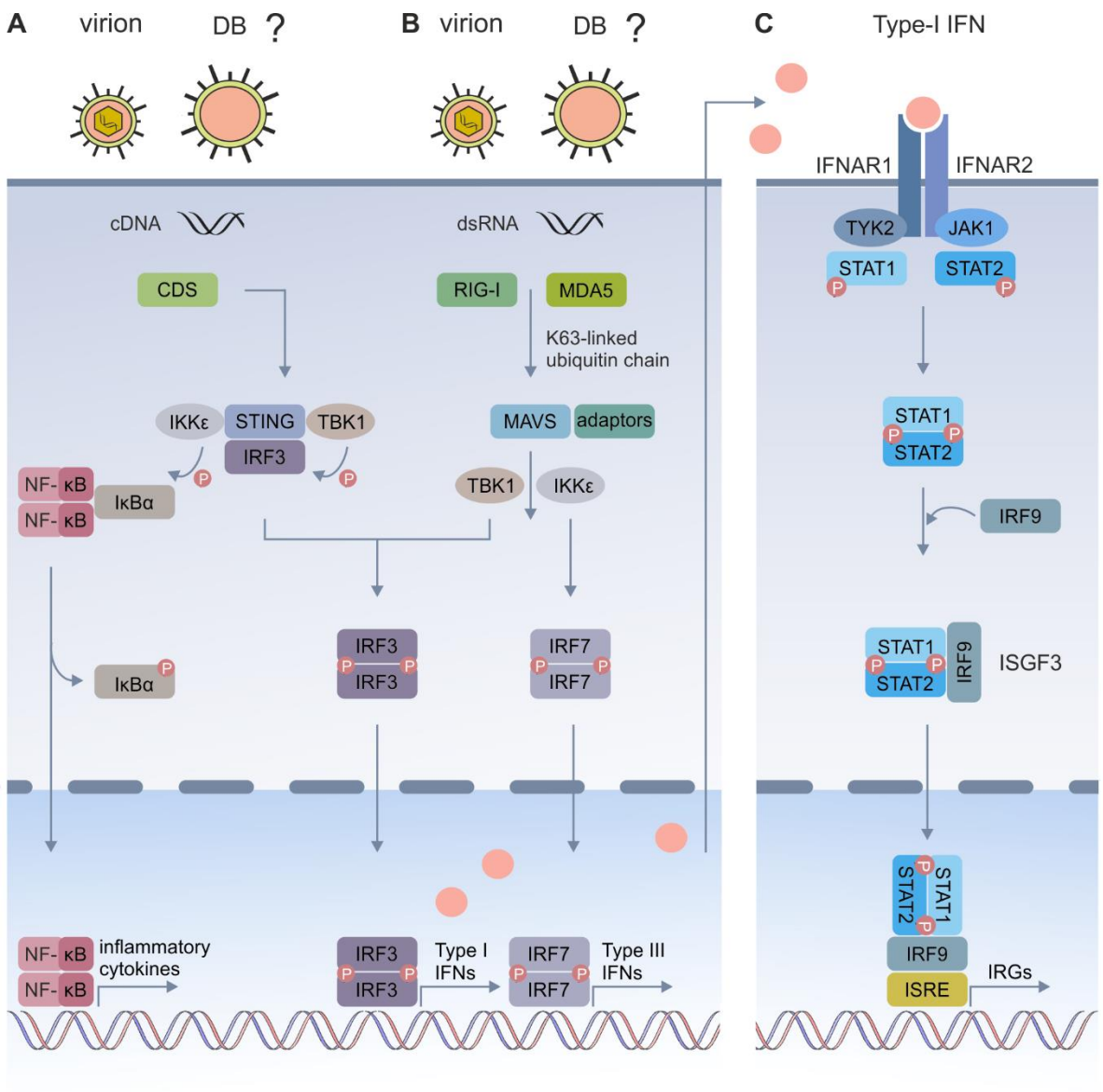

Fig 2. Schematic of IRG induction following virion sensing or possible DBs sensing and type-I IFN production. A Mechanism of cytosolic DNA-mediated type-I IFN induction**.** Cytosolic (virus)-DNA is sensed by cytosolic DNA sensors (CDS). This triggers the STING-TBK1-IRF3 or IKKs- NF-κB signalling cascades. Upon activation, STING translocates from the ER to the Golgi, where it recruits the kinases TBK1 and IKK, leading to the phosphorylation of IRF3 and IκBα, respectively. Phosphorylated IRF3 dimerizes, translocates to the nucleus, and activates transcription of type-I IFNs. Phosphorylation of IκBα leads to its dissociation from the complex and the translocation of NF-κB to the nucleus, where it activates transcription of genes encoding IFNs and proinflammatory cytokines. **B** RLR signalling pathway**.** RIG-I and MDA5 are activated by cytosolic (virus)- RNA and interact with MAVS. MAVS becomes associated with several adaptor proteins that lead to the activation of the cytosolic kinases TBK1 and IKKε. Phosphorylation of the transcription factors IRF3 and IRF7 leads to their translocation into the nucleus and the production of type I or type III IFNs. **C** Type-I IFN signalling through the JAK/STAT pathway. Binding of type-I IFNs to the heterodimeric receptor IFNAR, which

comprises IFNAR1 and IFNAR2, results in the autophosphorylation and activation of the kinases JAK1 and TYK2, which phosphorylate STAT1 and STAT2. The phosphorylated STATs dimerize and associate with IRF9 to form the transcriptional activator complex ISGF3. ISGF3 translocate to the nucleus where it binds to the IRSE element and activates the transcription of IRGs.

cDNA, cytosolic DNA; dsRNA, double stranded RNA; IκBα, Inhibitor of nuclear factor kappa B; IFNAR, Interferon- α/β receptor; IKK, Inhibitory kappa B kinase; IRF3, Interferon regulatory factor 3; IRSE, IFN-stimulated response element; JAK1, Janus kinase 1; NF-κB nuclear factor κappa B; STAT1/2, Signal transducer and activator of transcription 1/2; STING, Stimulator of interferon genes; TBK1, TANK- binding kinase 1; TYK2, Tyrosine kinase 2.

2 Materials and Methods

2.1. Materials

2.1.1 Devices

Device	Company
Blotting modules	
Novex™ Bolt™ Mini Blot Module	Thermo Fisher Scientific
Perfect Blue 'Semi-Dry Blotter Sedec M	VWR International GmbH
Cell Culture Laminar Flow:	
HERAsafe, HS12, Class II	Heraeus
HERAsafe, HS15, Class II	Heraeus
Centrifuges	
Eppendorf Centrifuge 5424/R	Eppendorf AG
Eppendorf Centrifuge 5430/R	Eppendorf AG
Mini Centrifuge SPROUT™	Heathrow Scientific
Ultracentrifuge Optima™ L-90K	Beckman Coulter
Electrophoresis	
Power Supply-EPS600	Pharmacia Biotech
Invitrogen®Mini Gel Tank	Thermo Fisher Scientific
ELISA MULTISKAN FC Type 357	Thermo Fisher Scientific
Flow cytometer Cytomics FC 500	Beckman Coulter
Freezer -86°C FORMA 88000	Thermo Fisher Scientific
Incubator	
Forma Steri-cult CO_2 Type B12	Thermo Fisher Scientific
Microscopes:	
Axiovert 25	Carl Zeiss Microscopy GmbH
Axio Vert.A1	Carl Zeiss Microscopy GmbH

Axiophot	Carl Zeiss Microscopy GmbH
Leitz DM IRB/SL	Leica
Microscope Camera:	
Axiocam 305 mono	Carl Zeiss Microscopy GmbH
Camera adapter 60N-C 2/3”	Carl Zeiss Microscopy GmbH
Microwave Samsung - M1712N	Samsung
Odyssey Infrared Imager CLx	LI-COR Biotechnology
PCR Workstation captair®bio Biocap DNA	Erlab
Pipettes:	
Gilson™ PIPETMAN Classic™	Thermo Fisher Scientific
P10 (1-10 µL) F144802	Thermo Fisher Scientific
P20 (2-20 µL) F123600	Thermo Fisher Scientific
P200 (20-200 µL) F123601	Thermo Fisher Scientific
P1000 (100-1000 µL) F123602	Thermo Fisher Scientific
RAININ Pipet-Lite XLS	Mettler- Toledo GmbH
Pipetboy	INTEGRA Biosciences
Pipetboy 2	INTEGRA Biosciences
IBS Pipetboy acu	INTEGRA Biosciences
Shaker	
IKA® MS 3 basic	IKA®- Werke GmbH & Co.
IKA® MS1 Minishaker	IKA®- Werke GmbH & Co
IKA® Shaker HS501 digital	IKA®- Werke GmbH & Co
IKA® Roller 10 basic	IKA®- Werke GmbH & Co.
Magnetic stirrer with heating Yellow MAG HS 7	IKA®- Werke GmbH & Co.
Orbital Shaker DOS-10L	neoLab Migge GmbH
pH meter FE20 FiveEasy™	Mettler- Toledo GmbH
7500 Real Time PCR System	Applied Biosystems

Scales	
BP 61	Sartorius AG
UW2200HV	SHIMADZU Germany GmbH
LP 5200P	Sartorius AG
ThermoMixer® F1.5	Eppendorf AG
Thermomixer compact	Eppendorf AG
UV-lamp	Carl Roth GmbH + Co. KG
Water bath WB7L1	Memmert

2.1.2 Consumables

Name	Description	Company
Cell culture dishes (10 cm)	TC Dish 100 No 83.3902	SARSTEDT AG & Co.KG
Cell culture dishes (6 cm)	BD Falcon™ 60 mm No. 353004	Becton Dickinson
Cell culture plates	TC Plate 6 Well No.83.3920	SARSTEDT AG & Co.KG
	TC Plate 24 Well No. 83.3922	SARSTEDT AG & Co.KG
	Costar 24 Well No. 3524	Corning
Cell culture flasks	CELLSTAR® TC 50 ml, T-25 cm^2 No. 690160	Greiner Bio-One International GmbH
	CELLSTAR® TC 250 ml, T-75 cm^2 No.658170	Greiner Bio-One International GmbH
	CELLSTAR® TC 550 ml, T-175 cm^2 No. 660160	Greiner Bio-One International GmbH
Centrifuge tubes	CELLSTAR® TUBES 15 mL	Greiner Bio-One International GmbH

	No. 188271	
	CELLSTAR® TUBES 50 mL No. 227261	Greiner Bio-One International GmbH
	Polypropylene, 13,2 mL No. 331372	Beckman Coulter
	Polyallomer, 38,5 mL No. 326823	Beckman Coulter
	Polycarbonate, 70 mL No.355655	Beckman Coulter
	Ultra-Clear™, 13,2 mL No.344059	Beckman Coulter
Chromatography Paper	Whatman® Cellulose No. 3030690	Thermo Fisher Scientific
Coverslips	Cover glasses, Ø 12mm No. 10062491	Thermo Fisher Scientific
Disposable syringe	BD Discardit™ II Syringe 20 mL No.300296	Becton Dickinson
Disposable needle	BD Microlane™3 No. 304622	Becton Dickinson
Filters	Millex®-GS Filter Unit MF-Millipore™ 0,22 µm No. SLGS033SS	Merck KGaA
	Filtropur V25, 250 mL No. 833940001	Sarstedt AG & Co
	Filtropur V50, 500 mL No.831823001	Sarstedt AG & Co
Filter tips	Rainin 20 µL No. GP-L10F	Mettler- Toledo
	Rainin 200 µL No. GP-L200F	Mettler- Toledo
	Rainin 1000 µL No. GP-L1000F	Mettler- Toledo
	Biosphere 0,1-10 µL No. 70.1130.210	Sarstedt AG & Co.

	Biosphere 2-20 µL No. 70.760.213	Sarstedt AG & Co.
	Biosphere 1-200 µL No. 70.760.211	Sarstedt AG & Co.
	Biosphere 50-1.000 µL No. 70.762.211	Sarstedt AG & Co.
Freezing tubes	Cryopure 1,8 mL No. 72.379	SARSTEDT AG & Co.KG
Flow cytometer tubes	Lab equip test tube No. 2523749	Beckman Coulter
Hemocytometer	Neubauer bright- line No. 0640130	Paul Marienfeld GmbH + Co. KG
Microscope slides	Cut edges 90°C No. BPB018	Rogo-Sampaic (RS)
Protein ladder	PageRuler™ Prestained No. 11812124	Thermo Fisher Scientific
Protein separation gels	Bolt™ 10% Bis-Tris Plus Gel, 10 Well No. NW00100BOX	Thermo Fisher Scientific
	Bolt™ 10% Bis-Tris Plus Gel, 15 Well No. NW00105BOX	Thermo Fisher Scientific
PVDF membrane	Immobilon-PSQ No. ISEQ00010	Merck KgaA
Reaction tubes (qPCR)	Sapphire PCR strip tube 1 x 8, 0.2 mL No. 673210	Greiner Bio-One International GmbH
	Sapphire PCR strip cap for 0.2 mL strip tubes 1 x 8 No. 373250	Greiner Bio-One International GmbH
Safe lock micro tube	Micro tube 2.0 mL No. 72.691	Sarstedt AG & Co.
	Micro tube 1.5 mL No. 72.690.001	Sarstedt AG & Co.

Serological pipettes	5 mL No. 606180	Greiner Bio-One International GmbH
	10 mL No. 607180	Greiner Bio-One International GmbH
	25 mL No. 760180	Greiner Bio-One International GmbH
	50 mL No. 768180	Greiner Bio-One International GmbH
Spot plate	12 cavities No.C768.1	Carl Roth GmbH + Co. KG

2.1.3 Chemicals and reagents

Name	Description	Company
Acetic acid	No.3738.1	Carl Roth GmbH + Co. KG
Acetone	No. 131007.1211	AppliChem
3-Amino-9-ethylcarbazole	AEC No. A6926	Sigma-Aldrich
Albumin fraction V	BSA No. 1.12018.0100	Merck KGaA
Aqua ad iniectabilia	Ampuwa® Rinsing solution Plastipur® No. B23067A	Fresenius Kabi
Aqua bidest.	Aqua B. Braun No. PET82423E	B. Braun Melsungen AG
Basic Fibroblast Growth Factor	bFGF No. 13256-029	Thermo Fisher Scientific
β- Mercaptoethanol	No. 4227.1	Carl Roth GmbH + Co. KG
Bromophenol Blue Sodium Salt	No. 1.11746.0005	Merck KGaA
Deoxynucleotide Triphosphates	dNTPs No.733-1855	VWR International GmbH
D- glucose	No.X997.2	Carl Roth GmbH + Co. KG
4′,6-Diamidin-2	DAPI	AppliChem GmbH

-phenylindol	No. A1001.0010	
N,N- Dimethylformamide	DMF No. D4254	Sigma-Aldrich
Dimethyl sulfoxide	DMSO ≥ 99,8% No.4720.2	Carl Roth GmbH + Co. KG
di-sodium tartrate dihydrate	$Na_2C_4H_4O_6$ No. A2662	AppliChem GmbH
1,4-Dithiothreit	DTT No. 6908.2	Carl Roth GmbH + Co. KG
Dulbecco's Phosphate Buffered Saline	DPBS No. D8537	Sigma-Aldrich
Endothelial Cell Growth Medium	ECGM No. C-22010	Promo Cell
Ethanol	Ethanol 99.6% No. P076.1	Carl Roth GmbH + Co. KG
Ethylenediaminetetraacetate	EDTA No. A3553	AppliChem GmbH
Gelatin solution	2% in H_2O No. G1393	Sigma-Aldrich
Glycerin 86%	No. 7533.3	Carl Roth GmbH + Co. KG
Hydrogen peroxide	H2O2 No.9683.1	Carl Roth GmbH + Co. KG
Isopropanol	No. 07001123B	Hedinger
Kaliumdihydrogenphosphat	KH2PO4 No. JB4921-04	Avantor Performance Materials
L-Alanyl-L-Glutamin	No. K0302	Biochrom GmbH
L-Glutamin	No. G7513	Sigma-Aldrich
Minimum Essential Medium	MEM No.21090-022	Thermo Fisher Scientific
Methanol	No. 20874307	VWR International GmbH
Milk powder	No. T145.2	Carl Roth GmbH + Co. KG
ROTI®Mount FluorCare	No. HP19.1	Carl Roth GmbH + Co. KG
Potassium chloride,	KCl No. P8041	Sigma-Aldrich
Powdered Milk	No. T145.2	Carl Roth GmbH + Co. KG
Rhodamine X	ROX No.80-3315-10	Genova Diagnostics

Sodium lauryl sulphate	SDS No. 4360.1	Carl Roth GmbH + Co. KG
Sodium chloride	NaCl No. 3957	Carl Roth GmbH + Co. KG
Sodium hydrogen carbonate	$NaHCO_3$ No. 6885.1	Carl Roth GmbH + Co. KG
Sodium Pyruvate	$C_3H_3NaO_3$ No. 11360-039	Thermo Fisher Scientific
SDS Running Buffer	Novex®, Bolt™ MES SDS Running Buffer No. B0002	Thermo Fisher Scientific
Supplement Mix Endothelial Cell Growth Medium	No. C-39215	Promo Cell
Transfer Buffer	Novex®, Bolt™ Transfer Buffer No.BT00061	Thermo Fisher Scientific
Tris-hydroxymethyl-amino methane	Tris No. 5429.2	Carl Roth GmbH + Co. KG
Triton-X-100	No. 3051.3	Carl Roth GmbH + Co. KG
Trypan Blue solution	No. T8154	Sigma-Aldrich
Trypsin	No.27250-018	Thermo Fisher Scientific
Trypsin-EDTA	No. 1540054	Thermo Fisher Scientific
Tween® 20	No. 8221840500	Merck KGaA

2.1.4 Solutions, buffers, and media

Acetate buffer	13.6 g/L sodium-acetate x 3 H_2O; 2.88 mL/L glacial acetic acid; pH= 4.9;
AEC-stock solution	4mg/mL n,n- dimethylformamide (DMF), 1 mL aliquots stored at -20°C
AEC-Staining solution	AEC-stock solution 1:20 diluted in acetate buffer and 1:1000 in H2O2 (30%)

bFGF	10 µg bFGF; lyophilized; Final concentration 0,1 mg/mL (w/v) dilution 1:10 in 10 mM; pH 7.6 TRIS-HCl + 0,1% BSA; 10 µg bFGF were mixed with 90 µL TRIS-HCl and 10 µL BSA. After centrifugation in a Spin-X Centrifuge Tube (filter 0,22 µm) at 14000 rpm for 1 minute, 5 µL aliquots were prepared and stored at -20°C.
Blocking buffer	5% (w/v) BSA in PBST
35% di-sodium tartrate	for 500 mL: 207.5 g di-sodium tartrate dihydrate; 325 mL 0.04 M sodiumphosphate buffer; pH= 7.4, solved at 65°C, autoclave, storage at room temperature
15% di-sodium tartrate-glycerol	500 mL: 80.9 g di-sodium tartrate dihydrate; 150 mL glycerol 86%; 275 mL 0.04 M sodiumphosphate buffer pH= 7.4, autoclave, store at room temperature
Doxycycline	Stock solution 2 mg/ml (dissolved in Ethanol, store at -20°C)
0.04 M sodium-phosphate	1.1 g/L NaH_2PO_4 x H_2O; 5.7 g /L Na_2HPO_4 x 2 H_2O; pH=7.4, autoclaved, storage at +4°C
Freezing medium	90% Fetal Bovine Serum FBS + 10 % dimethyl sulfoxide DMSO
0.1% gelatin solution	Diluted in ddH_2O, autoclaved, store at +4°C
Laemmli Buffer (2x)	125 mM Tris; 2% (v/v) β-Mercaptoethanol; 10% (v/v) glycerol; 2% (w/v) SDS; 1 mM EDTA, pH 8,0; 0.005% (v/v) bromphenolblue, ad 50 mL ddH_2O; store at -20°C
PBST	0.2% (v/v) Tween-20 in PBS

Solution A (Washing solution for HEC-LTT cells)	2.5 x stock solution in 500 mL ddH_2O: 10g NaCl; 0.5 g KCl; 0.44 g $NaHCO_3$; 1.13 g D-Glucose; filtered sterile and store at 4°C
Trypan blue solution	Final concentration 0,1% (v/v) dilution 1:4 in 1xPBS. 2.5 mL Trypan blue solution was mixed in 7.5 mL PBS.
Trypsin/ EDTA	0,5 g/L Trypsin; 0,2 g/L EDTA in 1xPBS (10x), 1:10 in *Aqua* B. Braun

Cell culture media

5% MEM	Minimal Essential Medium Eagle (MEM) supplemented with 25 ml FBS, 5 ml L-glutamine, 25 mg gentamicin, 2.5 µL bFGF.
5% MEM, bFGF free	Minimal Essential Medium Eagle (MEM) supplemented with 25 ml FBS, 5 ml L-glutamine, 25 mg gentamicin, without bFGF
10% MEM	Minimal Essential Medium Eagle (MEM) supplemented with 50 ml FCS, 5 ml L-glutamine, 25 mg gentamicin, 2.5 µL bFGF.
Freezing medium	90% Fetal Bovine Serum FBS + 10% dimethyl sulfoxide DMSO
Endothelial Cell Growth Medium	0.02 ml / ml Fetal Calf Serum; 0.004 ml / ml Endothelial Cell Growth Supplement; 0.1 ng / ml Epidermal Growth Factor (recombinant human) 1 ng / ml Basic Fibroblast Growth Factor (recombinant human); 90 µg / ml Heparin; 1 µg / ml Hydrocortisone

2.1.5 Commercial kits

Name	Catalog number	Company
Pierce™ BCA Protein Assay Kit	No. 23225	Thermo Fisher Scientific
HotStarTaq DNA Polymerase	No. 203207	Qiagen
High Pure Viral Nucleic Acid Kit	No. 11858874001	Roche Holding AG
Apoptosis/ Necrosis Assay (blue, green, red) Detection Kit	No. Ab176749	Abcam
Venor GeM-Mykoplasmen Detektions Kit	No. 1-1100	Minerva

2.1.6 Antibiotics

Antibiotics were stored at -20°C

Antibiotic	Solution stock	Final concentration	Catalog number	Company
BM-Cyclin 1	2,5 mg/mL	10 µg/mL	No. 10799050001	Roche Holding AG
BM-Cyclin2	1,25 mg/mL	5 µg/mL		
Doxycyclin	2 mg/mL	2 µg/mL	No. A2951,0025	Applichem
Gentamicin	50 mg/mL	50 µg/mL	No. 15750-037	Thermo Fisher Scientific

2.1.7 Cytokines

Name	Stock concentration	Company
IFN-β	100 U/mL diluted in 0.1% bovine serum albumin–ddH_2O; specific activity, according to the manufacturer's information, 5×10^8 U/mg; catalog number 300-02BC	PeproTech

2.1.8 Inhibitors

Inhibitor	End concentration	Catalog number	Company
Dynasore	80 µM/mL	No. S8047	Selleck Chemicals
JAK Inhibitor I	20 µM/mL	No. 420099	Merck Millipore
Letermovir (Prevymis)	50 nM	No. HY-15233	MedChemExpress

2.1.9 Antibodies

2.1.9.1 Primary Antibodies

WB: Western blot; IF: Immunofluorescence

Antibody	Designation	Isotype	Dilution		Company
GAPDH	mAb-GAPDH	mouse	WB:	1:500	Sigma-Aldrich No. G8795
IE1	mAb-IE1 (p63-27)	mouse			Dr. W. Britt, Birmingham, AL, USA
IFIT1	pAb-IFIT1	rabbit	WB:	1:500	Thermo Fisher Scientific No. PA5-31254
IFIT3	pAb-IFIT3	rabbit	WB:	1:1000	Thermo Fisher Scientific No. PA5-22230
ISG15	mAb-ISG15 (F-9)	mouse	WB:	1:500	Santa Cruz Biotechnology No. sc-166755
LC3B	mAb-LC3B (D11)	rabbit	WB:	1:1000	Cell Signaling Technology No. 3868S
MX1	pAb-MX1	rabbit	WB:	1:1000	Thermo Fisher Scientific PA5-22101
PML	pAb-PML	rabbit	IF:	1:100	Abcam

					No. ab53773
pp65	mAb-pp65 (p65-33)	mouse	WB: IF:	1:500 1:10	Dr. W. Britt, Birmingham, AL, USA
Sp100	Sp100	rabbit	IF:	1:100	Atlas Antibodies AB No. HPA017384
STAT1	mAb-STAT1 (42H3)	rabbit	WB:	1:500	Cell Signaling Technology No.9175
Transferrin	Transferrin Alexa Fluor™ 546 Conjugate	human			Thermo Fisher Scientific No. T23364
Tubulin-α	mAb-Tubulin-α (DM1A)	mouse	WB:	1:500	Sigma-Aldrich No. T6199
UL44	mAb-UL44 (BS510)	mouse	WB:	1:2	Biotest AG

2.1.9.2 Secondary Antibodies

Antibody	Designation		Dilution	Company
anti- rabbit	Donkey anti-Rabbit, Alexa Fluor 488	donkey	IF: 2 drops/ mL	Thermo Fisher Scientific No. R37118
anti- mouse	Goat anti-Mouse Alexa Fluor 546	goat	IF: 1:500	Thermo Fisher Scientific No. A-11003
anti- rabbit	Donkey anti- rabbit, Alexa Fluor 680	donkey	WB: 1:10000	Thermo Fisher Scientific No. A10043
anti- mouse	IRDye® 800CW Donkey anti-mouse	donkey	WB: 1:15000	LI-COR Biosciences No. 926-32212
anti-mouse	HRP-coupled rabbit anti-mouse	rabbit	IF: 1:500	Dako No.

2.1.10 Oligonucleotides for qPCR

Primer	Sequence (5‘to 3‘)	Company
CMV-FP	TCATCTACGGGGACACGGAC	Eurofins MWG Operon
CMV-RP	TGCGCACCAGATCCACG	Eurofins MWG Operon
TaqMan-CMV	CCACTTTGCCGATGTAACGTTTCTTGCAT	TIB MOLBIOL

2.1.11 HEC-LTT cell line

Human endothelial cell-large T antigen and telomerase (HEC-LTT)

HEC-LTT cells originate from human umbilical vein endothelial cells (HUVECs). This conditionally immortalized cell line contains gene expression cassettes for the human telomerase catalytic subunit (hTERT) and the simian virus 40 large T-antigen (SV40-TAg) [84, 85]. HEC-LTT cell proliferation and expansion can be controlled by the addition of doxycycline (DOX). In the presence of DOX, hTERT and SV40-TAg expression are activated and result in high cell proliferation and unlimited expansion. The cells were kindly provided by Christian Sinzger (Ulm University).

2.1.12 Viruses

All HCMV strains used for experiments were derived from Bacterial Artificial Chromosome (BAC) clones.

HCMV strain	Description
RV-KB14	UL83- deletion mutant. An AD169-derived recombinant virus where the complete coding sequence of pp65 was replaced by the tetracycline resistance gene, except for 150 bp at the 5’ end of UL83 and the stop codon (generated by Katrin Besold; Hesse et al., 2013)
RV-Towne-BAC	HCMV laboratory strain, based on ATCC-Towne strain (provided by Liu (USA) (Marchini et al., 2001)).

RV-TowneUL130repΔGFP (RV-Towne-repΔGFP)	Endotheliotropic strain; Towne-UL130repaired- derived recombinant virus where GFP was replaced by the GalK gene (modified by Christine Zimmermann; Gogesch et al., 2019),

2.1.13 Software and online tools

Software	Company/ Website
CorelDraw Graphics Suite X7	Corel Corporation
CXP Analysis Software	Beckman Coulter
GraphPad Prism 8 (Version 8.3.0)	GraphPad Software
Image Studio™ Lite	LI-COR Biotechnology
INTERFEROME database	http://www.interferome.org/interferome/home.jspx
Microsoft Office (Excel, Powerpoint, Word)	Microsoft
7000 System Sequence Detection Software RQ Study Application V.1.2.3	Applied Biosystems
STRING	https://string-db.org
UniProtKB database	https://www.uniprot.org
Zen 3.0 system Blue Edition	Carl Zeiss Microscopy GmbH

2.2 Methods

2.2.1 Cell culture

2.2.1.1 Cultivation of human cells

To provide an aseptic environment for cell culture experiments, all work with eukaryotic cells was performed under a Class II laminar flow clean bench and sterile implements. Human cells were maintained in a T-175 cm^2 cell culture flask at 37°C in a humidified atmosphere (80%) with 5% CO_2. The cells were frequently tested for mycoplasma contamination using the BM-cyclin mycoplasma detection kit. Provisionally cells were cultivated in the presence of BM Cyclin after thawing according to the manufacturer´s instructions.

Human foreskin fibroblasts (cell line Psf5)

Primary human foreskin fibroblasts (HFFs) at passage 13 to 21 were maintained in MEM medium supplemented with 5% FBS, 0.5 mg/ml L-glutamine, 0.5 ng/ml bFGF and 500 µL of the antibiotic gentamicin (50 mg/ml). HFFs were passaged once a week and 1,8 x 10^6 HFFs were reseeded into a T-175 cm^2 flask. For autophagy and apoptosis experiments, HFFs were maintained in MEM medium supplemented with 10% FBS. Confluent cells were washed once with PBS and incubated in trypsin/EDTA for five minutes at 37°C. The enzymatic digestion was stopped by addition of complete growth medium. Cells were centrifuged for five minutes at 1500 rpm, the supernatant was discarded, and cells were diluted in growth medium to determine the cell number.

Endothelial cells HEC-LTT

HEC-LTT cells from passage 41 to 56 were propagated in ECG medium in the presence of 2 µg/ml doxycycline. HEC-LTT cells were passaged twice a week. Before passaging, a T-175 cm^2 cell culture flask was coated with 6 ml of 0.1% gelatine and incubated at 37°C for 30 min. Afterwards, the excess solution was removed. Confluent cells were washed once with 10 ml solution A and incubated in 5 mL trypsin/EDTA 5% solution at room temperature until the cells detached. For trypsin neutralisation 10 mL of HFF 5% MEM medium without bFGF was added and the cells were transferred into a 50 mL tube. The cells were pelleted for five minutes at 1500 rpm. After the supernatant was discarded, the cells were resuspended in ECG medium and counted. 2x10^6 cells were reseeded into a new gelatine- coated flask with fresh ECG medium supplemented with DOX (final concentration 2 µg/ml) and incubated at 37°C. Hereafter HEC-LTT cells are designated as ECs.

2.2.1.2 Manual cell counting using a hemocytometer

To enable consistency between experiments an accurate cell number was determined. For cell counting and the assessment of cell viability, trypan blue staining was used. Dead cells with compromised membranes become blue, whereas cells with intact membranes exclude the dye and stay unstained. For cell counting, media was removed, and the cells were washed with PBS (HFFs) or solution A (ECS). Trypsin/EDTA 5% solution was added to detach the cells. Trypsinisation was stopped by the addition of 5% MEM (HFF) or 5% MEM without bFGF (ECS) respectively. The cell suspension was transferred into a tube and centrifuged for five minutes at 1500 rpm at room temperature. After the supernatant was removed the cell pellet was resuspended in PBS (HFFs) or solution A (ECS). The amount of PBs or solution A depended on the size of the cell pellet. To determine the cell number, 50 µL of the cell suspension and 50 µL of the trypan blue staining were mixed (1:1 dilution) in a well of a 96-well plate. 50 µL of this mixture were pipetted in the space between the cover slide and the Neubauer counting chamber, until the space was filled by capillarity. Unstained cells were counted under a 20 times magnification of an inverted microscope. To calculate the concentration, the average number of counted cells in the four quadrants was multiplied by 10^4 to get the number of cells per millilitre. To correct the dilution from the trypan blue addition, this number was multiplied by two. The final value represented the number of viable cells per millilitre in the original cell suspension. Depending on the experiment the required cell number was seeded into a new flask or dish and cultivated as described in 2.2.1.1 and 2.2.1.3.

$$\text{cells/ml} = \frac{\text{total number of counted cells (Quadrant I-IV)}}{\text{number of counted quadrants (I-IV)}} \times 10^4 \times \text{dilution factor}$$

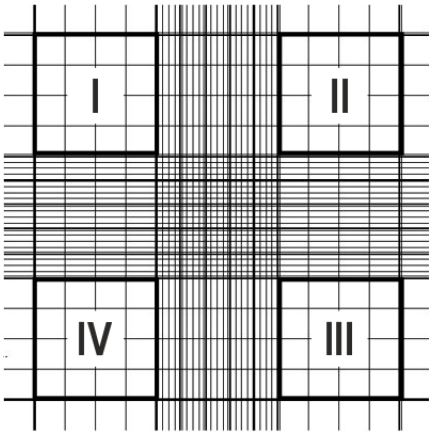

Neubauer counting chamber

2.2.1.3 Seeding of cells for different applications

For experiments, HFFs were seeded the day before infection or DBs exposure in their appropriate medium. ECS cells were maintained overnight in ECG medium devoid of doxycycline.

Cell line	Cultivation vessel	Seeded cell number	Medium volume
ECS	6-well plate	0.3 x 106	2 mL
	10 cm dish	0.6 x 106	10 mL
	175 cm2 flask	2 x 106	20 mL
HFFs	6-well plate	0.3 x 106	2 mL
	10 cm dish	0.5 x 106	10 mL
	175 cm2 flask	1.8 x 106	20 mL

2.2.1.4 Cryopreservation- Freezing of cells

For cryopreservation of human cells at -80°C, the cells were harvested at a confluence of 90-100% of a T-175 cm^2 flask. Therefore, the medium was removed, and the cells were washed and trypsinized. Once the cells were detached, media was added to stop the reaction and the cells were transferred into a centrifuge tube. The cells were pelleted at 1500 rpm for five minutes at room temperature. The supernatant was removed, and the cell pellet was resuspended in 2 mL freezing medium. 1 mL aliquots were dispensed into cryo tubes, which were stored in an isopropanol isolated cryo-box and transferred to -80°C.

2.2.1.5 Thawing of cells

To ensure the highest level of viability, the vial with frozen cells was thawed rapidly in a 37°C water bath. A 15 ml centrifuge tube containing 10 mL of the appropriate complete growth medium was prepared. After thawing, the cells were transferred into the fresh culture medium and centrifuged at 1500 rpm for five minutes. The supernatant was discarded, and the cells were washed with fresh medium again to completely remove DMSO. After centrifugation at 1500 rpm for five minutes the cell pellet was resuspended with the appropriate growth medium, dispensed into a T-25 cm^2 or T-75 cm^2 culture flask and incubated at 37°C and 5% CO_2. For ECS cells the flask was coated with 0.1% gelatine for 30 minutes before.

2.2.2 Virus cultivation and propagation

2.2.2.1 Preparation of virus “seed stocks”

For HCMV virus inoculations, supernatant stocks of the strains RV-Towne- BAC, RV-Towne-repΔGFP and RV-KB14 were used. These virus supernatant stocks were prepared from supernatants of transfected HFFs. Briefly, Towne- BAC, Towne-repΔGFP and KB14- BACmids were reconstituted to virus by transfection of BAC DNA into HFFs. Transfected cells were propagated until 100% of the cells showed cytopathic effects (CPE). The virus-containing supernatants from these cultures were used for further propagation of virus and declared as “seed-stocks”. The seed stocks, which were used to prepare supernatant stocks for the experiments in this thesis were already available.

2.2.2.2 Preparation of virus supernatant stocks

For the preparation of virus supernatant stocks, HFFs were seeded at a density of 1.8×10^6 in five T-175 cm^2 flasks one day before infection. The cells were incubated with virus inocula, consisting of 0.5 ml seed-stock- supernatant and 3.5 mL of 5% MEM medium for two hours with occasional swirling. After 1.5 hours, 16 ml of fresh 5% MEM medium was added, and the cells were maintained until the cultures showed a complete CPE. The supernatants were then harvested and precleared from cellular debris by centrifugation at 1,475 x g for 10 min at room temperature. Finally, the supernatants were stored in freezing tubes in 1 mL aliquots at -80°C.

2.2.2.3 TaqMan quantitative real-time polymerase chain reaction (TaqMan qPCR)

The detection of HCMV genomes was assessed by quantitative real-time polymerase chain reaction (qPCR) using TaqMan® technology based on the amplification of a conserved sequence of the HCMV UL54 gene, which encodes the catalytic subunit of the HCMV DNA polymerase.

The principle of the TaqMan® technology relies on the 5´ to 3´exonuclease activity of the Taq DNA polymerase to cleave a fluorophore-labelled probe during hybridization to a target sequence. The TaqMan® probe employs a gene-specific sequence within a DNA region amplified by a specific set of PCR primers. On the 5´end of the probe, a reporter-dye is attached to report the amplification of the template. On the 3´end of the probe a quencher is placed. The fluorescence of the reporter is quenched due to its proximity to the quencher. The quencher also blocks the 3´end of the probe, so that it cannot be extended by Taq DNA polymerase. During amplification, the primers and the probe anneal to the target. As the Taq DNA polymerase extends the primer and synthesizes the nascent strand, the 5' to 3' exonuclease activity of the Taq DNA polymerase degrades the probe. The degradation of the

probe releases a fragment containing the reporter dye. As a result, the reporter is separated from the quencher. The resulting fluorescence signal detected in the qPCR thermal cycler is directly proportional to the amount of amplified DNA template present in in the sample.

In this thesis, the TaqMan® probe 5′-CCACTTTGCCGATGTAACGTTTCTTGCAT-3′ was directed against the HCMV-specific sequence of the UL54 gene. At the 5´end of the probe, the reporter dye 6-carboxyfluorescein was attached and the 3´end was labelled with the quencher dye 6-carboxytetramethylrhodamine. For amplification the primers CMV-FP 5′-TCATCTACGGGGACACGGAC-3′ and CMV-RP 5′-TGCGCACCAGATCCACG-3′ were used. For determination of reference C_T values (cycle threshold), serial dilutions (10^5 to 10^1 copies) of the respective standard cosmid pCM1049 (Fleckenstein et al., 1982), which contains the UL54 gene of HCMV were analysed in parallel. A no-template control (NTC) was included to monitor unspecific amplification or contaminations.
TaqMan® qPCR was performed in a total reaction volume of 50 µl consisting of the components listed in the table XY “qPCR reaction mixture”, in 8 strip PCR tubes. All standard dilutions, controls and DNA samples were run in triplicates. The stripes were loaded into the Applied Biosystems 7500 Real-Time PCR instrument carried out with cycling parameters indicated in tableXY “qPCR cycling parameters”. The results were analysed using the corresponding 7000 System SDS (Sequence Detection Software) software version 1.2.3. The viral genome copy numbers were calculated using the sample specific C_T value, set into relation to the standard serial dilutions.

qPCR reaction mixture

Component	Concentration	Volume
PCR-Buffer (+ 15 mM $MgCl_2$)	10x	5 µL
$MgCl_2$	25 mM	2 µL
dNTP-Mix	2 mM	5 µL
TaqMan-CMV probe	1 µM	5 µL
CMV-FP	3 µM	5 µL
CMV-RP	3 µM	5 µL
HPLC water		17.25 µL
Template DNA		5 µL
Rox	100 µM	0.25 µL
HotStar Taq DNA polymerase	5 units/µl	0.5 µL
		50 µL

qPCR cycling parameters

Step	Temperature	Time	Cycles
Hold	95°C	10 min.	1x
Denaturation	95°C	15 sec.	45x
Annealing/Extension	60°C	60 sec.	

2.2.2.4 Titration of virus supernatant stocks by TaqMan® qPCR

Virus supernatant stocks were titrated based on viral genome copies released from infected HFFs into the supernatant, using TaqMan® qPCR. For this, three freezing tubes of the same virus supernatant stock were thawed. DNA from 200 µL supernatant was extracted using the High Pure Viral Nucleic Acid Kit (Roche) and eluted in 100 µL of elution buffer. 5 µL of the template DNA were subjected to qPCR for viral genome determination (2.2.2.3). Virus titres were indicated in number of genomes per mL supernatant (N x 10^8/mL; N = mean of genome number from three different supernatant tubes).

2.2.2.5 Infection of HFF cells with virus supernatant

HFF cells were seeded one day before infection. For infection, virus supernatant stocks were diluted in 5% MEM medium and applied for 1.5h at 37°C. To remove the virus inocula, cells were washed with PBS twice until fresh medium was added. The cells were cultivated at 37°C and 5%CO_2.

2.2.2.6 Infection of ECs cells with virus supernatant

Prior to experiments, ECs were seeded on 0.1% gelatine coated 10 cm dishes or 6-well plates and maintained in ECG medium in absence of doxycycline. On the day of infection or DB exposure, the medium was completely removed, and the cells were washed three times with solution A. In order to avoid HCMV interference with heparin that is supplemented in ECG medium, the cells were preincubated in 5% MEM medium

without bFGF for at least 30 min. in the common incubator. For infection, the medium was removed and virus inoculum, diluted in 5% MEM medium without bFGF, was applied to the cells for 2h. Virus inoculum was removed and fresh ECG medium without doxycycline was added to the cells. The cells were propagated at 37°C and 5%CO_2.

2.2.3 Infection of HFF cells with virus supernatant for gradient purification of DBs in presence of Letermovir

For gradient purification of DBs, seven days of incubation need to be considered until a complete CPE is achieved. One day prior to infection, HFFs cells were seeded at a density of 1.8 x 10^6 in 20 T-175cm^2 flasks. For infection, 10 mL (0.5 mL/ flask) of RV-Towne-BAC or RV-Towne-repΔGFP virus supernatant and 73,5 mL (3.5 mL/ flask) of 5% MEM were mixed. 4 mL of the virus inoculum was added to the cells and allowed to adsorb for 1.5 h at 37°C. During the incubation, 5% MEM medium supplemented with Letermovir was prepared. Letermovir is a highly specific inhibitor of the HCMV terminase complex and was shown to inhibit HCMV replication in cell culture by interfering with the proper cleavage/packaging of HCMV progeny DNA (Goldner et al., 2011). Subsequently, 336 mL 5% MEM and 2.1 mL Letermovir were mixed and 16 mL of the 5%MEM/ Letermovir medium was added to each flask. The cells were maintained at 37°C and 5% CO_2. Letermovir was added to the medium every three days. Therefore, the supernatants of the infected cells were collected in a fresh T-175cm^2 flask and adjusted with fresh 5%MEM to a volume of 420 mL. 2.1 mL of Letermovir were added and mixed properly. Finally, 20 mL of the medium/ Letermovir mix were added to the cells of each flask again. By 7 d.p.i, when the cells showed a complete CPE, the supernatants from the infected cells were harvested for gradient purification (2.2.4).

2.2.4 Gradient purification of Dense Bodies

For gradient purification of DBs, supernatants from infected HFFs that sowed a complete CPE were harvested and gross cellular debris was removed by centrifugation for 10 min at 1,300×g in 50 mL tubes. Supernatants from 20 flasks were then transferred into Beckman Coulter® 70 mL polycarbonate centrifuge bottles and centrifuged at 100.000×g at 10°C for 70 min in a Type SW32Ti rotor to pellet virions and DBs. During the last 15 minutes of centrifugation, two glycerol/tartrate gradients were pre-formed in a Beckman Coulter® Ultra-clear™ centrifuge tube. Therefore, a two-chambered gradient mixer was used. 5mL of 15% sodium tartrate were filled in the feeder chamber and 4 mL of 35% sodium tartrate were filled in the mixing chamber. After centrifugation, the pellets were resuspended in a total of 2 mL PBS.1 mL sample was

layered onto one gradient. The gradient was centrifuged for 90 min at 99,000×g and 10°C in a SW41Ti swing out rotor. Under these conditions, virions and DBs sediment to form two distinct, well separated, light scattering bands. When the gradient was illuminated from above, the upper band contained NIEPs while the diffuse lower band contained DBs. The DB-containing fraction was isolated with a syringe and transferred into a 50 mL tube. The DBs were washed in 20 mL PBS and pelleted by an additional ultracentrifugation for 90 min at 90,000×g in the same SW41 Ti rotor. After PBS was removed, the pellet was resuspended in 200-250 µL PBS. 30 µL aliquots were stored at -80°C.

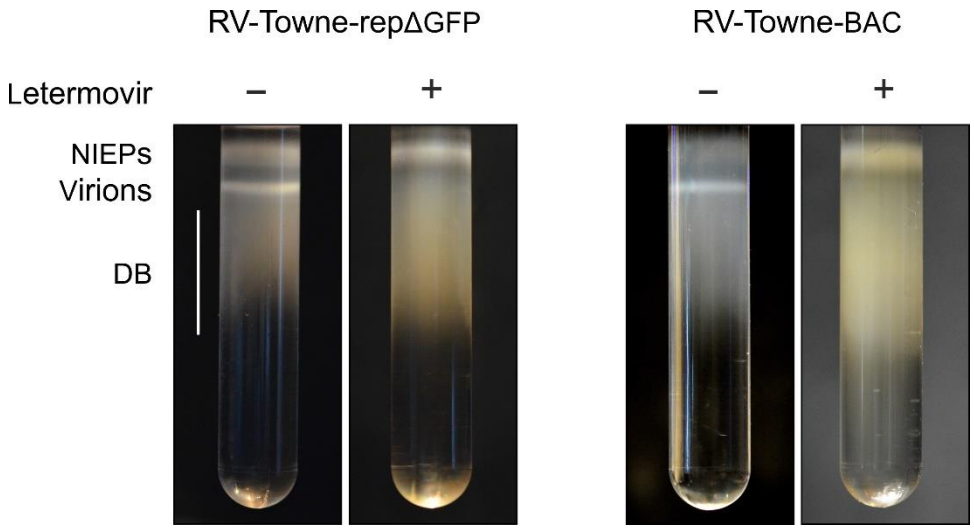

Fig. 3. Gradient purification of viral particles of RV-Towne-repΔGFP and RV-Towne-BAC. Infected HFFs exposed to Letermovir (+) released NIEPs and DBs, but no virions. NIEP, Noninfectious enveloped particle; DB, Dense Bodie.

2.2.5 Determination of protein concentration

The protein concentration of the purified DBs and virions was determined with the Pierce BCA Protein Assay Kit according to the manufacturers protocol.

2.2.6 UV- inactivation of DBs

Purified DBs were irradiated with ultra-violet (UV) light at a wavelength of 254 nm before they were applied to cells. Depending on the experiment, the appropriate amount of DBs was thawed and dispersed in PBS. For UV-irradiation a spot plate was used. To compensate the

volume loss on the surface of the cavity-like depressions of the spot plate, the amount of DBs and PBS was increased as indicated in the table “Amount of DBs used for UV-inactivation”. DBs were dispersed in PBS in a total volume of 120 µL PBS and transferred onto a spot plate. Following irradiation with UV-light for two minutes at a wavelength of 254 nm, 100 µL of the UV-irradiated DBs/PBS solution were mixed with culture medium and added to the cells (2.2.7).

Amount of DBs used for UV-inactivation

Cultivation vessel	**Well of a 6- well plate**			**10 cm dish**		
Cell type	HFF		ECs	HFF		ECs
DBs amount for UV-inactivation in 120 µL PBS	6 µg	12 µg	18 µg	12 µg	24 µg	48 µg
Final DBs amount in 100 µL PBS	5 µg	10 µg	15 µg	10 µg	20 µg	40 µg

2.2.7 Exposure of HFFs and ECS cells to DBs

For the penetration of DBs into HFFs, seeded on a 10 cm dish, 24 µg of DBs were diluted in 120 µL PBS and subjected for UV- irradiation (2.2.6). In a fresh tube, 1900 µL of 5% MEM were prepared and 100 µL of UV-irradiated DBs were transferred into the tube and mixed. A total volume of 2 mL was added to $0.5x10^6$ HFFs and incubated for 2h at 37°C for adsorption. Afterwards 8 mL of 5% MEM were added and the cells were further incubated at 37°C.

For the penetration of HEC-LLT cells, $0.6x10^6$ cells were seeded in absence of doxycycline on 0.1% gelatine coated 10 cm dishes one day before the addition of DBs. On the day of DBs exposure, the medium was completely removed, and the cells were washed two times with solution A to remove heparin and other ECGM supplements. Afterwards, the cells were preincubated with 5 mL 5% MEM without bFGF for 30 minutes in the common incubator.
During this time, 48 µg of DBs in 120 µL solution a were UV-irradiated (2.2.6). 100 µL were mixed with 2.9 mL 5% MEM bFGF-free. For DB-adsorption, the medium was removed, and 3 mL of the DBs-inoculum was applied to the cells for 2 h. Thereafter, fresh ECGM medium without doxycycline was added to the cells. The cells were incubated at 37°C and 5% CO_2.

2.2.8 Growth kinetics

For growth kinetics, an equivalent number of viral genomes per cell was prerequisite. Based on virus titres determined by qPCR, HFFs were initially infected with 25 viral genomes per cell

of RV-KB14 or RV-Towne-repΔGFP respectively. In some experiments, HFFs were preincubated with 10 µg of UV-irradiated DBs for two hours or applied to HFFs together with virus inocula. For analysis of intracellular genomes, viral DNA was isolated from 10^5 infected cells at different time points. To determine the number of genomes released into the supernatant, DNA from 200 µL of the supernatants collected at the same time points was isolated using the High Pure Viral Nucleic Acid Kit.

2.2.9 Infectivity assay via IE1 staining

The amount of infectious virus present in supernatants obtained from HCMV growth kinetics was determined by staining for HCMV IE1 protein. Infectivity assays were performed in 96-well microtiter plates. The day before infection, 5x 10^3 HFFs/well were seeded in 50 µL of 5% MEM and incubated at 37°C and 5% CO_2. For infection, virus supernatants were 10-fold serially diluted in 5% MEM from 10^{-1} to 10^{-4} to obtain eight replicates per dilution. Undiluted virus and uninfected cells were carried along as controls. 100 µL of the diluted or undiluted virus supernatants were subjected to the cells. Then, the microtiter plates with the inoculated HFFs were stored in a common incubator for 48 h. Afterwards, the medium was removed, the cells were washed with 200 µL PBS and fixed with 100 µL ethanol for 20 minutes at room temperature. After fixation the cells were washed with PBS again and probed with 50 µL of the primary IE1 (p63-27) mouse monoclonal hybridoma antibody against the HCMV immediate-early (IE1) protein. The microtiter plates were placed in a humidified chamber and incubated for an hour at 37°C. Thereafter, the primary antibody was removed, and the cells were washed twice with 200 µL PBS. 50 µl of a horseradish peroxidase (HRP)-conjugated rabbit anti-mouse IgG (Dako) secondary antibody was added (dilution 1:500 in PBS) and the plates were incubated for another hour under same conditions. During incubation fresh AEC-staining 3-amino-9-ethylcarbazole, Sigma-Aldrich) solution was prepared. Therefore, an AEC-Stock (4 mg/ mL dimethylformamide (DMF, Sigma-Aldrich)) was diluted 1:20 in acetate buffer and filtered. Afterwards, H_2O_2 (30%) was added to achieve a 1:1000 dilution. After incubation, the secondary antibody was removed, and the cells were washed twice with PBS. Subsequently, the cells were probed with 100 µL of the AEC-staining solution and incubated for another hour at 37°C. Finally, supernatant was discarded, and the cells were first washed and then covered with PBS. The samples were stored at 4°C in the dark. Microscopy was performed with a Leitz DM IRB/SL microscope (Leica). The mean of IE1-positive cells counted in six (undiluted samples) to eight (diluted samples) technical replicates from two independent experiments was taken as the relative measure of infectivity.

2.2.10 Immunofluorescence analysis of the inhibition of dynamin- dependent endocytosis using Dynasore

For immunofluorescence analysis, HFFs were grown on coverslips at a density of 0.3 x 10^6 cells/well in 6-well plates and cultured in complete 5% MEM medium for 24h at 37°C and 5% CO_2. Before ECs cells were seeded, the 6-well plates, including the coverslips were coated with 0.1% gelatine for 30 min. After the residual gelatine was removed, 0.3 x 10^6 ECs/well were seeded and maintained in ECG medium without doxycycline (Dox) for 24 h. One day after seeding, ECG medium was removed, and the cells were washed twice with Solution A. Prior to DB-application, ECs were pre-incubated in HFF 5% MEM medium without bFGF for 30 minutes.

For Dynasore inhibition experiments, the cells were pre-treated with 80 µM Dynasore in 5% MEM (HFFs) or 5% MEM without bFGF (ECs) for 30 minutes at 37°C. Dynasore was added during the whole DB-incubation process. 10 µg UV-irradiated DBs of the HCMV strain RV-Towne BAC and 10 µg (HFFs) and 15 µg (ECs) UV-irradiated DBs of the strain RV-Towne-repΔGFP were applied to the cells as described in 2.2.7. As a control for clathrin- mediated endocytosis (CME), HFFs and ECs were incubated with 35 µg/mLof human transferrin conjugated to AlexaFluor546. Labelled cells were washed with PBS, fixed in 90 % acetone, and processed for immunofluorescence. For fixation 1 mL of 90% acetone was prepared in 24-well plates. At 6, 8 or 24 h.p.a, the coverslips were briefly rinsed in PBS, transferred into the 1 mL 90% acetone and incubated at 4°C over night. Following fixation, the coverslips were transferred into fresh 24-well plates and washed three times with 0.1% Triton-X-100/ PBS. Afterwards the cells were probed with 200 µL of a primary antibody diluted in PBS directed against cellular or viral proteins. The plates were placed in a humidified chamber and incubated for an hour at 37°C. The cells were washed three times with 0.1 % Triton-X-100/PBS again and subsequently incubated with 200 µL of AlexaFluor-conjugated specific secondary antibodies for another hour at the same conditions. For counterstaining of cell nuclei 150 µL of a DAPI 1:5000 dilution in PBS was added to the cells. The samples were incubated for further 10 minutes in the dark at room temperature. Finally, the coverslips were washed three times with 0.1% Triton-X-100/PBS and once with ddH_2O and mounted onto slides using ROTI®Mount FluorCare mounting medium (Carl Roth GmbH + Co. KG). Images were acquired by the Axiophot (Zeiss) fluorescence microscope equipped with a SPOT Flex camera FX1520. For each time point 25-30 random pictures were taken.

2.2.11 Cell lysates

For immunoblotting, cells were lysed in 2x Laemmli buffer and heated to 99°C for 10 minutes. After 1 minute centrifugation at 11000 rpm the samples were stored at -20°C until further use. To enable a comparative load of protein amounts among the samples in an experiment, the cell number in 10 µL of 2x Laemmli buffer was defined as 1x 10^5. Briefly, cell monolayers were washed, harvested and the cells were counted as described in 2.2.1.2 and lysed in the appropriate amount of 2x Laemmli buffer.

2.2.12 Sodium dodecyl sulfate polyacrylamide gel electrophoresis (SDS-PAGE) and immunoblot analysis

For immunoblot analysis, 20 µL of total cell lysates from infected or DBs-treated cells (2.2.11) were heated for 10 min at 99°C and loaded on 10% Bolt Bis-Tris gels for protein separation. Before the transfer, the membranes and gels were incubated in transfer buffer for 5 minutes. The proteins were transferred to PVDF-membranes using a Mini Blot module at 20 V for 1h. Afterwards, the membranes were blocked in non-fat dry milk-blocking buffer for 1 h. The incubations with primary antibodies were performed overnight at 4°C on a roller mixer. Membranes were washed three times for 10 min with 0.1% TBST and then incubated with AlexaFluor secondary antibodies in 0.1% TBST for 2h protected from the light at RT. After another three washes with 0.1% TBST for 10 min, specific bands were detected by an Odyssey Infrared Scanner.

2.2.13 FACS analysis

Flow cytometry analysis was used to monitor apoptotic, necrotis and healthy cells after infection and DBs application using the Apoptosis/Necrosis Detection Kit (abcam). HFFs were seeded in 10 cm dishes at a density of 0.5x10^6 one day before infection and DB-application. Prior to infection, the cells of two dishes were primed with 20 µg of UV-irradiated DBs/dish of the HCMV strain RV-Towne-repΔGFP for two hours as described in 2.2.7. Following incubation, virus supernatant, normalized for an uptake of 50 viral genomes per cell was added and incubated for another two hours. In parallel, two dishes were inoculated with 50 genomes/cells of virus supernatant, two dishes with 50 genomes/cell virus supernatant and 20 µg of UV-irradiated DBs and the cells of two dishes were exposed to 20 µg of UV-irradiated DBs only. The inocula were allowed to adsorb for two hours at 37°C and 5% CO_2. Afterwards, the volume/dish was adjusted to 10 mL with 5% MEM medium and the cells were incubated

for further four hours. After a total incubation period of six hours, the inoculum was removed, and the cells were washed twice with PBS. Finally, the cells were maintained in new 5% MEM medium for six days. At the day of the flow cytometry assay, untreated and treated cells were collected on ice. Before the staining solution, comprising 200 µL of Assay Buffer, 2µL of Apopxin Green Indicator (100x) and 1µL of 7-AAD (200x) per sample was applied to the cells, a master mix was prepared to enable the same amount of the dye in each sample. One half of the cells was stained using the respective primary antibody while the rest was mock stained with FACS buffer which was included in the kit, to detect secondary antibody background staining. Cells were resuspended in 204 µL staining solution and staining was performed for 40 minutes at room temperature protected from light. To increase the volume before flow cytometer analysis, 300 µL of Assay Buffer were added to each sample. The fluorescence intensity was measured with a FACS Cytomics FC 500 (Becton Dickinson) flow cytometer. For the quantification of Apopxin Green Indicator binding, the FL1 channel (Ex/Em= 490/525 nm) was used. 7-AAD was measure by using the FL3 channel (Ex/Em=546/647). The Data were analysed using the corresponding BD CXP analysis software.

2.2.14 Mass spectrometry-based proteomics

2.2.14.1 Sample preparation

HFFs and ECs

For mass spectrometry analysis $0.5x10^6$ HFFs or $0.6x10^6$ ECs were seeded in two 10 cm dishes 1 day prior to DB-exposure. 10 µg (HFFs) or 40 µg (ECs) of UV-irradiated DBs were applied to the cells as described in 2.2.6 and 2.2.7. After 24 h incubation in a common incubator, $1x10^6$ cells were lysed in 20 µL 2x Laemmli buffer without bromophenol blue staining and heated at 99°C for 10 min. The samples were stored at -20°C until they were passed to the proteomics core facility (AG Butter, Proteomics Core Facility, IMB Mainz) for MS measurement. Therefore, the samples were thawed and mixed with 1x NuPAGE LDS Sample Buffer (Life technologies) and 100 mM DTT. Finally, the samples were incubated at 70°C for 10 min and subjected to AG Butter.

Monocytes and iDCs

The experiments on monocytes and iDCs were performed in collaboration with Marina Kreutz (Regensburg). Monocytes and iDCs were cultured in 6-well plates. $1x\ 10^6$ monocytes were incubated in 1 mL RPMI without human sera for 30 min. Afterwards, RPMI was removed and

the cells were exposed to 20 µg/100 µl PBS of UV inactivated DBs. As control, monocytes were incubated with PBS or lipopolysaccharide (LPS). After 2h, 880 µL RPMI+ 20 µL AB serum were added to the cells. Following 6h or 24h incubation, the supernatant was collected, centrifuged and stored at -20°C for further use. Monocytes were scraped off and washed in 500 mL PBS. After centrifugation PBS was removed and the cell pellet was stored at -80°C until they were send to us. Monocytes and iDCs were prepared in the same way as HFFs and ECs.

The following steps were performed by the group from Falk Butter from the proteomics core facility.

2.2.14.2 Mass spectrometry and data analysis

The proteins were run on the 10% SDS PAGE for 10 minutes at 180V to allow the proteins to move into the resolving gel and then proteins were fixated in the gel for 15 min in a 7% acetic acid/40% methanol solution and subsequently stained for 15 min with a solution of 0.25% Coomassie Blue G-250 (Biozym), 7% acetic acid and 45% ethanol. The SDS PAGE gels were washed several times with deionized water on the shaker to remove excess dye. The In-gel digestion was performed in principle as described previously [86] and detailed as follows. Each gel lane was cut separately using the new sharp scalpel and then minced and transferred to an Eppendorf tube. Gel pieces were destained (50% ethanol in 25 mM NH_4HCO_3) for 15 min to remove the Coomassie dye. The supernatant was removed, and the gel pieces were dehydrated by adding 100% acetonitrile for 10 minutes on the rotator. The acetonitrile was dispensed off by pipetting and the samples were dried to completion using a vacuum evaporator (Eppendorf). The dried samples were rehydrated and disulfide bonds in the proteins were reduced using reduction buffer (10 mM DTT in 50 mM NH_4HCO_3 pH 8.0) for 1 h at 56°C. Buffer was removed by pipetting and cysteine residues of proteins were subsequently alkylated with 50 mM iodoacetamide in 50mM NH_4HCO_3 pH 8.0 for 45 minutes at room temperature in the dark. Samples were dehydrated again by adding100% acetonitrile and dried by vacuum evaporation. The vacuum dried gel slices were incubated with 1 µg trypsin per tube in 50 mM triethylammonium bicarbonate buffer pH 8.0 at 37°C overnight. Digested peptides were extracted twice by adding 150 µL of 30% acetonitrile and the supernatant containing the digested peptides were transferred to the new Eppendorf tube. Second time, the peptide extraction was done by adding 150 µL of 100% acetonitrile to the gel pieces for 15 min at 25°C agitating at 1400 rpm in a Thermo shaker (Eppendorf) and the supernatant was transferred to the previous Eppendorf tube. The reductive demethylation step was performed as described previously [87]. Each sample pair including a replicate were switched with the dimethyl labels. Equal amounts of peptides from all labelled samples were

mixed and the purification and desalting of the peptides was done using the C18 stage-tips (M3 company) as previously described [88]. The eluted peptides were loaded on the silica column of 75 µm inner diameter (New Objective, FS360-75-8-N-5-C30) packed to 25cm length with 1.9µm C18 Reprosil beads (Dr. Maisch GmbH) using the EasyLC1000 liquid chromatography (Thermo).

Mass spectrometry and data analysis:

Peptides were separated on the C18 column using an EasyLC1000 HPLC (Thermo) with the following 4 hour reversed-phase chromatography gradient: 0-4 min, 2-5% solvent B; 4-157 min, 5-22% solvent B; 157-208 min, 22-40% solvent B; 208-212 min, 40-95% solvent B; 212-217 min, 95% solvent B; 217-221 min, 95-2% solvent B; and 221-225 min, 2% solvent B (solvent A: 0.1% formic acid, solvent B: 80% acetonitrile containing 0.1% formic acid) and directly sprayed into a Q-Exactive Plus mass spectrometer (Thermo Scientific) for the data acquision. The mass spectrometer was operated in the positive ion scan mode with a full scan resolution of 70,000; AGC target $3x10^6$; max. IT = 20ms; Scan range 300 - 1650 m/z with a top10 MS/MS DDA method. Normalized collision energy was set to 25 and MS/MS scan mode operated at a resolution of 17,000; AGC target $1x10^5$ and max IT of 120 ms.

MaxQuant Settings:

For database search, MaxQuant (V 1.5.2.8 and V 1.6.10.43 (Cox, J. and Mann, M. MaxQuant enables high peptide identification rates, individualized p.p.b.-range mass accuracies and proteome-wide protein quantification. Nat Biotechnol, 2008, 26, pp 1367-72.) was used with default settings. Trypsin/P was set as digestion mode allowing for 2 missed cleavages. Further settings were, variable modification: Acetyl (Protein N-term); Oxidation (M), fixed modifications: Carbamidomethyl (C), FDR of 1% on peptide and protein level was applied. Re-quantify was activated, quantification was based on razor and unique peptides. For labelling we used a Dimethyl label coupled to the Lysine residues and N-terminal ends of each peptide. Depending on the experimental design of the experiment, we used a double or triple labelling procedure, where always a standard Dimethyl group was used to label the light sample. And a modified Dimethyl with a mass shift of 4 Dalton was used to label Heavy sample in double labelling and as Medium label in triple label experiments. The heavy label in the triple labelling condition had a mass shift of 8 Dalton.

Database:

The search was performed against the protein databases in fasta format from the Uniprot website. The database where updated once a year and we combined all available sequences from Homo sapiens, Human Cytomegalovirus as well as the Towne strain from Human Cytomegalovirus.

Filtering MaxQuant results:

The results produced by MaxQuant where further processed to remove known contaminants (as provided within MaxQuant), reverse database binders (decoy) and protein groups only identified by site modifications. A second filtering step is removing all protein groups with less than 2 razor peptides (1 unique). Due to high similarity between our bait protein and other tegument proteins, the algorithm from MaxQuant accounts the razor peptides to the protein group with the most matching peptide IDs. In this case, we included our bait manually, although the overall ratio for the bait protein might not be accurate, due to missing razor peptide quantification and only based on a single unique peptide.

The quantification ratios of the dimethyl labels were log2 transformed and plotted forward against reverse experiment (label switch).

2.2.15 Statistical analysis

All statistics and calculations were conducted with Prism 8.0 software (Version 8.3.0, GraphPad, CA). The statistical significance between two groups was determined by unpaired student's two-tailed t-test. All significance tests were denoted as: n.s. means $p>0.05$; * means $0.01 < p < 0.05$; ** means $0.001 < p < 0.01$; *** means $p < 0.001$.

3 Results

Dense Bodies are a unique product of cytomegalovirus infected cells [89]. Isolation of these particles from cell culture supernatants allowed the biochemical characterization of their protein content [90-93]. Mass spectrometry provided a more detailed picture of the composition of DBs [94, 95]. These analyses demonstrated that important antigens of the adaptive immune response against HCMV were contained in DBs. Several publications have meanwhile demonstrated the immunologic potential of DBs both in-vitro and in laboratory animals [55, 67, 96-99]. Consequently, DBs have been identified as a promising vaccine candidate [55, 100-102]. However, very little information has been available about the impact of DBs on the host cell. From a vaccine perspective, knowledge about potential adverse effects of DBs, interacting with and intruding into cells is essential for projecting the tolerability of a future vaccine. With respect to HCMV infection, understanding the impact of DBs on the host cell is highly interesting, as these particles, which are concomitantly produced with infectious virions, may provide an either pro- or antiviral environment.

The following major questions were asked in this work:

1. What are the changes in the cellular proteome dependent on DBs with a focus on the innate defence mechanisms of the cell?
2. Are there cell-specific differences in the proteome after DB-application?
3. What is the impact of DBs on HCMV replication?
4. Is there an impact of DBs on crucial intracellular process like apoptosis or autophagy?

The aim of this study was to provide a comprehensive picture of the response of the cell to DBs in order to understand the role of these particles in HCMV infection and to assess their suitability as a vaccine.

3.1 Effects of HCMV- DBs on the proteome of different cell types

MS- based proteomic approaches provide powerful tools to characterize interactions between viruses and their hosts. The results of MS- analyses significantly contributed to our

understanding of HCMV biology [103]. Furthermore, proteomic analyses helped to determine the composition of virions and DBs [37, 38, 50, 104].

There are several studies that analysed the changes in the cellular proteome of different cell types upon HCMV infection [77, 103, 105, 106]. No data are, however, available that addressed the changes in the cellular proteome following DBs-application.

3.1.1 Impact of DBs on the cellular proteome of HFFs

3.1.1.1 Initial proteomic analysis of HFFs reveals the establishment of an antiviral cellular environment following DB-exposure

To analyse the impact of DBs on the cellular proteome of HFFs, an initial experiment was performed. HFFs were exposed to 10 µg of UV- inactivated, PC-positive DBs of the HCMV strain RV-Towne-rep∆GFP or were left untreated. The cells were collected at 24 hours post application (h.p.a) and processed for MS as describe in 2.2.14. The samples were measured with standard settings of 120 minutes on a Q Exactive Plus mass spectrometer (Thermo Fisher Scientific, Waltham, USA). MS analyses were performed in collaboration with the group of Falk Butter, head of the quantitative proteomics core facility at the Institute for Molecular Biology (IMB) in Mainz. MS data were processed as described in 2.2.14. A total of 990 proteins were identified in this experiment. The heatmap in Figure 4a was generated by filtering and hierarchically arranging proteins based on their log2 transformed ratios. 42 proteins exhibited log2Ratios of at least ± 0.58 (corresponding to a 1.5-fold-change) in one of the technical replicates. These proteins were considered as differentially regulated (Fig.4.a). The log2Ratio is represented by a colour gradient. The colour intensity indicates the degree of protein up- or downregulation. Black areas represent values that did not reach the threshold of ±0.58. At 24 h.p.a, 26 of these proteins were found to be upregulated and 16 proteins were found to be downregulated in the HFFs, treated with DBs (Fig.4a). Among these, 35 were known to be IFN responsive proteins according to the INTERFEROME database (http://www.interferome.org) of IFN Regulated Genes (Supplementary Table 1, S1). To get an idea of functional associations between the IRGs, a predicted protein-protein interaction (PPI) analysis was performed using the STRING (Search Tool for the Retrieval of Interacting Genes) database (http://string-DBs.org). The STRING PPI network analysis, shown in Fig. 4c revealed an enrichment in three clusters related to functional categories of antiviral defence, collagen organization and endocytosis. To examine the biological processes in which all the differentially regulated proteins were involved, gene ontology (GO)- analysis based on the UniProtKB database was performed (S2). As shown in the bar chart in Fig.4b, the categories

of antiviral defence, protein transport, cytoskeleton organization and endocytosis were enriched the most. However, in term of antiviral defence, the IRGs Interferon- induced guanylate-binding protein 1 (GBP1), Interferon-induced protein with tetratricopeptide repeats 3 (IFIT3), Ubiquitin-like protein ISG15 (ISG15), Interferon- induced GTP-binding protein MX1 (MX1), Protein kinase RNA-activated (PKR) and Signal transducer and activator of transcription 1-alpha/beta (STAT1) were all upregulated in DBs-treated HFFs (Fig.4a, c, d). Beside cytoskeletal proteins, endocytosis associated proteins were regulated in the DBs-treaded HFF- proteome (Fig. 4a, c, f). The collagen organizing proteins COL1A1, COL1A2 and COL5A1, that are also involved in cell motility were found to be downregulated in HFFs exposed to DBs (Fig.4a, c, e). The results indicated that DBs contribute to a remarkable upregulation of IRGs in HFFs. An antiviral function has been described for many of these IRGs.

(a)

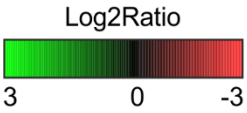

Replicate		Gene	Protein name
R1	R2		
3.04	1.45	MX1	Interferon-induced GTP-binding protein MXA
2.79	2.38	ISG15	Ubiquitin-like protein ISG15
2.78		IFIT3	Interferon-induced protein with tetratricopeptide repeats 3
	2.22	NUP93	Nuclear pore complex protein Nup93
1.68		EHD4	EH domain-containing protein 4
1.53		DPP7	Dipeptidyl peptidase 2
	1.43	REEP5	Receptor expression-enhancing protein 5
1.40	1.31	STAT1	Signal transducer and activator of transcription 1-alpha/beta
	1.17	ARPC1A	Actin-related protein 2/3 complex subunit 1A
	1.17	RPL23	60S ribosomal protein L23
1.06	0.80	H2BC13	Histone H2B type 1-L
	0.97	CNP	2,3-cyclic-nucleotide 3-phosphodiesterase
	0.87	NCKAP1	Nck-associated protein 1
	0.87	NAP1L4	Nucleosome assembly protein 1-like 4
0.86		SNX6	Sorting nexin-6, N-terminally processed
	0.85	PKR	Protein Kinase RNA-activated
0.76		NAPA	Alpha-soluble NSF attachment protein
0.72		DNAJA1	DnaJ homolog subfamily A member 1
	0.67	H3C15	Histone H3.2
0.66		ERH	Enhancer of rudimentary homolog
0.66		B2M	Beta-2-microglobulin
	0.65	CAPG	Macrophage-capping protein
0.62		STOML2	Stomatin-like protein 2, mitochondrial
	0.59	NAGK	N-acetyl-D-glucosamine kinase
0.60		GBP1	Interferon-induced guanylate-binding protein 1
0.58		NUDT5	ADP-sugar pyrophosphatase
-0.59		PTMA	Prothymosin alpha
-0.60		RPS10	40S ribosomal protein S10
-0.60		EHD2	EH domain-containing protein 2
-0.64		COL5A1	Collagen alpha-1(V) chain
-0.79	-0.64	COL1A2	Collagen alpha-2(I) chain
-0.65		COX7A2	Cytochrome c oxidase subunit 7A2, mitochondrial
	-0.66	KANK2	KN motif and ankyrin repeat domain-containing protein 2
-0.71		NUCB1	Nucleobindin-1
-0.71		EIF4H	Eukaryotic translation initiation factor 4H
-0.80		MYOF	Myoferlin
	-0.83	DYNLL2	Dynein light chain 2, cytoplasmic
-0.89		FHL2	Four and a half LIM domains protein 2
	-1.06	RAB3B	Ras-related protein Rab-3B
	-1.17	MANF	Mesencephalic astrocyte-derived neurotrophic factor
-1.14	-1.18	COL1A1	Collagen alpha-1(I) chain
	-2.44	KRT6B	Keratin, type II cytoskeletal 6B

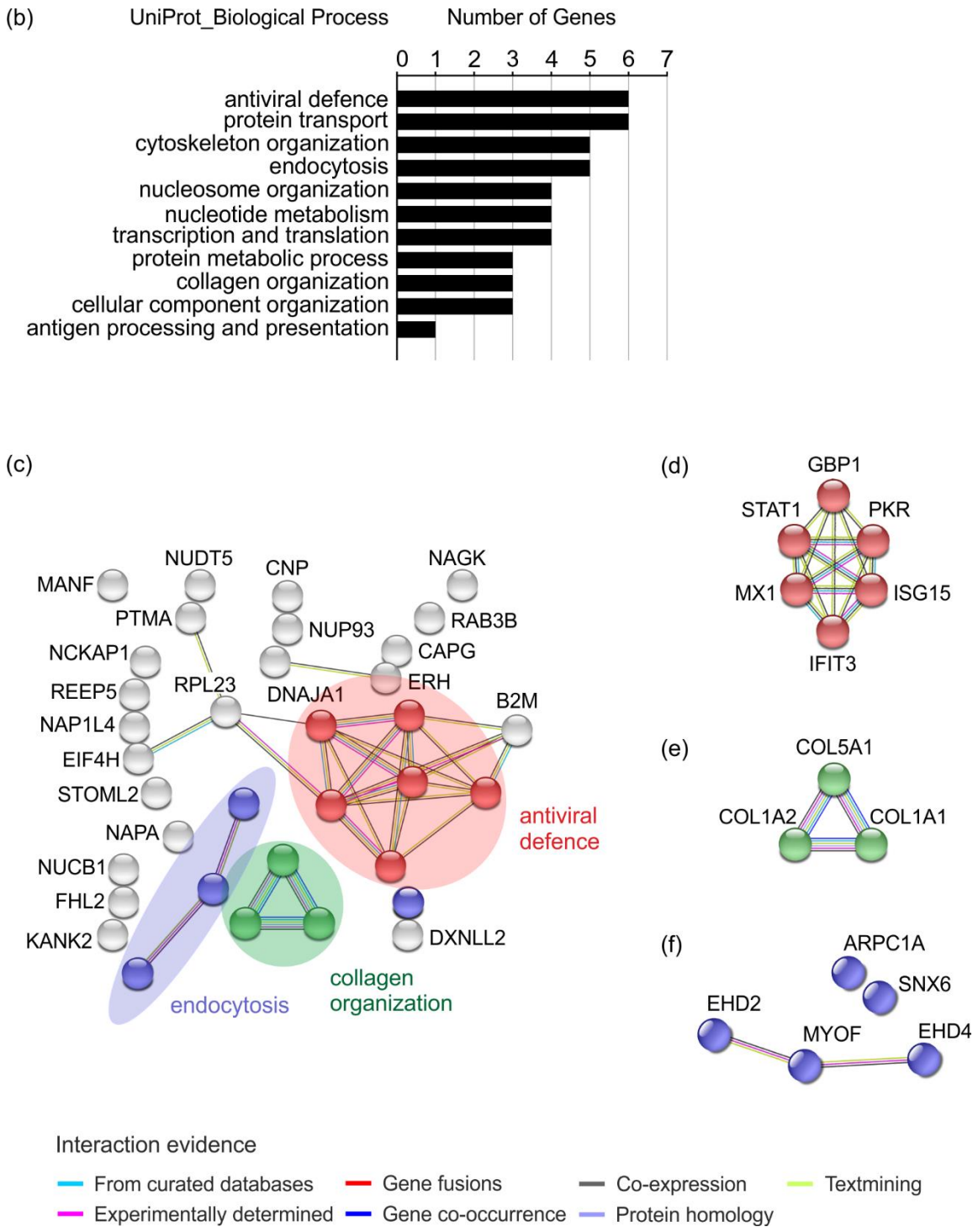

Fig. 4. DBs induce an upregulation of interferon regulated genes (IRGs) involved in antiviral defence. Proteomic analysis of HFFs exposed to PC-positive DBs (HCMV strain RV-Towne-repΔGFP, DB-PC+) and control cells at 24 h.p.i..The samples were measured at a standard setting of 120 min on a Q Exactive Plus mass spectrometer (Thermo Fisher Scientific, Waltham, USA) **(a)** Heatmap of 42 proteins differentially regulated in HFFs, exposed to 10 µg of DBs-PC+ and compared to untreated cells. The expression patterns of the proteins were arranged hierarchically based on the

log2 converted normalized ratio of two technical repilcates (R1; R2). The log2Ratio is represented with a colour gradient. 26 up-regulated (green) and 16 down-regulated (red) proteins with a fold-change of at least 1.5 (log2ratio ± 0.58) in one of the technical replicates were considered as differentially regulated. Black areas represent values that did not reach the threshold of ±0.58. **(b)** Bar chart of identified proteins grouped into biological processes based on Gene Ontology (GO) analysis using the UniProtKB database.The y-axis represents biological process categories, while the x-axis indicates the number of genes involved in each category. **(c)** Protein-protein interaction (PPI) network generated with the online STRING database showing only proteins that are regulated by interferons (IFNs) according to the INTERFEROME database of IFN regulated genes (IRGs). The clusters of antiviral defence (red), endocytosis (purple) and collagen organization (green) are highlighted. The proteins in these clusters were entered into the STRING database to obtain the subnetworks depicted in **(d-e)**. The Protein Actin-related protein 2/3 complex subunit 1A (ARPC1A) is not known to be IFN-stimulated and is therefore excluded in c. Each protein is represented as a node. Different line colours represent the types of evidence for the association between the proteins according to the STRING network database. The networks were generated with a minimum required interaction score of a medium confidence of 0.4. PC, Pentameric Complex; STRING, Search Tool for the Retrieval of Interacting Genes; UniProtKB, Universal Protein Resource Knowledgebase

3.1.1.2 Confirmation of MS analysis shows an upregulation of IRGs with known antiviral activity in response to DBs-application

The following two experiments were performed to confirm and expand the results of the initial MS analysis shown in 3.1.1.1. This time, the measurement time per sample was extended to 240 minutes. Sample preparation was performed as in 3.1.1.1. A total of 1446 proteins were identified. The heatmap in Fig.5a was generated from these two independent experiments and shows 92 differentially regulated proteins, hierarchically arranged based on their log2 transformed ratios. Proteins that exhibited a fold-change of at least 1.5 (log2Ratio ± 0.58) in one of the technical replicates in both experiments, were considered as differentially regulated (Fig.5a). The largest group of regulated proteins comprised 81 IRGs. At 24 h.p.a, 63 of them were upregulated and 18 were downregulated in HFFs after DBs-application. Eleven of the proteins are not regulated by IFNs (S3). One of them was the viral tegument protein pp65 of which detection was assessed as a criteria of successful DBs entry into HFFs. GO- analysis based on the UniProtKB database was again performed (Fig. 5b). Upregulated proteins involved in biological processes of antiviral defence, antigen processing and presentation, cell cycle and transcription and translation were found to be enriched (Fig.5.a, b, S4). Proteins involved in the ubiquitin conjugation pathway, apoptosis and ER Golgi transport were predominantly upregulated (Fig. 5a, b, S4). Proteins involved in biological processes like cell motility, cell adhesion, cell growth and cell migration as well as lipid metabolism were mostly

downregulated (Fig. 5a, b, S4). To get an idea of functional associations between the proteins, the 92 differentially regulated proteins were subjected to the STRING database. The PPI network analysis revealed four clusters of subnetworks in antiviral defence (red), cell motility (yellow), ubiquitin conjugation pathway (blue) and antigen processing and presentation (purple) (Fig. 5c). Proteins associated with apoptosis (green) were found to be distributed throughout the PPI network. (Fig.5 c). The subnetworks with the proteins related to the biological process are depicted seperately in Fig.5 d-h.

Both MS results indicated, that HFFs activated the antiviral immune response following DBs application. These data supported the hypothesis that DBs induce an antiviral environment in HFFs.

(a)

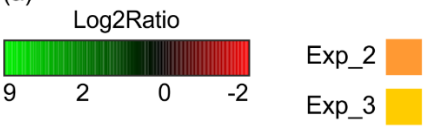

Replicate

R1	R2	R1	R2	Gene	Protein name
3.90	2.65	9.04	4.54	MX1	Interferon-induced GTP-binding protein MX1
1.00	1.83	6.98	2.74	MX2	Interferon-induced GTP-binding protein MX2
2.60	1.53	5.66	3.72	IFIT1	Interferon-induced protein with tetratricopeptide repeats 1
5.60		2.26	3.94	IFIH1	Interferon-induced helicase C domain-containing protein 1
1.37	1.03	5.47	3.14	OAS3	2-5-oligoadenylate synthase 3
1.45	1.02	5.36	1.60	STAT2	Signal transducer and activator of transcription 2
3.31	3.69	4.57	4.43	ISG15	Ubiquitin-like protein ISG15
	1.53	4.55	2.78	USP18	Ubl carboxyl-terminal hydrolase 18
4.08	1.70	2.71	1.50	pp65	65 kDa phosphoprotein
2.25	2.70	3.78	3.98	IFIT3	Interferon-induced protein with tetratricopeptide repeats 3
2.38	0.72	2.99	3.78	IFIT2	Interferon-induced protein with tetratricopeptide repeats 2
3.51		1.52		GSTT1	Glutathione S-transferase theta-1
1.00	1.03	3.12	2.76	DDX58	Antiviral innate immune response receptor-I
1.90	1.33	2.91	2.29	SAMHD1	Deoxynucleoside triphosphate triphosphohydrolase SAMHD1
2.85	1.24	2.23	2.10	PARP14	Poly [ADP-ribose] polymerase 14
2.68		0.70	0.84	TTC38	Tetratricopeptide repeat protein 38
1.28	0.93	2.63	2.25	UBE2L6	Ubiquitin/ISG15-conjugating enzyme E2 L6
2.49		1.49	1.90	IFITM1;2;3	Interferon-induced transmembrane protein 1;2;3
0.73		2.40	0.86	CIP2A	Protein CIP2A
1.69	1.91	2.33	2.38	STAT1	Signal transducer and activator of transcription 1-alpha/beta
1.53	0.96	1.51	2.32	DTX3L	E3 ubiquitin-protein ligase DTX3L
	0.59	2.29	1.33	TAPBP	Tapasin
	0.58	2.23	1.34	TRIM21	E3 ubiquitin-protein ligase TRIM21
1.01	0.67	2.01	1.94	TAP1	Antigen peptide transporter 1
1.56	0.98	1.99	1.46	PNPT1	Polyribonucleotide nucleotidyltransferase 1, mitochondrial
1.21	0.63	1.97	1.75	RNF213	E3 ubiquitin-protein ligase RNF213
1.16			1.91	PLSCR1	Phospholipid scramblase 1
1.09		1.22	1.88	PARP9	Poly [ADP-ribose] polymerase 9
1.49	1.89	1.48	1.82	TOP2A	DNA topoisomerase 2-alpha
0.84		1.79	1.76	CMPK2	UMP-CMP kinase 2, mitochondrial
1.77	0.90	1.43	1.53	TRIM22	E3 ubiquitin-protein ligase TRIM22
0.93		1.72	1.32	PML	Protein PML
1.15	1.28	1.70	1.56	LAP3	Cytosol aminopeptidase
1.63	1.27	1.53	1.68	GBP1	Guanylate-binding protein 1
0.83	0.94	1.05	1.67	PKR	Protein Kinase RNA-activated
1.12	0.87	1.65	1.36	TAP2	Antigen peptide transporter 2
	1.34	1.59	1.13	CASP1	Caspase-1
0.69	0.63	1.59	0.87	SP100	Nuclear autoantigen Sp-100
	0.63		1.49	EPHA2	Ephrin type-A receptor 2
0.88		1.47		COG7	Conserved oligomeric Golgi complex subunit 7
1.34	1.24	1.41	1.47	B2M	Beta-2-microglobulin
1.19		1.39	1.16	IFIT5	Interferon-induced protein with tetratricopeptide repeats 5
1.12		1.39	1.37	CNP	2,3-cyclic-nucleotide 3-phosphodiesterase
1.06	0.69	1.24	1.37	TRIM25	E3 ubiquitin/ISG15 ligase TRIM25
1.31		0.73	0.92	NAPA	Alpha-soluble NSF attachment protein
1.27		1.13		RACGAP1	Rac GTPase-activating protein 1
1.26		0.62	0.98	MKI67	Proliferation marker protein Ki-67
	0.79	1.25	1.00	IFI16	Gamma-interferon-inducible protein 16
0.66		1.23	0.93	ZNFX1	NFX1-type zinc finger-containing protein 1
1.16		0.66	0.73	DNAJA1	DnaJ homolog subfamily A member 1
1.15	1.15		0.95	AURKB	Aurora kinase B

	1.11	0.59		NEDD4	E3 ubiquitin-protein ligase NEDD4
1.10	0.74		0.94	NUSAP1	Nucleolar and spindle-associated protein 1
1.08			0.79	HERC6	Probable E3 ubiquitin-protein ligase HERC6
0.74	0.59	1.05	0.87	WARS	Tryptophan--tRNA ligase, cytoplasmic
1.01			1.00	SNRPA	U1 small nuclear ribonucleoprotein A
	0.64	0.97	0.58	EMC2	ER membrane protein complex subunit 2
0.71		0.96		SLC25A13	Calcium-binding mitochondrial carrier protein Aralar2
	0.70	0.93	0.58	MYD88	Myeloid differentiation primary response protein MyD88
0.87		0.92	0.89	XRN1	5-3 exoribonuclease 1
	0.90		0.73	CBX1	Chromobox protein homolog 1
	0.62		0.81	PBK	Lymphokine-activated killer T-cell-originated protein kinase
0.66		0.76	0.59	NUDCD1	NudC domain-containing protein 1
0.60		0.66		PSME2	Proteasome activator complex subunit 2
0.66			0.63	SPART	Spartin
0.63		0.61	0.53	ITGA2	Integrin alpha-2
	-0.61	-0.62	-0.59	ARHGEF40	Rho guanine nucleotide exchange factor 40
	-0.67		-0.64	PCOLCE	Procollagen C-endopeptidase enhancer 1
-0.67	-0.68		-0.65	COL1A2	Collagen alpha-2(I) chain
-0.26	-0.91	-0.80	-0.45	COL5A1	Collagen alpha-1(V) chain
-0.62	-0.81	-0.65	-0.65	PDGFRB	Platelet-derived growth factor receptor beta
-0.63			-0.84	FADS2	Acyl-CoA 6 desaturase
	-0.66		-0.88	TPBG	Trophoblast glycoprotein
	-0.61	-0.96	-0.30	TRAPPC11	Trafficking protein particle complex subunit 11
-0.92	-0.97	-0.68	-0.62	COL1A1	Collagen alpha-1(I) chain
-0.97	-0.99		-0.86	CSPG4	Chondroitin sulfate proteoglycan 4
	-1.05	-0.64	-0.06	RNF20	E3 ubiquitin-protein ligase BRE1A
	-1.03		-1.06	UBE4B	Ubiquitin conjugation factor E4 B
-0.68		-1.08		NSA2	Ribosome biogenesis protein NSA2 homolog
	-1.11		-0.90	WASF2	Wiskott-Aldrich syndrome protein family member 2
-1.05			-1.25	NOC2L	Nucleolar complex protein 2 homolog
	-0.70	-1.25	-0.43	ARMC9	LisH domain-containing protein ARMC9
-0.92		-0.71	-1.26	JUP	Junction plakoglobin
	-1.17		-1.36	VPS25	Vacuolar protein-sorting-associated protein 25
-1.53			-0.64	SGCD	Delta-sarcoglycan
	-1.71	-1.47		CORO7	Coronin-7
-1.80		-0.64		SLC27A4	Long-chain fatty acid transport protein 4
-0.84		-1.82		CKB	Creatine kinase B-type
	-1.29	-2.08	-1.33	CEMIP	Cell migration-inducing and hyaluronan-binding protein
	-0.58	-2.09	-1.47	RPP25L	Ribonuclease P protein subunit p25-like protein

(b)

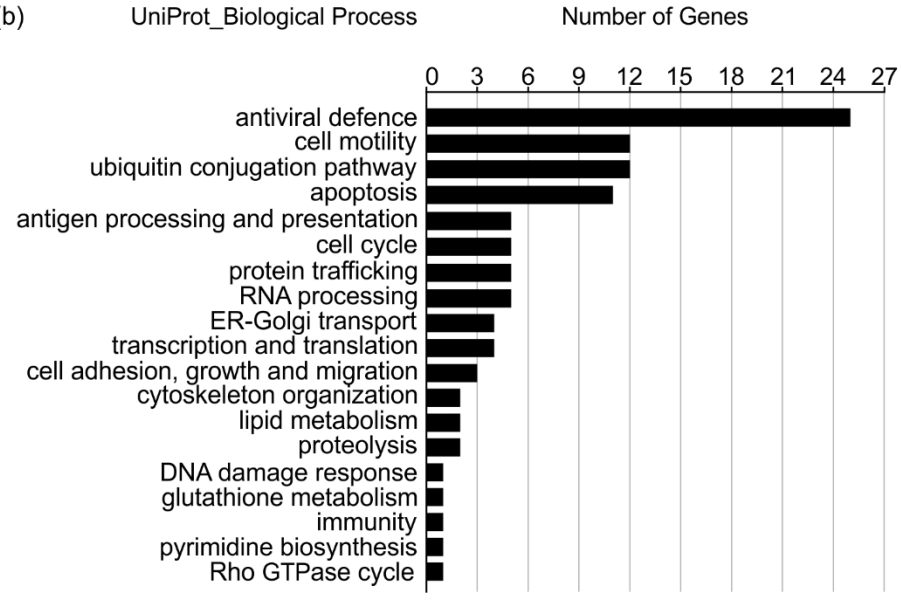

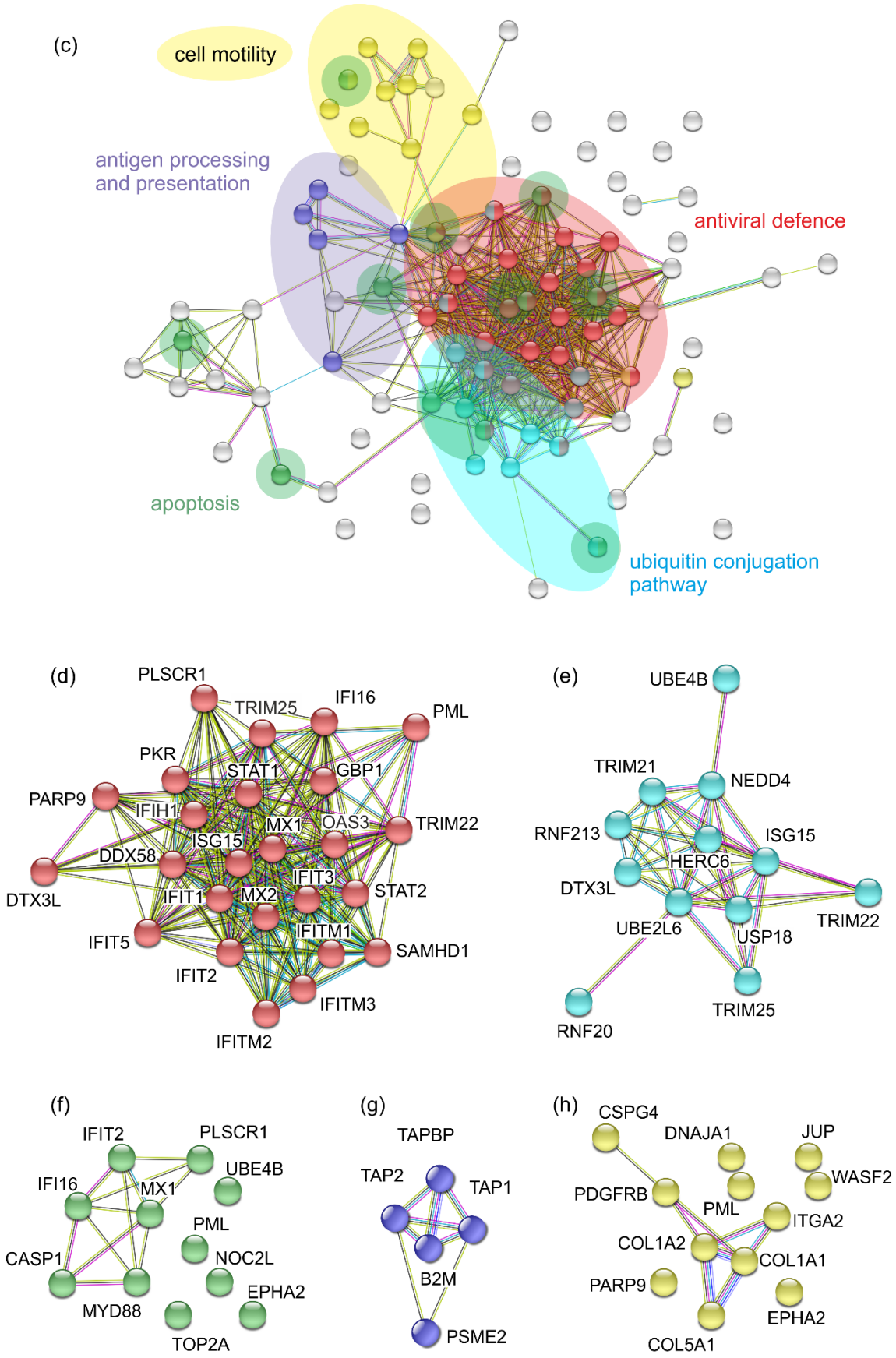
(c)
cell motility
antigen processing and presentation
antiviral defence
apoptosis
ubiquitin conjugation pathway
(d)
PLSCR1
TRIM25
IFI16
PML
PKR
STAT1
GBP1
PARP9
IFIH1
MX1
OAS3
TRIM22
ISG15
DDX58
IFIT3
DTX3L
IFIT1
MX2
STAT2
IFITM1
IFIT5
SAMHD1
IFIT2
IFITM3
IFITM2
(e)
UBE4B
TRIM21
NEDD4
RNF213
ISG15
HERC6
DTX3L
TRIM22
UBE2L6
USP18
TRIM25
RNF20
(f)
IFIT2
PLSCR1
UBE4B
IFI16
MX1
PML
CASP1
NOC2L
EPHA2
MYD88
TOP2A
(g)
TAPBP
TAP2
TAP1
B2M
PSME2
(h)
CSPG4
DNAJA1
JUP
WASF2
PDGFRB
PML
ITGA2
COL1A2
COL1A1
PARP9
EPHA2
COL5A1
Interaction evidence
From curated databases
Gene fusions
Co-expression
Textmining
Experimentally determined
Gene co-occurrence
Protein homology

Fig. 5. DBs-application induces an antiviral cellular environment in HFFs. MS- analysis of HFFs exposed to PC-positive DBs for 24 hours (HCMV strain RV-Towne-repΔGFP, DB-PC+). Untreated cells were used as control. The measurement period per sample was 240 minutes. **(a)** The expression patterns of the 92 regulated proteins were hierarchically arranged, based on the log2 converted normalized ratio of two technical repilcates (R1; R2) and plotted in a heatmap. The log2Ratio is represented with a colour gradient. 68 up-regulated (green) and 24 down-regulated (red) proteins with a fold- change of at least 1.5 (log2ratio ± 0.58) in one of the technical replicates of the two experiments were considered as differentially regulated. Black areas represent values that did not reach the threshold of ±0.58 **(b)** Bar chart of the regulated proteins grouped into biological processes based on Gene Ontology (GO) analysis using the UniProtKB database. The y-axis represents biological processes categories, while the x-axis indicates the number of genes involved in each category. **(c)** Protein-protein interaction (PPI) network generated by using the STRING database. Five highlighted clusters related to antiviral defence (red), cell motility (yellow), ubiquitin conjugation pathway (blue), antigen processing and presentation (purple) and apoptosis (green) are shown. The proteins associated with these enriched processes were depicted in separate subnetworks in **(d-h)**. Each protein is represented as a node. Different line colours represent the types of evidence for the association between the proteins according to the STRING network database. The networks were generated with a minimum required interaction score of a medium confidence of 0.4.

3.1.2 Validation of proteome analysis of HFFs

3.1.2.1 Immunoblot analyses confirmed DBs- induced upregulation of the IRGs STAT1, MX1, IFIT1, IFIT3 and ISG15

To validate the MS data, immunoblot analyses were performed using antibodies directed against the IRGs STAT1, MX1, IFIT1, IFIT3 and ISG15 (Fig.6). HFFs were incubated with 10 µg of UV-inactivated PC-positive DBs (DBs-PC+). Control cells were either left untreated or infected with HCMV strain RV-Towne-repΔGFP (virus, 100- 300 genomes per cell). Cell lysates were prepared at 4, 24 48 and 72 h.p.a, respectively. Control cells were prepared at 24 h.p.a. Equal amounts of total protein were subjected to SDS-PAGE and analyzed by immunoblot. In accordance with the MS data, a significant increase in the expression levels of all five IRGs upon DBs-treatment could be confirmed at 24 h.p.a (Fig.6). Although the fold-changes were not identical in immunoblot analyses compared to MS data, the tendencies were similar thus confirming the proteomic analyses.

3.1.2.2 IRGs induction in HFFs is not dependent on the PC

To determine if IRGs were also upregulated upon incubation with DBs that are devoid of the PC, RV-Towne-BAC-derived DBs were used, and immunoblot analysis were performed as described before. Briefly, HFFs were incubate with 10 µg of UV-inactivated PC-negative DBs (DBs-PC-). Mock- treated and virus-infected HFFs (RV-Towne-repΔGFP, 100- 300 genomes per cell) served as controls. Equal protein amounts were subjected to SDS-PAGE and examined by immunoblot using anti- MX1 and anti- ISG15 antibodies. As shown in Fig. 7, the application of PC-negative DBs also increased the protein levels of MX1 and ISG15 in a time course of three days.

In conclusion, these data confirm that DBs elicit IRGs expression in HFFs and show that the induction of IRGs by DBs is independent of the presence of the PC.

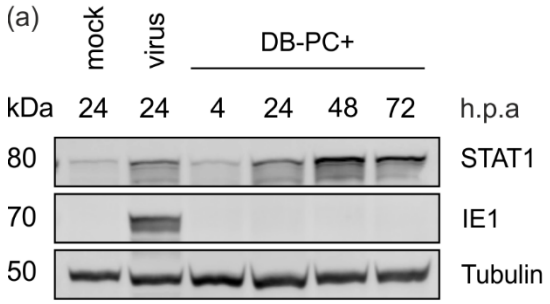
(a)
mock
virus
DB-PC+
kDa 24 24 4 24 48 72 h.p.a
80 STAT1
70 IE1
50 Tubulin

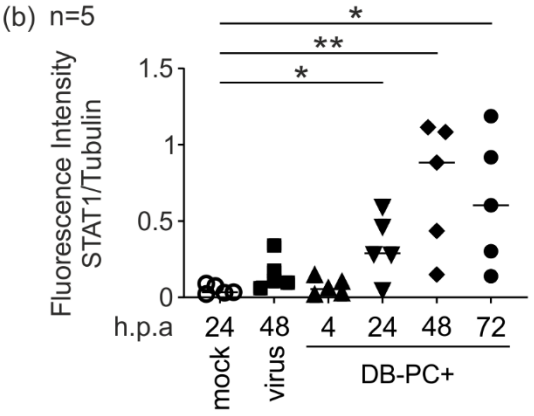
(b) n=5
Fluorescence Intensity STAT1/Tubulin
1.5
1
0.5
0
h.p.a 24 48 4 24 48 72
mock
virus
DB-PC+

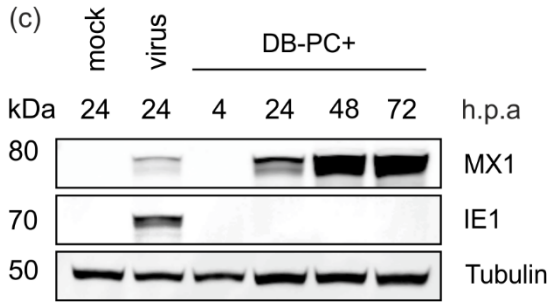
(c)
mock
virus
DB-PC+
kDa 24 24 4 24 48 72 h.p.a
80 MX1
70 IE1
50 Tubulin

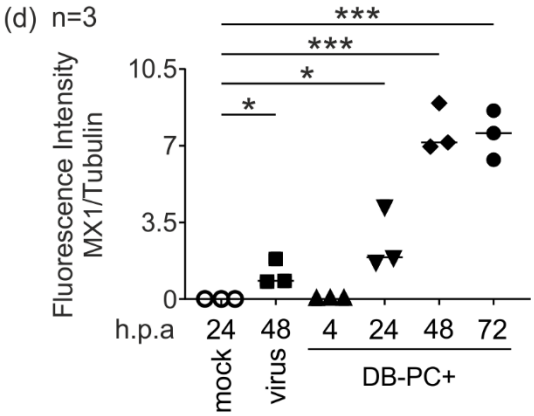
(d) n=3
Fluorescence Intensity MX1/Tubulin
10.5
7
3.5
0
h.p.a 24 48 4 24 48 72
mock
virus
DB-PC+

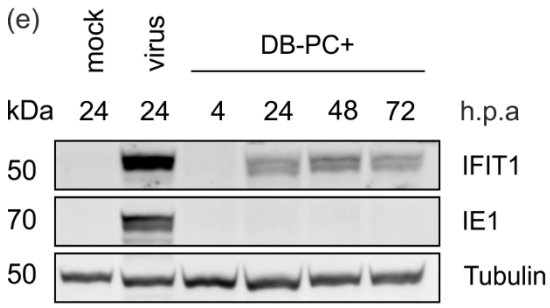
(e)
mock
virus
DB-PC+
kDa 24 24 4 24 48 72 h.p.a
50 IFIT1
70 IE1
50 Tubulin

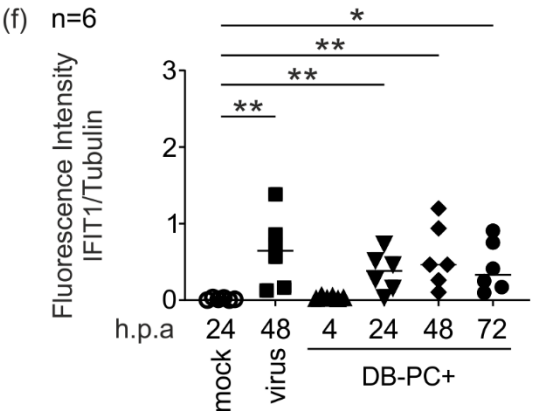
(f) n=6
Fluorescence Intensity IFIT1/Tubulin
3
2
1
0
h.p.a 24 48 4 24 48 72
mock
virus
DB-PC+

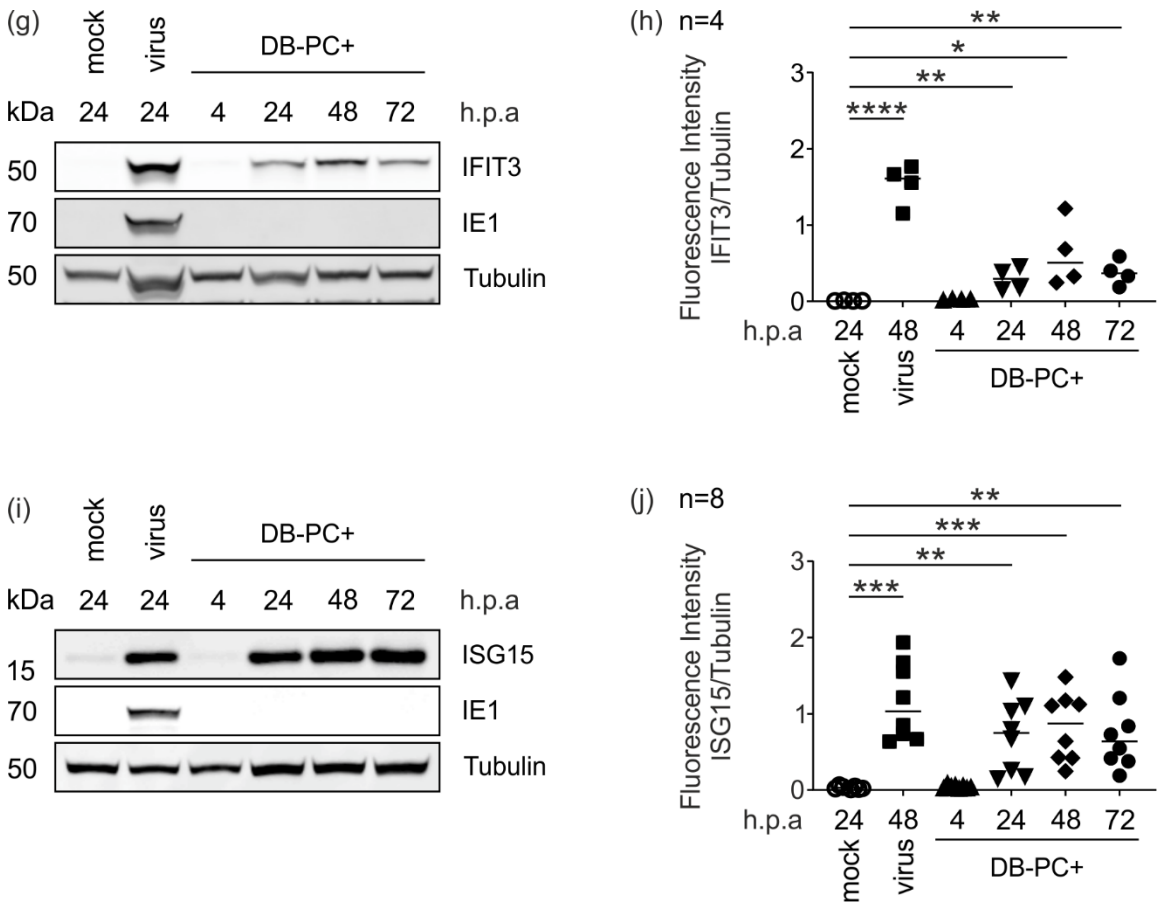

Fig. 6. DBs induce the expression of IRGs. Validation of MS data by immunoblot analyses. Expression of IRGs in HFFs treated with DBs. 5x10exp5 HFFs were incubated with 10 µg UV-inactivated DBs of the PC-positive HCMV strain RV-Towne-repΔGFP (DBs-PC+). Cell lysates were prepared at the indicated times and subjected to SDS-PAGE and immunoblot analyses. Untreated cells (mock) and HCMV infected cells (strain RV-Towne-repΔGFP, 100-300 genomes per cell, virus) served as controls. The membranes were probed with antibodies against the IRGs STAT1, MX1, IFIT1, IFIT3 and ISG15 (a, c, e, g and i). The viral IE1-protein was used to exclude contamination of the DBs with infectious virus. Tubulin was probed as sample loading control. For quantification, the ratio of the fluorescence intensity of each IRG protein band to the corresponding tubulin band was measured using the LICOR Image Studio Lite (Ver 5.2) software. The values of three to eight independent experiments were plotted. Comparisons between groups were calculated using an unpaired, two-tailed t test for the indicated group compared with the untreated (mock) group. * $p<0.05$; ** $p < 0.01$; *** $p < 0.001$.

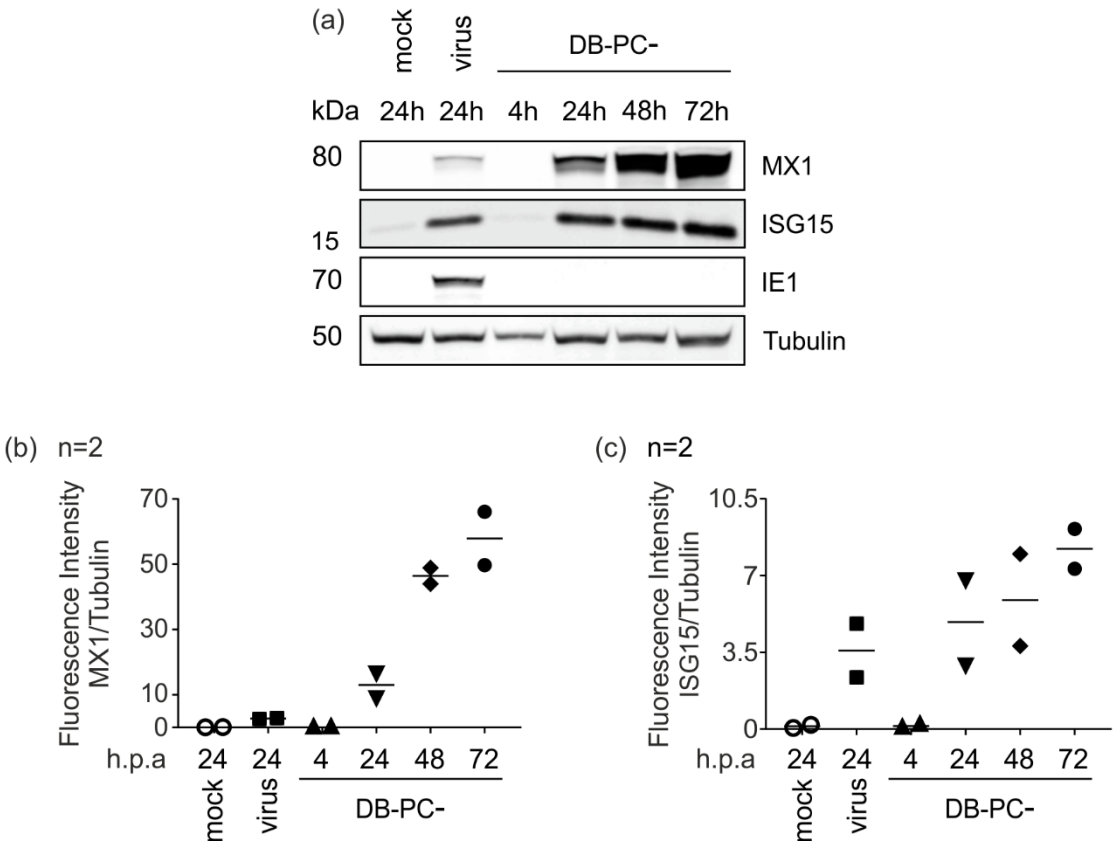

Fig. 7. DBs induce the expression of IRGs regardless of the PC. Immunoblot analyses of HFFs treated with PC-negative DBs. (a) 10 µg of UV-inactivated DBs derived from the PC-negative HCMV strain RV-Towne-BAC (DBs-PC-) were applied to 5x10exp5 HFFs. Untreated- (mock) or infected cells (HCMV strain RV-Towne-repΔGFP, 100-300 genomes per cell, virus) served as controls. Cell lysates were prepared at indicated times and submitted to immunoblot analyses. The membranes were probed with antibodies against MX1 and ISG15. An antibody against the viral IE1-protein was used to exclude contamination of the DBs with infectious virus. An anti-tubulin antibody was used to visualize the loading control. For quantification, the ratio of the fluorescence intensity of MX1 (b) or ISG15 (c) band to the corresponding tubulin band was measured using the LICOR Image Studio Lite (Ver 5.2) software. The values of two independent experiments were plotted.

3.1.2.3 The IRGs STAT1, MX1, IFIT3 and ISG15 are not incorporated into purified DBs

MS-based studies of purified HCMV DBs revealed, that in addition to viral structural proteins, several host cell proteins including e.g. Annexin A2(ANXA2), Actin-α-2 and Actin-β (ACTN2, ACTB), or Collagen alpha 2 chain (COL1A2) associated with DBs [38, 104].

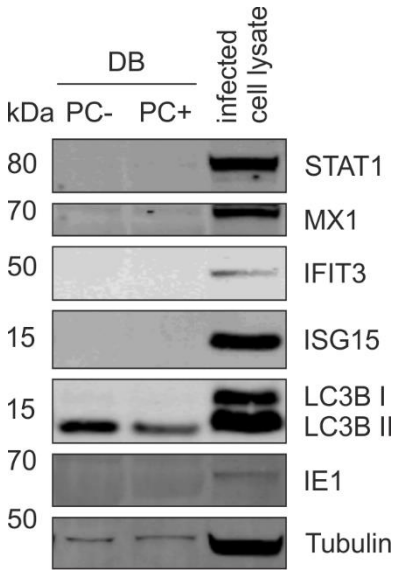

Fig. 8. The cellular proteins STAT1, MX1, IFIT3 and ISG15 are not incorporated into purified DBs. Immunoblot analysis of purified PC-negative and PC-positive. DBs. HCMV DBs were gradient purified from culture supernatants of HFFs infected with the HCMV strain RV-Towne-BAC (PC-) or RV-Towne-repΔGFP (PC+). 30 µg of each preparation were lysed, subjected to SDS-PAGE and analysed by immunoblot using antibodies against the STAT1, MX1, IFIT3 and ISG15. Infected cell lysate (HCMV strain RV-Towne-repΔGFP) was subjected as expression control. As integral parts of DBs, LC3B and tubulin were visualized and used as positive control. The detection of the viral IE1 confirmed infection.

To exclude the packaging of STAT1, MX1, IFIT3 and ISG15 and delivery of these proteins into cells was accountable for their detection in HFFs, following DBs-applications, immunoblot analyses were performed using purified DBs (Fig.8). HCMV DBs were gradient purified from culture supernatants of HFFs infected with the HCMV strain RV-Towne-BAC (PC-) or RV-Towne-repΔGFP (PC+). 30 µg of each preparation were lysed and analysed by immunoblot, using antibodies against STAT1, MX1, IFIT3 and ISG15 (Fig.8). An infected cell lysate (HCMV

strain RV-Towne-repΔGFP) was subjected as expression control. As integral parts of DBs, LC3B and Tubulin were visualized and used as positive control [38, 107, 108]. IE1 expression confirmed infection. As shown in Fig. 8 neither PC-negative nor PC-positive, purified DBs contained either STAT1, MX1, IFIT3 or ISG15.

These findings verified that the cellular proteins STAT1, MX1, IFIT3 or ISG15 were not packaged into DBs in the course of their morphogenesis and excluded that the MS analyses on DBs-treated cells were confounded by introduction of these proteins by incoming particles.

3.1.2.4 DBs do not induce the dispersion of ND10 proteins PML and Sp100

Among the differentially regulated proteins identified in the proteome of HFFs after treatment with DBs, the Promyelocytic Leukemia protein (PML) and the Speckled protein of 100 kDa (Sp100) were increased > 3-fold (PML, 3,3-fold-change; Sp100, 3-fold change). PML and SP100 compose, next to Death domain- associated protein (hDaxx), major constituents of nuclear domain 10 (ND10) [109, 110]. ND10 proteins are iIFN regulated and act as host restriction factors (RFs) with repressive effects on viral replication [110-112]. Consequently, HCMV has developed mechanisms to antagonize these antiviral restrictions. In the case of HCMV, the IE1 protein was shown to be responsible for the disruption of ND10 during infection [113-116].

To test, if DBs would have the same effect on ND10, the particles were applied to HFFs for 24 h and double immunofluorescence staining was performed (Fig. 9). For this PC-negative and PC-positive DBs were analysed. Additionally, cells were infected with 50 genomes per cell with HCMV strain RV-Towne-repΔGFP (virus) to confirm ND10 disruption. Following fixation, cells were stained with anti-PML (Fig.6a, green) or anti-SP100 (Fig. 9b, green), IE1 (Fig. 9, red) or pp65 (Fig. 9, red). Nuclei were visualized with DAPI. Uninfected cells (mock) showed the typical dot-like distribution of PML and SP100. Cells exposed to DBs showed the speckled profile of uninfected cells. HCMV infected cells (virus), carried along as positive control showed disruption of PML nuclear bodies in the presence of IE1 expression.

The experiments showed that DBs do not share the ND10-disruptive effects seen after HCMV infection.

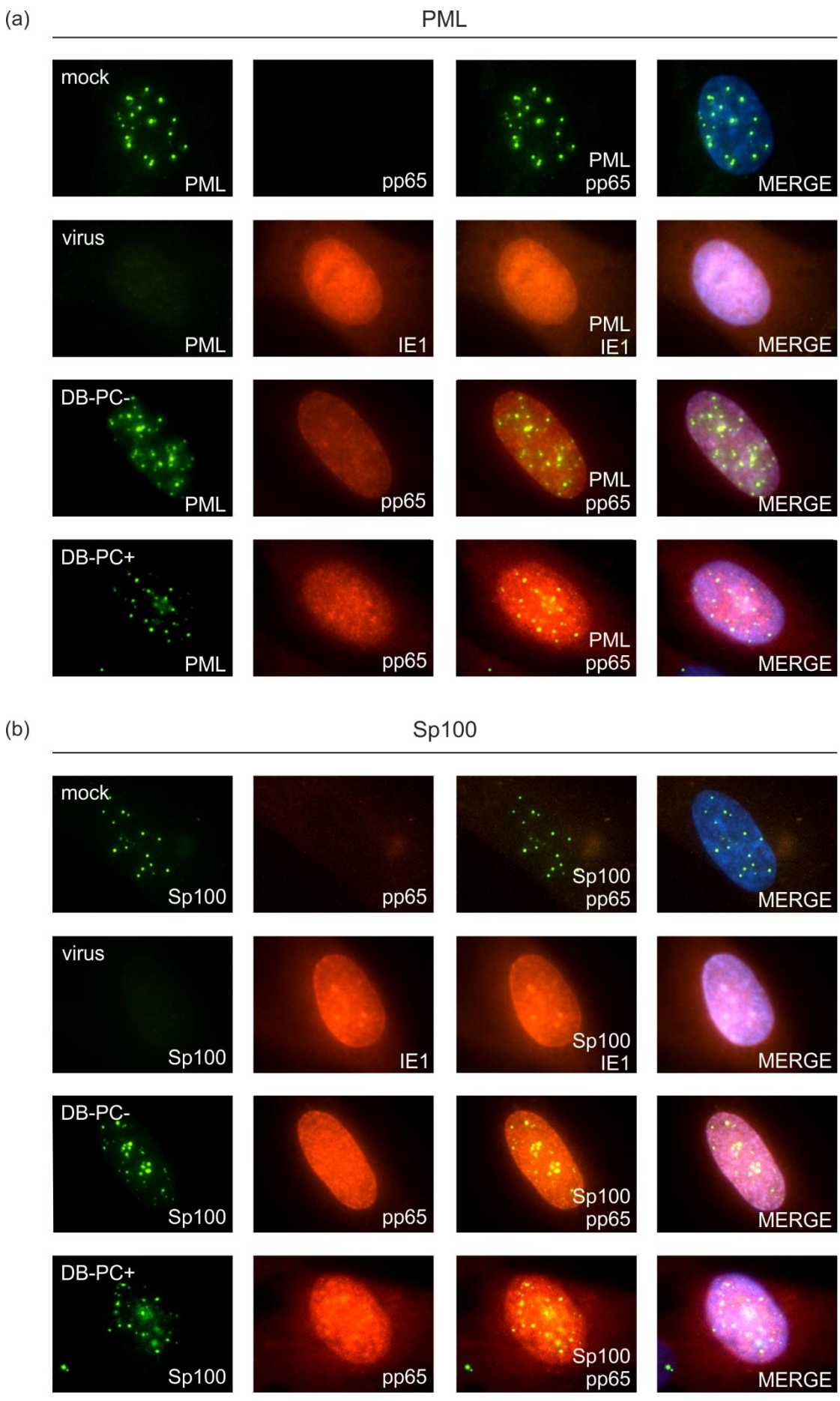
(a)
PML
mock
PML
pp65
PML
pp65
MERGE
virus
PML
IE1
PML
IE1
MERGE
DB-PC-
PML
pp65
PML
pp65
MERGE
DB-PC+
PML
pp65
PML
pp65
MERGE
(b)
Sp100
mock
Sp100
pp65
Sp100
pp65
MERGE
virus
Sp100
IE1
Sp100
IE1
MERGE
DB-PC-
Sp100
pp65
Sp100
pp65
MERGE
DB-PC+
Sp100
pp65
Sp100
pp65
MERGE

Fig. 9. DBs fail to disperse the primary ND10 proteins PML and SP100. Immunofluorescence analysis examining the effects of PC-negative (DBs-PC-) and PC-positive (DBs-PC+) DBs on ND10 disruption after 24 h, using antibodies directed against the major ND10 proteins PML (a) and SP100 (b). 3x10exp5 HFFs were grown on glass coverslips and treated with 5 µg of either DBs-PC- or DBs-PC+. After 24 h, cells were fixed in 90% acetone, washed and stained for PML (a, green) or SP100 (b, green), IE1 (red) or pp65 (red). Nuclei were visualized with DAPI. As control for ND10 disruption, HFFs were infected with HCMV strain RV-Towne-repΔGFP (virus, 50 genomes per cell). Representative single and merged fluorescent stains of each protein and nucleus are shown. Magnification of 400x. Mock cells were used to show the common dot-like nuclear distribution of PML or SP100 respectively. Cells exposed to DBs showed the speckled profile of uninfected cells for both proteins PML and Sp100. In HCMV infected cells (virus) the disruption of PML and SP100 in presence of IE1 expression was confirmed. ND 10, Nuclear Domain 10; PML, Promyelocytic Leukemia bodies; SP100, Speckled protein of 100 kDa

3.1.3 Impact of DBs on the cellular proteome of ECs

3.1.3.1 Initial proteomic analysis of ECs reveals the upregulation of IRGs related to antiviral defence following DB-exposure

ECs are one predominant target of HCMV infection both in vivo and in vitro [19, 33, 117]. EC seem to play an important role in viral dissemination. The ability of HCMV to replicate in ECs enables the virus to establish latency and persistence within the host [3, 118]. However, it has been shown that the PC is indispensable for virus entry and growth in ECs [33, 119].

To analyse the impact of DBs on the cellular proteome of ECs, an initial experiment was performed. ECs [85] were exposed to 40 µg of UV- irradiated PC-positive DBs (DBs-PC+) or were left untreated (mock). The cells were collected at 24 h.p.a and processed for MS as describe in 2.2.14. A total of 3087 proteins were identified in this experiment. For compilation of the data, the proteins with a minimum fold-change of 1.5 up- or downregulation (Log2Ratio ± 0.58) in both technical replicates were considered as regulated by DBs. At 24 h.p.a, 16 of these proteins were found to be upregulated (green) and 3 proteins downregulated (red) in ECs treated with DBs (Fig.10a) Except for the viral tegument protein pp65 and the cellular proteins ATP synthase subunit (ATP5I,↓), Gasdermin E (GSDME,↑) and Quinone oxidoreductase PIG3 (TP53I3,↑), all proteins were known to be regulated by IFNs according

to the INTERFEROME database (S5). To investigate the biological processes in which the regulated proteins were involved, GO-analysis was performed using the UniProtKB database. As shown in the bar chart, ten of the proteins were enriched in the category of antiviral defence (Fig.10b, S6)). The category of lipid metabolism was represented by the two proteins Fatty acid desaturase 2 (FSDS2, ↓) and Estradiol 17-beta-dehydrogenase 11 (HSD17B11,↓). The two upregulated proteins SAFB-like transcription modulator (SLTM, ↑) and Protein mono-ADP-ribosyltransferase PARP14 (PARP14, ↑) are functionally active in transcription. Further analysis, using STRING PPI network, revealed a central cluster of ten highly interacting proteins that associated with antiviral defence (Fig.10c, red). All proteins involved in this cluster were upregulated in ECs and were known to be responsive to IFNs.

The evaluation of the initial MS-data revealed that DBs elicit an upregulation of IRG in EC which are associated with antiviral functions.

(a)

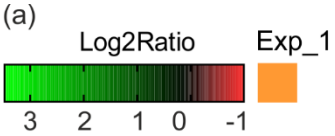

Replicate

R1	R2	Gene	Protein name
3.48	3.19	MX1	Tegument protein pp65
2.39	2.38	pp65	Interferon-induced GTP-binding protein MX1
2.28	1.37	IFIT1	Interferon-induced protein with tetratricopeptide repeats 1
1.44	2.08	SLTM	SAFB-like transcription modulator
1.93	1.40	OAS2	2-5-oligoadenylate synthase 2
1.91	1.84	ISG15	Ubiquitin-like protein ISG15
1.04	1.32	BST2	Bone marrow stromal antigen 2
0.96	1.06	DDX58	Probable ATP-dependent RNA helicase DDX58
0.81	1.04	TP53I3	Quinone oxidoreductase PIG3
0.98	0.74	OAS3	2-5-oligoadenylate synthase 3
0.79	0.86	STAT1	Signal transducer and activator of transcription 1-alpha/beta
0.72	0.80	PARP14	Protein phosphatase methylesterase 1
0.77	0.69	SERPINB2	Plasminogen activator inhibitor 2
0.72	0.63	SAMHD1	Deoxynucleoside triphosphate triphosphohydrolase SAMHD1
0.71	0.67	STAT2	Signal transducer and activator of transcription 2
0.59	0.61	GSDME	Gasdermin E
-0.59	-0.65	FADS2	Fatty acid desaturase 2
-0.70	-0.62	HSD17B11	Estradiol 17-beta-dehydrogenase 11
-0.87	-0.87	ATP5I	ATP synthase subunit e, mitochondrial

(b)

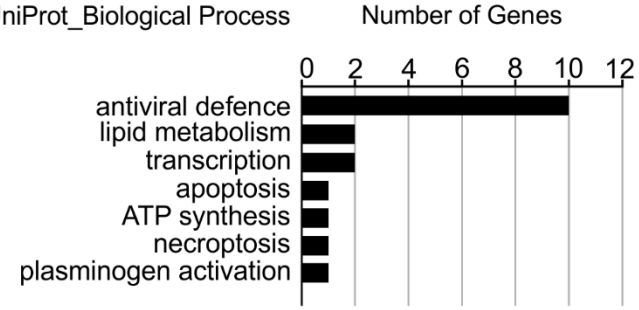

(c)

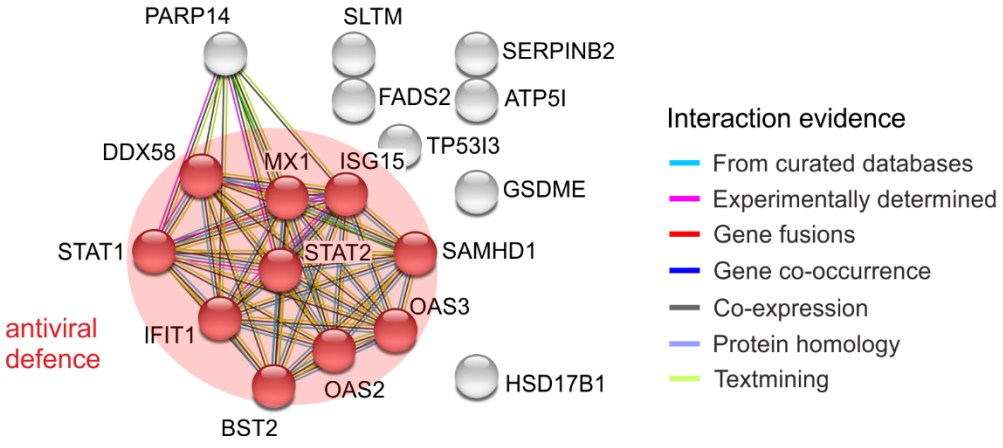

Fig. 10. IRGs, related to antiviral defence are upregulated in ECs after DBs exposure. MS- data analysis of ECs 24 h after incubation with DBs. The samples were measured at 240 min on a Q Exactive Plus mass spectrometer (Thermo Fisher Scientific, Waltham, USA **(a)** Hierarchically arranged proteins that were differrentially regulated in ECs, exposed to PC-positive DBs of the HCMV strain RV-Towne-repΔGFP. The expression patterns were arranged based on the log2 converted normalized ratio of two technical repilcates (R1; R2). The log2Ratio is represented with a colour gradient. 16 up-regulated (green) and 3 down-regulated (red) proteins with a fold- change of at least 1.5 (log2ratio ± 0.58) in both technical replicates were considered as differentially regulated. **(b)** Regulated proteins grouped into biological processes based on GO analysis using the UniProtKB database.The y-axis represents categories, while the x-axis indicates the number of genes in each category. **(c)** PPI network generated with the online STRING database software showing a cluster (red), of proteins involved in antiviral defence. Each protein is represented as a node. Different line colours represent the types of evidence for the association between the proteins according to the STRING network database. The networks were generated with a minimum required interaction score of a medium confidence of 0.4.

3.1.3.2 MS data show a downregulation of cell cycle and chromosome organization regulating proteins in ECs after DBs exposure

A total of 2263 proteins were identified in this experiment. Only proteins with a minimum log2Ratio of ± 0.58 in both technical replicates of the two experiments were considered as regulated by DBs. The 51 regulated proteins were hierarchically clustered according to their log2Rations and plotted in a heatmap (Fig. 11a). 25 of these proteins were found to be upregulated (green) and 26 proteins downregulated (red) in ECs treated with DBs. According to the INTERFEROME database, 46 of the filtered proteins are listed as IFN- regulated (S7). For biological process analysis, the proteins were subjected to GO functional categorization (S8). The bar chart in Fig. 11b demonstrates that the proteins related to cell cycle and chromosome organization were enriched in ECs after treatment with DBs. Strikingly, all these proteins were downregulated, except for protein phosphatase methylesterase 1 (PPME1). The STRING PPI network analysis revealed that the proteins associated with cell cycle (yellow) were connected to proteins involved in chromosome organization (purple) (Fig. 11c-e). Interestingly, proteins related to apoptosis were distributed throughout the network (Fig. 11c). In contrast to previous results, proteins involved in antiviral defence were only represented by the three ISGs MX1, ISG15 and Nucleolar RNA helicase 2 (DDX21) (Fig. 11a+g).

According to this result, the application of PC-positive DBs to EC resulted in a downregulation of cell cycle control mechanisms.

(a)

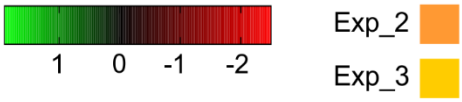

Replicate				Gene	Protein name
R1	R2	R1	R2		
2.72	0.85	2.18	0.43	pp65	Tegument protein pp65
1.43	2.42	1.77	1.85	CMBL	Carboxymethylenebutenolidase homolog
1.05	2.20	0.82	2.22	TP53I3	Quinone oxidoreductase PIG3
1.63	1.40	2.01	1.44	FDXR	NADPH:adrenodoxin oxidoreductase, mitochondrial
1.04	1.89	1.60	1.30	TAGLN	Transgelin
1.29	1.33	1.76	0.89	MX1	Interferon-induced GTP-binding protein MX1
1.39	1.48	1.75	1.11	ITGA3	Integrin alpha-3
1.32	1.40	1.50	1.49	ISG15	Ubiquitin-like protein ISG15
1.35	1.10	1.50	0.99	MVP	Major vault protein
1.05	1.16	0.70	1.38	CD99	CD99 antigen
0.86	1.30	0.91	0.74	S100A6	Protein S100-A6
0.76	1.27	0.89	1.16	PPME1	Protein phosphatase methylesterase 1
1.01	0.92	1.24	1.24	ICAM2	Intercellular adhesion molecule 2
0.75	1.20	0.66	0.84	FTH1	Ferritin heavy chain
0.80	1.16	0.79	0.62	PSAT1	Phosphoserine aminotransferase
0.95	0.91	1.07	0.84	ANPEP	Aminopeptidase N
1.04	0.70	0.79	0.74	CAVIN2	Caveolae-associated protein 2
1.01	1.07	0.79	0.69	SERPINE1	Plasminogen activator inhibitor 1
0.96	0.82	0.95	0.89	PLEC	Plectin
0.94	0.63	0.88	0.85	AHNAK	Neuroblast differentiation-associated protein AHNAK
0.88	0.93	0.94	0.92	ANXA4	Annexin A4
0.84	0.73	0.88	0.61	PLOD2	Procollagen-lysine,2-oxoglutarate 5-dioxygenase 2
0.60	0.70	0.59	0.82	STOM	Erythrocyte band 7 integral membrane protein
0.80	0.78	0.74	0.73	FLNC	Filamin-C
0.70	0.70	0.80	0.61	EHD1	EH domain-containing protein 1
-0.64	-0.60	-0.59	-0.64	CBR3	Carbonyl reductase [NADPH] 3
-0.58	-0.58	-0.65	-0.60	DDX21	Nucleolar RNA helicase 2
-0.81	-0.72	-0.79	-0.75	DBI	Acyl-CoA-binding protein
-0.83	-0.87	-0.83	-0.84	HIST1H1B	Histone H1.5
-0.91	-0.70	-0.83	-0.84	H4C1	Histone H4
-0.93	-0.76	-0.71	-0.64	MCM5	DNA replication licensing factor MCM5
-0.94	-0.63	-0.65	-0.69	DEK	Protein DEK
-0.85	-0.95	-0.79	-0.83	MCM2	DNA replication licensing factor MCM2
-0.78	-0.96	-0.95	-0.64	MCM6	DNA replication licensing factor MCM6
-0.94	-0.96	-0.84	-0.65	SMC1A	Structural maintenance of chromosomes protein 1A
-1.03	-0.92	-0.83	-0.88	MCM4	DNA replication licensing factor MCM4
-0.90	-0.98	-0.75	-1.04	SMC4	Structural maintenance of chromosomes protein 4
-0.83	-1.03	-1.05	-0.97	MSH6	DNA mismatch repair protein Msh6
-0.92	-0.84	-1.06	-0.81	STMN1	Stathmin
-0.96	-0.84	-1.11	-0.84	HMGB2	High mobility group protein B2
-1.12	-1.21	-1.03	-1.13	ALDH1A1	Retinal dehydrogenase 1
-1.24	-1.06	-0.62	-0.81	DHCR24	Delta(24)-sterol reductase
-1.27	-1.07	-1.15	-0.62	EIF1	Eukaryotic translation initiation factor 1
-1.46	-1.10	-1.15	-0.86	PTMA	Prothymosin alpha
-1.55	-1.30	-1.64	-1.29	TP53	Cellular tumor antigen p53
-1.72	-1.28	-1.68	-1.66	CDK1	Cyclin-dependent kinase 1
-1.75	-1.34	-1.61	-1.79	TOP2A	DNA topoisomerase 2-alpha
-0.75	-1.34	-1.87	-1.22	DNMT1	DNA (cytosine-5)-methyltransferase 1
-1.93	-1.47	-1.18	-1.29	DHFR	Dihydrofolate reductase
-1.94	-1.78	-1.91	-1.54	KPNA2	Importin subunit alpha-1
-3.18	-2.73	-2.92	-1.97	RRM2	Ribonucleoside-diphosphate reductase subunit M2

(b)

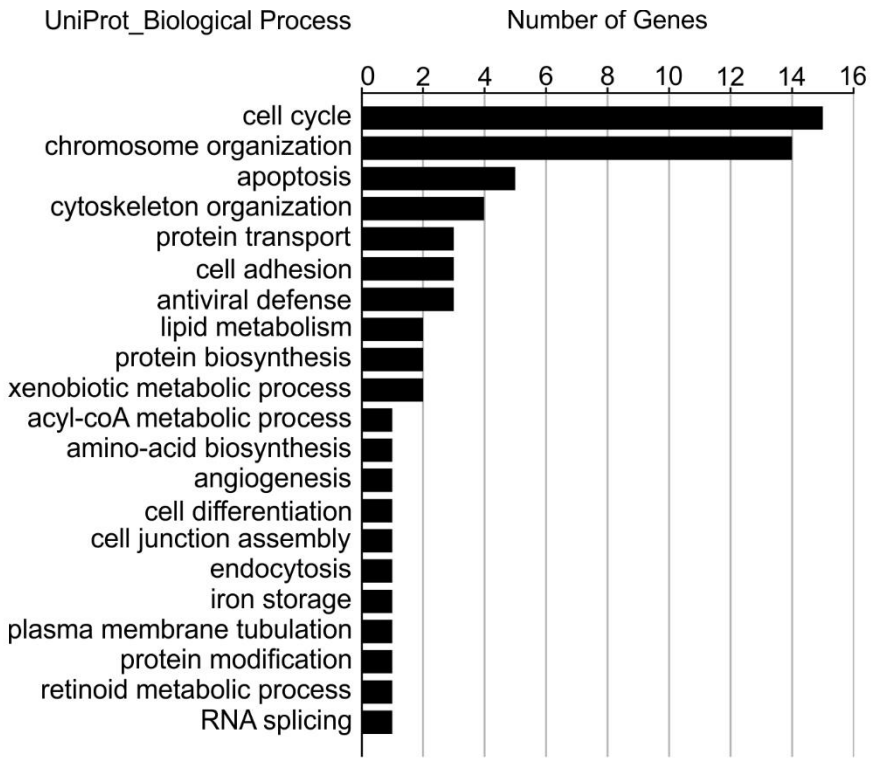
UniProt_Biological Process
Number of Genes
0 2 4 6 8 10 12 14 16
cell cycle
chromosome organization
apoptosis
cytoskeleton organization
protein transport
cell adhesion
antiviral defense
lipid metabolism
protein biosynthesis
xenobiotic metabolic process
acyl-coA metabolic process
amino-acid biosynthesis
angiogenesis
cell differentiation
cell junction assembly
endocytosis
iron storage
plasma membrane tubulation
protein modification
retinoid metabolic process
RNA splicing

(c)

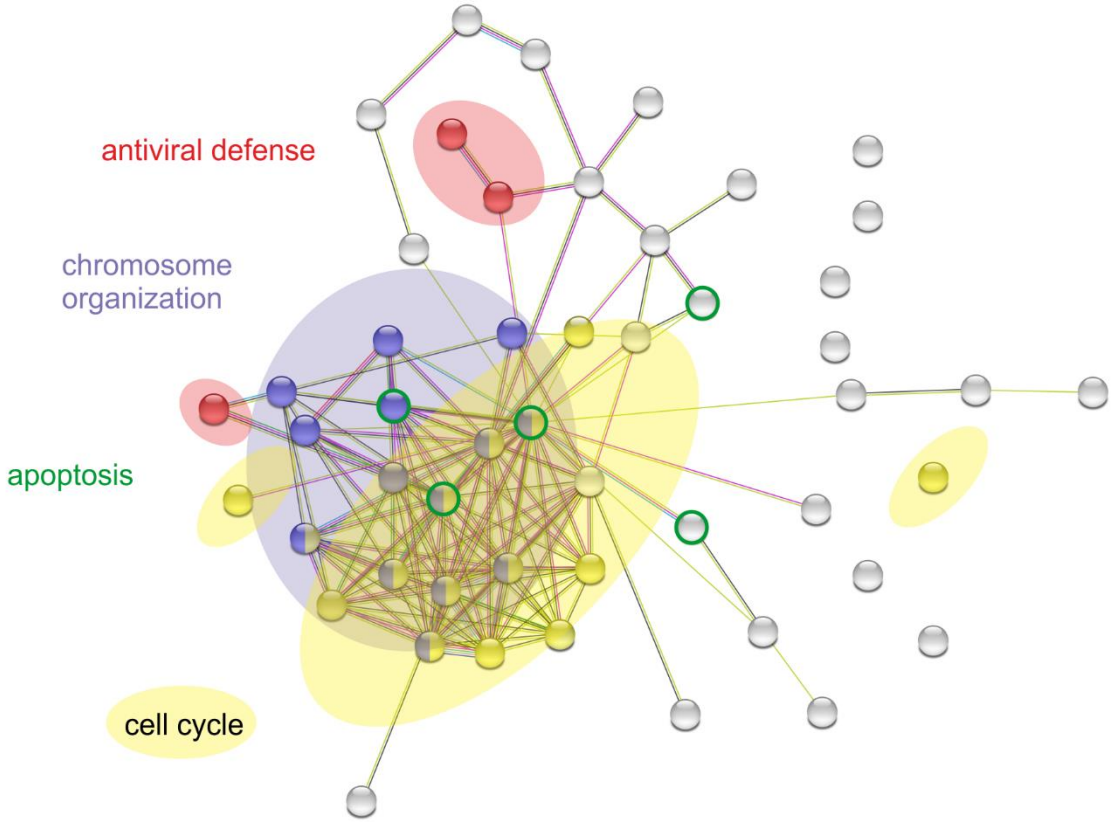
antiviral defense
chromosome organization
apoptosis
cell cycle

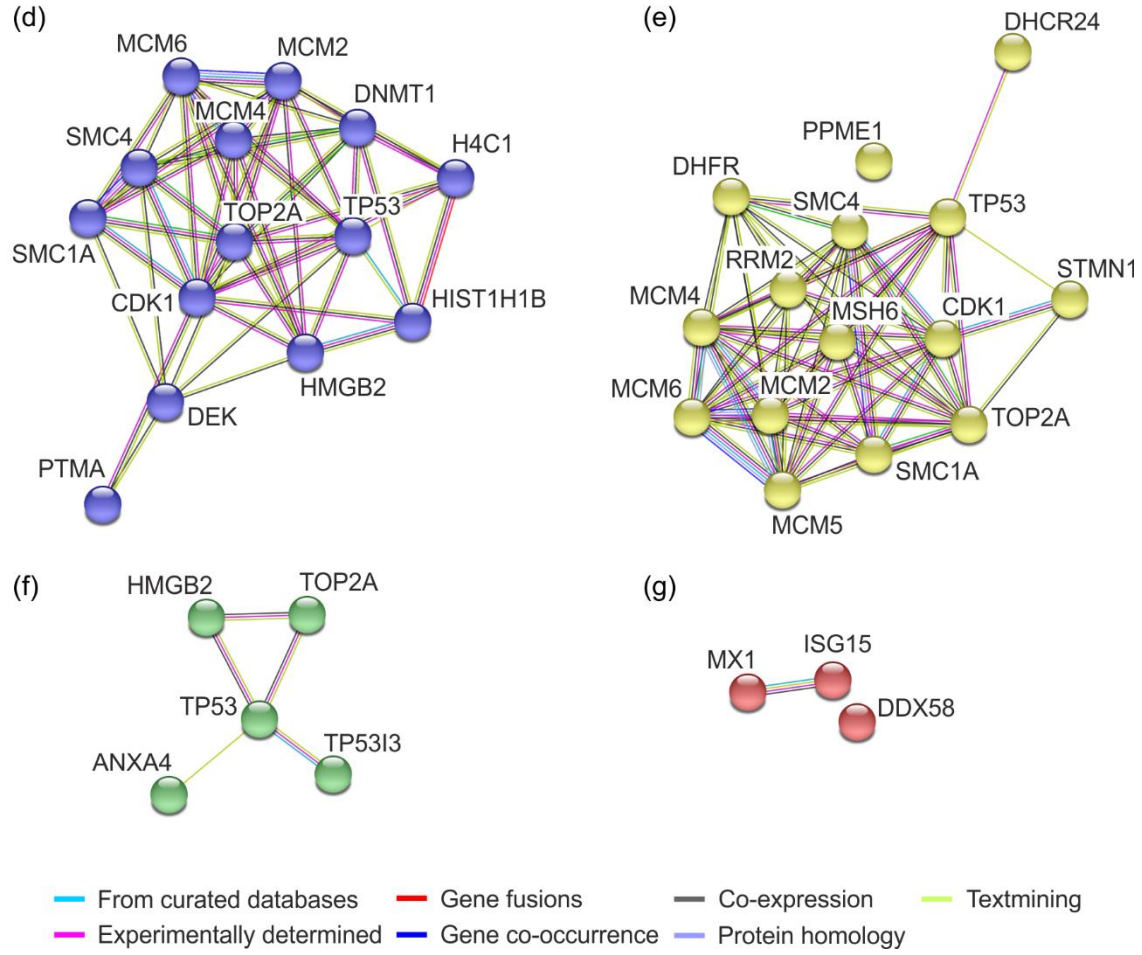

Fig. 11. ECs exhibit a regulation of IRGs mainly involved in cell cycle and chromosome organization upon DBs treatment. Quantitative MS analysis of ECs exposed to 40 µg UV-inactivated PC-positive DBs (strain RV-Towne-repΔGFP). (a) Heatmap of 51 proteins differentially regulated in Ecs exposed to DBs compared to untreated cells. The expression patterns of the proteins were hierarchically arranged, based on the log2 converted normalized ratio of two technical repilcates (R1; R2). The log2Ratio is represented with a colour gradient. 25 up-regulated (green) and 26 down-regulated (red) proteins with a fold- change of at least 1.5 (log2ratio ± 0.58) in both technical replicates of two independent experiments were considered as being differentially regulated. (b) Catergorization of the identified proteins into biological processes based on GO analysis using the UniProtKB database. (c) PPI network shows one major cluster of proteins related to biological processes cell cycle, chromosome organization, apoptosis and antiviral defence. The association between proteins regulated in these processes are depicted in subnetworks d, e, f and g. Each node represents all the proteins produced by a single, protein-coding gene locus. Different line colours represent the types of evidence for the association according to STRING network database. The networks were generated with a minimum required interaction score of medium confidence 0.4.

3.1.4 Validation of proteomic results of endothelial cells in immunoblot analysis

3.1.4.1 PC-positive DBs promote the induction of IRGs in ECs

To verify the proteomic results, immunoblot analysis were performed on the proteins STAT1, MX1, IFIT3 and ISG15 (Fig. 12). ECs were incubated with 30 µg of UV-inactivated PC-positive DBs (DBs-PC+). Control cells were either left untreated or infected with HCMV strain RV-Towne-repΔGFP (virus, 300 genomes per cell). Immunoblot analysis from total cell lysates prepared at 24, 48 and 72 h.p.a. were evaluated. As shown in Fig. 12, application of DBs-PC+ increased the protein levels of all four IRGs in ECs compared to control cells. The results were in agreement with those obtained from the initial MS analysis.

In conclusion, the data above indicated that DBs promote IRG- induction in ECs.

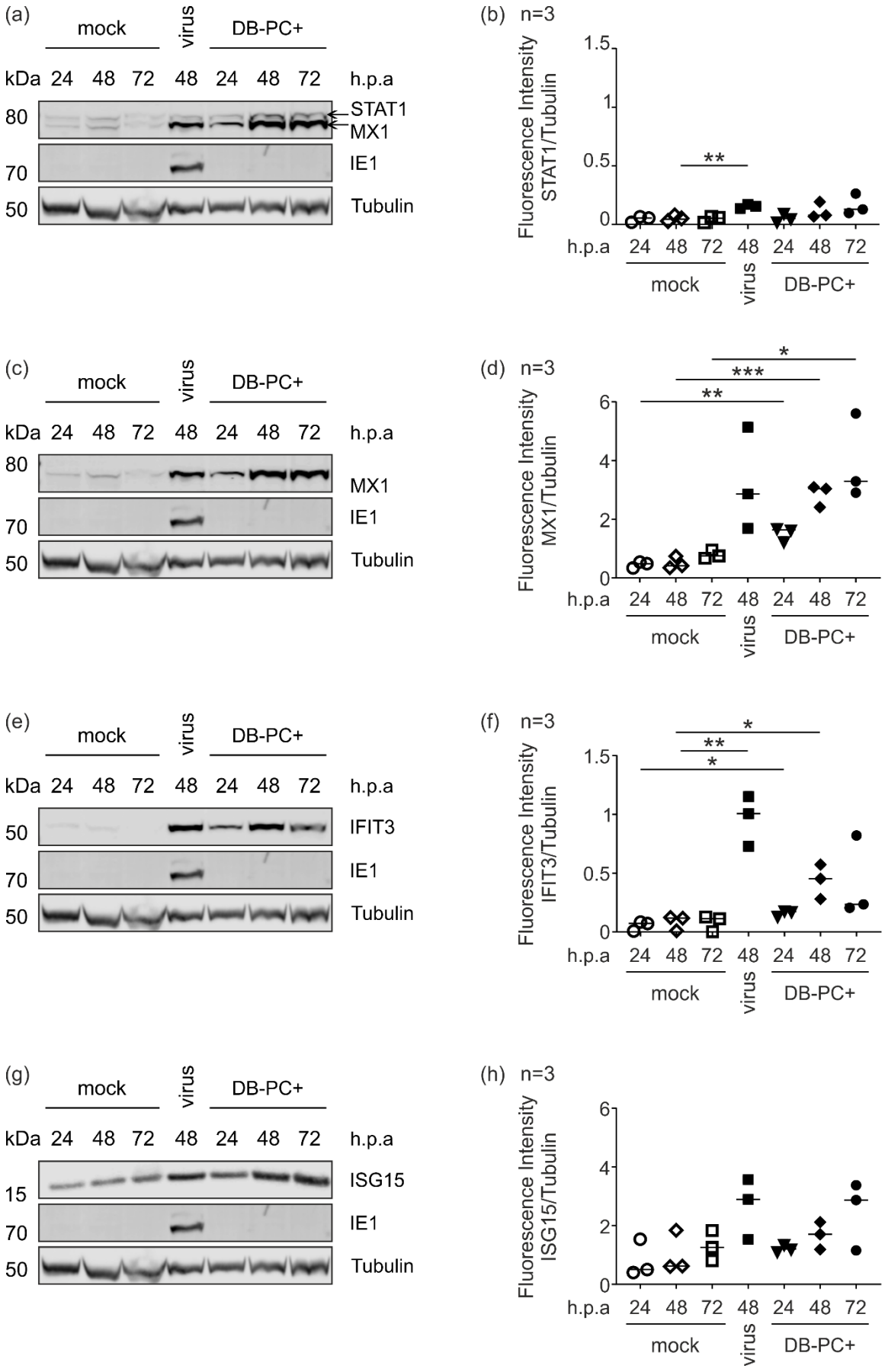
(a)
mock
virus
DB-PC+
kDa 24 48 72 48 24 48 72 h.p.a
80
STAT1
MX1
70
IE1
50
Tubulin
(b) n=3
Fluorescence Intensity STAT1/Tubulin
1.5
1
0.5
0
**
h.p.a 24 48 72 48 24 48 72
mock
virus
DB-PC+
(c)
mock
virus
DB-PC+
kDa 24 48 72 48 24 48 72 h.p.a
80
MX1
70
IE1
50
Tubulin
(d) n=3
Fluorescence Intensity MX1/Tubulin
6
4
2
0
*
***
**
h.p.a 24 48 72 48 24 48 72
mock
virus
DB-PC+
(e)
mock
virus
DB-PC+
kDa 24 48 72 48 24 48 72 h.p.a
50
IFIT3
70
IE1
50
Tubulin
(f) n=3
Fluorescence Intensity IFIT3/Tubulin
1.5
1
0.5
0
*
**
*
h.p.a 24 48 72 48 24 48 72
mock
virus
DB-PC+
(g)
mock
virus
DB-PC+
kDa 24 48 72 48 24 48 72 h.p.a
15
ISG15
70
IE1
50
Tubulin
(h) n=3
Fluorescence Intensity ISG15/Tubulin
6
4
2
0
h.p.a 24 48 72 48 24 48 72
mock
virus
DB-PC+

Fig. 12. Confirmation of IRG-induction in ECs by DBs using immunoblot analyses. Expression profiles of antiviral IRGs STAT1, MX1, IFIT3 and ISG15 in ECs after treatment with DBs. For immunoblot analysis 30 µg of UV-inactivated PC- positive DBs of the HCMV strain RV-Towne-repΔGFP (DBs-PC+) were applied to 6x10exp5 ECs. Untreated cells (mock) and HCMV infected cells (strain RV-Towne-repΔGFP, virus) served as controls. Cells were harvested at 24, 48, and 72 h.p.a. Equal protein amounts were applied to SDS-PAGE and transferred onto PVDF-membranes. The membranes were incubated with antibodies specific for STAT1, MX1, IFIT3 and ISG15 (a, c, e and g). Infection was confirmed by antibody-staining of viral IE1-protein. An antibody against tubulin was used for controlling the amount of loaded protein. For each protein, one representative immunoblot is shown. For quantification, the ratio of the fluorescence intensity of each protein and the corresponding tubulin intensity was determined. The values of all three experiments were plotted. The ratios between groups were calculated using an unpaired, two-tailed t test for the indicated group, compared with the untreated (mock) group and the appropriate time point. (b, d, f and h). * $p<0.05$; ** $p < 0.01$; *** $p < 0.001$. PVDF, Polyvinylidene fluoride.

3.1.4.2 DBs devoid of the PC, induce an increase in MX1 expression in ECs

Previous work by others had shown, that IRGs and inflammatory cytokines are robustly induced independent of HCMV replication [77]. Furthermore, cells treated with HCMV glycoprotein B (gB) strongly induced IRGs [120]. To test, if mere interaction of DBs with the host cell membrane in the absence of membrane fusion was already sufficient for IRG-induction, ECs were incubated with DBs lacking the PC. In this setting, membrane fusion is not initiated due to the lack of the PC. Cell lysates were collected and subjected to immunoblot analysis using antibodies directed against STAT1, MX1, IFIT3 and ISG15 (Fig.13). Except for MX1, no significant increase in IRG-upregulation was observed in ECs exposed to DBs-PC- in the time course of three days. MX1 expression levels were elevated at 24 h.p.a and continued to increase until 72 h.p.a (Fig. 13c). The MX1 expression in EC exposed to PC-negative DBs was lower that the expression of MX1 in PC-positive DBS treated ECs.

Altogether these data indicate that the upregulation of selected IRGs is dependent on the internalization of DBs into the cell. For some of the IRGs the interaction with the plasma membrane seems to be sufficient to induce an upregulation.

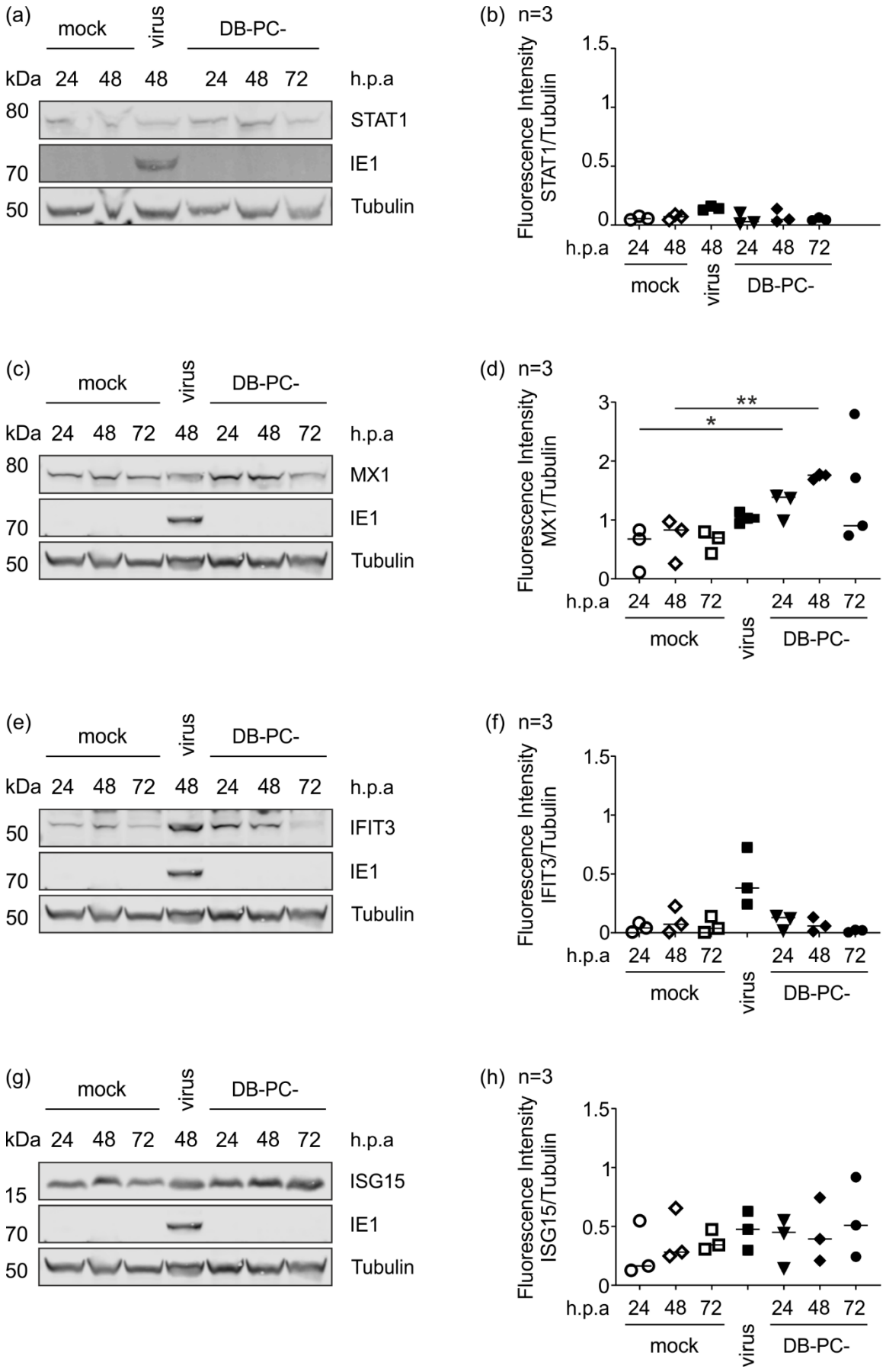
(a)
mock
virus
DB-PC-
kDa 24 48 48 24 48 72 h.p.a
80
STAT1
70
IE1
50
Tubulin
(b) n=3
Fluorescence Intensity STAT1/Tubulin
1.5
1
0.5
0
h.p.a 24 48 48 24 48 72
mock
virus
DB-PC-
(c)
mock
virus
DB-PC-
kDa 24 48 72 48 24 48 72 h.p.a
80
MX1
70
IE1
50
Tubulin
(d) n=3
Fluorescence Intensity MX1/Tubulin
**
*
3
2
1
0
h.p.a 24 48 72 24 48 72
mock
virus
DB-PC-
(e)
mock
virus
DB-PC-
kDa 24 48 72 48 24 48 72 h.p.a
50
IFIT3
70
IE1
50
Tubulin
(f) n=3
Fluorescence Intensity IFIT3/Tubulin
1.5
1
0.5
0
h.p.a 24 48 72 24 48 72
mock
virus
DB-PC-
(g)
mock
virus
DB-PC-
kDa 24 48 72 48 24 48 72 h.p.a
15
ISG15
70
IE1
50
Tubulin
(h) n=3
Fluorescence Intensity ISG15/Tubulin
1.5
1
0.5
0
h.p.a 24 48 72 24 48 72
mock
virus
DB-PC-

Fig. 13. DBs, devoid of the PC, only induce an increase in MX1 expression in ECs. Representative immunoblots of IRGs expression levels in ECs after treatment with DBs. For immunoblot analysis, 40 µg of UV-inactivated PC-negative DBs of the HCMV strain RV-Towne-BAC (DBs-PC-) were applied to 6x10exp5 endothelial cells. Control cells were left untreated (mock) or infected with HCMV strain RV-Towne-repΔGFP (300 genomes per cell, virus). Cell lysates were prepared at 24, 48, and 72 h.p.a. Following SDS-PAGE and transfer onto a PVDF-membrane, the proteins were visualized using antibodies specific for STAT1, MX1, IFIT3 and ISG15 (a, c, e and g). Infection was confirmed by antibody-staining of viral IE1-protein. Tubulin indicated the amount of loaded protein. For quantification the ratio of the fluorescence intensity of each protein and the corresponding tubulin intensity was determined. The values of all three experiments were plotted and comparisons between groups were calculated using an unpaired, two-tailed t test for the indicated group compared with the untreated (mock) group and the appropriate time point (b, d, f and h). * $p<0.05$; ** $p < 0.01$; *** $p < 0.001$. BAC, Bacterial Artificial Chromosome

3.1.5 Impact of DBs on the cellular proteome of monocytes

Monocytes are primary targets of HCMV infection *in vivo* and play a pivotal role in viral dissemination and the establishment of latency and persistence in the host tissue [20, 121, 122]. However, viral gene expression or replication is restricted in monocytes until their differentiation into macrophages [25, 123]. Furthermore, monocytes have a short lifespan in circulation of around 48-72 h [124]. Based on published reports, it has been suggested that HCMV establishes a pro-viral phenotype in monocytes that is directed towards macrophage differentiation. By extending the survival of infected monocytes, HCMV enables viral spread, effective viral replication and persistence [125-127]. DBs stimulated the secretion of inflammatory cytokines in monocytes, promoting viral dissemination [127, 128]. To obtain an understanding of cellular changes in monocytes following DBs exposure, proteomic analyses were performed.

3.1.5.1 Proteins enriched in defence response, exocytosis and cell death were altered in monocytes exposed to DBs

Incoming virus particles stimulated the secretion of inflammatory cytokines in monocytes, what is thought to promote viral dissemination [127]. To obtain an understanding of cellular changes in monocytes following DBs exposure, proteomic analyses were performed.

For compilation of the data, analyses from six independent donors were used. Proteins with a minimum fold-change of 1.5 up- or downregulation in one technical replicate of at least three of six donors were considered as regulated by DBs. Proteins, that showed another regulation direction in the donor were accepted. The heatmap in Figure 14a shows a hierarchical cluster of the 30 proteins that were identified to be regulated in monocytes exposed to PC-negative as well as PC-positive DBs. Another 27 proteins were regulated by only PC-negative DBs (Fig. 11b) and 20 by only PC-positive DBs (Fig.14c). Except for Immunoglobulin kappa constant (IGKC,↑), Pleckstrin homology domain-containing family O member 2 (PLEKHO2,↑), 40S ribosomal protein S2 (RPS2,↑) and 40S ribosomal protein S25 (RPS25,↑), all proteins are known to be IRGs (S9,10). Analysis of functional classifications revealed that the majority of the upregulated proteins was mainly involved in biological processes of defence response, exocytosis and cell death (Fig.14d, e, f). Strikingly, proteins involved in lipid metabolism were downregulated (Fig. 14a, S11). STRING analysis revealed functional interactions between the 30 proteins, that were found to be regulated by both, PC-negative and PC-positive DBs (Fig. 14A,S12,13). Three major clusters with proteins related to defence response (red), exocytosis (green) and lipid metabolism (yellow) evolved (Fig. 14A). Especially proteins involved in defence response and exocytosis were densely connected and overlapped. (Fig. 14A a). When these proteins were entered for STRING analysis, again to generate subnetworks, the proteins clustered in two separate subnetworks with no connecton between the networks. (Fig. 14A b, c). The network map of the 27 proteins regulated by only PC-negative DBs (Fig.14B,S12) segregated into three networks representing functions in defence response, exocytosis and translation (Fig.14B). Again, proteins that contributed to defence response were also active in exocytosis. The cluster related to translation comprised upregulated ribosomal subunits RPL7A, RPS16, RPS25 and RPS7 as well as the RNA- helicase DDX3X. The 20 proteins which were regulated by PC-positive DBs shared biological functions in defence response, endocytosis and exocytosis and ER translocation (Fig. 14C a-e). The analysis revealed a very modest functional interaction pattern of the regulated proteins (Fig. 14 C,a).

(a)

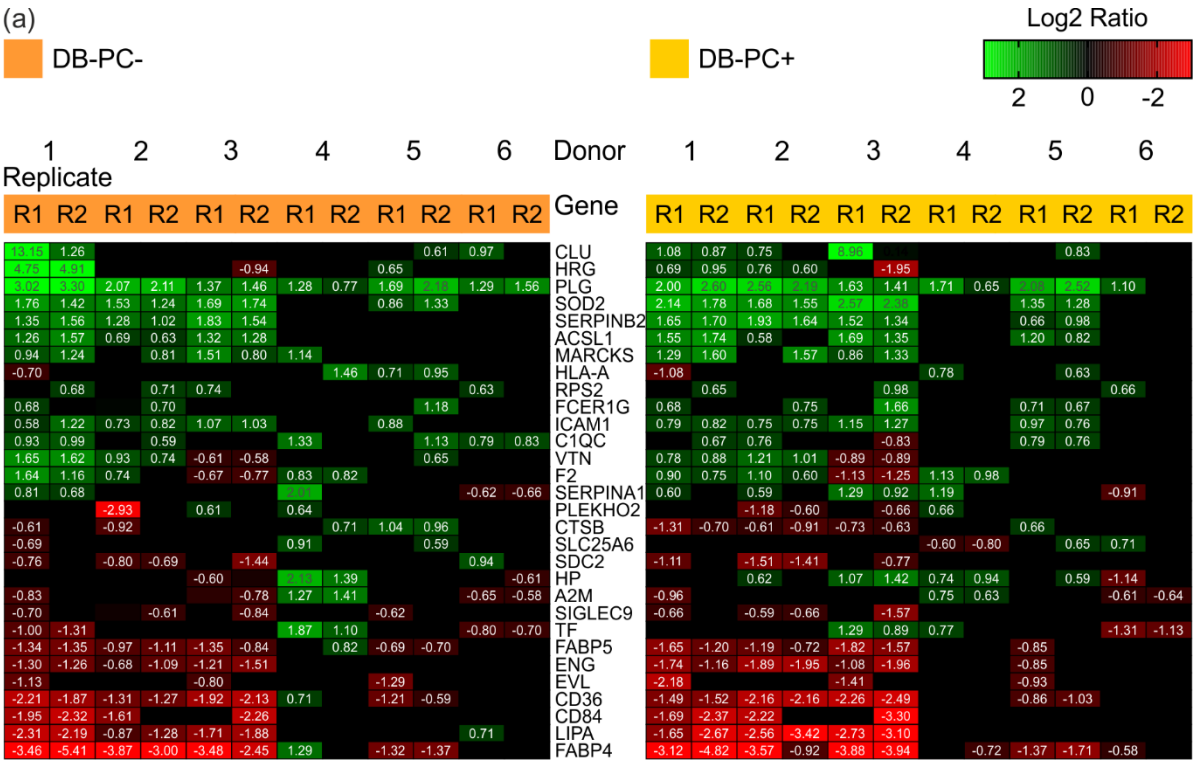

(b)

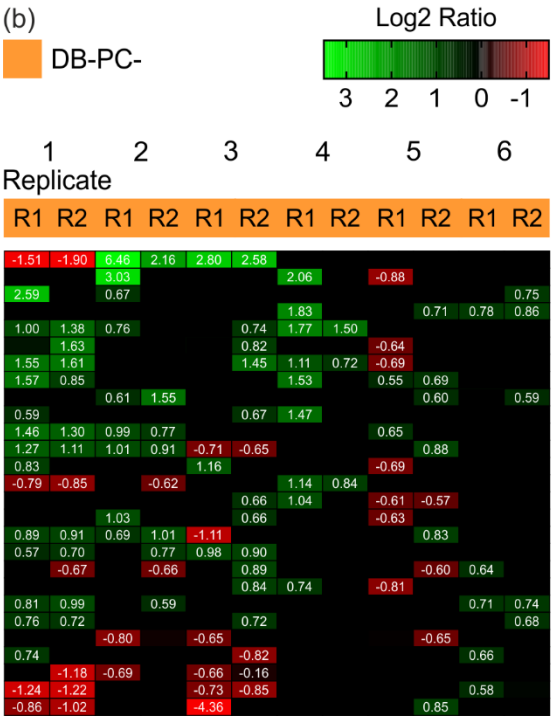

Gene	Protein name
HIST2H2AB	Histone H2A type 2-B
RPS7	40S ribosomal protein S7
CLEC5A	C-type lectin domain family 5 member A
CP	Ceruloplasmin
C4A	Complement C4-A
S100A4	Protein S100-A4
S100A8	Protein S100-A8
RPS7	40S ribosomal protein S7
DDX3X	ATP-dependent RNA helicase DDX3X
RPS16	40S ribosomal protein S16
FGA	Fibrinogen alpha chain
FGG	Fibrinogen gamma chain
CDC37	Hsp90 co-chaperone Cdc37
CTSS	Cathepsin S
COTL1	Coactosin-like protein
CCL24	C-C motif chemokine 24
FGB	Fibrinogen beta chain
MMP9	Matrix metalloproteinase-9
SH3BGRL3	SH3 domain-binding glutamic acid-rich-like protein 3
PFN1	Profilin-1
C1QC	Complement C1q subcomponent subunit C
RPS25	40S ribosomal protein S25
M6PR	Cation-dependent mannose-6-phosphate receptor
RPL7A	60S ribosomal protein L7a
NPC2	NPC intracellular cholesterol transporter 2
PECAM1	Platelet endothelial cell adhesion molecule
NUCB1	Nucleobindin-1

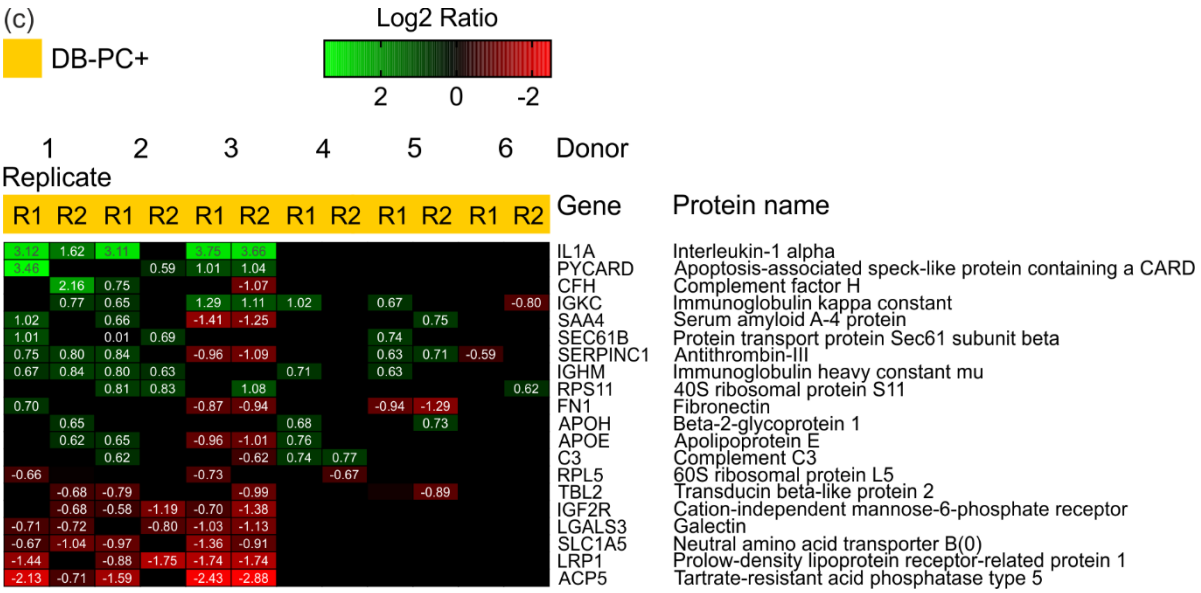
(c)
DB-PC+
Log2 Ratio
2
0
-2
1
2
3
4
5
6
Donor
Replicate
R1 R2 R1 R2 R1 R2 R1 R2 R1 R2 R1 R2
Gene
Protein name
IL1A Interleukin-1 alpha
PYCARD Apoptosis-associated speck-like protein containing a CARD
CFH Complement factor H
IGKC Immunoglobulin kappa constant
SAA4 Serum amyloid A-4 protein
SEC61B Protein transport protein Sec61 subunit beta
SERPINC1 Antithrombin-III
IGHM Immunoglobulin heavy constant mu
RPS11 40S ribosomal protein S11
FN1 Fibronectin
APOH Beta-2-glycoprotein 1
APOE Apolipoprotein E
C3 Complement C3
RPL5 60S ribosomal protein L5
TBL2 Transducin beta-like protein 2
IGF2R Cation-independent mannose-6-phosphate receptor
LGALS3 Galectin
SLC1A5 Neutral amino acid transporter B(0)
LRP1 Prolow-density lipoprotein receptor-related protein 1
ACP5 Tartrate-resistant acid phosphatase type 5

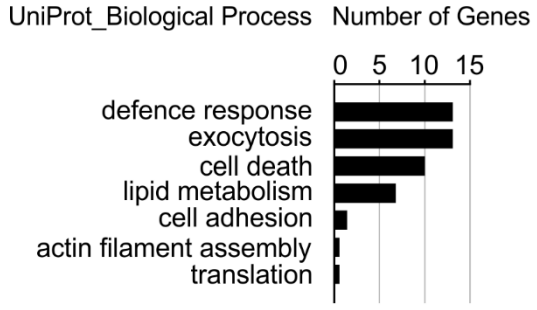
(d)
DB-PC- and DB-PC+
UniProt_Biological Process
Number of Genes
0 5 10 15
defence response
exocytosis
cell death
lipid metabolism
cell adhesion
actin filament assembly
translation

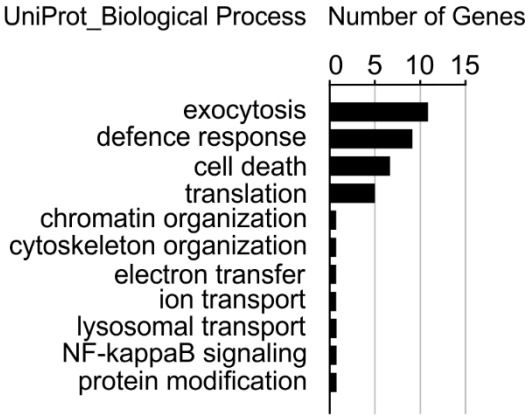
(e)
DB-PC-
UniProt_Biological Process
Number of Genes
0 5 10 15
exocytosis
defence response
cell death
translation
chromatin organization
cytoskeleton organization
electron transfer
ion transport
lysosomal transport
NF-kappaB signaling
protein modification

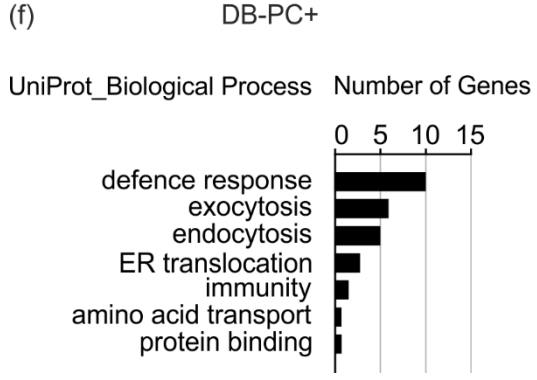
(f)
DB-PC+
UniProt_Biological Process
Number of Genes
0 5 10 15
defence response
exocytosis
endocytosis
ER translocation
immunity
amino acid transport
protein binding

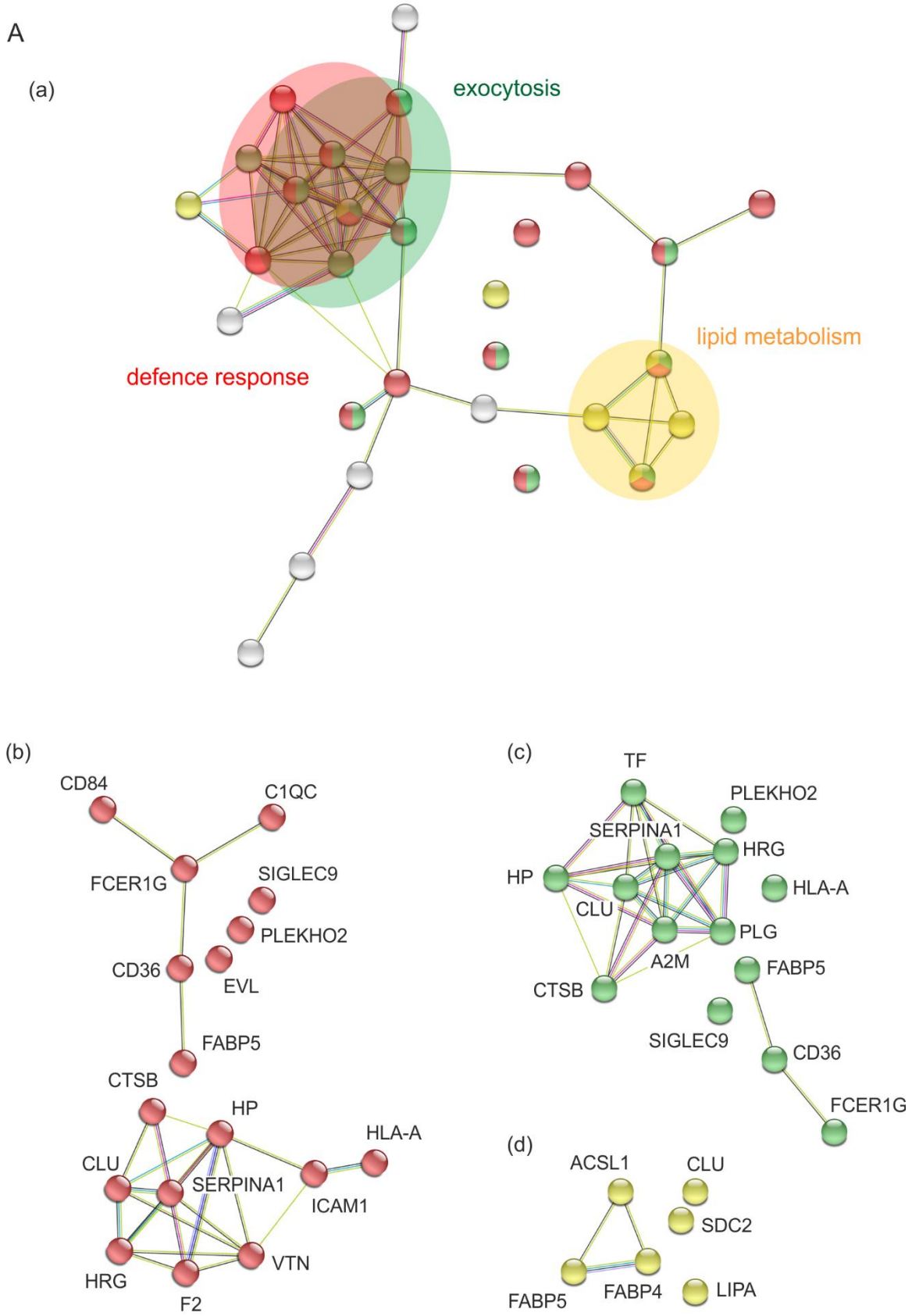
A
(a)
exocytosis
lipid metabolism
defence response
(b)
CD84
C1QC
FCER1G
SIGLEC9
PLEKHO2
CD36
EVL
FABP5
CTSB
HP
HLA-A
CLU
SERPINA1
ICAM1
VTN
HRG
F2
(c)
TF
PLEKHO2
SERPINA1
HRG
HP
HLA-A
CLU
PLG
A2M
FABP5
CTSB
SIGLEC9
CD36
FCER1G
(d)
ACSL1
CLU
SDC2
FABP5
FABP4
LIPA
Interaction evidence
From curated databases
Gene fusions
Co-expression
Textmining
Experimentally determined
Gene co-occurrence
Protein homology

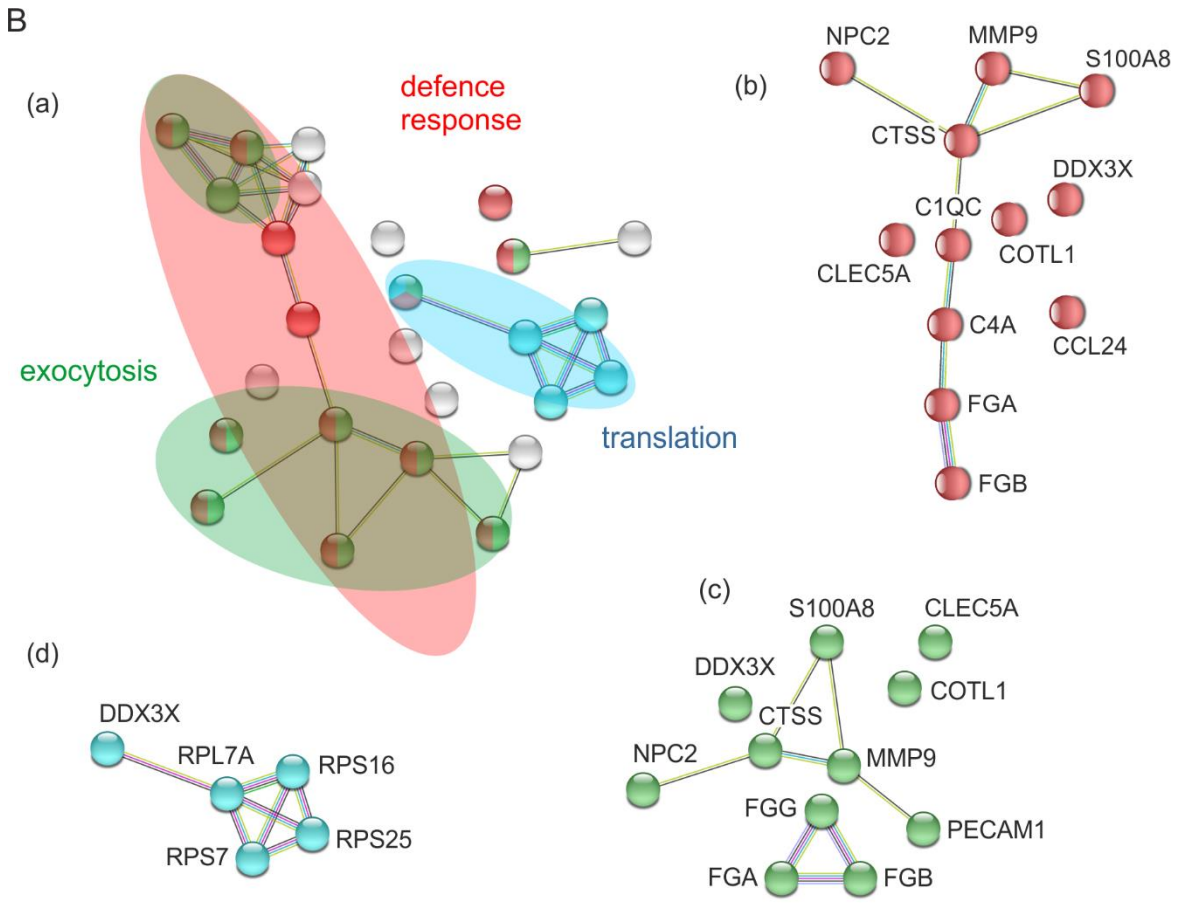
B
(a)
defence response
exocytosis
translation
(b)
NPC2
MMP9
S100A8
CTSS
DDX3X
C1QC
COTL1
CLEC5A
C4A
CCL24
FGA
FGB
(c)
S100A8
CLEC5A
DDX3X
COTL1
CTSS
NPC2
MMP9
FGG
PECAM1
FGA
FGB
(d)
DDX3X
RPL7A
RPS16
RPS25
RPS7

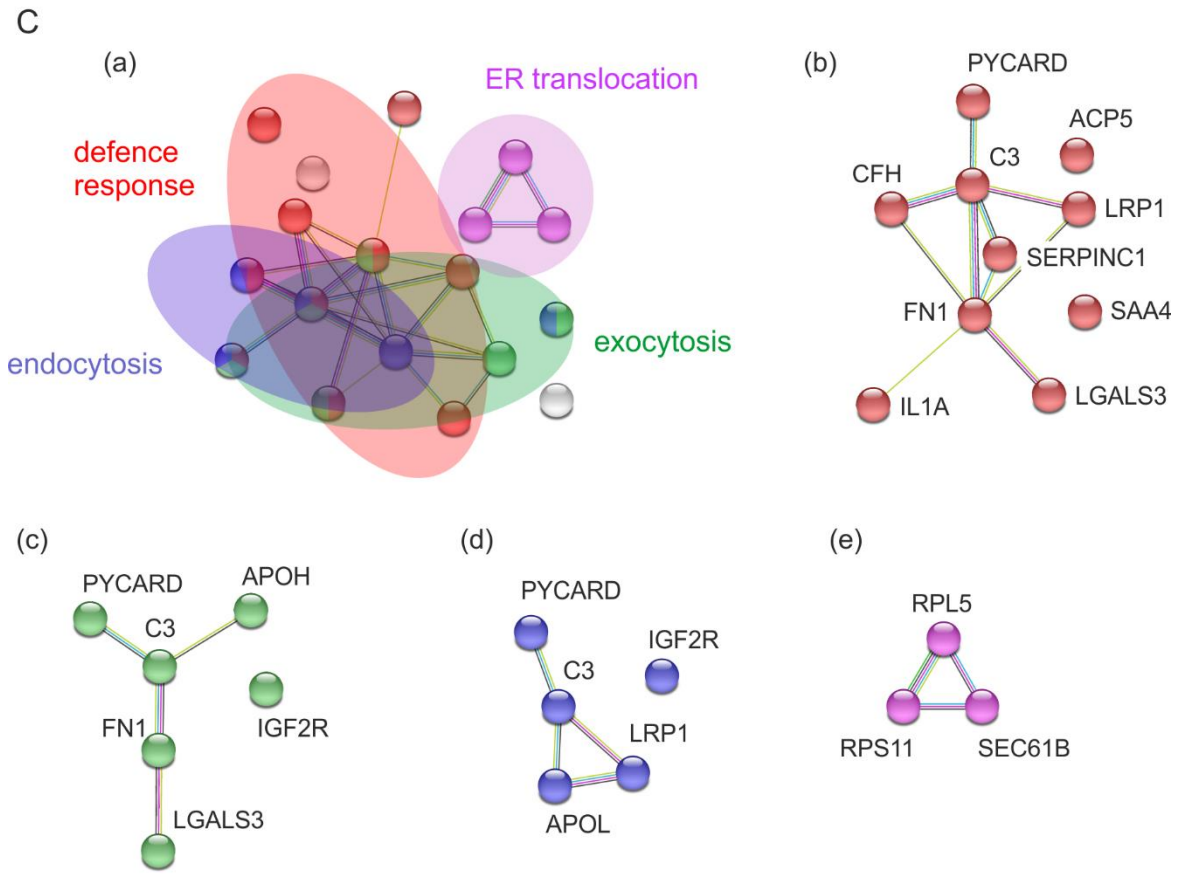
C
(a)
ER translocation
defence response
endocytosis
exocytosis
(b)
PYCARD
ACP5
C3
CFH
LRP1
SERPINC1
FN1
SAA4
IL1A
LGALS3
(c)
PYCARD
APOH
C3
FN1
IGF2R
LGALS3
(d)
PYCARD
IGF2R
C3
LRP1
APOL
(e)
RPL5
RPS11
SEC61B

Fig. 14. Biological processes of defence response, exocytosis and cell death are enriched in monocytes exposed to DBs. Heatmap of the differentially regulated proteins which were found in monocytes exposed to both, PC-negative and PC-positive DBs (a). Proteins that only were found to be regulated in PC-negative (b) or PC-positive (c) DBs were depicted separately. Each row represents a protein and two colums represent the two technical replicates (R1; R2) of one donor. Regulated proteins with a minimum log2ratio ± 0.58 in one technical replicate of at least three of six donors were hierarchically arranged.The log2Ratio is represented with a colour gradient. Green indicates upregulation, red downregulation. Black areas represent values that did not reach the threshold of ±0.58. (d) Functional classification of the identified proteins according to biological processes based on GO analysis using the UniProtKB database. The y-axis represents biological processes categories, while the x-axis indicates the number of genes involved in each category. **A-C** STRING analysis of PPI network of regulated proteins affected by DBs-PC- or DBs-PC+ (A), only by DBs-PC- (B) and only by DBs-PC+(C). Each node represents a protein. The coloured lines between the proteins indicate the type of interaction evidence according to the STRING network database. The networks were generated with a minimum required interaction confidence level of 0.4.

3.1.6 Impact of DBs on the cellular proteome of immature dendritic cells (iDCs)

Dendritic cells (DC) are specialized antigen-presenting cells (APCs) that are important for the immune response against invading microorganisms. Immature DCs reside in peripheral tissues and become activated upon contact to pathogens. MHC class I and II molecules present the captured pathogen- derived antigens to immature DCs, which mature (mDCs) and migrate to lymph nodes to prime naïve T cells. mDCs are fully permissive to HCMV replication [129], but infection of these cells is restricted to strains expressing the viral genes UL128 to UL131A [33, 35]. Regarding HCMV, some studies reported that HCMV infection inhibited DC maturation, downregulated MHC class I and class II molecules and decreased cytokine release [130-132]. Surprisingly, the incubation of iDCs with DBs induced their maturation and activation towards a myeloid DC (mDC) phenotype [73]. To investigate the impact of DBs on the proteome of iDCs, MS analyses were also performed on these cells.

Human iDCs were generated from peripheral blood mononuclear cells (PBMC) were exposed to 20 µg of PC-positive DBs for 24 hours. Cells were then subjected to MS. Based on the MS data, the mean of 2414 protein were identified from 3 different donors. The proteins were sorted according to their log2 transformed expression ratio and plotted in a heatmap (Fig.15a, b, c) Proteins with a minimum fold-change of 1.5 up- or downregulation (log2Ratio of ±0.58) in one technical replicate of at least two of the donors were considered as regulated by DBs. Among the regulated proteins, 19 were detected in iDCs exposed to both PC-negative or PC-positive DBs (Fig.15a, S14). Remarkably, all these proteins were upregulated by PC-positive

DBs (Fig.15a, heatmap on the right, S15). In iDCs treated with PC-negative DBs, seven proteins were downregulated in at least one of the donors (Fig.15a, heatmap on the left). Ten proteins were regulated in iDC only treated with PC-negative DBs and only four proteins comprising Long-chain-fatty-acid--CoA ligase 1(ACSL1), Interferon-induced protein with tetratricopeptide repeats 3 (IFIT3), Raftlin (RFTN1) and Transferrin receptor protein 1 (TFRC) were upregulated in iDCs by PC-positive DBs. To elucidate the biological processes in iDCs affected by DBs, a GO analysis was conducted (S16). Most of the upregulated proteins were related to biological processes of exocytosis, antiviral defence, antigen processing and presentation and endocytosis (Fig. 15d). All regulated proteins were entered into STRING database to identify possible physical and functional interactions between the proteins. The PPI network in Fig. 15e shows two interacting clusters comprised of antiviral defence (red) and protein translation (yellow) and one cluster of interacting proteins associated with exocytosis (green). Proteins related to antigen processing and presentation are distributed in the network (purple). When the proteins of each cluster were submitted to STRING analysis again, most of them clustered in subnetworks and interacted with each other (Fig.15 f-h). Only the proteins related to antigen processing and presentation did not interact (Fig. 15 i).

(a)

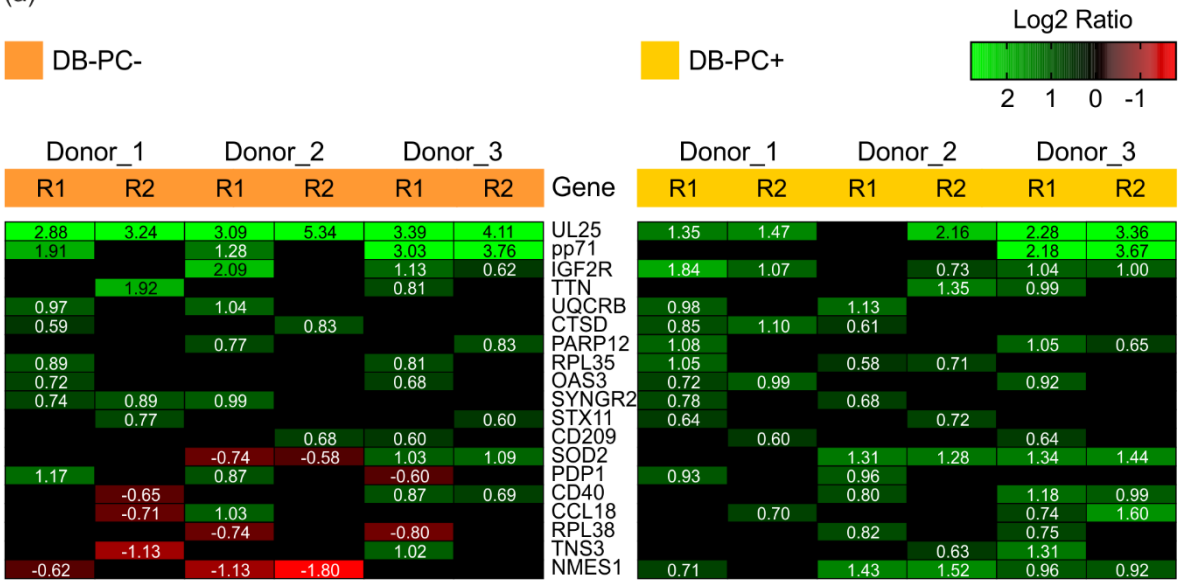
DB-PC-
DB-PC+
Log2 Ratio
2 1 0 -1
Donor_1 Donor_2 Donor_3
R1 R2 R1 R2 R1 R2
Gene
UL25 2.88 3.24 3.09 5.34 3.39 4.11
pp71 1.91 1.28 3.03 3.76
IGF2R 2.09 1.13 0.62
TTN 1.92 0.81
UQCRB 0.97 1.04
CTSD 0.59 0.83
PARP12 0.77 0.83
RPL35 0.89 0.81
OAS3 0.72 0.68
SYNGR2 0.74 0.89 0.99
STX11 0.77 0.60
CD209 0.68 0.60
SOD2 -0.74 -0.58 1.03 1.09
PDP1 1.17 0.87 -0.60
CD40 -0.65 0.87 0.69
CCL18 -0.71 1.03
RPL38 -0.74 -0.80
TNS3 -1.13 1.02
NMES1 -0.62 -1.13 -1.80
Donor_1 Donor_2 Donor_3
R1 R2 R1 R2 R1 R2
1.35 1.47 2.16 2.28 3.36
2.18 3.67
1.84 1.07 0.73 1.04 1.00
1.35 0.99
0.98 1.13
0.85 1.10 0.61
1.08 1.05 0.65
1.05 0.58 0.71
0.72 0.99 0.92
0.78 0.68
0.64 0.72
0.60 0.64
1.31 1.28 1.34 1.44
0.93 0.96
0.80 1.18 0.99
0.70 0.74 1.60
0.82 0.75
0.63 1.31
0.71 1.43 1.52 0.96 0.92

(b)

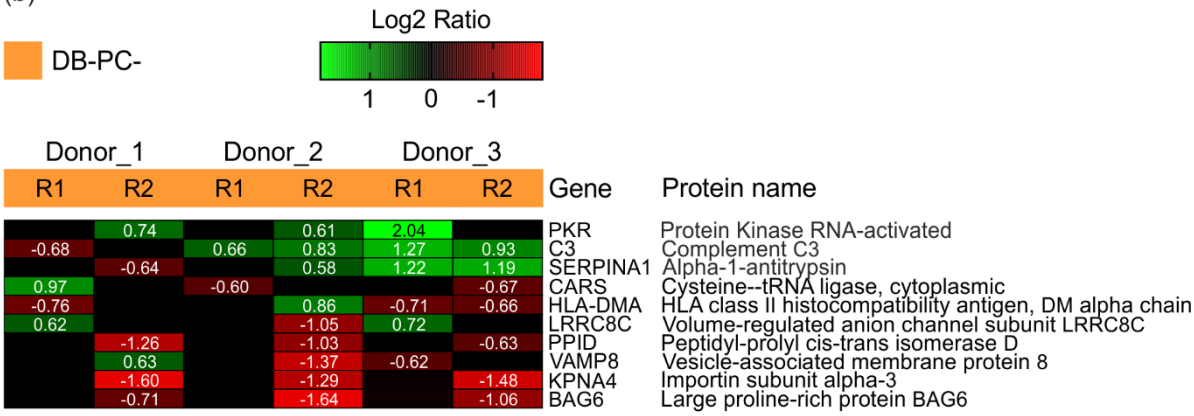
DB-PC-
Log2 Ratio
1 0 -1
Donor_1 Donor_2 Donor_3
R1 R2 R1 R2 R1 R2
Gene
Protein name
PKR 0.74 0.61 2.04 Protein Kinase RNA-activated
C3 -0.68 0.66 0.83 1.27 0.93 Complement C3
SERPINA1 -0.64 0.58 1.22 1.19 Alpha-1-antitrypsin
CARS 0.97 -0.60 -0.67 Cysteine--tRNA ligase, cytoplasmic
HLA-DMA -0.76 0.86 -0.71 -0.66 HLA class II histocompatibility antigen, DM alpha chain
LRRC8C 0.62 -1.05 0.72 Volume-regulated anion channel subunit LRRC8C
PPID -1.26 -1.03 -0.63 Peptidyl-prolyl cis-trans isomerase D
VAMP8 0.63 -1.37 -0.62 Vesicle-associated membrane protein 8
KPNA4 -1.60 -1.29 -1.48 Importin subunit alpha-3
BAG6 -0.71 -1.64 -1.06 Large proline-rich protein BAG6

(c)

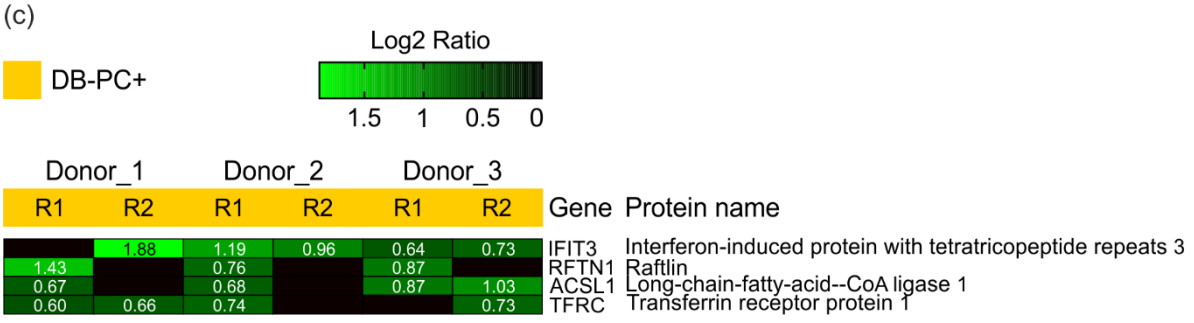
DB-PC+
Log2 Ratio
1.5 1 0.5 0
Donor_1 Donor_2 Donor_3
R1 R2 R1 R2 R1 R2
Gene
Protein name
IFIT3 1.88 1.19 0.96 0.64 0.73 Interferon-induced protein with tetratricopeptide repeats 3
RFTN1 1.43 0.76 0.87 Raftlin
ACSL1 0.67 0.68 0.87 1.03 Long-chain-fatty-acid--CoA ligase 1
TFRC 0.60 0.66 0.74 0.73 Transferrin receptor protein 1

(d)

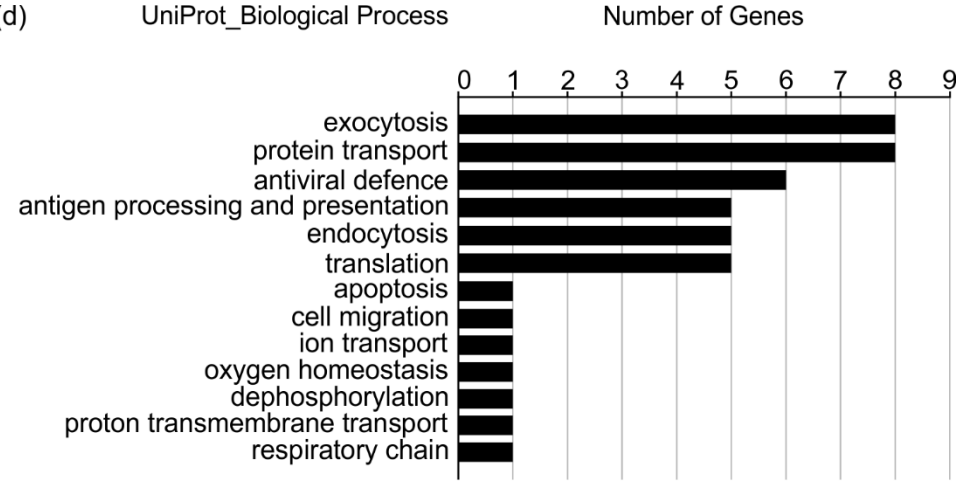
UniProt_Biological Process
Number of Genes
0 1 2 3 4 5 6 7 8 9
exocytosis
protein transport
antiviral defence
antigen processing and presentation
endocytosis
translation
apoptosis
cell migration
ion transport
oxygen homeostasis
dephosphorylation
proton transmembrane transport
respiratory chain

(e)

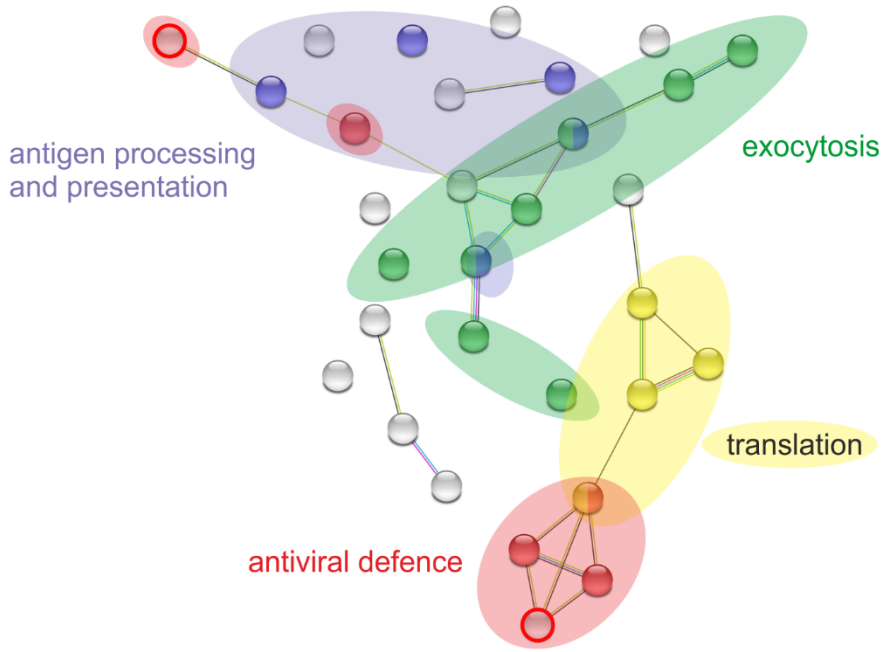
antigen processing
and presentation
exocytosis
translation
antiviral defence

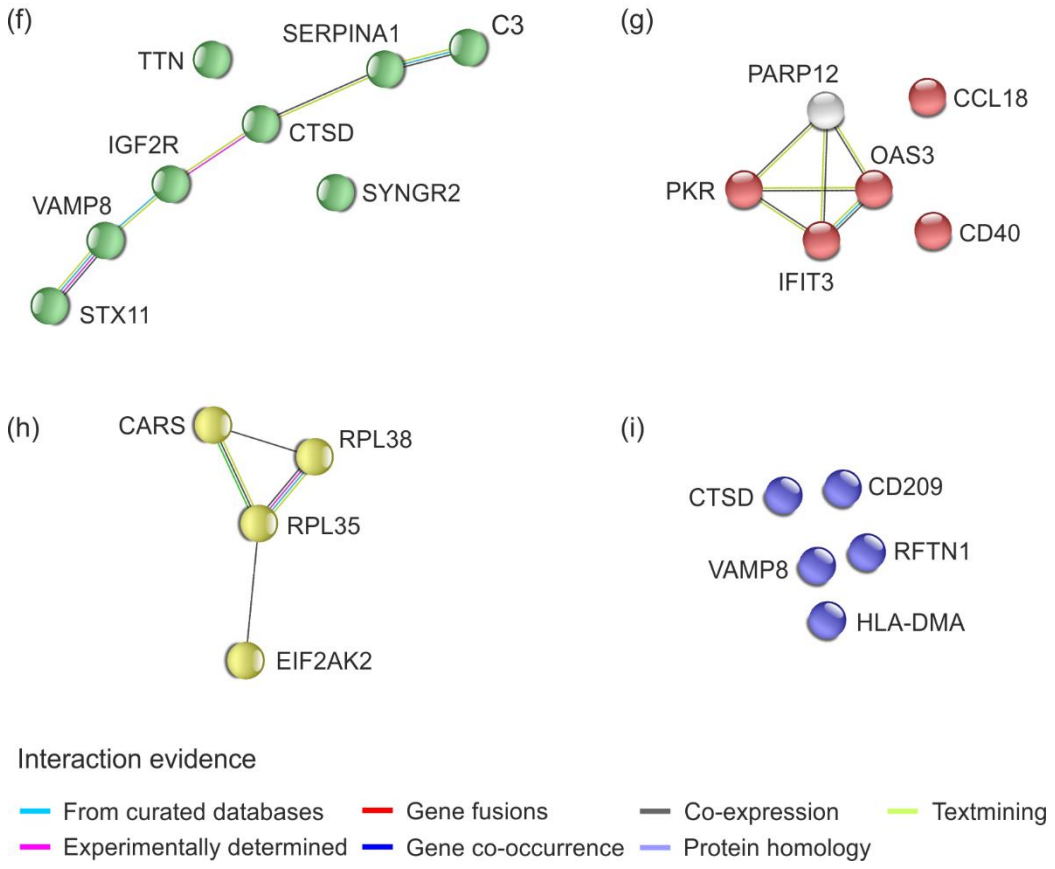

Fig. 15. Biological processes of exocytosis, protein transport and antiviral defence are stimulated in iDCs exposed to DBs. Heatmap of the differentially regulated proteins in iDCs exposed to PC-negative or PC-positive DBs (DB-PC-; DB-PC+) (a), to only PC-negative DBs (b) and to only PC-positive DBs (c) after 24 h. Each row represents a protein and two colums represent the two technical replicates (R1; R2) of one donor. Regulated proteins with a minimum log2ratio ± 0.58 in one technical replicate of at least two of three donors were hierarchically arranged.The log2Ratio is represented with a colour gradient. Green indicates upregulation, red downregulation. Black areas represent values that did not reach the threshold of ±0.58. (d) Functional classification of the identified proteins according to biological processes based on Gene Ontology GO analysis using the UniProtKB database. The y-axis represents biological processes categories, while the x-axis indicates the number of genes involved in each category. (e-i) STRING analysis of protein-protein interaction (PPI) network of DB-regulated proteins . Each node represents a protein. The coloured lines between the proteins indicate the type of interaction evidence according to STRING network database. The networks were generated with a minimum required interaction confidence level of 0.4.

3.2 Involvement of the JAK/STAT signalling pathway in DBs-induced IRGs upregulation.

Canonical induction of IRG transcription is mediated by activation of the Janus tyrosine Kinase/ Signal Transducer and Activator of Transcription (JAK/ STAT) signalling pathway, initiated by type I, II and III IFNs [133, 134]. In the context of HCMV infection, Ashley and colleagues demonstrated that the upregulated transcription of several core IRGs, including IFIT1, IFIT3, MX1 and ISG15 was independent of type I IFN, but required IRF3 activation [135].

To investigate whether the increased expression of the IRGs STAT1, MX1, IFIT3 and ISG15 upon incubation with DBs was dependent on type I IFN- initiated JAK/STAT- signalling or in an IFN- independent manner, JAK inhibitor I (JAK-I.) (synonyms: Pyridone6, P6) was used to block the activity of the Janus kinase family enzymes JAK1, JAK2, JAK3 and TYK2, consequently impairing STAT phosphorylation and the downstream transcription initiation. The effect on IRGs expression was examined by immunoblot (Fig. 16 A, B). HFFs treated with 100U/ ml of IFN-ß (IFN-beta) or with 20 µg of UV- irradiated PC- negative or PC- positive DBs induced strong protein expression levels for all four IRGs after 24h (Fig. 16 A). Blocking the JAK/STAT pathway with JAK-I. abolished the DB-mediated induction of STAT1, MX1 and IFIT3 (Fig. 16A, B). Interestingly, ISG15 protein levels were decreased, but were incompletely reduced to basal levels in samples cotreated with JAK -I, indicating an alternative, JAK/STAT-independent DB-signalling mechanism to be operative in this instance.

Furthermore, a striking difference in the amount of pp65 protein between HFFs incubated with PC- negative or PC- positive DBs was noticed (Fig. 16A). Although the protein concentration of purified DBs was determined via the BCA protein assay kit, the staining for pp65 revealed considerable differences in protein quantity. The tubulin loading control indicated no notable differences. Cell lysates prepared of HFFs incubated with PC-negative DBs had an approximately 9.4-times higher amount in pp65 protein than lysates of HFFs incubated with PC- positive DBs. To investigate the relevance of this difference related to the efficiency to enhance the protein expression levels of IRGs, the fluorescence intensity ratio of each IRG to the corresponding pp65 intensity (IRG/pp65) was calculated (Fig. 16C). The estimated values showed that STAT1, MX1, IFIT3 and ISG15 were more potently induced by DBs expressing the PC compared to PC-negative DBs (Fig.16C).

These results demonstrate that the initiation of IRG expression in HFFs upon DBs treatment relies on the activity of JAKs for signal transduction. Interference of the JAK/STAT signalling pathway abolishes IRG expression completely and cannot be compensated by another pathway, except for ISG15. Furthermore, these data indicated that PC-positive DBs elicit a stronger IRG induction than PC-negative DBs.

A

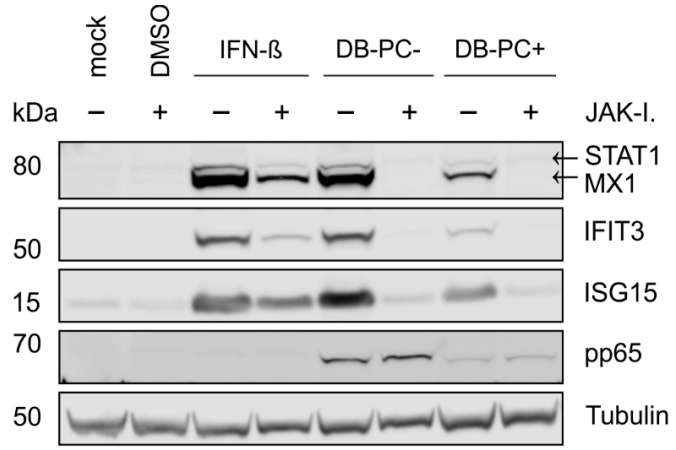
mock
DMSO
IFN-ß
DB-PC-
DB-PC+
kDa
JAK-I.
80
50
15
70
50
STAT1
MX1
IFIT3
ISG15
pp65
Tubulin

B

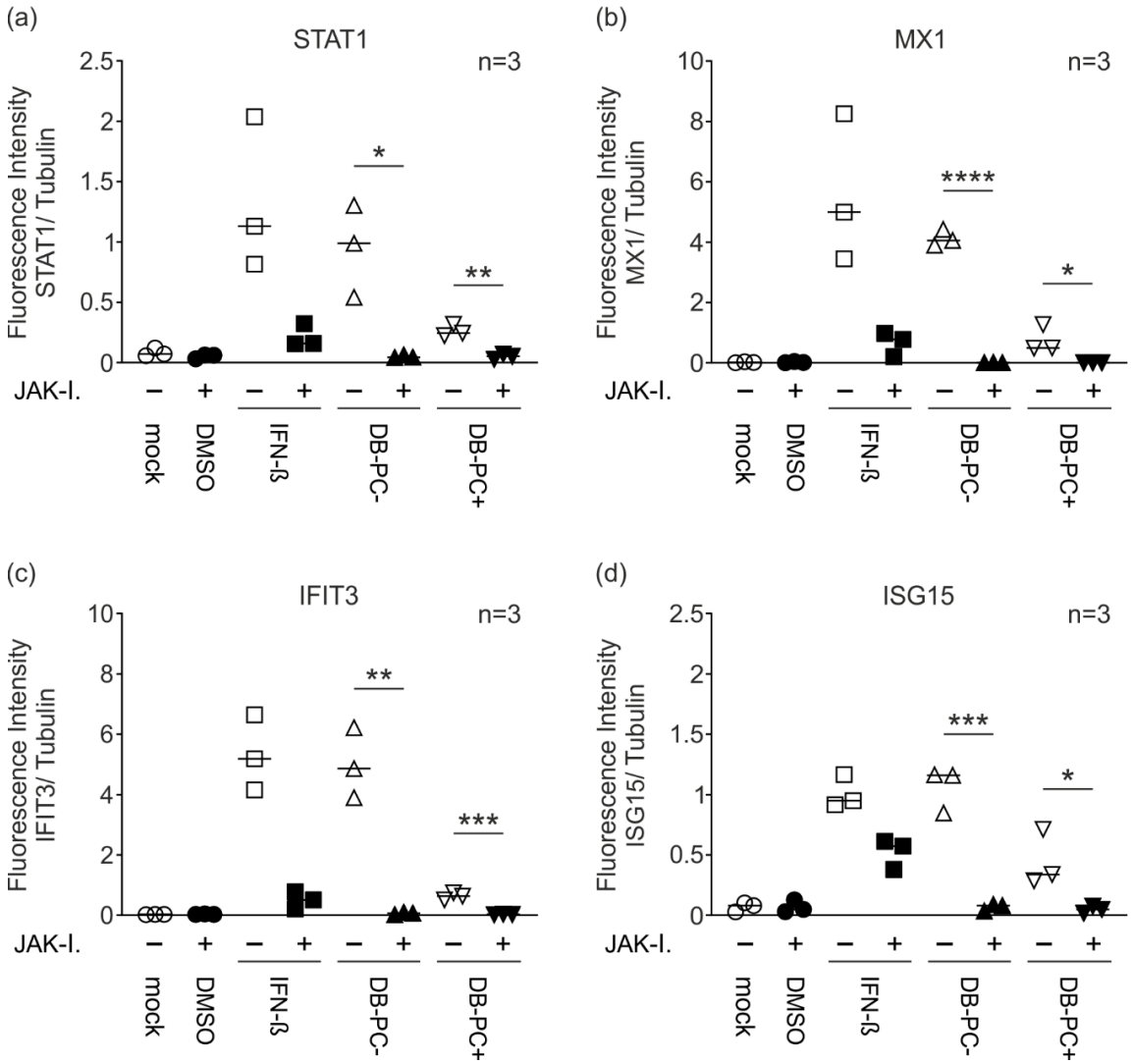
(a)
STAT1
n=3
Fluorescence Intensity
STAT1/ Tubulin
(b)
MX1
n=3
Fluorescence Intensity
MX1/ Tubulin
(c)
IFIT3
n=3
Fluorescence Intensity
IFIT3/ Tubulin
(d)
ISG15
n=3
Fluorescence Intensity
ISG15/ Tubulin
JAK-I.
mock
DMSO
IFN-ß
DB-PC-
DB-PC+

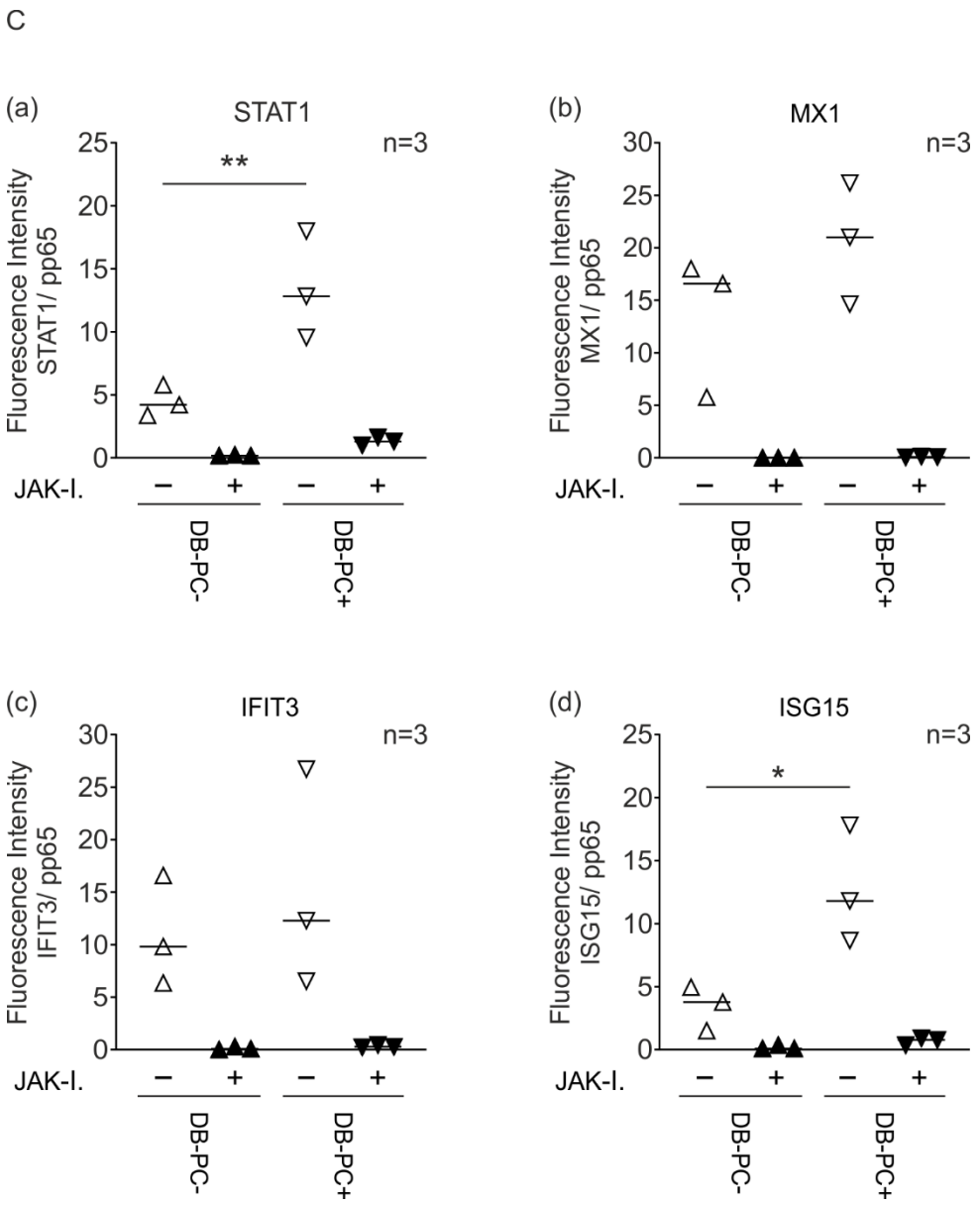

Fig. 16. JAK inhibitor I (JAK-I.) abrogates DBs-induced IRG expression. HFFs were either pre-treated with DMSO or JAK inhibitor I (20 µM/ ml). After one-hour incubation the cells were either left untreated (mock), treated with IFN-ß (100U/ ml) or treated with 20 µg PC- negative (DBs-PC-) or positive (DBs-PC+) DBs respectively. Each sample was further co-treated with JAK inhibitor I for 24 hours. **A** Representative immunoblot analysis of STAT1 expression and the downstream IRG protein levels of MX1, IFIT3 and ISG15 in HFFs upon JAK inhibitor I treatment compared to untreated control cells. IFN-ß treatment was used to assess the effects on JAK/STAT signalling cascade. Tubulin was used as protein loading control. Pp65 was used as DBs internalization control. All samples for the respective antibody were analysed on the same membrane. **B** For immunoblot quantification the ratio of the fluorescence intensity IRG to tubulin (IRG/Tubulin) was calculated for each protein (B a, b, c and d). The values of three independent experiments were plotted. Comparisons between groups were calculated using an unpaired, two-tailed t test for the DBs and the JAK-I. treated group,

compared with the appropriate untreated group. * p<0.05; **p < 0.01; ***p < 0.001. **C** Comparison of protein expression levels between DBs-PC- and DBs-PC+, dependent on the amount of pp65.

3.3 Endocytosis as optional pathway for the uptake of DBs into HFFs and ECs

3.3.1 Inhibition of dynamin-dependent endocytosis delayed the uptake of DBs into HFFs

HCMV is generally assumed to enter fibroblasts by direct fusion with the plasma membrane in a pH-independent process [136, 137]. However, macropinocytosis was suggested as an alternative entry-mechanism for HCMV into fobroblasts [138]. The infection of endothelial (EC), epithelial cells (EPC), or dendritic cells (DC) is dependent on the PC, consisting of gH/gL/UL128-131 [21, 34, 35]. Experiments showed that HCMV particles entered endothelial and epithelial cells by endocytosis followed by low-pH-dependent fusion with endosomes [139, 140].
The inhibitor Dynasore provides a rapid and reversible inhibition of dynamin-dependent endocytosis [141]. Dynasore inhibits the GTPase of dynamin, which is crucial for membrane remodelling and fission of clathrin- coated vesicles formed during endocytosis [141, 142].

To assess whether the inhibition of dynamin-dependent endocytosis affected DBs- entry, HFFs were incubated with 80 µM Dynasore prior to and during DB-incubation. Cells were analysed by immunofluorescence (Fig. 17). PC- negative (DBs-PC-) and PC-positive DBs (DBs-PC+) were analysed. The entry of DBs into HFFs was monitored by pp65 staining (green) in the nucleus (DAPI). The efficiency by which of DBs entered the cells was quantified by counting cells with a pp65- positive staining in the nucleus in absence or in presence of Dynasore at 6 h.p.a and 8 h.p.a. (Fig. 17b, c). The uptake of transferrin (red) was used to monitor endocytosis (Fig. 17 a). Whereas endocytosis of transferrin was inhibited in cells incubated with Dynasore (Fig. 17a), an effective entry of PC-negative DBs was still detected (Fig. 14b). Addition of Dynasore, in contrast led to a significant decrease in the number of pp65-positive cells exposed to PC- positive DBs at 6 h.p.a. However, a slight decrease in pp65-positive cells was still observed at 8 h.p.a (Fig. 17c). Interestingly, when approximately 100 % of the cells exposed to PC-negative DBs were pp65-positive, only 61 % of HFFs incubated with PC-positive DBs showed pp65 in their nucleus at 6 h.p.a, indicating the use of a different, co-existent pathway for entry.

These experiments show that PC-negative DBs do not require endocytosis to enter HFFs. Whereas, the entry of PC-positive DBs is to some extent dependent on dynamin. Furthermore

the results indicate that there is a general delay in the uptake of PC-positive DBs into HFFs when compared to PC-negative DBs.

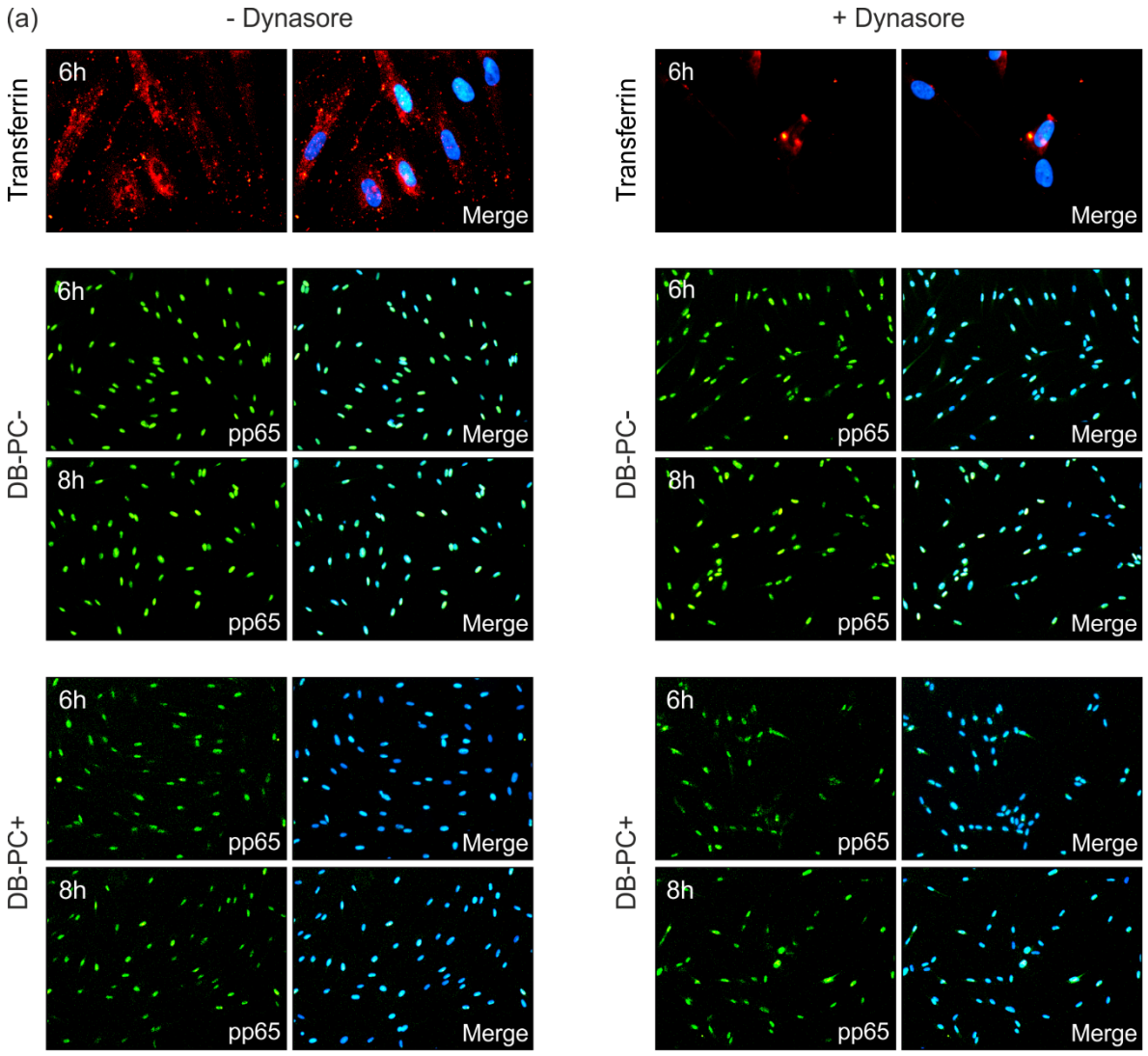
(a)
- Dynasore
+ Dynasore
Transferrin
DB-PC-
DB-PC+
6h
8h
pp65
Merge

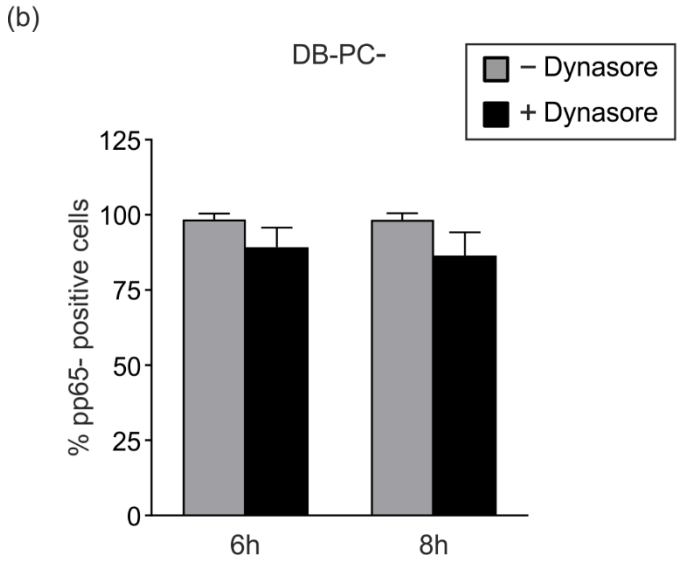
(b)
DB-PC-
– Dynasore
+ Dynasore
% pp65- positive cells
125
100
75
50
25
0
6h
8h

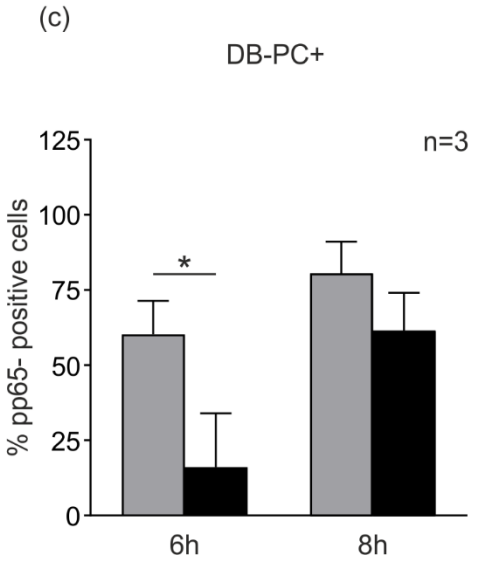
(c)
DB-PC+
n=3
*
% pp65- positive cells
125
100
75
50
25
0
6h
8h

Fig. 17. Inhibition of dynamin-dependent endocytosis delayes the uptake of DBs into HFFs. Immunofluorescence analysis of HFFs exposed to DBs in absence or presence of Dynasore. (a) HFFs were either mock treated (- Dynasore) or pre-incubated with 80 µM Dynasore (+ Dynasore) for 30 min. Cells were subsequently incubated with AlexaFluor546 labeled transferrin (red) or 10 µg of DBs-PC- and DBs-PC+ in absence and presence of 80 µM Dynasore. Cells were fixed with 90% acetone at 6h and 8h post DBs-application. Immunostaining was performed using a pp65-specific antibody (green). DAPI was used to visualize the nuclei. Cells were examined by immunofluorescence microscopy. 25-30 random micrographs representing different areas of the cover slip were taken. Magnification of 100-200x. (b) To calculate the uptake efficiency, approximately 500 cell nuclei (DAPI, blue) were counted for each timepoint. Entry of DBs into the cell was determined by counting pp65- positive cells (green). The percentage of pp65-positive cell was calculated. The data represent mean values ± SD from three independent experiments for each timepoint.

3.3.2 Entry of DBs into ECs was diminished after inhibition of dynamin-dependent endocytosis

Recently published data demonstrated, that only DBs that expressed the PC on their surface were able to enter ECs [75]. Based on this report, only PC- positive DBs were considered to examine the impact of endocytosis- inhibition on their uptake into ECs. For immunofluorescence analyses, ECs were grown on cover slips and incubated with 80 µM Dynasore prior to and during DBs- incubation for 24 h (Fig. 18). As indication for the uptake of DBs, nuclear staining of the major protein pp65 (green) was assessed. The uptake of transferrin (red) was used to monitor endocytosis. The percentage of pp65-positive cells was determined by counting cell nuclei (DAPI) and pp65-positive nuclei (green) in the absence or in presence of Dynasore at 24 h.p.a (Fig 18b). Roughly 47% of ECs showed a nuclear pp65-staining in control cells (- Dynasore). Addition of Dynasore led to a highly significant decrease in the number of pp65-positive cells to 27 % (Fig. 18b).

These experiments showed that inhibition of endocytosis affected the uptake of DBs into ECs.

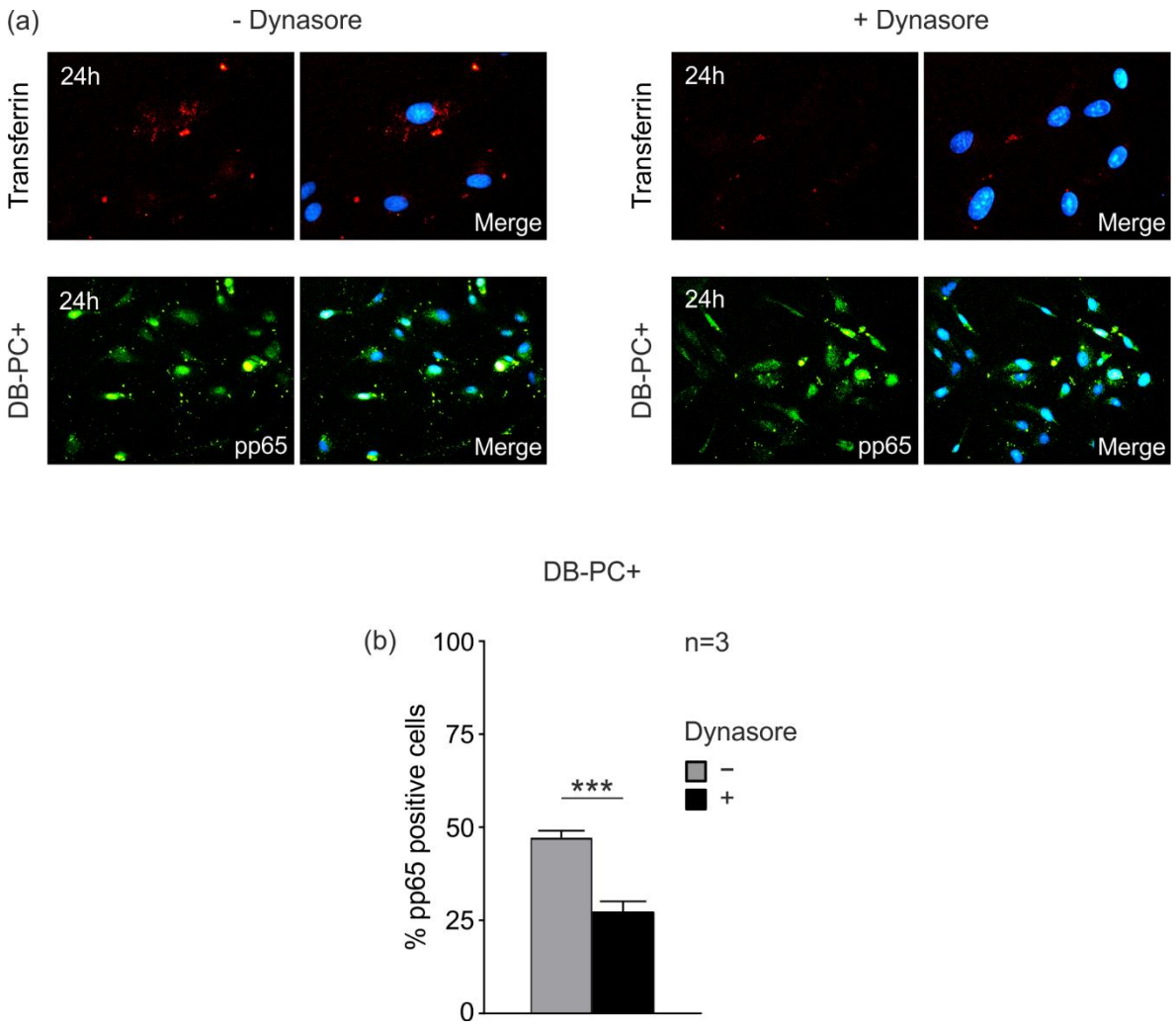

Fig. 18. Incubation of ECs with the dynamin inhibitor Dynasore decreased the uptake of DBs. Inhibition of DBs-uptake into ECs by adding the dynamin inhibitor Dynasore to the culture medium. (a) For immunofluorescence analysis ECs were grown on 0.1% gelatin-covered glass coverslips. Cells were left untreated (- Dynasore) or were pre-incubated with 80 µM Dynasore (+ Dynasore) for 30 min. Subsequently, AlexaFluor546 labeled transferrin or 15 µg of PC-positive DBs (DBs-PC+) were added to the cells together with 80 µM Dynasore. Control cells were incubated without Dynasore. Following fixation in 90% acetone, immunostaining was performed using a pp65-specific antibody. Nuclei were stained by DAPI. Cells were examined by immunofluorescence microscopy. 25-30 random micrographs were taken from the cover slip. Magnification: 200x. (b) To calculate the uptake efficiency, approximately 500 cell nuclei were counted. Entry of DBs into the cells was quantified by counting pp65- positive cells (green). The percentage of pp65-positive cell was determined. The data represent mean values ± SD from three independent experiments.

3.4 Impact of DBs on infected HFFs

3.4.1 DBs abrogate the downregulation of IRG-expression at late stages of HCMV infection

Infected cells release DBs concomitantly with infectious virions. DBs also enter cells together with virions in the process of infection in cell culture [47, 48]. Others have shown that HCMV infection leads to the upregulation of IRG-expression at early time points, followed by a decrease at later stages [77].

To investigate the impact of DBs on the IRGs expression in infected HFFs, immunoblot analyses were performed using antibodies directed against MX1, IFIT3 and ISG15 (Fig.19). In order to ensure the same infection levels in the samples, the viral IE1 protein was carried along (Fig.19e). HFFs infected with the HCMV strain RV-Towne-repΔGFP (virus) exhibited increased expression levels for all three IRGs at 24 h.p.i (Fig. 19b, c and d). Consistent with the observations made by Weekes et al. (2014), these levels decreased at 48 h.p.i. MX1 and IFIT3 protein levels were elevated in cells that were infected and co-treated with DBs at 24 h.p.i and 48 h.p.i compared to the virus control (Fig 19b and c). DBs seemed to antagonize the repression of IRGs by the virus at 48 h.p.i. Interestingly, DBs alone induced a higher expression of MX1 and IFIT3 than cells that were additionally infected with HCMV, indicating an interference caused by the virus. In infected cells that were exposed to DBs, the expression levels of ISG15 stayed at elevated levels comparable to levels of cells treated with DBs alone (Fig. 19d).

These results showed that DBs prevented the decrease in IRG expression levels in late-stage HCMV-infected HFFs. Simultaneously, these data demonstrated that virus infection antagonized DB-induced IRGs expression (compare DB-treated cells +/- virus infection).

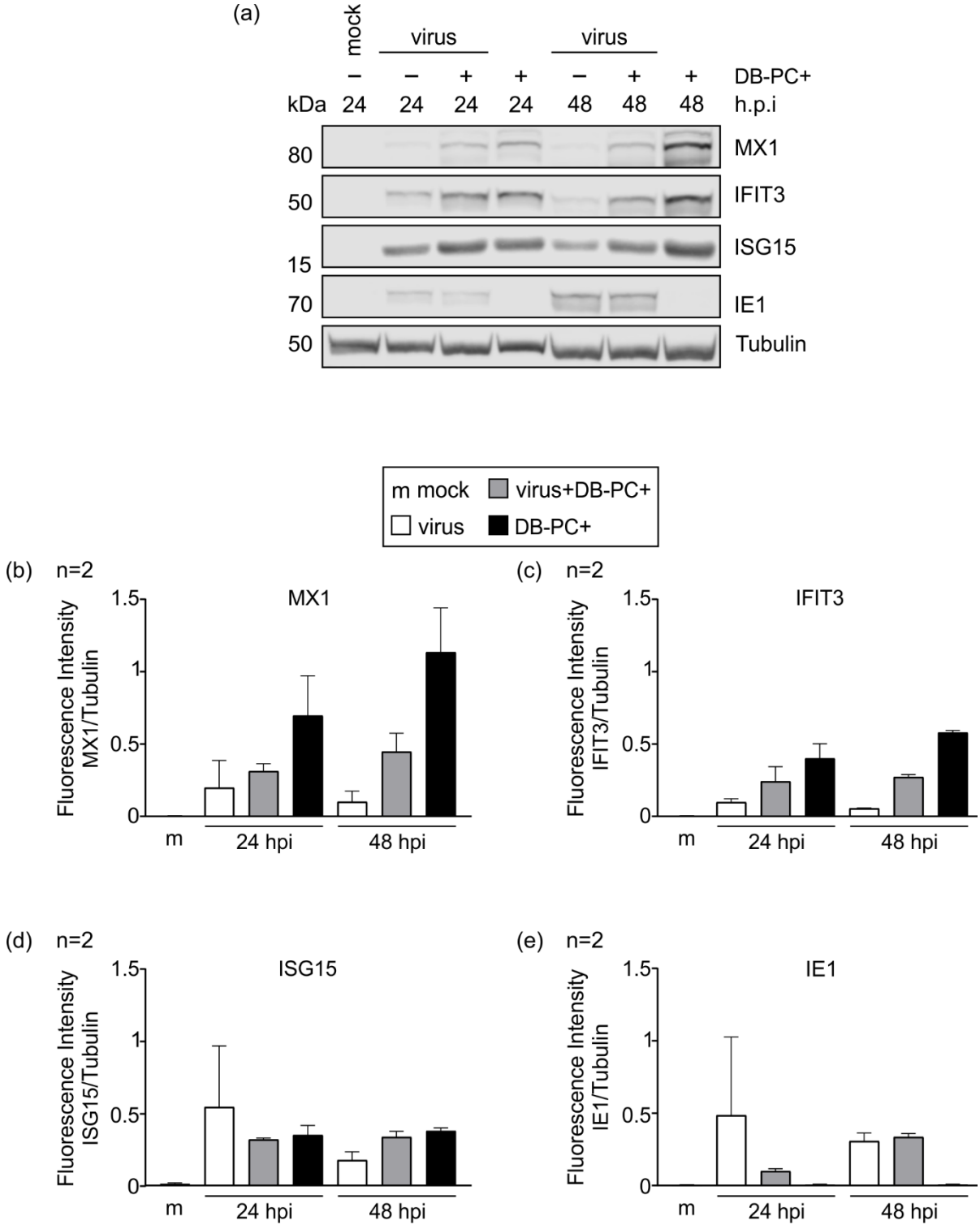

Fig. 19. DBs antagonize the repression of IRGs in infected HFFs. Expression of IRGs in infected HFFs, cotreated with PC-positive DBs (DBs-PC+). (a) Representative immunoblot analysis of 5x10exp5 HFFs infected with HCMV strain RV-Towne-repΔGFP (50 genomes, virus) or infected and co-incubated with 10 µg of UV-inactivated PC-positive DBs. Cell lysates were prepared at 24 h.p.i and 48 h.p.i and subjected to SDS-PAGE and immunoblot analyses. Untreated cells (mock) and cells

exposed to 10 µg UV-inactivated PC-positive DBs served as controls. The membranes were probed with antibodies against MX1, IFIT3 and ISG15. An antibody directed against the viral IE1 protein was used to confirm infection. Anti-tubulin served as sample loading control. (b) For quantification the fluorescence intensity ratio of each IRG and the corresponding tubulin intensity was determined (IRG/tubulin ratio). The means ± SD of two independent experiments are shown for each IRG and timepoint.

3.4.2 Impact of DBs on HCMV infection

3.4.2.1 Preincubation of HFFs with DBs before infection diminished the release of viral genomes

HCMV strains lacking the UL83 gene coding for pp65 do not produce DBs but show no gross impairment in virus replication or virus progeny production in fibroblasts [143, 144]. Nevertheless, growth defects of pp65- deletion mutants were reported at low multiplicity of infection (m.o.i) in fibroblasts and in monocyte-derived macrophages [145, 146]. There is evidence that pUL83 contributes to transcription of immediate-early (IE) genes by acting directly at the major immediate-early promoter/enhancer (MIEP) [146]. Along with pp65, the tegument protein pp71 is associated with DBs as one of the minor proteins with approximately 1.7 % of the total protein content [38, 104]. Pp71 has been identified as an essential viral transactivator of IE promoters, necessary for efficient viral replication. It was shown to be responsible for an increased infectivity of viral DNA when transfected into cultured cells [147-149]. The amount of pp71 delivered into a cell correlated with IE gene expression and an enhanced viral particle release [150].

To address the question whether exogenous addition of DBs to infected HFFs would have any effect on viral growth kinetics, viral DNA in cells and culture supernatants was quantified by real time PCR (qRT-PCR), using primers targeting the sequence of the catalytic subunit UL54 of HCMV DNA polymerase. To avoid an interference with endogenously produced DBs from infected fibroblasts, the pp65-deletion mutant RV-KB14, which is unable to produce DBs, was used for one set of experiments (Hesse et al., 2013). To determine whether the addition of DBs affected the growth properties of an endotheliotropic HCMV strain that produces DBs, the recombinant virus RV-Towne-repΔGFP was also used [59, 75]. HFFs were infected with 25 genomes/cell of RV-KB14 or RV-Towne-repΔGFP and co-incubated with 10 µg of UV-irradiated PC- positive DBs of the HCMV strain RV-Towne-repΔGFP. In a parallel approach, HFFs were also pre-treated with 10 µg of UV-irradiated PC-positive DBs for 2h to investigate whether DBs would sensitise the cells to subsequent infection (Fig. 20, pre-DBs+wt). This was

based on published data that showed that incoming, particle-delivered pp71 primed host cells to facilitate viral replication [149, 150]. DBs treated cells were carried along for control without infection (Fig.20, DBs-PC+). Cell culture supernatants and cells were harvested at indicated time points. Viral DNA from 10^5 cells or 200 µL of supernatants was isolated and the numbers of genomes were determined by qRT-PCR. The data were calculated in genome copies per cell (Fig. 20A) or genome copies per ml cell culture supernatant (Fig. 20B), irrespective to whether DBs were added or not. No significant differences in viral replication or genome release were observed within 8 days after infection for both viruses (Fig.20). Surprisingly, a decrease of viral genome copies was observed in supernatants of HFFs that were preincubated with DBs before infection (Fig. 20B(b). Very low genome levels were detected in control cells and their supernatants, that were incubated with only purified DBs (Fig. 20, DBs-PC+). The very low DNA yields were probably caused by contaminating virions. However, the viral DNA remained unchanged, suggesting that DBs alone were not able to replicate or produce viral progeny.

The experiments showed that replication and progeny production of an DB-producing HCMV strain was unaltered when DBs were exogenously added to the virus inoculum at the time of infection. However, the data also indicated that the release of viral DNA decreased when HFFs were pre-incubated with DBs before infection, indicating that DBs induced an antiviral state in cells when applied prior to infection

A Genome replication

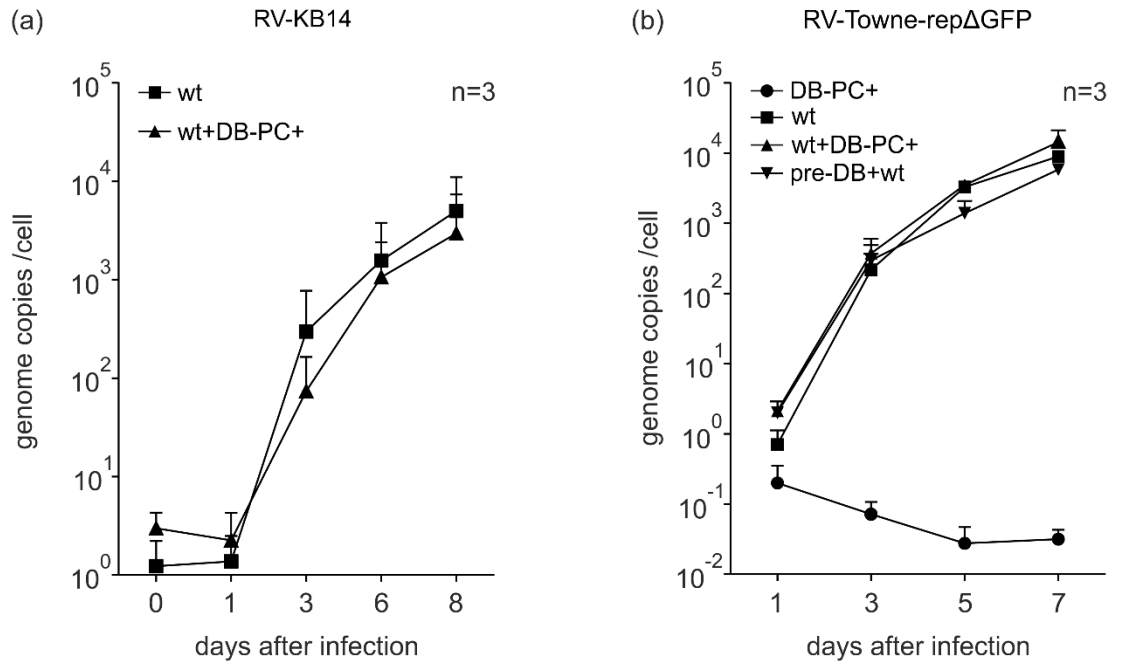

B Genome release

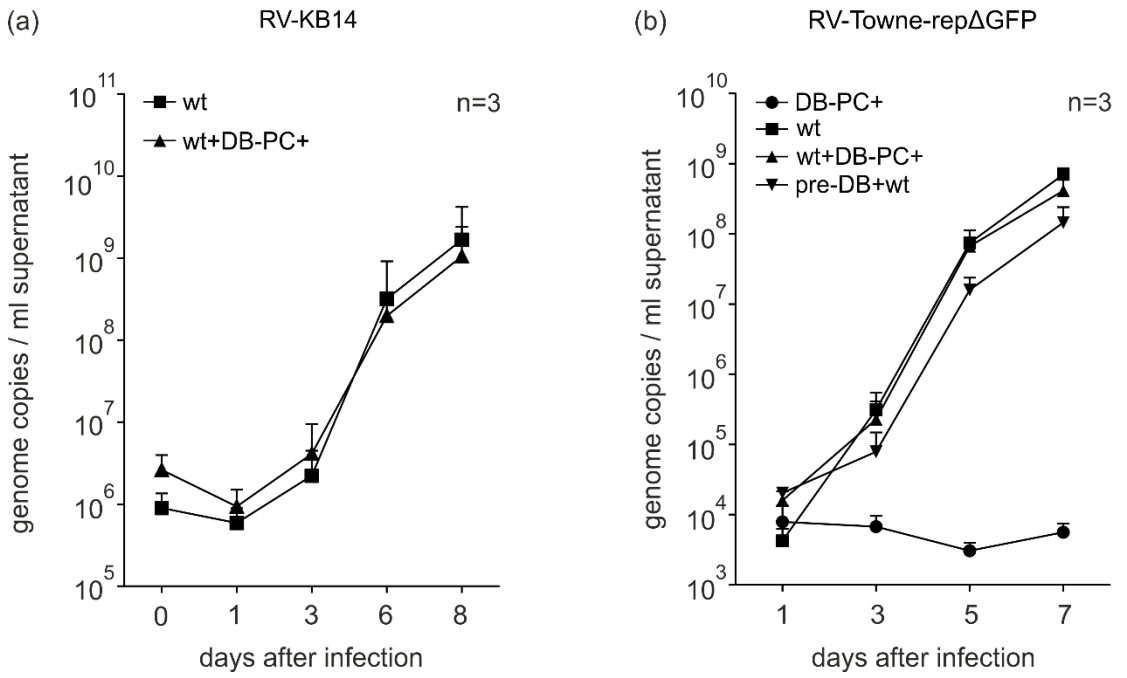

Fig. 20. Impact of DBs on HCMV replication and genome release. Quantitative real time PCR (qRT-PCR) analysis of viral genome replication (**A**) and viral genome release (**B**) from HFFs. **(A,a)** Cells were infected with 25 genomes per cell with RV-KB14 (wt) or infected and concomitantly incubated with DBs (wt+DB-PC+). **(A,b)** 10 µg of UV-inactivated PC-positive DBs were added to HFFs either 2h prior to infection with RV-Towne-repΔGFP (pre-DB+wt) or concomitantly with virus (wt+DB-PC+). As a control HFFs were infected with RV-Towne-repΔGFP (wt)or only incubated with 10 µg of UV-inactivated PC-positive DBs alone (DBs-PC+). The cells were collected at the indicated time points. DNA from 10xexp5 cells was isolated and the number of viral genomes was determined by qRT-PCR analysis. The means ± SD of three technical replicates measured in three independent experiments are shown for each time point. (**B**) HFFs were infected and DBs were applied as in A. Cell culture supernatants were collected at the indicated time points and cleared from cell debris by centrifugation. DNA from 200 µl of each supernatant was isolated and subjected to qRT-PCR analysis for genome determination. The means ± SD of three technical replicates measured in three independent experiments are shown for each timepoint. The data represent mean values ± SD of triplicate determinations from three independent experiments for each timepoint. KB14, HCMV strain AD169 deletion mutant lacking the pp65 gene

3.4.2.2 Preincubation of HFFs with DBs before infection potentiates the decrease in infectious progeny release

In a next set of experiments, it was investigated, whether there was a difference in the amount of infectious virus released from the cells, collected in the previous experiment (3.4.2.1). Supernatants obtained on the indicated days after infection were thawed and subjected to HFFs in serial dilutions. Infected cells were visualized using a hybridoma anti-IE1 antibody and counted in eight technical replicates [151]. The results were displayed as IE1-positive cells per ml supernatant. Surprisingly, the number of IE1-positive cells was up to 3 times lower in supernatants from RV-KB14 infected cells incubated with DBs (Fig. 21a, wt+DB-PC+), compared to control infected cells (Fig. 21a, wt). The results indicated that infected HFFs that were cotreated with DBs released less progeny. The decreased infectivity was not attributed to genome replication defects, as evidenced by the experiments shown in 3.4.2.1. Interestingly, this decrease was enhanced when HFFs were primed with DBs before infection (Fig. 21, b, pre-DB+ virus).

These results showed that pre-incubation of HFFs with DBs prior to infection result in a marked decrease in the release of infectious virus, exceeding the effect seen after co-incubation. These data confirm experiments obtained by using qPCR as readout and underscore the hypothesis that DBs sensitize cells against HCMV infection.

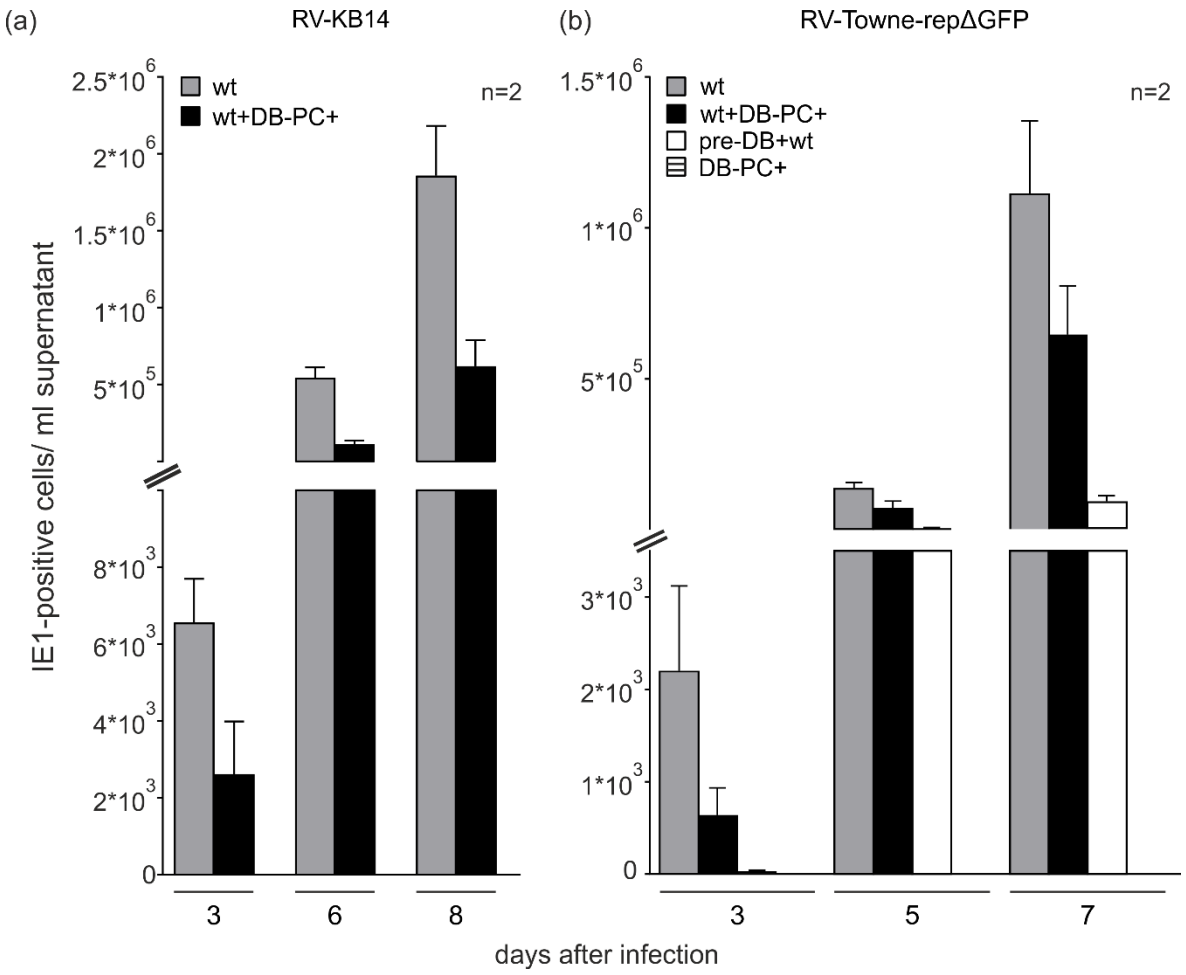

Fig. 21. The decrease in the infectivity of viral progeny is augmented by pre-incubation of HFFs with DBs. Release of infectious virus from infected HFFs exposed to DBs determined via IE1-staining **(a)** HFFs were infected with 25 genome copies per cell of HCMV virus RV-KB14 (wt) or infected and simultaneously exposed to 10 µg of PC-positive DBs (wt+DBs-PC+). Cell culture supernatants were collected at the indicated time points, cleared from cell debris by centrifugation and frozen at -80°C until further use. To determine the levels of infectious virus contained in the cell culture supernatants, serial dilutions of the supernatants obtained on day 3, 6 and 8 h.p.i were subjected to HFFs. (b). Virus supernatants from HFF pre-incubated with 10 µg of UV-inactivated PC-positive DBs for 2 h and subsequently infected with RV-Towne-repΔGFP (25 genomes per cell) (pre-DB+wt) or infected and cotreated with 10 µg of UV-inactivated PC-positive DBS (wt+DBs-PC+) were collected at 3, 5 and 7 days after infection. As a control, supernatants from HFFs infected or treated with DBs alone (DB-PC+) were also collected. Supernatants were centrifuged to remove cell debris

and stored at – 80°C until further use. To determine infectiousness of virus supernatants, HFFs were incubated with these supernatants in serial dilutions. Infected cells were visualized using an IE1-specific antibody. Infectivity of viral progeny was determined by counting the numbers of IE1-positive cells. Shown are the mean values ± SD of 8 technical replicates from two independent experiments for each time point.

3.4.2.3 Concomitant DBs-application and HCMV infection diminished early gene (UL44) expression

As constituents of viral particles, the tegument proteins pp65 and pp71 appear to facilitate optimal expression of viral genes in the early stages of cellular infection [146-150]

The impact of DBs-associated proteins was investigated on viral immediate early and early (IE1) and early (UL44) protein expression in HFFs infected with the HCMV strain RV-KB14 or RV-Towne-repΔGFP and infected and co-treated with PC- positive DBs (Fig.22). No significant differences in IE1-expression levels were found in cells that were infected compared to infected and DB-treated cells (Fig. 22, B, a, b). Interestingly, UL44 expression levels were decreased in in infected and DB-co-treated cells (Fig. 22B, c, d).

The data shows that the co-incubation of DBs with infected HFFs results in a decrease of early gene (UL44) expression.

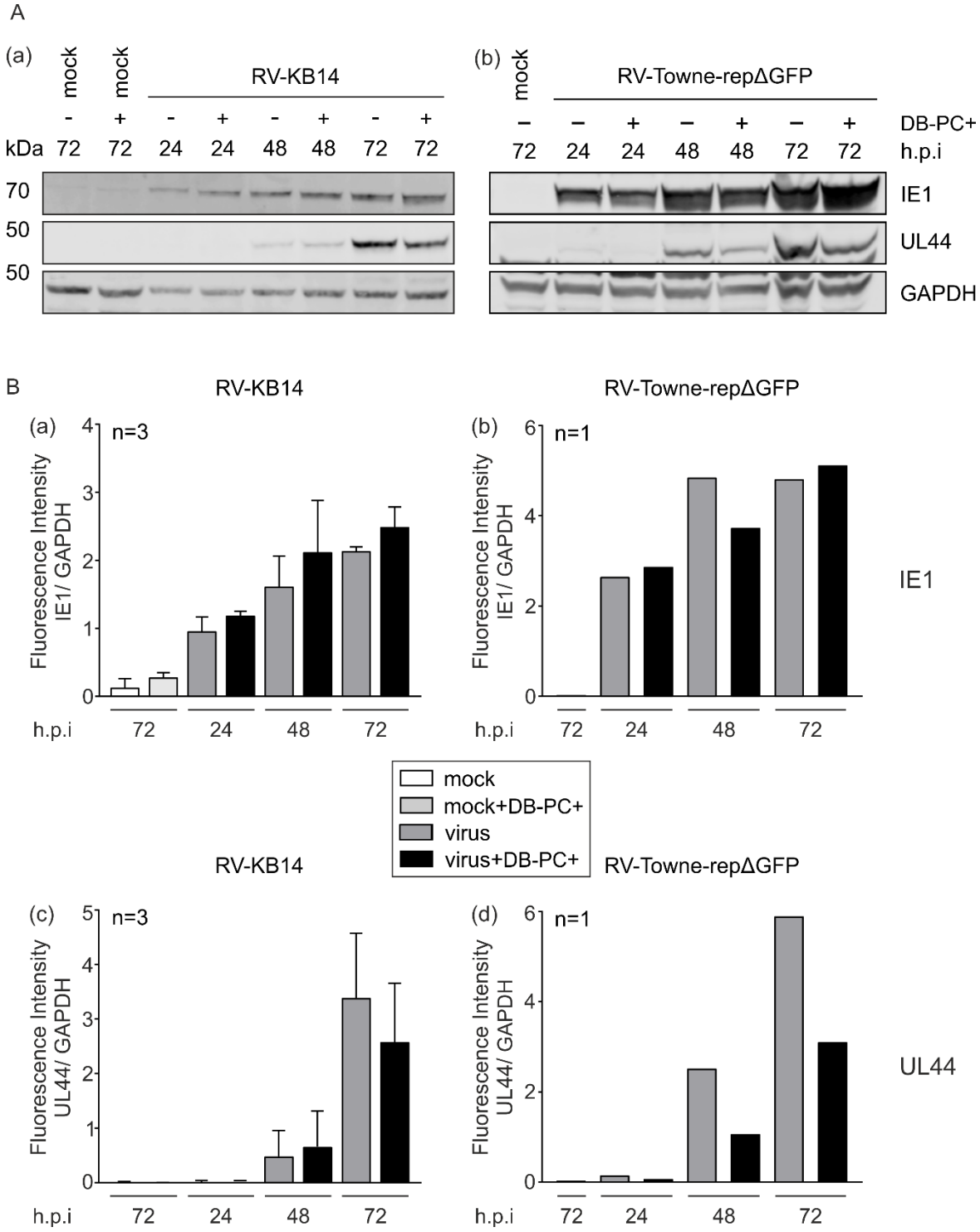

Fig. 22. Exogenous addition of DBs to infected HFFs showed no effect on viral immediate early (IE1) gene expression but diminished early gene (UL44) expression. (A) Immunoblot analysis of viral immediate- early (IE1) and early (UL44) protein levels in (a) HFFs infected with 50 genomes of RV-KB14 or infected and simultaneously exposed to 10 µg PC-positive DBs (DBs-PC+) and (b) HFFs infected with 50 genomes of RV-Towne-repΔGFP (virus) or infected and simultaneously exposed to 10 µg DBs-PC+. Mock cells were left untreated as a control. Cell lysates were prepared at indicated

times and analysed by immunoblot. Membranes were probed with hybridoma antibodies specific for IE1 (p63-27) and UL44 (BS510). GAPDH was used as a sample loading control. (**B)** Quantification of the protein expression level of IE1 and UL44. (a, b) The fluorescence intensity ratio of IE1 to GAPDH was calculated and plotted as individual values for all three experiments. (c, d) The ratios of UL44 to GAPDH were calculated and plotted as individual values for all three experiments.

3.4.3 Cytopathic effects (CPE) were accelerated in infected fibroblasts co-treated, or pre-treated with DBs compared to infected cells

Consistent with earlier reports, infection with HCMV strain RV-Towne-repΔGFP exhibited cytopathogenic effects (CPE) in HFFs, comparable to those of other endotheliotropic HCMV strains [34, 59, 75]. A characteristic phenotype of an infection with such endotheliotropic HCMV strains is their ability to form large multinucleated syncytia [34, 59].

In the experiments focussing on the replication kinetics of RV-Towne-repΔGFP in cell culture (3.4.2.), cytopathic changes were also monitored and photographed. The changes started to appear at 3 days post infection (dpi) in RV-Towne-repΔGFP (Fig.23, virus) infected cells as well as in infected cells that were pre- or co-incubated with PC-positive DBs (Fig. 23, virus+ DBs-PC+; DBs-PC+ pre.+ virus). The CPE of swollen and syncytial cells was progressing during incubation period. A markedly increased CPE was observed in virus infected cells co- or pre-incubated with DBs, compared to virus infected cells after 6 days. The extent of CPE at 6 dpi and 7 dpi was similar in infected cells that additionally were co- or pre-incubated with DBs (Fig. 23). On the contrary, a delayed CPE, mainly showing an intact HFF monolayer with remaining cells on the surface was observed in virus infected HFFs. These data demonstrated that the exposure of infected HFFs to DBs resulted in morphological changes of the cells that were clearly more distinct compared to the CPE of infected cells. A CPE was not seen, when DBs were applied to cells without infection (data not shown). The results indicated that DBs induced alterations in infected cells that eventually lead to enhanced cell death.

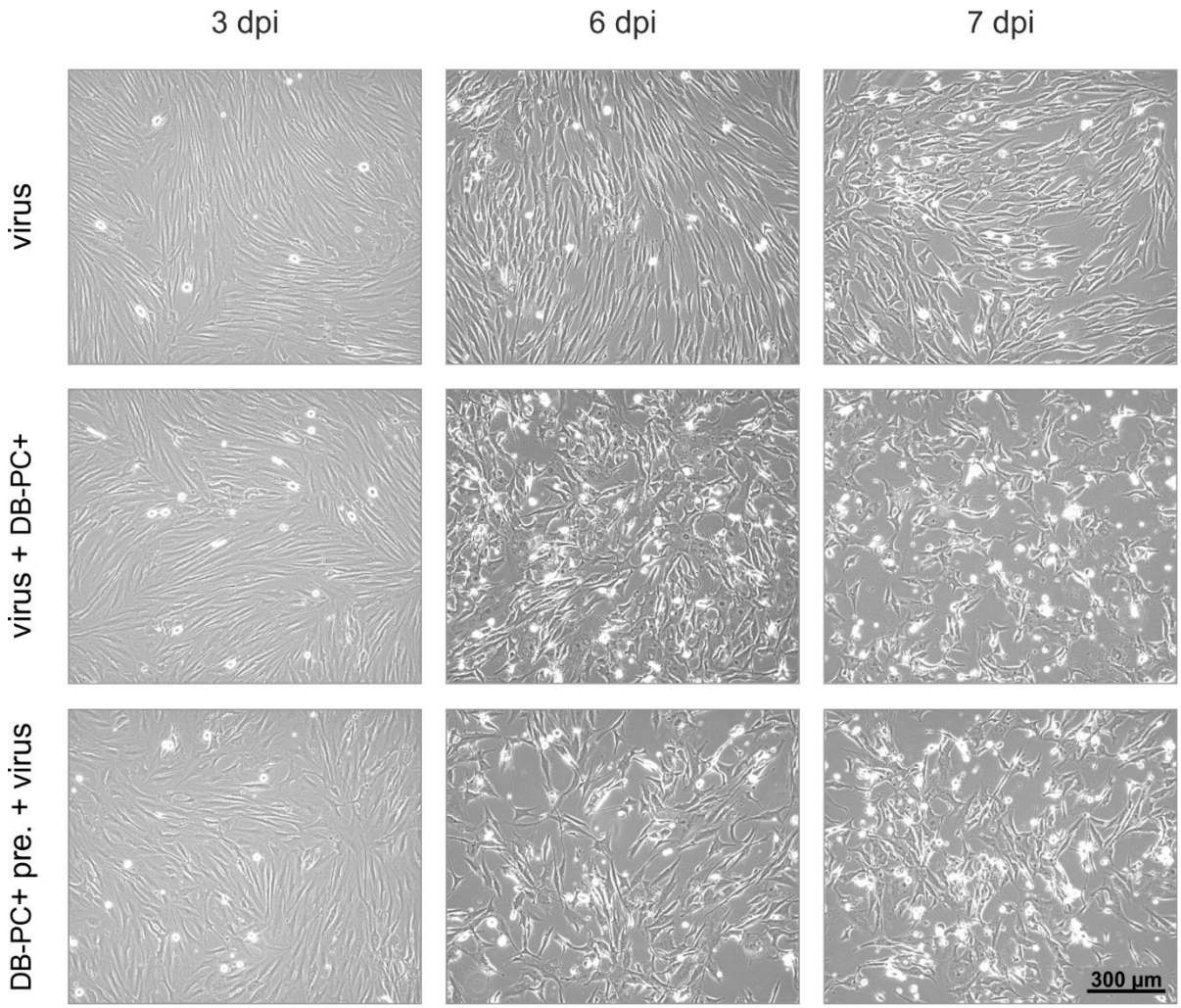

Fig. 23. Incubation of infected HFFs with DBs enhances the cytopathic effects in cell culture. HFFs were incubated with 25 genomes/cell of RV-Towne-repΔGFP together with 10 µg of UV-inactived PC-positive DBs (virus+ DBs-PC+) of the same strain, or pre-incubated with 10 µg DBs for two hours and infected subsequently (DBs-PC+ pre. + virus). Infected cells served as controls. Following 6h incubation, the inocula were removed and the cells washed two times with PBS. Fresh medium was added, and the cells cultivated. The cytopathic effect in these cultures was documented at 3, 6 and 7 dpi by light microscopy in 100x magnification.

3.4.4 Early apoptosis is increased in infected HFFs exposed to DBs

Application of DBs before or at the time of HCMV infection had a marked impact on cell morphology. Consequently, the hypothesis was addressed that DBs induce enhanced programmed cell death in HCMV infected cells.

In order to investigate the effect of DBs on cell apoptosis and necroptosis, HFFs were infected in presence or absence of DBs for 6 days and analysed in a flow cytometry assay (Fig. 24). Several conditions were evaluated. First, control cells were left untreated (b, d, d and e), incubated with 20 µg of UV-irradiated PC-positive DBs (DBs-PC+) (f) or infected with 50 genomes per cells with the HCMV strain RV-Towne-repΔGFP (g). Second, virus inoculum including 20 µg of UV- inactivated PC-positive DBs was applied to HFF (h). (i) Last, prior to infection, HFFs were primed with 20 µg of UV-inactivated PC- positive DBs for 2 h. Cell death was assessed by double-staining of the cells with 7-Aminoactinomycin D (7-AAD) and Apopxin Green, using flow cytometry (Fluorescence-activated Cell Sorting, FACS). 7-AAD labels both apoptotic and necroptotic cells, whereas Apopxin is used to detect apoptotic cells. In accordance with the manufacturers reference, Apopxin Green single labelling detected innate apoptosis in untreated cells, which should be around 2-6% of all cells (Fig. 24.c). Compared to infected cells (10.4%), the percentage of early apoptotic cells significantly increased up to 13.5 % in infected cells that were co-incubated with DBs (virus+DBs-PC+); Fig. 24h, j). An even higher level of 16.4% apoptotic cells was found in cells that had been initially primed with DBs before infection (Fig. 24i, j). In contrast, the late apoptotic/necrotic rate showed no difference between infected or infected and DBs- treated cells (Fig.24, j).

Taken together the results indicate that DBs exert an early-apoptotic effect on infected fibroblasts and that this could be further potentiated by sensitizing the cells by preincubation with DBs.

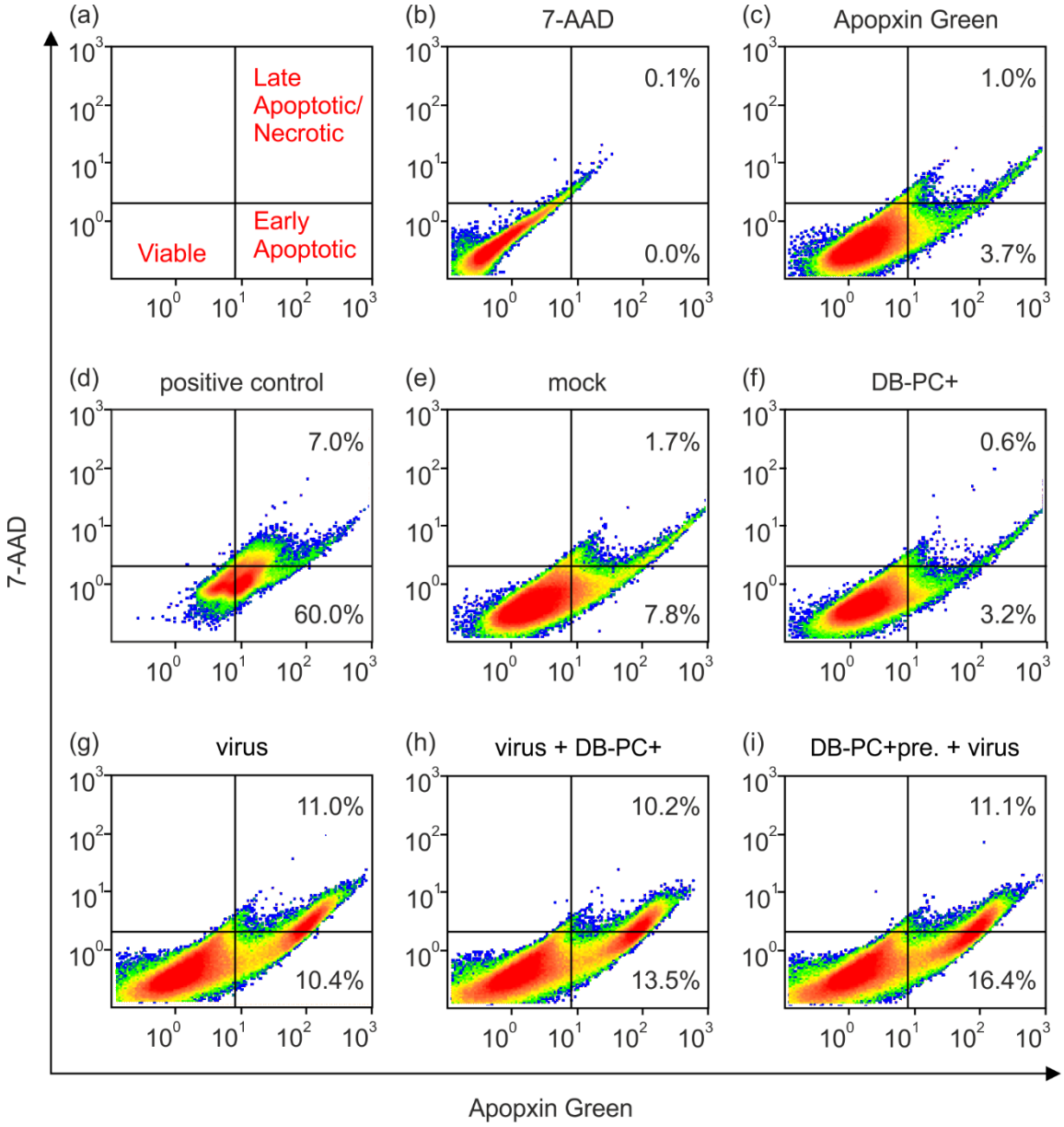
(a)
Late Apoptotic/ Necrotic
Viable
Early Apoptotic
(b) 7-AAD
0.1%
0.0%
(c) Apopxin Green
1.0%
3.7%
(d) positive control
7.0%
60.0%
(e) mock
1.7%
7.8%
(f) DB-PC+
0.6%
3.2%
(g) virus
11.0%
10.4%
(h) virus + DB-PC+
10.2%
13.5%
(i) DB-PC+pre. + virus
11.1%
16.4%
7-AAD
Apopxin Green

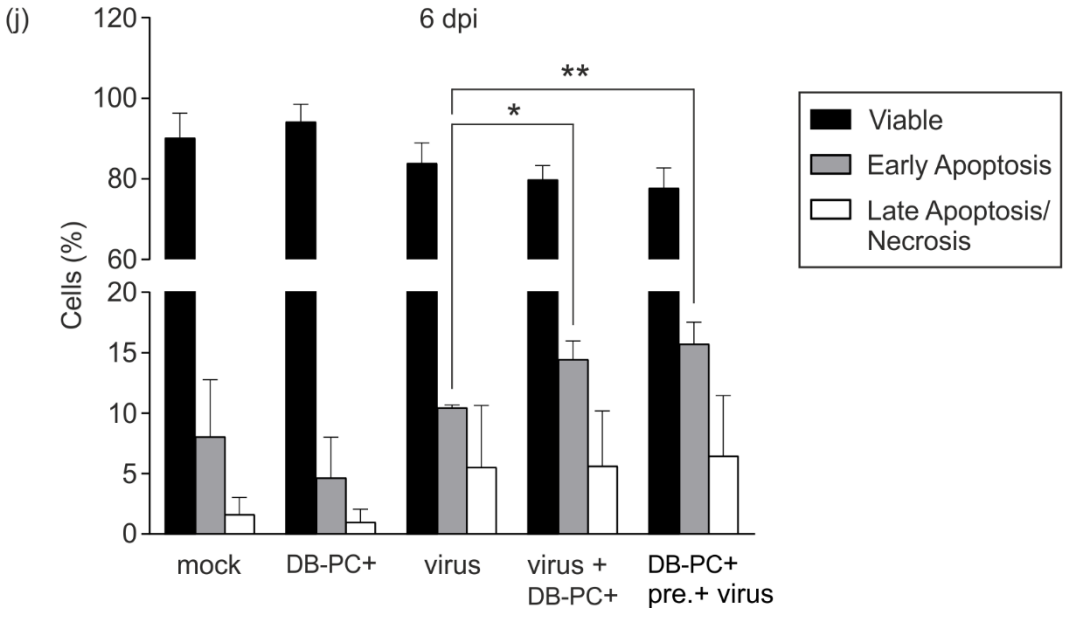
(j)
6 dpi
Cells (%)
**
*
Viable
Early Apoptosis
Late Apoptosis/ Necrosis
mock
DB-PC+
virus
virus + DB-PC+
DB-PC+ pre.+ virus

Fig. 24. Addition of DBs to infected HFFs increases early apoptotic events. Flow cytometry analysis of apoptosis and necrosis in HFFs six days after infection and concurrent DBs exposure. (a) Gating strategy for the different staining patterns used in the FACS analyses. Viable cells appear in the lower left quadrant, early apoptotic cells appear in the lower right quadrant, and late apoptotic/necrotic cells are shown in the upper right quadrant. (b) Untreated cells only stained with 7-AAD. (c) Untreated cells only stained with Apopxin Green. (d) HFFs incubated at 99°C for 30 min. on day six. (e) FACS analysis of untreated cells (mock). (f) Cells incubated with 20 µg UV- inactivated and PC- positive DBs (DBs-PC+). (g) HFFs infected with HCMV strain RV-Towne-repΔGFP (50 genomes per cell; virus). (h) Cells infected and simultaneously treated with 20 µg UV- inactivated PC-positive DBs (i) Prior to infection HFFs were preincubated with 20 µg of UV-inactivated PC- positive DBs. After 2 hours, virus inoculum (HCMV strain RV-Towne-repΔGFP; 50 genomes per cell) was added to the cells. The different inocula in (f-i) were applied to HFFs for 2 hours. Subsequently fresh medium was added, and the cells were incubated at 37°C and 5% CO_2 for another 4hours. After a total incubation period of six hours, the inoculum was removed, the cells were washed twice with PBS, and cultivated for six days in fresh medium. For the samples g-i, floating cells from supernatants were combined with adherent cells. Apoptotic and necrotic cells in d-I, were double labelled with Apopxin Green and 7-AAD. The percentages of cells in the different quadrants are shown. The results are representative for three independent experiments. (j) Quantification of apoptotic/necrotic cells from the results, described in (e-i). Data represent mean ±SD of three independent experiments. Comparisons between groups were calculated using an unpaired, two-tailed t test for the indicated group, compared with the appropriate untreated group. *p<0.05; **p<0.01. 7-AAD, 7-aminoactinomycin D. 7-AAD stains late apoptotic/necrotic cells; Apopxin Green stains apoptotic cells; FACS, Fluorescence-activated Cell Sorting

3.5 Effect of DBs on autophagy

3.5.1 Effects of DBs on autophagy in HFFs

Autophagy is a fundamental lysosome-dependent degradation process. It operates at basal levels in most cells to maintain cellular viability and homeostasis (Mizushima and Komatsu, 2011). However, autophagy is induced by different stress conditions including starvation, cytokines or upon virus infection [152, 153]. One role of autophagy in cellular defence is the elimination of invading pathogens, termed xenophagy, [154, 155]. Depending on the virus, autophagy can be manipulated to promote viral immune evasion, replication or the release of progeny virus from infected cells [156, 157].

Microtubule-associated protein light chain 3 (LC3) is widely used as a marker for autophagosome formation and therefore to monitor autophagy. Endogenous LC3 is detectable

in two forms following SDS-PAGE and immunoblotting. Cytosolic LC3 is represented by LC3I whereas LC3II is conjugated with phosphatidylethanolamine (PE) and is membrane bound [158, 159]. LC3II correlates with the number of autophagosomes and conversion of LC3I to LC3II is used as indicator for the induction of autophagy [158, 159].

3.5.1.1 DBs increase the lipidation of LC3BII in HFFs at 24h independent of the PC

McFarlane et al. demonstrated that purified DBs failed to increase LC3II protein levels at 6 h.p.a in HFFs suggesting that viral DNA was responsible for the induction of autophagy [160]. However, to ascertain whether DBs could induce autophagy at later time points, LC3 conjugation was monitored throughout three days after DB-application by immunoblot analyses (Fig. 25). HFFs were incubated with 20 µg of UV-irradiated DBs. Both, PC-positive (Fig. 25A) and PC-negative DBs (Fig. 25B) were investigated. Uninfected HFFs (mock) and cells infected with RV-Towne-repΔGFP (virus) were carried along as controls. For LC3 detection, a monoclonal antibody against the splice variant LC3B was used. An increase in the intensity of LC3BII was detected at 24h in cell lysates incubated with PC-positive (Fig.25A) and PC-negative DBs, respectively (Fig. 25B). LC3B expression declined to mock levels at 48h and 72h.

The results show that induction of autophagy is a cellular response to incoming non-infectious DBs that occurs even in the absence of viral gene expression

A

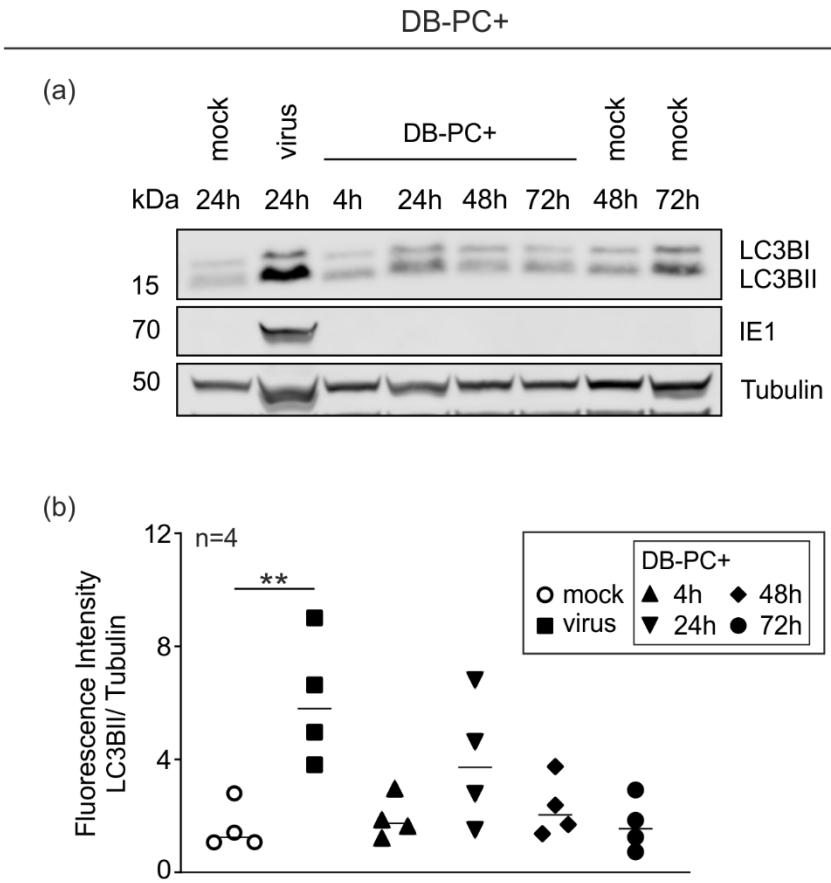
DB-PC+
(a)
mock
virus
DB-PC+
mock
mock
kDa 24h 24h 4h 24h 48h 72h 48h 72h
15
70
50
LC3BI
LC3BII
IE1
Tubulin
(b)
n=4
**
Fluorescence Intensity
LC3BII/ Tubulin
12
8
4
0
DB-PC+
mock
virus
4h
48h
24h
72h

B

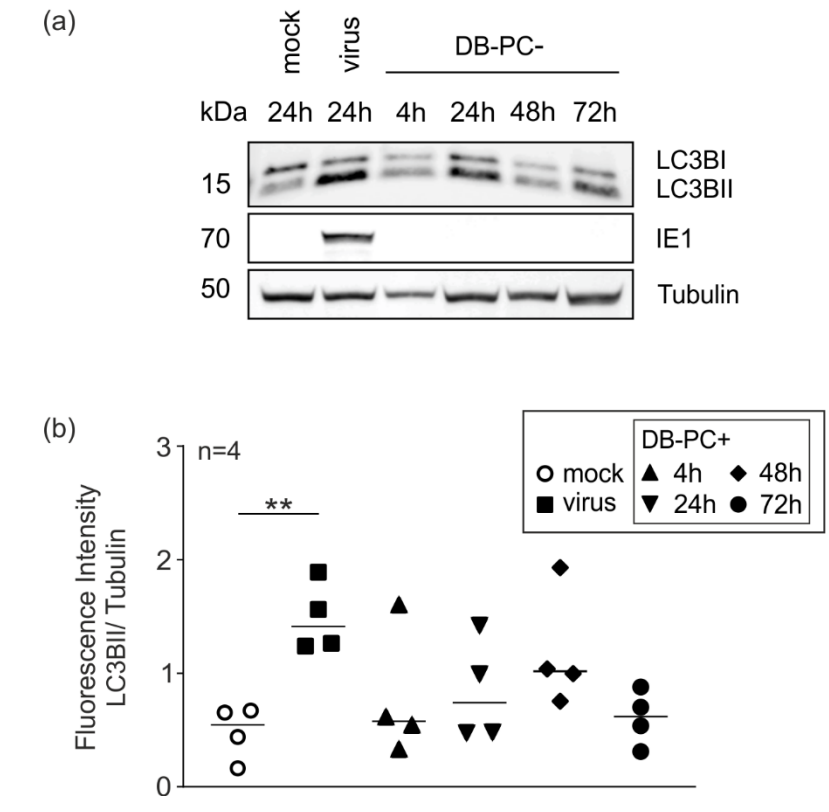
DB-PC-
(a)
mock
virus
DB-PC-
kDa 24h 24h 4h 24h 48h 72h
15
70
50
LC3BI
LC3BII
IE1
Tubulin
(b)
n=4
**
Fluorescence Intensity
LC3BII/ Tubulin
3
2
1
0
DB-PC+
mock
virus
4h
48h
24h
72h

Fig. 25. Autophagy is increased in HFFs upon incubation with DBs at 24 h. Expression levels of LC3BI and LC3II in HFFs during incubation with PC-positive DBs (DBs-PC+) in **A** and with PC-negative DBs (DBs-PC-) in **B**. **A** (a) 5x10exp5 HFFs were exposed to 20 µg UV- irradiated DBs-PC+. Untreated cells and cells infected with HCMV (strain RV-Towne-repΔGFP; 100 genomes per cell; virus) were carried along as controls. At the indicated times, total cell lysates were prepared and subjected to immunoblot analysis. The turnover of LC3BI to LC3BII was detected with an antibody directed against the LC3 splice variant LC3B. Expression levels of the viral IE1 were visualized using an anti-IE1 specific monoclonal antibody. Labelling of tubulin with a specific antibody served as loading control. Shown is one representative immunoblot out of four independent experiments. (b) The fluorescence intensity band ratios of LC3BII to tubulin were calculated and plotted as individual values for all four experiments. Comparisons between groups were calculated using an unpaired, two-tailed t test for the indicated group compared with the untreated (mock) group. **$p < 0.01$. **B** (a) Samples for immunoblot analysis were prepared as described in A(a), but PC-negative DBs were used. (b) The fluorescence intensity band ratios of LC3BII to tubulin were calculated and plotted as individual values for all four experiments. Comparisons between groups were calculated using an unpaired, two-tailed t test for the indicated group compared with the untreated (mock) group. **$p < 0.01$.

3.5.1.2 DBs potentiate the lipidation of LC3BII in HCMV infected HFFs

HCMV infection is a potent autophagy stimulus (see Fig. 25, virus). In order to investigate whether DBs could additionally boost autophagy during infection, immunoblot analyses of HFFs infected with RV-Towne-repΔGFP (virus) and co-treated with DBs were performed (Fig. 26). Virus infection alone resulted in a significant increase of LC3BII protein expression compared to mock cells at 24 h and 48 h. When compared to virus infected cells, additional application of DBs enhanced levels of LC3BII expression (Fig. 26b).

Collectively, these results demonstrated that DBs enhance the induction of autophagy in infected cells.

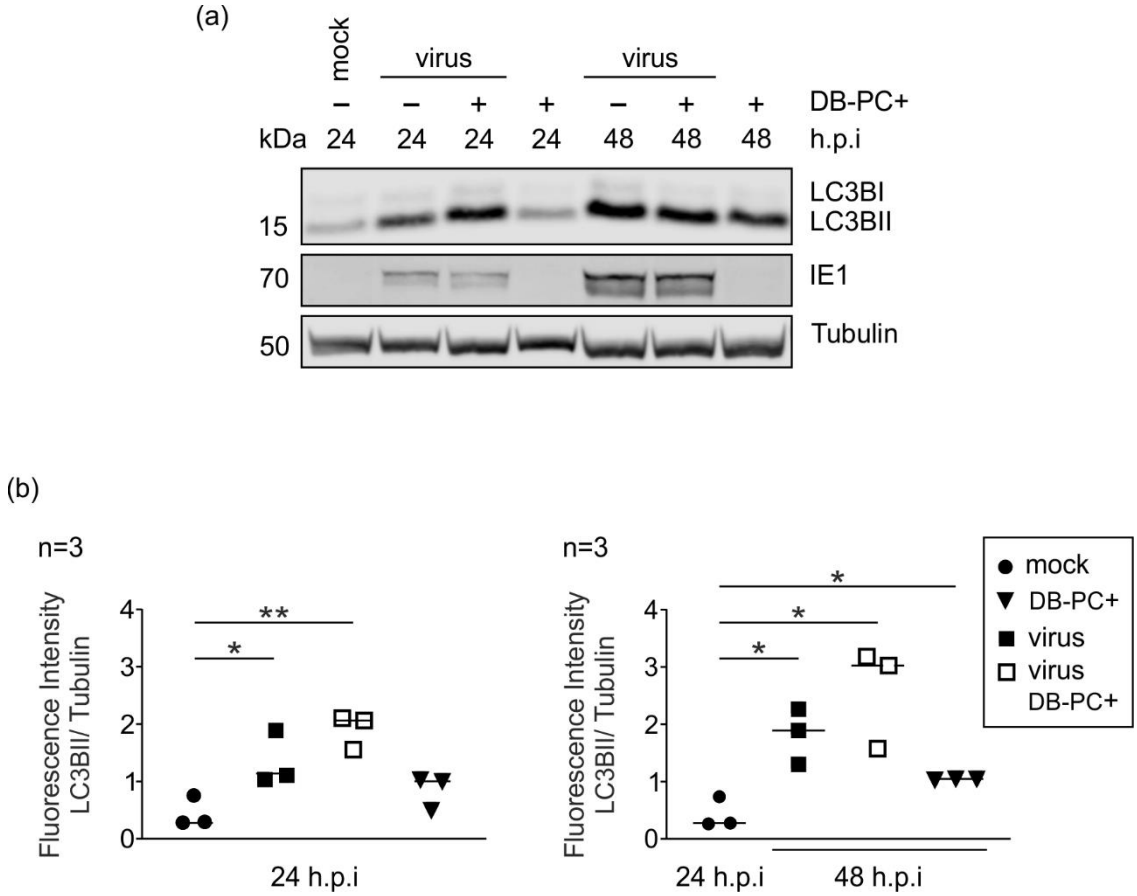

Fig. 26. DBs enhance autophagy in infected HFFs. (a) Immunoblot analyses of LC3BI and LC3II expression levels in HFFs during infection and co- incubation with PC-positive DBs (strain, RV-Towne-repΔGFP, DBs-PC+). 5x10exp5 HFFs were infected with 100 genomes per cell of HCMV strain RV-Towne-repΔGFP (virus) or infected and cotreated with 20 µg of UV-inactivated DBs-PC+. As control, cells were left untreated (mock) or exposed to 20 UV- inactivated DBs-PC+. Total cell lysates were prepared at indicated times and subjected to immunoblot analysis. The turnover of LC3BI to LC3BII was detected using a monoclonal antibody directed against the LC3B splice variant. Expression levels of viral IE1 were analysed using an anti-IE1 monoclonal antibody. Labelling of tubulin with a specific antibody served as loading control. Shown is one representative immunoblot out of three independent experiments. (b) Fluorescence intensity band ratio of LC3BII to tubulin at 24 h.p.i and 48 h.p.i. The ratios of LC3BII to tubulin were determined and plotted as individual values for all three experiments. Comparisons between groups were calculated using an unpaired, two-tailed t test for the indicated group compared with the corresponding untreated group. *p<0.05; **p < 0.01.

3.5.1.3 Inhibition of JAK/STAT signalling pathway has no effect on LC3BII lipidation

Several studies demonstrated that autophagy is induced in different cancer cell lines by type I IFNs [161, 162]. The JAK/STAT signalling pathway was suggested to play an important role in IFN-mediated induction of autophagy.
To investigate the correlation between the JAK-STAT pathway and the autophagy status in HFFs exposed to DBs, immunoblot analyses in presence of JAK Inhibitor I (JAK-I.) were performed (Fig. 27). Changes in LC3B levels were detected at 24 h.p.a. of DBs. Unexpectedly, IFN-ß treatment did not result in induction of autophagy in this experiment. MX1 expression, used as control was induced. Addition of JAK-I. did not change LC3B levels, neither in control cells nor in cells treated with DBs. MX1 expression was completely diminished by JAK-I. proving its functionality (Fig. 27a).

Based on these results, IFN-ß-mediated induction of autophagy in HFFs could not be found in HFFs. Inhibition of JAK/STAT signalling pathways had no effect on LC3B levels in HFFs.

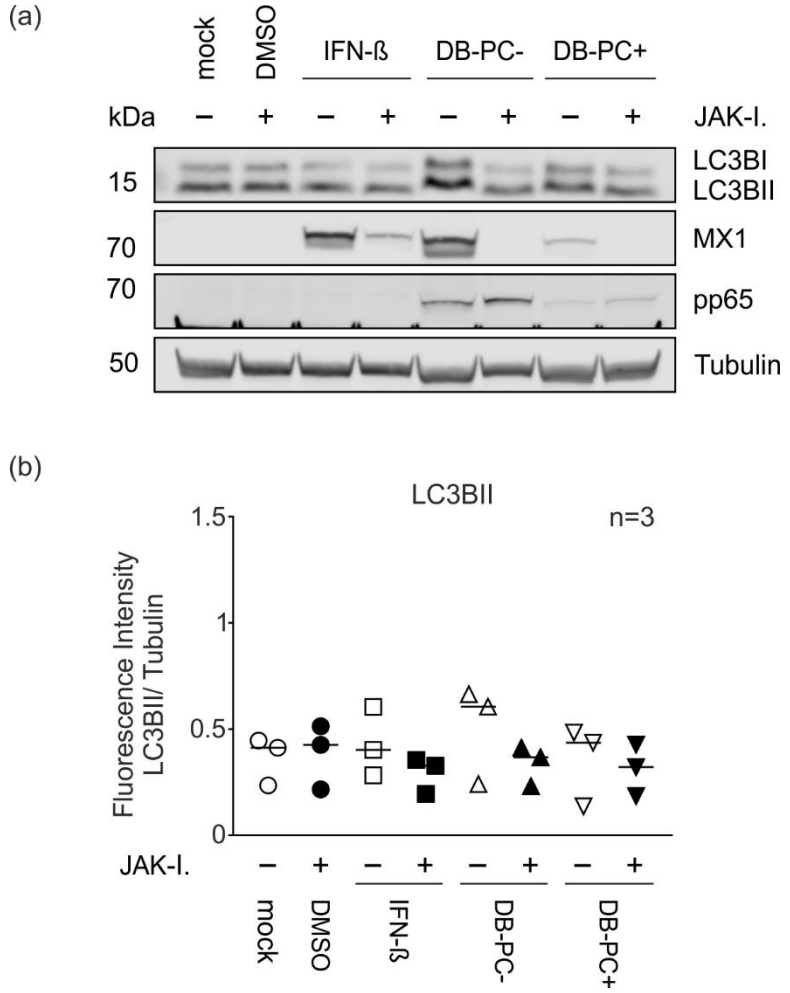

Fig. 27. DBs-induced autophagy is not dependent on JAK/STAT signalling pathways. Protein levels of LC3BI and LC3BII in HFFs after incubation with DBs in presence and absence of JAK inhibitor I (JAK-I.). (a) HFFs were either pre-treated with DMSO or JAK-I. (20 µM/ ml) for one hour. Cells were incubated with DMSO (mock), treated with IFN-ß (100U/ ml) or exposed to 20 µg of UV-inactivated DBs-PC- or DBs-PC+. Each sample was further cotreated with JAK-I. for 24 hours. Immunoblot analysis of LC3BI and LC3BII expression upon JAK-I.- treatment compared to the appropriate untreated control. IFN-ß treatment was used to assess effects of JAK/STAT signalling cascade on autophagy. The IRG MX1 was used as positive control for IFN-ß and JAK-I. activity. Tubulin was used as protein loading control. Pp65 was used as DBs internalization control. A representative immunoblot out of three independent experiments is shown. (b) The ratios of LC3BII to tubulin were estimated for each sample and plotted as individual values for all four experiments. Comparisons between groups revealed no significant differences in LC3BII expression.

3.5.2 Effects of DBs on autophagy in endothelial cells

3.5.2.1 LC3BII levels in endothelial cell do not change upon DBs incubation

In human umbilical vein endothelial cells (HUVEC), autophagy was shown to be induced upon HCMV infection until 24 h.p.i and was inhibited afterwards [163](Zhao et al., 2018). Concordant with the observations made in fibroblasts, this stimulation was independent of viral protein synthesis [160, 163].

To investigate the ability of DBs to induce autophagy in ECs, immunoblot analyses were performed (Fig. 28). ECs cells were incubated with 30 µg of UV-inactivated PC-positive DBs (DB-PC+) (Fig. 28A) or PC-negative DBs (DB-PC-) respectively (Fig. 28B). A constant increase in LC3BI to LCB3II conversion was detected in ECs in a time course of 24-72 h.p.a. However, the levels of increase were comparable to the increase seen in mock controls.

These results thus did not indicate that DBs-application had a measurable impact on autophagy in endothelial cells.

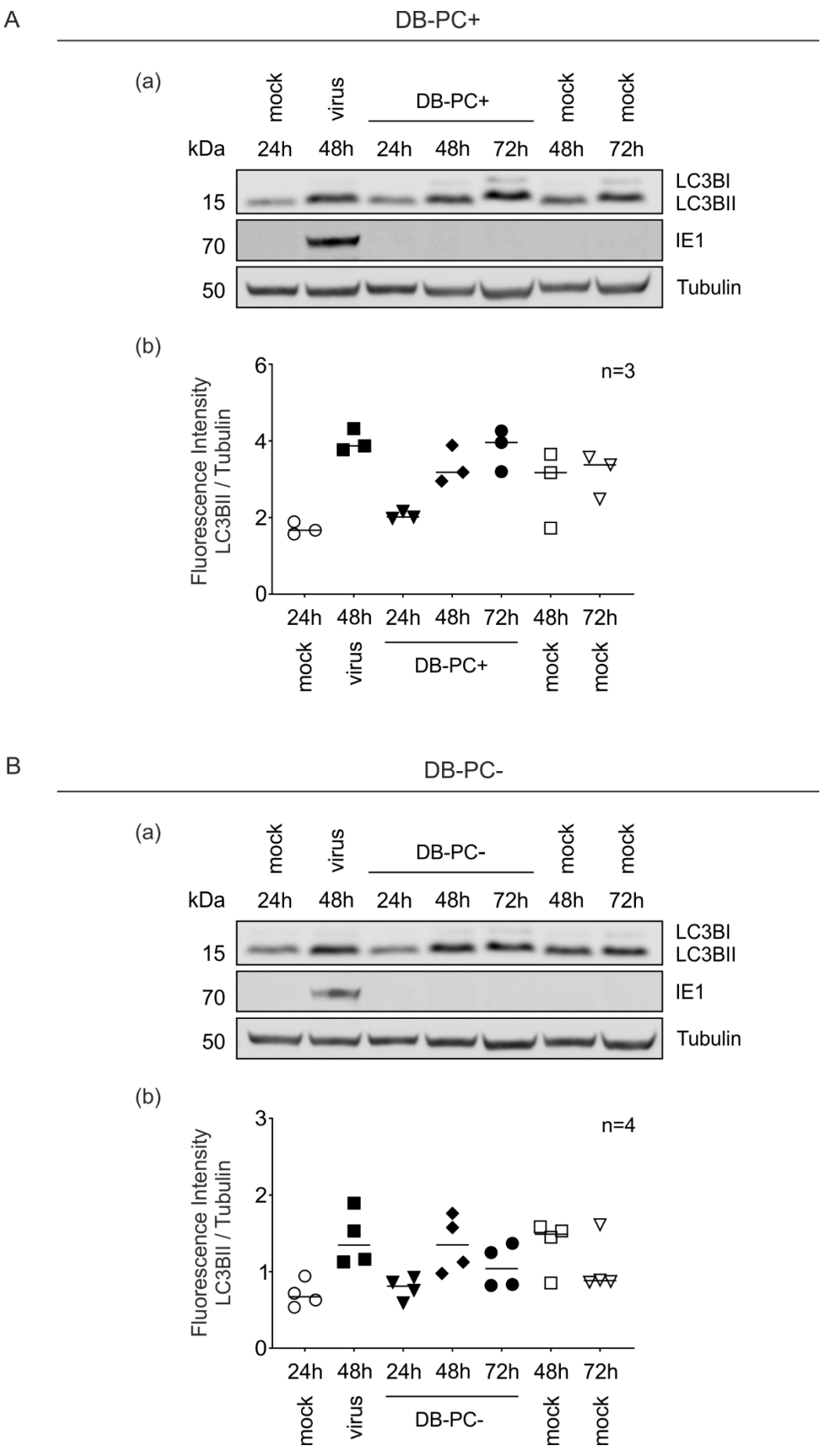
A
DB-PC+
(a)
mock
virus
DB-PC+
mock
mock
kDa
24h
48h
24h
48h
72h
48h
72h
15
70
50
LC3BI
LC3BII
IE1
Tubulin
(b)
Fluorescence Intensity
LC3BII / Tubulin
n=3
6
4
2
0
24h
48h
24h
48h
72h
48h
72h
mock
virus
DB-PC+
mock
mock
B
DB-PC-
(a)
mock
virus
DB-PC-
mock
mock
kDa
24h
48h
24h
48h
72h
48h
72h
15
70
50
LC3BI
LC3BII
IE1
Tubulin
(b)
Fluorescence Intensity
LC3BII / Tubulin
n=4
3
2
1
0
24h
48h
24h
48h
72h
48h
72h
mock
virus
DB-PC-
mock
mock

Fig. 28. DBs do not induce autophagy in ECs. A+B Protein expression levels of LC3BI and LC3BII in endothelial cells after incubation with PC-positive (strain RV-Towne-repΔGFP, DBs-PC+, A) or PC-negative DBs (strain RV-Towne-BAC, DBs-PC-, B). **A** (a) Immunoblot of whole cell lysates of endothelial cells (ECs), incubated with 30 µg of UV- inactivated DBs-PC+ after 24, 48 and 72 hours. Control cells were either left untreated (mock) for the same period or infected with the HCMV virus strain RV-Towne-repΔGFP (300 genomes per cell, virus) for 48 hours. The turnover of LC3BI to LC3BII was detected by using a monoclonal anti-LC3B antibody. Infection was confirmed by viral IE1 protein expression. Labelling of tubulin served as sample loading control. Shown is one representative immunoblot out of three independent experiments. (b) The fluorescence intensity ratios of LC3BII to tubulin were calculated for each sample and plotted as individual values for all three experiments. Comparisons between groups revealed no significant differences. **B** (a) The samples for immunoblot analyses were prepared as in A(a), but PC-negative DBs were used. (b) The fluorescence intensity ratios of LC3BII to tubulin were determined for each sample and plotted as individual values for all four experiments. Comparisons between groups revealed no significant differences in LC3BII expression.

4. Discussion

DBs are enveloped particles that resemble HCMV virions in their viral glycoprotein and tegument protein composition but they are devoid of DNA and a capsid. DBs are not infectious and non-replicating [37, 38, 164]. The fact that DBs are synthesized during HCMV replication in vitro and in vivo [53] indicates that these particles have a relevant role in HCMV infection. Considering this, it is astonishing that their function in HCMV infection is still unknown.

4.1 Effect of DBs on the proteome of HFFs, ECs, monocytes and iDCs

In this work, we used MS-based proteomics to analyse the impact of DBs on host cells. The exposure of HFFs to DBs altered the abundance of 92 proteins 1.5-fold or more. Interestingly, 88% of these are known to be IFN responsive proteins (IRGs). Among these IRGs, 26 belong to a core set of 62 IRGs that are upregulated in response to type I IFN by 10 vertebrate species analysed in a recently published study [165].

The biological processes in which the regulated proteins are mainly involved covered antiviral response, ubiquitination, antigen processing and presentation, cell motility and apoptosis. Most of these proteins are induced by IFNs. This raises the question, how DBs are sensed by target cells for the induction of the IFN-IRG pathways. Surprisingly, essential immune sensors for double stranded RNA (dsRNA) and dsRNA-binding proteins (e.g., IFIH1/MDA5 and DDX58/RIG-I, PKR, OAS3 etc.) were strikingly upregulated among the IRGs in HFFs, ECs and iDCs. Detection of dsRNAs is a potent inducer of type I IFNs and antiviral immunity [166]. A study by Weber and co-workers, demonstrated that DNA viruses produce dsRNA during their replication cycle [167]. These authors hypothesized that dsRNA might be an erroneous product of convergent transcription from bidirectional promoters It has indeed been demonstrated that dsRNA is produced during HCMV- infection [168]. In addition to DNA, viral RNA is also packaged into virions and delivered to cells upon viral entry [149]. Notably, several types of viral and host RNA molecules have also been found incorporated into DBs [54]. The function of these RNA species remains unclear. It is however reasonable to assume, that DBs deliver RNAs into host cells and these RNAs are detected by RNA- sensors, leading to the activation of antiviral signalling pathways. Interestingly, HCMV encodes two proteins, namely pIRS1 and pTRS1, that have been shown to block dsRNA- mediated antiviral pathways [168]. This indicates that RNA-sensing of incoming HCMV is an important antiviral pathway that may be subverted by the expression of pIRS and pTRS. As DBs do not express these proteins upon

cellular uptake, RNA-sensing may be one important pathway by which these particles induce the IFN-IRG pathways.

The only DNA sensor found to be upregulated upon DB-treatment was the IFN -γ-inducible protein 16 (IFI16). DNA sensors like IFI16 promote the expression and secretion of IFNs. DB preparations contain traces of viral and cellular DNA. It is thus reasonable to assume that DNA-sensing, e.g. mediated by IFI16 contribute to IFN-IRG induction. However, DBs treated with DNase showed induction of selected IRG expression at levels, comparable to untreated DBs. These preliminary experiments indicate that DNA sensing is not a major pathway required for IFN- IRG induction upon DB application. Still more detailed analyses are required to approach this issue.

Toll-like receptors (TLRs) are considered as being primary pathogen sensors [80]. HCMV is recognized by a variety of members from the TLR family. TLR2 and CD14 have been identified as membrane bound PRRs that recognize HCMV virions and DBs in monocytes [83]. Furthermore, both were able to trigger inflammatory cytokine production in a CD14 and TLR2 dependent manner [83]. In our work, the myeloid differentiation factor 88 (MyD88), the downstream key adaptor protein of the TLR signalling pathway, was found to be upregulated upon DB-treatment in HFFs. However, no other component of the TLR signal transduction was found to be regulated by DBs in these cells. In monocytes, TLR2 was upregulated after DB-incubation. However, TLR2 upregulation was found in the monocytes of only three of six donors, challenging the significance of this finding. Still, based on these proteomic data, the involvement of TLR-signalling in DB-recognition cannot be excluded, as components of these pathways do not necessarily have to be upregulated to be functional. Again, further investigations are needed to approach this.

Following viral infection, IRGs are primarily stimulated by engagement of IFN with its cognate receptor and the subsequent downstream activation of the JAK/STAT pathway. Recently published data, however, demonstrated IFN-independent upregulation of some of the antiviral IRGs, e.g., IFIT1, IFIT2, IFIT3, MX1 and ISG15 upon HCMV infection [135]. These studies identified IRF3 as transcriptional regulator, which is indispensable for constitutive expression of these IRGs in the absence of IFNs [135]. This raised the question, if DBs would directly induce selected IRGs independent of IFN. The inhibition of the JAK/STAT signalling pathway in HFFs exposed to DBs potently blocked the induction of the IRGs STAT1, MX1, and IFIT3, indicating that the expression of these IRGs is IFN-dependent and cannot be compensated by another pathway. The upregulation of STAT1 and STAT2, the key downstream transcription

factors in the JAK/STAT pathway in the proteome analyses performed in this work support this, suggesting that induction of IRGs upon DB-application in HFFs is IFN-dependent.

4.2 Upregulation of the major histocompatibility complex (MHC) class I and II antigen presentation pathways in response to DBs

Essential proteins of the antigen processing and presentation machinery (APM), namely Beta-2-microglobulin (B2M), Proteasome activator complex subunit 2 (PSME2), Antigen peptide transporter 1 (TAP1), Antigen peptide transporter 2 (TAP2) and Tapasin (TAPBP) were considerably upregulated upon DBs exposure in HFFs. These proteins are key factors that orchestrate the stringent assembly process of MHC class I molecules for antigen presentation; the recognition of viral peptides in the context of MHC class I molecules by cytotoxic T lymphocytes (CTLs) is a key event in the elimination of virus-infected cells [169]. Fittingly, proteins involved in the pathway of ubiquitin conjugation were also upregulated in these cells. It is well established that virus-derived proteins are targeted for degradation by the ubiquitin-proteasome pathway prior to MHC class I presentation [170].

Previous studies from this laboratory have shown that DBs induce the maturation and activation of immature dendritic cells and an induction of HLA-ABC in these cells [73]. Further to that DBs exogenously introduce viral antigens into the MHC-class I presentation pathway in fibroblasts, rendering them susceptible to CD8-T lymphocyte attack [57, 69]. This latter exceptional property of DBs could not be explained until now. The finding that both components of the MHC class I pathway and the ubiquitin-proteasome pathway are induced by DBs in fibroblasts provide a rationale, how DB-derived proteins can so efficiently be introduced in the MHC-class I presentation pathway in somatic cells. Taken together the results of this work provide further experimental explanation why DBs are so highly immunogenic, as evidenced by the induction of HCMV-specific CD8+ T lymphocyte responses in mice [55, 57, 69, 171].

Additionally, the application of DBs resulted in the upregulation of proteins involved in MHC class II restricted antigen presentation in iDCs. Especially the enhanced expression of the lectin receptor CD209 (DC-SIGN), which enables the acquisition of antigens by receptor-mediated endocytosis, appears to be interesting. It has been shown that ligands, internalized by lectin receptors enhance the efficiency of antigen processing and presentation to CD4+ T cells [172, 173]. The upregulation of DC-SIGN upon DB treatment may be one reason for the marked induction of CD4+ T cell responses in laboratory animals [57, 67]. Taken together, the results obtained here provide further insight into the pathways that lead to the exceptional antigenicity of DBs and will aid in the process of development of DBs as a vaccine against HCMV.

4.3 Impact of DBs on autophagy

Autophagy is a cellular process that promotes the proteolytic degradation of cytosolic components at the lysosome [174]. In times of starvation and stress, it provides nutrients for maintaining cell viability [175]. Furthermore, autophagy contributes to pathogen restriction (also termed as xenophagy) by regulating the expression of IFNs and antigen presentation on MHC class I and II molecules [176, 177]. It is estimated that approximately 20-30% of the cytoplasmic and nuclear antigens are provided by autophagy [172]. Upon DB-incubation, autophagy was induced at 24 h.p.a. in an IFN independent manner (Fig. 27). This result has to be observed with caution, because lipidated LC3B, a marker which is widely used to monitor autophagy, is also present in purified DBs (Fig. 5). Thus, it can´t be excluded that DBs- derived lipidated LC3B contributed to the increase of lipidated LC3B in the cell lysate. In a study performed by McFarlane et al., the induction of autophagy was analysed at 6 h.p.a. At this timepont, DBs did not induce autophagy. Furthermore, they haven´t observe an increase in lipidated LC3B that could refer to DB- derived protein [160]. Additional experiments are warranted to confirm that DBs indeed induce autophagy.

4.4 Activation of apoptosis of HCMV infected HFFs by DBs

Apoptosis is induced as a defence mechanism of the host cell in response to infection in order to restrict viral spread [178]. HCMV encodes proteins that block key apoptotic steps to ensure complete viral replication and progeny virus production [179, 180]. This study revealed that cells infected with HCMV and treated with DBs induced rather than repressed apoptosis. This effect was not seen, when DBs were applied to the cells in the absence of infection. In accordance with this, infected+DB-treated cells showed a markedly enhanced cytopathic effect upon microscopic inspection, compared to infected cells. Together, this indicates that DBs induced an antiviral environment in infected cells by subverting the anti-apoptotic effects of proteins, expressed by the virus.

How apoptosis is induced upon DBs application to infected cells remains unclear. However, one explanation could imply an effect of IRGs as mediators of apoptosis. Microarray studies have identified IRGs with proapoptotic functions [181]. Some of these IRGs were found to be upregulated in HFF incubated with DBs. It could be hypothesized that induction of these IRGs in combination with the pro-apoptotic response of the cell to HCMV infection leads to enhanced cell death of infected/DB-treated cells.

4.5 The ND10 antiviral restriction factor (RF) is not targeted by DBs

Antiviral RFs are constitutively expressed in cells. Their expression can be increased in either an IFN- dependent and IFN- independent manner (Landolfo et al., 2016; Ashley et al., 2019). The application of DBs to HFFs induced an upregulation of several known RF for HCMV, namely IFI16, MX1 and the proteins PML and SP100 of the ND10 complex. ND10 are spherical nuclear substructures which represent accumulations of the major cellular proteins PML, SP100 and hDaxx. ND10 are thought to be the key RF of HCMV replication (Landolfo et al., 2016). HCMV has developed strategies to circumvent the antiviral functions of ND10, which rely on the viral proteins IE1 and pp71. It is well established that the HCMV IE1 induces the dispersal of PML thereby preventing ND10 oligomerization and activation (Korioth et al., 1996; Lee et al., 2004; Schilling et al., 2017). DBs do not support viral IE1 expression. We thus hypothesized that DBs would not share the ND10-dispersing activity seen in HCMV infected cells. Immunofluorescence analysis performed in this work proved this as the application of DBs to HFFs had no effect on the ND10 complex as shown by intact dot-like PML and SP100 staining. Thus, DBs do not exhibit evasive mechanism to counteract the antiviral activity of ND10 as seen during HCMV infection, providing another argument for their suitability for vaccine development.

4.6 Interference of DBs with virus infection

During HCMV replication, DBs are synthesized and released from infected HFFs into the cell culture supernatant concomitantly with virions [47, 182]. DBs have also been documented in endothelial cells obtained from HCMV-infected patients [53], disproving the notion that DBs were aberrant products of cell culture. This raises the question about the function of these particles in the context of HCMV infection. The most likely assumption was that DBs serve a pro-viral role during infection. However, no alterations in viral genome replication or genome release was seen when DBs were applied simultaneously with the virus inoculum. Interestingly, the release of infectious progeny was reduced when DBs were applied together with the virus to cell cultures, as compared to cultures that were infected without DBs. And notably, the “priming” of HFFs with DBs prior to infection decreased both the release of viral genomes and even enhanced the release of infectious virus, compared to the co-application of DBs with virus. These experiments indicate that DBs impair rather than support HCMV infection, thus imposing an anti-viral effect. This is concordant with the marked induction of IRGs in different cells by DBs and the induction of mechanisms of programmed cell death.

In addition, the protein expression levels of MX1, IFIT3 and ISG15 were sustained for 48h in virus+DB- infected cells, whereas they are normally degraded within 48h during HCMV infection [77, 183, 184]. All of that together suggests that DBs induce an antiviral environment in cells that impedes viral productivity.

An interesting finding was that co-application of DBs with virus had only moderate effects on virus release and but little impact on genome replication. These results resemble the observations regarding the insensitivity of HCMV infection to the effects of IFN exposure [185]. It has been described that only cells pre-treated with IFNs prior to infection, but not after infection, exhibited antiviral effects [186]. This could provide an explanation, why viral genome replication, genome release and protein expression levels of IE1 kinetics were not altered when DBs were applied to HFFs simultaneously with the virus inoculum. It is tempting to assume that DBs act in a way comparable to IFNs that protect cells against infection in a paracrine rather than an autocrine fashion. Could it be that infected cells synthesize and release DBs in order to protect neighbouring cells? Although this is certainly a speculative notion it is certainly an attractive explanation why DBs are produced in-vivo.

Surprisingly, the application of DBs to infected HFFs resulted in a repression of expression of the early UL44 protein. Recently published data identified the HCMV DNA polymerase subunit UL44 as an inhibitor of the host antiviral immune response [187]. UL44 has been shown to interact with IRF3 and NF-κB, thereby inhibiting the binding of IRF3 and NF-κB to the promoters of their downstream antiviral genes [187]. DBs induce the expression IFI16, a cellular RF for HCMV that was shown to suppress the transcriptional activity of the viral DNA polymerase gene (UL54) and the UL44 gene [188]. Interestingly, in the later phase of infection, IFI16 is redirected from the nucleus to the virion assembly compartment (vAC) where it is incorporated into mature virions [189]. The current hypothesis is, that HCMV includes IFI16 into virions to counteract its restriction activity and to exploit its capacity to enhance IE gene transcription [189]. A similar effect might be imposed by DBs, as unpublished proteomic work from our laboratory proved that IFI16 was packaged into these particles (Plachter et al., unpublished).

HCMV infected cells release DBs both in vitro and in vivo. Based on the results of this work, we would propose the hypothesis that these DBs bind to cells in an autocrine or, more likely paracrine fashion. Components of DBs are then recognized via PRRs following their attachment to and entry into cells, leading to the induction of type I IFN expression. The PRRs that are important in this process still have to be determined. IFNs are then released and bind to their cognate receptor, again in a paracrine and autocrine fashion, leading to the

downstream induction of broad spectrum of antiviral IRGs via the JAK/STAT signalling pathway. This induces the establishment of a broad antiviral state both in cells that have received DBs and in neighbouring cells, thereby impeding HCMV infection and spread in an infected organ tissue. Work in progress is intended to further elucidate, in more detail, the molecular mechanisms of DB- cell interaction with a particular focus on the impact of DBs on the course of HCMV infection.

4.7 Effect of Dynamin inhibition on DBs internalization

Immunofluorescence analyses demonstrated that pp65, the main constituent of DBs, can be detected in the nuclei of HFFs incubated with purified DBs within 30 minutes [190]. Electron microscopy (EM) studies of HFFs revealed that the uptake of DBs follows the same kinetics as complete virions and NIEPs, suggesting direct fusion with the plasma membrane as the common entry mechanism in HFFs [137]. It has been shown that the glycoprotein complex gH/gL/gO (TC) in the virion envelope mediates the entry into HFFs via membrane fusion. However, other cell types are primarily infected by endocytic entry. This entry process depends on the TC and, in addition, on the presence of the gH/gL/pUL128/pUL130/pUL131A-pentamer (PC) [119, 191].

The studies that investigated the entry events of viral particles mostly focused on HCMV virions. Here we investigated the pathways necessary for DB-entry in HFFs and ECs.

The initial uptake efficiency of PC-positive DBs by HFF was significantly lower compared to PC-negative DBs. This indicated that the kinetics of internalization of PC-positive DBs lagged behind the uptake kinetics of PC-negative DBs. Concordant with this was the finding that the dynamin-inhibitor Dynasore significantly reduced, but not abolished the entry of PC-positive DBs into HFFs. The uptake of PC-negative DBs, in contrast was independent of Dynasore, indicating that these particles use membrane fusion for fibroblast entry, similar to the uptake of PC-negative virions from laboratory strains [138, 192, 193].

The results thus indicate that the expression of the PC on DBs is a determinant for DB-entry into fibroblasts and that there are alternative pathways of entry. A study by Hetzenacker et al, demonstrated that majority of infectious HCMV virions entered HFFs by actin- dependent endocytosis, designated as macropinocytosis [138]. A study, where scanning transmission electron microscopy (STEM) tomography was used recorded macropinocytic-like protrusion enclosing virions and DBs [192]. Our data seem to support these alternative entry pathways for HCMV into fibroblasts.

PC-negative DBs do not enter ECs. A direct comparison of DB entry in these cells, depending on the PC was thus impossible. Still there was a marked reduction of DB uptake by ECs in the presence of Dynasore. The most likely explanation for this may be that endocytosis is a major entry pathway for DB into ECs. However, in general, data obtained with the use of Dynasore should be viewed with caution. Dynamin is essential for membrane remodelling and fission of vesicles during clathrin- mediated endocytosis (CME) [194]. Dynasore is a dynamin GTPase inhibitor that is known to prevent CME [141]. Dynamin- independent “off target” effects of Dynasore have been described, including reduction of plasma membrane cholesterol and the disruption of the actin cytoskeleton [194, 195]. The rearrangement of the actin cytoskeleton is essential for the formation of plasma membrane protrusions that engulf surrounding cargo and lead to macropinocytosis [196]. Thus, the observed decrease in DB-uptake could result from an inhibited mobilization of the cellular membrane as an indirect effect of Dynasore, thereby targeting macropinocytosis. Further experiments are necessary to investigate the uptake pathway of DBs in host cells. Hence, dynamin inhibition does not completely abrogate the endocytic uptake of PC-positive DBs in HFFs and ECs, and thus the entry mechanism should be verified by alternative approaches.

4.8 Conclusion and future directions

There is a high medical need for the development of an HCMV vaccine. DBs are a promising candidate that is due to be evaluated in clinical trials. Major issues that have to be addressed prior to human studies are possible adverse events and the impact of DBs on concurrent viral infection. In this work it has been shown that DBs induce the upregulation of IRGs which serve to mount an antiviral state within the host cell. No impact on cell viability was found. In addition, proteins and pathways are stimulated that are involved in the induction of adaptive T lymphocyte responses, thereby explaining the immunogenicity of DBs. Importantly, no evidence was found that DBs enhance viral replication, but rather restrict progeny production. Conclusively the results are highly supportive to use DBs in human trials.

A couple of questions, however, arise from this work. (i), what are the cellular mechanisms that sense DBs? (ii), what are the mechanisms that restrict viral progeny production after “DB-priming” of the cell? (iii), what is the role of autophagy induction in the pronounced stimulation of CD4- and CD8- T lymphocyte responses by DBs? and (iv), are DBs really suitable to protect neighbouring cells against HCMV infection and thus provide an antiviral environment in organ tissues. Studies are under way to address these issues.

References

1. Khanna, R. and D.J. Diamond, *Human cytomegalovirus vaccine: time to look for alternative options.* Trends Mol Med, 2006. **12**(1): p. 26-33.
2. Gerna, G. and D. Lilleri, *Human cytomegalovirus (HCMV) infection/re-infection: development of a protective HCMV vaccine.* New Microbiol, 2019. **42**(1): p. 1-20.
3. Gugliesi, F., et al., *Where do we Stand after Decades of Studying Human Cytomegalovirus?* Microorganisms, 2020. **8**(5).
4. Dolan, A., et al., *Genetic content of wild-type human cytomegalovirus.* J Gen Virol, 2004. **85**(Pt 5): p. 1301-1312.
5. Wyatt, J.P., J. Saxton, and et al., *Generalized cytomegalic inclusion disease.* J Pediatr, 1950. **36**(3): p. 271-94, illust.
6. Riley, H.D., Jr., *History of the cytomegalovirus.* South Med J, 1997. **90**(2): p. 184-90.
7. Landolfo, S., et al., *The human cytomegalovirus.* Pharmacol Ther, 2003. **98**(3): p. 269-97.
8. Griffiths, P., I. Baraniak, and M. Reeves, *The pathogenesis of human cytomegalovirus.* J Pathol, 2015. **235**(2): p. 288-97.
9. Zuhair, M., et al., *Estimation of the worldwide seroprevalence of cytomegalovirus: A systematic review and meta-analysis.* Rev Med Virol, 2019. **29**(3): p. e2034.
10. Horwitz, C.A., et al., *Clinical and laboratory evaluation of cytomegalovirus-induced mononucleosis in previously healthy individuals. Report of 82 cases.* Medicine (Baltimore), 1986. **65**(2): p. 124-34.
11. Rafailidis, P.I., et al., *Severe cytomegalovirus infection in apparently immunocompetent patients: a systematic review.* Virol J, 2008. **5**: p. 47.
12. Gianella, S., et al., *The Sordid Affair Between Human Herpesvirus and HIV.* J Infect Dis, 2015. **212**(6): p. 845-52.
13. Perello, R., et al., *Cytomegalovirus infection in HIV-infected patients in the era of combination antiretroviral therapy.* BMC Infect Dis, 2019. **19**(1): p. 1030.
14. Kenneson, A. and M.J. Cannon, *Review and meta-analysis of the epidemiology of congenital cytomegalovirus (CMV) infection.* Rev Med Virol, 2007. **17**(4): p. 253-76.
15. Dollard, S.C., S.D. Grosse, and D.S. Ross, *New estimates of the prevalence of neurological and sensory sequelae and mortality associated with congenital cytomegalovirus infection.* Rev Med Virol, 2007. **17**(5): p. 355-63.
16. Fowler, K.B. and S.B. Boppana, *Congenital cytomegalovirus infection.* Semin Perinatol, 2018. **42**(3): p. 149-154.
17. Nance, W.E., B.G. Lim, and K.M. Dodson, *Importance of congenital cytomegalovirus infections as a cause for pre-lingual hearing loss.* J Clin Virol, 2006. **35**(2): p. 221-5.
18. Fowler, K.B. and S.B. Boppana, *Congenital cytomegalovirus (CMV) infection and hearing deficit.* J Clin Virol, 2006. **35**(2): p. 226-31.
19. Sinzger, C., et al., *Fibroblasts, epithelial cells, endothelial cells and smooth muscle cells are major targets of human cytomegalovirus infection in lung and gastrointestinal tissues.* J Gen Virol, 1995. **76 (Pt 4)**: p. 741-50.
20. Sinzger, C. and G. Jahn, *Human cytomegalovirus cell tropism and pathogenesis.* Intervirology, 1996. **39**(5-6): p. 302-19.
21. Sinzger, C., M. Digel, and G. Jahn, *Cytomegalovirus cell tropism.* Curr Top Microbiol Immunol, 2008. **325**: p. 63-83.
22. Plachter, B., C. Sinzger, and G. Jahn, *Cell types involved in replication and distribution of human cytomegalovirus.* Adv Virus Res, 1996. **46**: p. 195-261.
23. Gerna, G., et al., *Human cytomegalovirus infection of the major leukocyte subpopulations and evidence for initial viral replication in polymorphonuclear leukocytes from viremic patients.* J Infect Dis, 1992. **166**(6): p. 1236-44.

24. Gerna, G., et al., *Human cytomegalovirus replicates abortively in polymorphonuclear leukocytes after transfer from infected endothelial cells via transient microfusion events.* J Virol, 2000. **74**(12): p. 5629-38.
25. Gerna, G., F. Baldanti, and M.G. Revello, *Pathogenesis of human cytomegalovirus infection and cellular targets.* Hum Immunol, 2004. **65**(5): p. 381-6.
26. Grefte, A., et al., *Presence of human cytomegalovirus (HCMV) immediate early mRNA but not ppUL83 (lower matrix protein pp65) mRNA in polymorphonuclear and mononuclear leukocytes during active HCMV infection.* J Gen Virol, 1994. **75 (Pt 8)**: p. 1989-98.
27. Jackson, J.W. and T. Sparer, *There Is Always Another Way! Cytomegalovirus' Multifaceted Dissemination Schemes.* Viruses, 2018. **10**(7).
28. Sinclair, J. and M. Reeves, *The intimate relationship between human cytomegalovirus and the dendritic cell lineage.* Front Microbiol, 2014. **5**: p. 389.
29. Gerna, G., A. Kabanova, and D. Lilleri, *Human Cytomegalovirus Cell Tropism and Host Cell Receptors.* Vaccines (Basel), 2019. **7**(3).
30. Cha, T.A., et al., *Human cytomegalovirus clinical isolates carry at least 19 genes not found in laboratory strains.* J Virol, 1996. **70**(1): p. 78-83.
31. Prichard, M.N., et al., *A review of genetic differences between limited and extensively passaged human cytomegalovirus strains.* Rev Med Virol, 2001. **11**(3): p. 191-200.
32. Sinzger, C., et al., *Modification of human cytomegalovirus tropism through propagation in vitro is associated with changes in the viral genome.* J Gen Virol, 1999. **80 (Pt 11)**: p. 2867-2877.
33. Hahn, G., et al., *Human cytomegalovirus UL131-128 genes are indispensable for virus growth in endothelial cells and virus transfer to leukocytes.* J Virol, 2004. **78**(18): p. 10023-33.
34. Wang, D. and T. Shenk, *Human cytomegalovirus UL131 open reading frame is required for epithelial cell tropism.* J Virol, 2005. **79**(16): p. 10330-8.
35. Gerna, G., et al., *Dendritic-cell infection by human cytomegalovirus is restricted to strains carrying functional UL131-128 genes and mediates efficient viral antigen presentation to CD8+ T cells.* J Gen Virol, 2005. **86**(Pt 2): p. 275-284.
36. Vanarsdall, A.L. and D.C. Johnson, *Human cytomegalovirus entry into cells.* Curr Opin Virol, 2012. **2**(1): p. 37-42.
37. Buscher, N., et al., *The proteome of human cytomegalovirus virions and dense bodies is conserved across different strains.* Medical Microbiology and Immunology, 2015. **204**(3): p. 285-293.
38. Varnum, S.M., et al., *Identification of proteins in human cytomegalovirus (HCMV) particles: the HCMV proteome.* J Virol, 2004. **78**(20): p. 10960-6.
39. Kabanova, A., et al., *Platelet-derived growth factor-alpha receptor is the cellular receptor for human cytomegalovirus gHgLgO trimer.* Nature Microbiology, 2016. **1**(8).
40. Wu, Y., et al., *Human cytomegalovirus glycoprotein complex gH/gL/gO uses PDGFR-alpha as a key for entry.* PLoS Pathog, 2017. **13**(4): p. e1006281.
41. Martinez-Martin, N., et al., *An Unbiased Screen for Human Cytomegalovirus Identifies Neuropilin-2 as a Central Viral Receptor.* Cell, 2018. **174**(5): p. 1158-1171 e19.
42. Nguyen, C.C. and J.P. Kamil, *Pathogen at the Gates: Human Cytomegalovirus Entry and Cell Tropism.* Viruses, 2018. **10**(12).
43. Liu, J., et al., *The Human Cytomegalovirus Trimer and Pentamer Promote Sequential Steps in Entry into Epithelial and Endothelial Cells at Cell Surfaces and Endosomes.* J Virol, 2018. **92**(21).
44. Vanarsdall, A.L., et al., *CD147 Promotes Entry of Pentamer-Expressing Human Cytomegalovirus into Epithelial and Endothelial Cells.* mBio, 2018. **9**(3).
45. Stein, K.R., et al., *CD46 facilitates entry and dissemination of human cytomegalovirus.* Nat Commun, 2019. **10**(1): p. 2699.
46. E, X., et al., *OR14I1 is a receptor for the human cytomegalovirus pentameric complex and defines viral epithelial cell tropism.* Proc Natl Acad Sci U S A, 2019. **116**(14): p. 7043-7052.

47. Craighead, J.E., R.E. Kanich, and J.D. Almeida, *Nonviral microbodies with viral antigenicity produced in cytomegalovirus-infected cells.* J Virol, 1972. **10**(4): p. 766-75.
48. Sarov, I. and I. Abady, *The morphogenesis of human cytomegalovirus. Isolation and polypeptide characterization of cytomegalovirions and dense bodies.* Virology, 1975. **66**(2): p. 464-73.
49. Talbot, P. and J.D. Almeida, *Human cytomegalovirus: purification of enveloped virions and dense bodies.* J Gen Virol, 1977. **36**(2): p. 345-9.
50. Irmiere, A. and W. Gibson, *Isolation and characterization of a noninfectious virion-like particle released from cells infected with human strains of cytomegalovirus*. Virology, 1983. **130**(1): p. 118-33.
51. Severi, B., M.P. Landini, and E. Govoni, *Human cytomegalovirus morphogenesis: an ultrastructural study of the late cytoplasmic phases.* Arch Virol, 1988. **98**(1-2): p. 51-64.
52. Stinski, M.F., *Human cytomegalovirus: glycoproteins associated with virions and dense bodies.* J Virol, 1976. **19**(2): p. 594-609.
53. Grefte, A., et al., *Circulating cytomegalovirus (CMV)-infected endothelial cells in patients with an active CMV infection.* J Infect Dis, 1993. **167**(2): p. 270-7.
54. Mohammad, A.A., et al., *Human cytomegalovirus microRNAs are carried by virions and dense bodies and are delivered to target cells.* J Gen Virol, 2017. **98**(5): p. 1058-1072.
55. Cayatte, C., et al., *Cytomegalovirus vaccine strain towne-derived dense bodies induce broad cellular immune responses and neutralizing antibodies that prevent infection of fibroblasts and epithelial cells.* J Virol, 2013. **87**(20): p. 11107-20.
56. Forghani, B. and N.J. Schmidt, *Humoral immune response to virions and dense bodies of human cytomegalovirus determined by enzyme immunofluorescence assay.* J Med Virol, 1980. **6**(2): p. 119-27.
57. Pepperl, S., et al., *Dense bodies of human cytomegalovirus induce both humoral and cellular immune responses in the absence of viral gene expression.* J Virol, 2000. **74**(13): p. 6132-46.
58. Pepperl-Klindworth, S., N. Frankenberg, and B. Plachter, *Development of novel vaccine strategies against human cytomegalovirus infection based on subviral particles.* Journal of Clinical Virology, 2002. **25**: p. S75-S85.
59. Lehmann, C., et al., *Dense Bodies of a gH/gL/UL128/UL130/UL131 Pentamer-Repaired Towne Strain of Human Cytomegalovirus Induce an Enhanced Neutralizing Antibody Response.* J Virol, 2019. **93**(17).
60. Wussow, F., et al., *Neutralization of Human Cytomegalovirus Entry into Fibroblasts and Epithelial Cells.* Vaccines, 2017. **5**(4).
61. Vanarsdall, A.L., et al., *HCMV trimer- and pentamer-specific antibodies synergize for virus neutralization but do not correlate with congenital transmission.* Proc Natl Acad Sci U S A, 2019. **116**(9): p. 3728-3733.
62. Gerna, G., et al., *Human cytomegalovirus serum neutralizing antibodies block virus infection of endothelial/epithelial cells, but not fibroblasts, early during primary infection.* J Gen Virol, 2008. **89**(Pt 4): p. 853-865.
63. Macagno, A., et al., *Isolation of human monoclonal antibodies that potently neutralize human cytomegalovirus infection by targeting different epitopes on the gH/gL/UL128-131A complex.* J Virol, 2010. **84**(2): p. 1005-13.
64. Fouts, A.E., et al., *Antibodies against the gH/gL/UL128/UL130/UL131 complex comprise the majority of the anti-cytomegalovirus (anti-CMV) neutralizing antibody response in CMV hyperimmune globulin.* J Virol, 2012. **86**(13): p. 7444-7.
65. Wussow, F., et al., *Human cytomegalovirus vaccine based on the envelope gH/gL pentamer complex.* PLoS Pathog, 2014. **10**(11): p. e1004524.
66. Bachmann, M.F. and G.T. Jennings, *Vaccine delivery: a matter of size, geometry, kinetics and molecular patterns.* Nat Rev Immunol, 2010. **10**(11): p. 787-96.

67. Becke, S., et al., *Optimized recombinant dense bodies of human cytomegalovirus efficiently prime virus specific lymphocytes and neutralizing antibodies without the addition of adjuvant.* Vaccine, 2010. **28**(38): p. 6191-8.
68. Pepperl-Klindworth, S., et al., *Protein delivery by subviral particles of human cytomegalovirus.* Gene Ther, 2003. **10**(3): p. 278-84.
69. Mersseman, V., et al., *Exogenous introduction of an immunodominant peptide from the non-structural IE1 protein of human cytomegalovirus into the MHC class I presentation pathway by recombinant dense bodies.* J Gen Virol, 2008. **89**(Pt 2): p. 369-379.
70. Banchereau, J. and R.M. Steinman, *Dendritic cells and the control of immunity.* Nature, 1998. **392**(6673): p. 245-52.
71. Pozzi, L.A., J.W. Maciaszek, and K.L. Rock, *Both dendritic cells and macrophages can stimulate naive CD8 T cells in vivo to proliferate, develop effector function, and differentiate into memory cells.* J Immunol, 2005. **175**(4): p. 2071-81.
72. Banchereau, J., et al., *Immunobiology of dendritic cells.* Annu Rev Immunol, 2000. **18**: p. 767-811.
73. Sauer, C., et al., *Subviral dense bodies of human cytomegalovirus stimulate maturation and activation of monocyte-derived immature dendritic cells.* J Virol, 2013. **87**(20): p. 11287-91.
74. Schneider-Ohrum, K., et al., *Production of Cytomegalovirus Dense Bodies by Scalable Bioprocess Methods Maintains Immunogenicity and Improves Neutralizing Antibody Titers.* J Virol, 2016. **90**(22): p. 10133-10144.
75. Gogesch, P., et al., *Production Strategies for Pentamer-Positive Subviral Dense Bodies as a Safe Human Cytomegalovirus Vaccine.* Vaccines (Basel), 2019. **7**(3).
76. Schoggins, J.W. and C.M. Rice, *Interferon-stimulated genes and their antiviral effector functions.* Curr Opin Virol, 2011. **1**(6): p. 519-25.
77. Weekes, M.P., et al., *Quantitative temporal viromics: an approach to investigate host-pathogen interaction.* Cell, 2014. **157**(6): p. 1460-1472.
78. Abe, T. and S.D. Shapira, *Negative Regulation of Cytosolic Sensing of DNA.* Int Rev Cell Mol Biol, 2019. **344**: p. 91-115.
79. Motwani, M., S. Pesiridis, and K.A. Fitzgerald, *DNA sensing by the cGAS-STING pathway in health and disease.* Nat Rev Genet, 2019. **20**(11): p. 657-674.
80. Marques, M., A.R. Ferreira, and D. Ribeiro, *The Interplay between Human Cytomegalovirus and Pathogen Recognition Receptor Signaling.* Viruses, 2018. **10**(10).
81. Rehwinkel, J. and M.U. Gack, *RIG-I-like receptors: their regulation and roles in RNA sensing.* Nat Rev Immunol, 2020. **20**(9): p. 537-551.
82. Aaronson, D.S. and C.M. Horvath, *A road map for those who don't know JAK-STAT.* Science, 2002. **296**(5573): p. 1653-5.
83. Compton, T., et al., *Human cytomegalovirus activates inflammatory cytokine responses via CD14 and Toll-like receptor 2.* J Virol, 2003. **77**(8): p. 4588-96.
84. May, T., et al., *Synthetic gene regulation circuits for control of cell expansion.* Tissue Eng Part A, 2010. **16**(2): p. 441-52.
85. Lieber, D., et al., *A permanently growing human endothelial cell line supports productive infection with human cytomegalovirus under conditional cell growth arrest.* Biotechniques, 2015. **59**(3): p. 127-36.
86. Shevchenko, A., et al., *In-gel digestion for mass spectrometric characterization of proteins and proteomes.* Nat Protoc, 2006. **1**(6): p. 2856-60.
87. Boersema, P.J., et al., *Multiplex peptide stable isotope dimethyl labeling for quantitative proteomics.* Nat Protoc, 2009. **4**(4): p. 484-94.
88. Rappsilber, J., M. Mann, and Y. Ishihama, *Protocol for micro-purification, enrichment, pre-fractionation and storage of peptides for proteomics using StageTips.* Nat Protoc, 2007. **2**(8): p. 1896-906.
89. Craighead, J.E., R.E. Kanich, and J.D. Almeida, *Nonviral microbodies with viral antigenicity produced in cytomegalovirus-infected cells.* J. Virol, 1972. **10**: p. 766-775.

90. Sarov, I. and I. Abady, *The morphogenesis of human cytomegalovirus. Isolation and polypeptide characterization of cytomegalovirions and dense bodies.* Virology, 1975. **66**: p. 464-473.
91. Stinski, M.F., *Human cytomegalovirus: glycoproteins associated with virions and dense bodies.* J. Virol, 1976. **19**(2): p. 594-609.
92. Fiala, M., et al., *Cytomegalovirus proteins. I. Polypeptides of virions and dense bodies.* J. Virol, 1976. **19**(1): p. 243-254.
93. Roby, C. and W. Gibson, *Characterization of phosphoproteins and protein kinase activity of virions, noninfectious enveloped particles, and dense bodies of human cytomegalovirus.* J. Virol, 1986. **59**: p. 714-727.
94. Varnum, S.M., et al., *Identification of proteins in human cytomegalovirus (HCMV) particles: the HCMV proteome.* J. Virol, 2004. **78**(20): p. 10960-10966.
95. Büscher, N., et al., *The proteome of human cytomegalovirus virions and dense bodies is conserved across different strains.* Med. Microbiol. Immunol, 2015. **204**(3): p. 285-293.
96. Sarov, I., et al., *Stimulation of human lymphocytes by cytomegalovirions and dense bodies.* Med. Microbiol. Immunol. Berl, 1978. **166**: p. 81-89.
97. Pepperl, S., et al., *Dense bodies of human cytomegalovirus induce both humoral and cellular immune responses in the absence of viral gene expression.* J. Virol, 2000. **74**(13): p. 6132-6146.
98. Sauer, C., et al., *Subviral dense bodies of human cytomegalovirus stimulate maturation and activation of monocyte-derived immature dendritic cells.* J. Virol, 2013. **87**(20): p. 11287-11291.
99. Lehmann, C., et al., *Dense bodies of a gH/gL/UL128-131 pentamer repaired Towne strain of human cytomegalovirus induce an enhanced neutralizing antibody response.* J Virol, 2019. **93**(17).
100. Plotkin, S.A. and B. Plachter, *Cytomegalovirus Vaccine: On the Way to the Future?*, in *Cytomegaloviruses: From Molecular Pathogenesis to Intervention*, M.J. Reddehase, Editor. 2013, Caister Academic Press: Norfolk, U.K. p. 424-449.
101. Schleiss, M.R., *Cytomegalovirus vaccine development.* Curr. Top. Microbiol. Immunol, 2008. **325**: p. 361-382.
102. Khanna, R. and D.J. Diamond, *Human cytomegalovirus vaccine: time to look for alternative options.* Trends Mol. Med, 2006. **12**(1): p. 26-33.
103. Jean Beltran, P.M. and I.M. Cristea, *The life cycle and pathogenesis of human cytomegalovirus infection: lessons from proteomics.* Expert Rev Proteomics, 2014. **11**(6): p. 697-711.
104. Baldick, C.J., Jr. and T. Shenk, *Proteins associated with purified human cytomegalovirus particles.* J Virol, 1996. **70**(9): p. 6097-105.
105. Karniely, S., et al., *Human Cytomegalovirus Infection Upregulates the Mitochondrial Transcription and Translation Machineries.* mBio, 2016. **7**(2): p. e00029.
106. Poole, E. and J. Sinclair, *Understanding HCMV Latency Using Unbiased Proteomic Analyses.* Pathogens, 2020. **9**(7).
107. Taisne, C., et al., *Human cytomegalovirus hijacks the autophagic machinery and LC3 homologs in order to optimize cytoplasmic envelopment of mature infectious particles.* Sci Rep, 2019. **9**(1): p. 4560.
108. Zimmermann, C., et al., *Autophagy interferes with human cytomegalovirus genome replication, morphogenesis, and progeny release.* Autophagy, 2020: p. 1-17.
109. Ishov, A.M., et al., *PML is critical for ND10 formation and recruits the PML-interacting protein daxx to this nuclear structure when modified by SUMO-1.* J Cell Biol, 1999. **147**(2): p. 221-34.
110. Tavalai, N., et al., *Nuclear domain 10 components promyelocytic leukemia protein and hDaxx independently contribute to an intrinsic antiviral defense against human cytomegalovirus infection.* J Virol, 2008. **82**(1): p. 126-37.

111. Tavalai, N., et al., *Evidence for a role of the cellular ND10 protein PML in mediating intrinsic immunity against human cytomegalovirus infections.* J Virol, 2006. **80**(16): p. 8006-18.
112. Tavalai, N. and T. Stamminger, *Intrinsic cellular defense mechanisms targeting human cytomegalovirus.* Virus Res, 2011. **157**(2): p. 128-33.
113. Korioth, F., et al., *The nuclear domain 10 (ND10) is disrupted by the human cytomegalovirus gene product IE1.* Exp Cell Res, 1996. **229**(1): p. 155-8.
114. Ahn, J.H. and G.S. Hayward, *The major immediate-early proteins IE1 and IE2 of human cytomegalovirus colocalize with and disrupt PML-associated nuclear bodies at very early times in infected permissive cells.* J Virol, 1997. **71**(6): p. 4599-613.
115. Wilkinson, G.W., et al., *Disruption of PML-associated nuclear bodies mediated by the human cytomegalovirus major immediate early gene product.* J Gen Virol, 1998. **79 (Pt 5)**: p. 1233-45.
116. Schilling, E.M., et al., *The Human Cytomegalovirus IE1 Protein Antagonizes PML Nuclear Body-Mediated Intrinsic Immunity via the Inhibition of PML De Novo SUMOylation.* J Virol, 2017. **91**(4).
117. Ho, D.D., et al., *Replication of human cytomegalovirus in endothelial cells.* J Infect Dis, 1984. **150**(6): p. 956-7.
118. Jarvis, M.A. and J.A. Nelson, *Human cytomegalovirus persistence and latency in endothelial cells and macrophages.* Curr Opin Microbiol, 2002. **5**(4): p. 403-7.
119. Ryckman, B.J., M.C. Chase, and D.C. Johnson, *HCMV gH/gL/UL128-131 interferes with virus entry into epithelial cells: evidence for cell type-specific receptors.* Proc Natl Acad Sci U S A, 2008. **105**(37): p. 14118-23.
120. Simmen, K.A., et al., *Global modulation of cellular transcription by human cytomegalovirus is initiated by viral glycoprotein B.* Proc Natl Acad Sci U S A, 2001. **98**(13): p. 7140-5.
121. Rice, G.P., R.D. Schrier, and M.B. Oldstone, *Cytomegalovirus infects human lymphocytes and monocytes: virus expression is restricted to immediate-early gene products.* Proc Natl Acad Sci U S A, 1984. **81**(19): p. 6134-8.
122. Soderberg-Naucler, C., et al., *Reactivation of latent human cytomegalovirus in CD14(+) monocytes is differentiation dependent.* J Virol, 2001. **75**(16): p. 7543-54.
123. Smith, M.S., et al., *Human cytomegalovirus induces monocyte differentiation and migration as a strategy for dissemination and persistence.* J Virol, 2004. **78**(9): p. 4444-53.
124. Whitelaw, D.M., *Observations on human monocyte kinetics after pulse labeling.* Cell Tissue Kinet, 1972. **5**(4): p. 311-7.
125. Chan, G., et al., *Transcriptome analysis reveals human cytomegalovirus reprograms monocyte differentiation toward an M1 macrophage.* J Immunol, 2008. **181**(1): p. 698-711.
126. Chan, G., et al., *PI3K-dependent upregulation of Mcl-1 by human cytomegalovirus is mediated by epidermal growth factor receptor and inhibits apoptosis in short-lived monocytes.* J Immunol, 2010. **184**(6): p. 3213-22.
127. Stevenson, E.V., et al., *HCMV reprogramming of infected monocyte survival and differentiation: a Goldilocks phenomenon.* Viruses, 2014. **6**(2): p. 782-807.
128. Bentz, G.L., et al., *Human cytomegalovirus (HCMV) infection of endothelial cells promotes naive monocyte extravasation and transfer of productive virus to enhance hematogenous dissemination of HCMV.* J Virol, 2006. **80**(23): p. 11539-55.
129. Riegler, S., et al., *Monocyte-derived dendritic cells are permissive to the complete replicative cycle of human cytomegalovirus.* J Gen Virol, 2000. **81**(Pt 2): p. 393-9.
130. Raftery, M.J., et al., *Targeting the function of mature dendritic cells by human cytomegalovirus: a multilayered viral defense strategy.* Immunity, 2001. **15**(6): p. 997-1009.
131. Beck, K., et al., *Human cytomegalovirus impairs dendritic cell function: a novel mechanism of human cytomegalovirus immune escape.* Eur J Immunol, 2003. **33**(6): p. 1528-38.
132. Moutaftsi, M., et al., *Human cytomegalovirus inhibits maturation and impairs function of monocyte-derived dendritic cells.* Blood, 2002. **99**(8): p. 2913-21.

133. Kiu, H. and S.E. Nicholson, *Biology and significance of the JAK/STAT signalling pathways.* Growth Factors, 2012. **30**(2): p. 88-106.
134. Shuai, K. and B. Liu, *Regulation of JAK-STAT signalling in the immune system.* Nat Rev Immunol, 2003. **3**(11): p. 900-11.
135. Ashley, C.L., et al., *Interferon-Independent Upregulation of Interferon-Stimulated Genes during Human Cytomegalovirus Infection is Dependent on IRF3 Expression.* Viruses, 2019. **11**(3).
136. Compton, T., R.R. Nepomuceno, and D.M. Nowlin, *Human cytomegalovirus penetrates host cells by pH-independent fusion at the cell surface.* Virology, 1992. **191**(1): p. 387-95.
137. Topilko, A. and S. Michelson, *Hyperimmediate entry of human cytomegalovirus virions and dense bodies into human fibroblasts.* Res Virol, 1994. **145**(2): p. 75-82.
138. Hetzenecker, S., A. Helenius, and M.A. Krzyzaniak, *HCMV Induces Macropinocytosis for Host Cell Entry in Fibroblasts.* Traffic, 2016. **17**(4): p. 351-68.
139. Bodaghi, B., et al., *Entry of human cytomegalovirus into retinal pigment epithelial and endothelial cells by endocytosis.* Invest Ophthalmol Vis Sci, 1999. **40**(11): p. 2598-607.
140. Ryckman, B.J., et al., *Human cytomegalovirus entry into epithelial and endothelial cells depends on genes UL128 to UL150 and occurs by endocytosis and low-pH fusion.* J Virol, 2006. **80**(2): p. 710-22.
141. Macia, E., et al., *Dynasore, a cell-permeable inhibitor of dynamin.* Dev Cell, 2006. **10**(6): p. 839-50.
142. Ferguson, S.M. and P. De Camilli, *Dynamin, a membrane-remodelling GTPase.* Nat Rev Mol Cell Biol, 2012. **13**(2): p. 75-88.
143. Schmolke, S., et al., *The dominant phosphoprotein pp65 (UL83) of human cytomegalovirus is dispensable for growth in cell culture.* J Virol, 1995. **69**(10): p. 5959-68.
144. Hesse, J., et al., *Human cytomegalovirus pp71 stimulates major histocompatibility complex class i presentation of IE1-derived peptides at immediate early times of infection.* J Virol, 2013. **87**(9): p. 5229-38.
145. Chevillotte, M., et al., *Major tegument protein pp65 of human cytomegalovirus is required for the incorporation of pUL69 and pUL97 into the virus particle and for viral growth in macrophages.* J Virol, 2009. **83**(6): p. 2480-90.
146. Cristea, I.M., et al., *Human cytomegalovirus pUL83 stimulates activity of the viral immediate-early promoter through its interaction with the cellular IFI16 protein.* J Virol, 2010. **84**(15): p. 7803-14.
147. Liu, B. and M.F. Stinski, *Human cytomegalovirus contains a tegument protein that enhances transcription from promoters with upstream ATF and AP-1 cis-acting elements.* J Virol, 1992. **66**(7): p. 4434-44.
148. Baldick, C.J., Jr., et al., *Human cytomegalovirus tegument protein pp71 (ppUL82) enhances the infectivity of viral DNA and accelerates the infectious cycle.* J Virol, 1997. **71**(6): p. 4400-8.
149. Bresnahan, W.A. and T.E. Shenk, *UL82 virion protein activates expression of immediate early viral genes in human cytomegalovirus-infected cells.* Proc Natl Acad Sci U S A, 2000. **97**(26): p. 14506-11.
150. Tavalai, N., et al., *Insertion of an EYFP-pp71 (UL82) coding sequence into the human cytomegalovirus genome results in a recombinant virus with enhanced viral growth.* J Virol, 2008. **82**(21): p. 10543-55.
151. Andreoni, M., et al., *A rapid microneutralization assay for the measurement of neutralizing antibody reactive with human cytomegalovirus.* J Virol Methods, 1989. **23**(2): p. 157-67.
152. Mortimore, G.E. and A.R. Poso, *Intracellular protein catabolism and its control during nutrient deprivation and supply.* Annu Rev Nutr, 1987. **7**: p. 539-64.
153. Mizushima, N. and M. Komatsu, *Autophagy: renovation of cells and tissues.* Cell, 2011. **147**(4): p. 728-41.
154. Levine, B., *Eating oneself and uninvited guests: autophagy-related pathways in cellular defense.* Cell, 2005. **120**(2): p. 159-62.

155. Kwon, D.H. and H.K. Song, *A Structural View of Xenophagy, a Battle between Host and Microbes.* Mol Cells, 2018. **41**(1): p. 27-34.
156. Chiramel, A.I., N.R. Brady, and R. Bartenschlager, *Divergent roles of autophagy in virus infection.* Cells, 2013. **2**(1): p. 83-104.
157. Choi, Y., J.W. Bowman, and J.U. Jung, *Autophagy during viral infection - a double-edged sword.* Nat Rev Microbiol, 2018. **16**(6): p. 341-354.
158. Kabeya, Y., et al., *LC3, a mammalian homologue of yeast Apg8p, is localized in autophagosome membranes after processing.* EMBO J, 2000. **19**(21): p. 5720-8.
159. Kabeya, Y., et al., *LC3, GABARAP and GATE16 localize to autophagosomal membrane depending on form-II formation.* J Cell Sci, 2004. **117**(Pt 13): p. 2805-12.
160. McFarlane, S., et al., *Early induction of autophagy in human fibroblasts after infection with human cytomegalovirus or herpes simplex virus 1.* J Virol, 2011. **85**(9): p. 4212-21.
161. Schmeisser, H., et al., *Type I interferons induce autophagy in certain human cancer cell lines.* Autophagy, 2013. **9**(5): p. 683-96.
162. Schmeisser, H., J. Bekisz, and K.C. Zoon, *New function of type I IFN: induction of autophagy.* J Interferon Cytokine Res, 2014. **34**(2): p. 71-8.
163. Zhao, J., et al., *Human cytomegalovirus infection-induced autophagy was associated with the biological behavioral changes of human umbilical vein endothelial cell (HUVEC).* Biomed Pharmacother, 2018. **102**: p. 938-946.
164. Gibson, W. and A. Irmiere, *Selection of particles and proteins for use as human cytomegalovirus subunit vaccines.* Birth Defects Orig Artic Ser, 1984. **20**(1): p. 305-24.
165. Shaw, A.E., et al., *Fundamental properties of the mammalian innate immune system revealed by multispecies comparison of type I interferon responses.* PLoS Biol, 2017. **15**(12): p. e2004086.
166. Hur, S., *Double-Stranded RNA Sensors and Modulators in Innate Immunity.* Annu Rev Immunol, 2019. **37**: p. 349-375.
167. Weber, F., et al., *Double-stranded RNA is produced by positive-strand RNA viruses and DNA viruses but not in detectable amounts by negative-strand RNA viruses.* J Virol, 2006. **80**(10): p. 5059-64.
168. Marshall, E.E., et al., *Essential role for either TRS1 or IRS1 in human cytomegalovirus replication.* J Virol, 2009. **83**(9): p. 4112-20.
169. Hewitt, E.W., *The MHC class I antigen presentation pathway: strategies for viral immune evasion.* Immunology, 2003. **110**(2): p. 163-9.
170. Leone, P., et al., *MHC class I antigen processing and presenting machinery: organization, function, and defects in tumor cells.* J Natl Cancer Inst, 2013. **105**(16): p. 1172-87.
171. Besold, K., et al., *Processing and MHC class I presentation of human cytomegalovirus pp65-derived peptides persist despite gpUS2-11-mediated immune evasion.* J Gen Virol, 2007. **88**(Pt 5): p. 1429-1439.
172. Roche, P.A. and K. Furuta, *The ins and outs of MHC class II-mediated antigen processing and presentation.* Nat Rev Immunol, 2015. **15**(4): p. 203-16.
173. Engering, A., et al., *The dendritic cell-specific adhesion receptor DC-SIGN internalizes antigen for presentation to T cells.* J Immunol, 2002. **168**(5): p. 2118-26.
174. Glick, D., S. Barth, and K.F. Macleod, *Autophagy: cellular and molecular mechanisms.* J Pathol, 2010. **221**(1): p. 3-12.
175. Deretic, V. and B. Levine, *Autophagy, immunity, and microbial adaptations.* Cell Host Microbe, 2009. **5**(6): p. 527-49.
176. Tian, Y., M.L. Wang, and J. Zhao, *Crosstalk between Autophagy and Type I Interferon Responses in Innate Antiviral Immunity.* Viruses, 2019. **11**(2).
177. Munz, C., *Autophagy proteins in antigen processing for presentation on MHC molecules.* Immunol Rev, 2016. **272**(1): p. 17-27.
178. Fliss, P.M. and W. Brune, *Prevention of cellular suicide by cytomegaloviruses.* Viruses, 2012. **4**(10): p. 1928-49.

179. McCormick, A.L., *Control of apoptosis by human cytomegalovirus.* Curr Top Microbiol Immunol, 2008. **325**: p. 281-95.
180. Collins-McMillen, D., et al., *HCMV Infection and Apoptosis: How Do Monocytes Survive HCMV Infection?* Viruses, 2018. **10**(10).
181. Chawla-Sarkar, M., et al., *Apoptosis and interferons: role of interferon-stimulated genes as mediators of apoptosis.* Apoptosis, 2003. **8**(3): p. 237-49.
182. Roby, C. and W. Gibson, *Characterization of phosphoproteins and protein kinase activity of virions, noninfectious enveloped particles, and dense bodies of human cytomegalovirus.* J Virol, 1986. **59**(3): p. 714-27.
183. Goodwin, C.M., J.H. Ciesla, and J. Munger, *Who's Driving? Human Cytomegalovirus, Interferon, and NFkappaB Signaling.* Viruses, 2018. **10**(9).
184. Dell'Oste, V., et al., *Tuning the Orchestra: HCMV vs. Innate Immunity.* Front Microbiol, 2020. **11**: p. 661.
185. Glasgow, L.A., et al., *Interferon and cytomegalovirus in vivo and in vitro.* Proc Soc Exp Biol Med, 1967. **125**(3): p. 843-9.
186. Holmes, A.R., L. Rasmussen, and T.C. Merigan, *Factors affecting the interferon sensitivity of human cytomegalovirus.* Intervirology, 1978. **9**(1): p. 48-55.
187. Fu, Y.Z., et al., *Human Cytomegalovirus DNA Polymerase Subunit UL44 Antagonizes Antiviral Immune Responses by Suppressing IRF3- and NF-kappaB-Mediated Transcription.* J Virol, 2019. **93**(11).
188. Gariano, G.R., et al., *The intracellular DNA sensor IFI16 gene acts as restriction factor for human cytomegalovirus replication.* PLoS Pathog, 2012. **8**(1): p. e1002498.
189. Dell'Oste, V., et al., *Innate nuclear sensor IFI16 translocates into the cytoplasm during the early stage of in vitro human cytomegalovirus infection and is entrapped in the egressing virions during the late stage.* J Virol, 2014. **88**(12): p. 6970-82.
190. Plachter, B., K. Weise, and M.J. Reddehase, *[Pathogenesis and diagnosis of cytomegalovirus infection].* Dtsch Med Wochenschr, 1996. **121**(44): p. 1365-8.
191. Nogalski, M.T., et al., *The HCMV gH/gL/UL128-131 complex triggers the specific cellular activation required for efficient viral internalization into target monocytes.* PLoS Pathog, 2013. **9**(7): p. e1003463.
192. Abdellatif, M.E.A., C. Sinzger, and P. Walther, *Investigating HCMV entry into host cells by STEM tomography.* J Struct Biol, 2018. **204**(3): p. 406-419.
193. Archer, M.A., et al., *Inhibition of endocytic pathways impacts cytomegalovirus maturation.* Sci Rep, 2017. **7**: p. 46069.
194. Preta, G., J.G. Cronin, and I.M. Sheldon, *Dynasore - not just a dynamin inhibitor.* Cell Commun Signal, 2015. **13**: p. 24.
195. Ivanov, A.I., *Pharmacological inhibitors of exocytosis and endocytosis: novel bullets for old targets.* Methods Mol Biol, 2014. **1174**: p. 3-18.
196. Swanson, J.A., *Shaping cups into phagosomes and macropinosomes.* Nat Rev Mol Cell Biol, 2008. **9**(8): p. 639-49.

Appendix

S1:

HFFs_Interferon Regulated protein groups 24h after DBs exposure in Experiment_1

Threshold: log2Ratio 0.58 in minimum one of the 2 replicates
log2Ratio 0.58 = fold increase of 1.5

upregulated
downregulated

Protein.ID	Protein.name	Gene.name	Mass (kDa)	Razor + unique peptides	Experiment 1 log2.Ratio.DB/Contr replicate 1	replicate 2
P20591	Interferon-induced GTP-binding protein Mx1	MX1	75,519	13	3,037	1,446
P05161	Ubiquitin-like protein ISG15	ISG15	17,887	5	2,789	2,380
O14879	Interferon-induced protein with tetratricopeptide repeats 3	IFIT3	55,984	3	2,782	
Q9H223	EH domain-containing protein 4	EHD4	61,155	2	1,676	
P42224	Signal transducer and activator of transcription 1-alpha/beta	STAT1	87,334	18	1,399	1,312
Q9UNH7-2	Sorting nexin-6, N-terminally processed	SNX6	33,818	6	0,857	0,191
P54920	Alpha-soluble NSF attachment protein	NAPA	9,8571	2	0,755	
P31689-2	DnaJ homolog subfamily A member 1	DNAJA1	37,044	5	0,720	0,562
P84090	Enhancer of rudimentary homolog	ERH	12,259	3	0,658	
P61769	Beta-2-microglobulin	B2M	13,946	3	0,658	0,319
Q9UJZ1-2	Stomatin-like protein 2, mitochondrial	STOML2	33,337	4	0,619	0,136
P32455	Interferon-induced guanylate-binding protein 1	GBP1	41,27	3	0,596	
Q9UKK9	ADP-sugar pyrophosphatase	NUDT5	25,895	5	0,583	0,395
Q9UJ70	N-acetyl-D-glucosamine kinase	NAGK	36,888	4	0,303	0,591
P40121-2	Macrophage-capping protein	CAPG	36,248	5	0,079	0,648
Q00765	Receptor expression-enhancing protein 5	REEP5	17,758	4	0,076	1,426
Q99733	Nucleosome assembly protein 1-like 4	NAP1L4	18,152	3	0,022	0,867
Q8N1F7	Nuclear pore complex protein Nup93	NUP93	93,381	2		2,220
P62829	60S ribosomal protein L23	RPL23	8,8994	2		1,175
P09543-2	2,3-cyclic-nucleotide 3-phosphodiesterase	CNP	20,245	2		0,969
Q9Y2A7	Nck-associated protein 1	NCKAP1	128,79	2		0,868
P19525-2	Interferon-induced, double-stranded RNA-activated protein kinase	PKR	40,68	3		0,849
Q63ZY3-3	KN motif and ankyrin repeat domain-containing protein 2	KANK2	90,043	4	-0,057	-0,661
P20337	Ras-related protein Rab-3B	RAB3B	24,741	4	-0,187	-1,055
P06454-2	Prothymosin alpha	PTMA	11,758	2	-0,586	
Q9NZN4	EH domain-containing protein 2	EHD2	61,161	16	-0,603	-0,392
P20908	Collagen alpha-1(V) chain	COL5A1	178,51	6	-0,641	-0,110
Q02818	Nucleobindin-1	NUCB1	51,62	3	-0,709	-0,255
Q15056-2	Eukaryotic translation initiation factor 4H	EIF4H	25,2	7	-0,709	-0,106
P08123	Collagen alpha-2(I) chain	COL1A2	129,15	24	-0,794	-0,642
Q9NZM1-5	Myoferlin	MYOF	134,71	2	-0,800	
Q14192	Four and a half LIM domains protein 2	FHL2	30,949	5	-0,888	-0,246
P02452	Collagen alpha-1(I) chain	COL1A1	138,94	40	-1,138	-1,177
P55145	Mesencephalic astrocyte-derived neurotrophic factor	MANF	21,143	4		-1,174
Q96FJ2	Dynein light chain 2, cytoplasmic	DYNLL2	10,35	2		-0,827

HFFs_Not interferon regulated protein groups 24h after DBs exposure in Experiment_1

Threshold: log2Ratio 0.58 in minimum one of the 2 replicates
log2Ratio 0.58 = fold increase of 1.5

upregulated
downregulated

Protein.ID	Protein.name	Gene.name	Mass (kDa)	Razor + unique peptides	Experiment 1 log2.Ratio.DB/Contr replicate 1	replicate 2
Q9UHL4	Dipeptidyl peptidase 2	DPP7	41,324	3	1,531	
Q99880	Histone H2B type 1-L	H2BC13	13,834	4	1,059	0,800
Q92747	Actin-related protein 2/3 complex subunit 1A	ARPC1A	41,569	3		1,175
Q71DI3	Histone H3.2	H3C15	10,334	2		0,668
P46783	40S ribosomal protein S10	RPS10	18,898	5	-0,595	-0,523
P14406	Cytochrome c oxidase subunit 7A2, mitochondrial	COX7A2	9,4259	2	-0,648	
P04259	Keratin, type II cytoskeletal	KRT6B	60,066	2		-2,436

S2:

HFFs_ Classification of regulated protein groups according to GO - Biological processes (UniProtKB) in Experiment_1

Threshold: log2Ratio 0.58 in minimum one of the 2 replicates = upregulated
log2Ratio 0.58 = fold increase of 1.5 = downregulated

Antiviral Defense

Protein.ID	Protein.name	Gene.name	Mass (kDa)	Razor + unique peptides	Experiment 1 log2.Ratio.DB/Contr replicate 1	replicate 2
P20591	Interferon-induced GTP-binding protein Mx1	MX1	75,519	13	3,037	1,446
P05161	Ubiquitin-like protein ISG15	ISG15	17,887	5	2,789	2,380
O14879	Interferon-induced protein with tetratricopeptide repeats 3	IFIT3	55,984	3	2,782	
P42224	Signal transducer and activator of transcription 1-alpha/beta	STAT1	87,334	18	1,399	1,312
P19525-2	Interferon-induced, double-stranded RNA-activated protein kinase	PKR	40,68	3		0,849
P32455	Interferon-induced guanylate-binding protein 1	GBP1	41,27	3	0,596	

Protein Transport

Protein.ID	Protein.name	Gene.name	Mass (kDa)	Razor + unique peptides	Experiment 1 log2.Ratio.DB/Contr replicate 1	replicate 2
Q9UNH7-2	Sorting nexin-6, N-terminally processed	SNX6	33,818	6	0,857	0,191
P54920	Alpha-soluble NSF attachment protein	NAPA	9,8571	2	0,755	
P31689-2	DnaJ homolog subfamily A member 1	DNAJA1	37,044	5	0,720	0,562
Q8N1F7	Nuclear pore complex protein Nup93	NUP93	93,381	2		2,220
P20337	Ras-related protein Rab-3B	RAB3B	24,741	4	-0,187	-1,055
Q96FJ2	Dynein light chain 2, cytoplasmic	DYNLL2	10,35	2		-0,827

Cytoskeleton Organization

Protein.ID	Protein.name	Gene.name	Mass (kDa)	Razor + unique peptides	Experiment 1 log2.Ratio.DB/Contr replicate 1	replicate 2
Q92747	Actin-related protein 2/3 complex subunit 1A	ARPC1A	41,569	3		1,175
Q9Y2A7	Nck-associated protein 1	NCKAP1	128,79	2		0,868
P40121-2	Macrophage-capping protein	CAPG	36,248	5	0,079	0,648
Q63ZY3-3	KN motif and ankyrin repeat domain-containing protein 2	KANK2	90,043	4	-0,057	-0,661
P04259	Keratin, type II cytoskeletal	KRT6B	60,066	2		-2,436

Endocytosis

Protein.ID	Protein.name	Gene.name	Mass (kDa)	Razor + unique peptides	Experiment 1 log2.Ratio.DB/Contr replicate 1	replicate 2
Q92747	Actin-related protein 2/3 complex subunit 1A	ARPC1A	41,569	3		1,175
Q9UNH7-2	Sorting nexin-6, N-terminally processed	SNX6	33,818	6	0,857	0,191
Q9H223	EH domain-containing protein 4	EHD4	61,155	2	1,676	
Q9NZN4	EH domain-containing protein 2	EHD2	61,161	16	-0,603	-0,392
Q9NZM1-5	Myoferlin	MYOF	134,71	2	-0,800	

Transcription and Translation

Protein.ID	Protein.name	Gene.name	Mass (kDa)	Razor + unique peptides	Experiment 1 log2.Ratio.DB/Contr replicate 1	replicate 2
P62829	60S ribosomal protein L23	RPL23	8,8994	2		1,175
P46783	40S ribosomal protein S10	RPS10	18,898	5	-0,595	-0,523
Q15056-2	Eukaryotic translation initiation factor 4H	EIF4H	25,2	7	-0,709	-0,106
Q14192	Four and a half LIM domains protein 2	FHL2	30,949	5	-0,888	-0,246

Nucleotide metabolism

Protein.ID	Protein.name	Gene.name	Mass (kDa)	Razor + unique peptides	Experiment 1 log2.Ratio.DB/Contr replicate 1	replicate 2
Q9UKK9	ADP-sugar pyrophosphatase	NUDT5	25,895	5	0,583	0,395
Q9UJZ1-2	Stomatin-like protein 2, mitochondrial	STOML2	33,337	4	0,619	0,136
P09543-2	2,3-cyclic-nucleotide 3-phosphodiesterase	CNP	20,245	2		0,969
P84090	Enhancer of rudimentary homolog	ERH	12,259	3	0,658	

Nucleosome Assembly

Protein.ID	Protein.name	Gene.name	Mass (kDa)	Razor + unique peptides	Experiment 1 log2.Ratio.DB/Contr replicate 1	replicate 2
Q99880	Histone H2B type 1-L	H2BC13	13,834	4	1,059	0,800
Q71DI3	Histone H3.2	H3C15	10,334	2		0,668
Q99733	Nucleosome assembly protein 1-like 4	NAP1L4	18,152	3	0,022	0,867
P06454-2	Prothymosin alpha	PTMA	11,758	2	-0,586	

Cellular Component Organization

Protein.ID	Protein.name	Gene.name	Mass (kDa)	Razor + unique peptides	Experiment 1 log2.Ratio.DB/Contr replicate 1	replicate 2
Q00765	Receptor expression-enhancing protein 5	REEP5	17,758	4	0,076	1,426
P55145	Mesencephalic astrocyte-derived neurotrophic factor	MANF	21,143	4		-1,174
P14406	Cytochrome c oxidase subunit 7A2, mitochondrial	COX7A2	9,4259	2	-0,648	

Protein Metabolic Process

Protein.ID	Protein.name	Gene.name	Mass (kDa)	Razor + unique peptides	Experiment 1 log2.Ratio.DB/Contr replicate 1	replicate 2
Q9UHL4	Dipeptidyl peptidase 2	DPP7	41,324	3	1,531	
Q9UJ70	N-acetyl-D-glucosamine kinase	NAGK	36,888	4	0,303	0,591
Q02818	Nucleobindin-1	NUCB1	51,62	3	-0,709	-0,255

Collagen Organization

Protein.ID	Protein.name	Gene.name	Mass (kDa)	Razor + unique peptides	Experiment 1 log2.Ratio.DB/Contr replicate 1	replicate 2
P02452	Collagen alpha-1(I) chain	COL1A1	138,94	40	-1,14	-1,18
P08123	Collagen alpha-2(I) chain	COL1A2	129,15	24	-0,79	-0,64
P20908	Collagen alpha-1(V) chain	COL5A1	178,51	6	-0,64	-0,11

Antigen Processing and Presentation

Protein.ID	Protein.name	Gene.name	Mass (kDa)	Razor + unique peptides	Experiment 1 log2.Ratio.DB/Contr replicate 1	replicate 2
P61769	Beta-2-microglobulin	B2M	13,946	3	0,658	0,319

S3:
HFFs_Interferon regulated protein groups 24h after DBs exposure in Expermint 2 and 3

Threshold: log2Ratio 0.58 in minimum one of the 2 replicates
log2Ratio 0.58 = fold increase of 1.5

upregulated
downregulated

Protein.ID	Protein.name	Gene.name	Mass (kDa)	Experiment 2 Razor + unique peptides	Experiment 3 Razor + unique peptides	Experiment 2 log2.Ratio.DB/Contr replicate 1	replicate 2	Experiment 3 log2.Ratio.DB/Contr replicate 1	replicate 2
P20591	Interferon-induced GTP-binding protein Mx1	MX1	75,519	38	40	3,899	2,650	9,036	4,535
P20592	Interferon-induced GTP-binding protein Mx2	MX2	82,088	16	21	0,999	1,832	6,976	2,741
P09914-2	Interferon-induced protein with tetratricopeptide repeats 1	IFIT1	51,713	22	31	2,602	1,526	5,657	3,719
Q9Y6K5	2-5-oligoadenylate synthase 3	OAS3	121,21	13	20	1,374	1,030	5,473	3,139
P52630-4	Signal transducer and activator of transcription 2	STAT2	97,701	14	22	1,449	1,018	5,360	1,598
P05161	Ubiquitin-like protein ISG15	ISG15	17,887	7	7	3,313	3,689	4,571	4,494
Q9UMW8	Ubl carboxyl-terminal hydrolase 18	USP18	41,351	3	5		1,530	4,550	2,783
O14879	Interferon-induced protein with tetratricopeptide repeats 3	IFIT3	55,984	16	16	2,252	2,705	3,777	3,984
O95786	Antiviral innate immune response receptor-I	DDX58	101,38	24	36	1,001	1,034	3,124	2,764
Q05DN2	Interferon-induced protein with tetratricopeptide repeats 2	IFIT2	54,704	9	19	2,379	0,723	2,989	3,785
Q9Y3Z3	Deoxynucleoside triphosphate triphosphohydrolase SAMHD1	SAMHD1	72,2	16	20	1,896	1,331	2,909	2,290
O14933	Ubiquitin/ISG15-conjugating enzyme E2 L6	UBE2L6	17,769	6	7	1,279	0,929	2,630	2,246
P42224	Signal transducer and activator of transcription 1-alpha/beta	STAT1	87,334	34	39	1,695	1,911	2,334	2,384
O15533-2	Tapasin	TAPBP	47,625	3	6	0,408	0,593	2,290	1,326
Q9BYX4	Interferon-induced helicase C domain-containing protein 1	IFIH1	112,28	7	9	5,596		2,255	3,939
P19474	E3 ubiquitin-protein ligase TRIM21	TRIM21	54,169	4	9		0,582	2,234	1,339
Q460N5-1	Poly [ADP-ribose] polymerase 14	PARP14	193,75	28	30	2,855	1,238	2,230	2,097
Q03518	Antigen peptide transporter 1	TAP1	80,964	4	5	1,011	0,675	2,009	1,936
Q8TCS8	Polyribonucleotide nucleotidyltransferase 1, mitochondrial	PNPT1	85,95	13	19	1,558	0,981	1,991	1,460

Q63HN8	E3 ubiquitin-protein ligase RNF213	RNF213	591,4	34	60	1,207	0,630	1,973	1,751
Q5EBM0	UMP-CMP kinase 2, mitochondrial	CMPK2	49,447	5	6	0,838	0,485	1,787	1,760
P29590	Protein PML	PML	92,563	9	15	0,928	0,504	1,717	1,318
P28838-2	Cytosol aminopeptidase	LAP3	56,049	19	26	1,147	1,277	1,697	1,558
Q03519	Antigen peptide transporter 2	TAP2	75,663	4	5	1,117	0,866	1,648	1,358
P29466-3	Caspase-1	CASP1	40,943	2	3		1,337	1,591	1,128
P23497	Nuclear autoantigen Sp-100	SP100	96,548	4	4	0,688	0,627	1,586	0,869
P32455	Guanylate-binding protein 1	GBP1	41,27	16	18	1,629	1,270	1,531	1,685
P30711	Glutathione S-transferase theta-1	GSTT1	24,739	3	2	3,514	0,296	1,521	
Q8TDB6	E3 ubiquitin-protein ligase DTX3L	DTX3L	83,553	5	12	1,531	0,961	1,515	2,321
P13164	Interferon-induced transmembrane protein 1	IFITM1	13,938	2	2	2,492	0,464	1,492	1,898
Q01629	Interferon-induced transmembrane protein 2	IFITM2	13,938	2	2	2,492	0,464	1,492	1,898
Q01628	Interferon-induced transmembrane protein 3	IFITM3	13,938	2	2	2,492	0,464	1,492	1,898
P11388	DNA topoisomerase 2-alpha	TOP2A	174,38	36	35	1,491	1,890	1,482	1,816
Q8IYM9-2	E3 ubiquitin-protein ligase TRIM22	TRIM22	56,372	5	6	1,771	0,899	1,433	1,534
P61769	Beta-2-microglobulin	B2M	13,946	3	4	1,342	1,237	1,409	1,466
Q13325	Interferon-induced protein with tetratricopeptide repeats 5	IFIT5	55,846	7	8	1,191	0,284	1,392	1,155
P09543-2	2,3-cyclic-nucleotide 3-phosphodiesterase	CNP	20,245	8	5	1,118	0,571	1,392	1,374
Q16666-3	Gamma-interferon-inducible protein 16	IFI16	82,422	16	23	0,505	0,792	1,248	1,001
Q14258	E3 ubiquitin/ISG15 ligase TRIM25	TRIM25	70,973	20	21	1,062	0,692	1,238	1,369
Q9P2E3	NFX1-type zinc finger-containing protein 1	ZNFX1	146,22	4	4	0,655		1,234	0,933
Q8IXQ6-2	Poly [ADP-ribose] polymerase 9	PARP9	92,27	9	10	1,094	0,373	1,221	1,879
Q9H0H5	Rac GTPase-activating protein 1	RACGAP1	70,968	4	6	1,268		1,126	0,306
P19525-2	Interferon-induced, double-stranded RNA-activated protein kinase	PKR	40,68	14	16	0,830	0,936	1,052	1,665
P23381	Tryptophan--tRNA ligase, cytoplasmic	WARS	53,165	23	29	0,736	0,590	1,045	0,866
Q15006	ER membrane protein complex subunit 2	EMC2	34,761	3	4	0,361	0,637	0,974	0,584
Q9UJS0	Calcium-binding mitochondrial carrier protein Aralar2	SLC25A13	74,116	10	5	0,708	0,333	0,961	0,081
Q99836-2	Myeloid differentiation primary response protein MyD88	MYD88	9,4461	2	3		0,702	0,929	0,579
Q8IZH2-2	5-3 exoribonuclease 1	XRN1	130,08	5	12	0,873	0,211	0,922	0,893
Q96RS6	NudC domain-containing protein 1	NUDCD1	63,501	7	7	0,661	0,148	0,757	0,592
P54920	Alpha-soluble NSF attachment protein	NAPA	9,8571	13	13	1,312	0,162	0,733	0,920
Q5R3I4	Tetratricopeptide repeat protein 38	TTC38	50,74	4	4	2,678	0,136	0,700	0,840
P31689-2	DnaJ homolog subfamily A member 1	DNAJA1	37,044	6	11	1,160	0,574	0,665	0,729
Q9UL46	Proteasome activator complex subunit 2	PSME2	27,401	8	8	0,600	0,231	0,661	0,545
P46013	Proliferation marker protein Ki-67	MKI67	358,69	16	17	1,262	0,442	0,623	0,981
P17301	Integrin alpha-2	ITGA2	129,29	20	24	0,627	0,490	0,612	0,528
P46934-4	E3 ubiquitin-protein ligase NEDD4	NEDD4	104,16	2	5		1,112	0,587	0,233
Q96KB5	Lymphokine-activated killer T-cell-originated protein kinase	PBK	36,085	7	7	0,467	0,620	0,490	0,807
Q9BXS6-7	Nucleolar and spindle-associated protein 1	NUSAP1	49,438	3	2	1,103	0,742	0,465	0,938
P29317	Ephrin type-A receptor 2	EPHA2	73,014	3	3		0,630	0,225	1,491
P83916	Chromobox protein homolog 1	CBX1	20,03	2	3		0,896	0,002	0,728
O15162-2	Phospholipid scramblase 1	PLSCR1	27,081	4	4	1,162			1,914
Q96GD4-4	Aurora kinase B	AURKB	27,956	2	2	1,154	1,147		0,955
Q8IVU3-2	Probable E3 ubiquitin-protein ligase HERC6	HERC6	68,048	2	5	1,077			0,788
Q9Y3T9	Nucleolar complex protein 2 homolog	NOC2L	84,916	5	5	-1,047	-0,308	0,000	-1,249
Q92629-2	Delta-sarcoglycan	SGCD	32,202	4	5	-1,533	-0,078	-0,211	-0,643
Q6UVK1	Chondroitin sulfate proteoglycan 4	CSPG4	250,53	6	9	-0,965	-0,993	-0,221	-0,865
O95155-3	Ubiquitin conjugation factor E4 B	UBE4B	121,37	3	5	-0,022	-1,033	-0,310	-1,057
O95864	Acyl-CoA 6 desaturase	FADS2	52,259	7	7	-0,628	-0,542	-0,404	-0,844
Q15113	Procollagen C-endopeptidase enhancer 1	PCOLCE	47,972	5	6	-0,190	-0,670	-0,436	-0,644
P08123	Collagen alpha-2(I) chain	COL1A2	129,15	24	29	-0,668	-0,683	-0,543	-0,650
Q8TER5	Rho guanine nucleotide exchange factor 40	ARHGEF40	162,79	3	3		-0,611	-0,617	-0,590
Q6P1M0	Long-chain fatty acid transport protein 4	SLC27A4	57,194	3	3	-1,803		-0,643	
Q5VTR2	E3 ubiquitin-protein ligase BRE1A	RNF20	113,66	2	4		-1,046	-0,644	-0,064
P09619	Platelet-derived growth factor receptor beta	PDGFRB	123,97	10	12	-0,616	-0,809	-0,649	-0,655
P02452	Collagen alpha-1(I) chain	COL1A1	138,94	31	32	-0,922	-0,966	-0,682	-0,616
P14923	Junction plakoglobin	JUP	81,744	5	4	-0,916		-0,708	-1,257
P20908	Collagen alpha-1(V) chain	COL5A1	178,51	7	8	-0,265	-0,911	-0,802	-0,448
Q7Z392	Trafficking protein particle complex subunit 11	TRAPPC11	83,018	2	2	-0,518	-0,613	-0,957	-0,301
O95478	Ribosome biogenesis protein NSA2 homolog	NSA2	30,065	2	2	-0,676		-1,083	
Q7Z3E5-2	LisH domain-containing protein ARMC9	ARMC9	22,221	3	5		-0,697	-1,252	-0,429
P12277	Creatine kinase B-type	CKB	42,644	3	3	-0,840		-1,823	

S4:
HFFs_Classification of regulated protein groups according to GO - Biological processes (UniProtKB) in Experiment 2 and 3

Threshold: log2Ratio 0.58 in minimum one of the 2 replicates
log2Ratio 0.58 = fold increase of 1.5

upregulated
downregulated

Viral Protein

				Experiment 2 Razor + unique peptides	Experiment 3 Razor + unique peptides	Experiment 2 log2.Ratio.DB/Contr		Experiment 3 log2.Ratio.DB/Contr	
Protein.ID	Protein.name	Gene.name	Mass (kDa)			replicate 1	replicate 2	replicate 1	replicate 2
P18139	65 kDa phosphoprotein	pp65	62,896	16	21	4,080	1,704	2,713	1,503

Antiviral Defense

Protein.ID	Protein.name	Gene.name	Mass (kDa)	Experiment 2 Razor + unique peptides	Experiment 3 Razor + unique peptides	Experiment 2 log2.Ratio.DB/Contr replicate 1	Experiment 2 log2.Ratio.DB/Contr replicate 2	Experiment 3 log2.Ratio.DB/Contr replicate 1	Experiment 3 log2.Ratio.DB/Contr replicate 2
O95786	Antiviral innate immune response receptor-l	DDX58	101,38	24	36	1,001	1,034	3,124	2,764
Q8TDB6	E3 ubiquitin-protein ligase DTX3L	DTX3L	83,553	5	12	1,531	0,961	1,515	2,321
P19525-2	Interferon-induced, double-stranded RNA-activated protein kinase	PKR	40,68	14	16	0,830	0,936	1,052	1,665
P32455	Guanylate-binding protein 1	GBP1	41,27	16	18	1,629	1,270	1,531	1,685
Q16666-3	Gamma-interferon-inducible protein 16	IFI16	82,422	16	23	0,505	0,792	1,248	1,001
Q9BYX4	Interferon-induced helicase C domain-containing protein 1	IFIH1	112,28	7	9	5,596		2,255	3,939
P09914-2	Interferon-induced protein with tetratricopeptide repeats 1	IFIT1	51,713	22	31	2,602	1,526	5,657	3,719
Q05DN2	Interferon-induced protein with tetratricopeptide repeats 2	IFIT2	54,704	9	19	2,379	0,723	2,989	3,785
O14879	Interferon-induced protein with tetratricopeptide repeats 3	IFIT3	55,984	16	16	2,252	2,705	3,777	3,984
Q13325	Interferon-induced protein with tetratricopeptide repeats 5	IFIT5	55,846	7	8	1,191	0,284	1,392	1,155
P13164	Interferon-induced transmembrane protein 1	IFITM1	13,938	2	2	2,492	0,464	1,492	1,898
Q01629	Interferon-induced transmembrane protein 2	IFITM2	13,938	2	2	2,492	0,464	1,492	1,898
Q01628	Interferon-induced transmembrane protein 3	IFITM3	13,938	2	2	2,492	0,464	1,492	1,898
P05161	Ubiquitin-like protein ISG15	ISG15	17,887	7	7	3,313	3,689	4,571	4,494
P20591	Interferon-induced GTP-binding protein Mx1	MX1	75,519	38	40	3,899	2,650	9,036	4,535
P20592	Interferon-induced GTP-binding protein Mx2	MX2	82,088	16	21	0,999	1,832	6,976	2,741
Q9Y6K5	2-5-oligoadenylate synthase 3	OAS3	121,21	13	20	1,374	1,030	5,473	3,139
Q8IXQ6-2	Poly [ADP-ribose] polymerase 9	PARP9	92,27	9	10	1,094	0,373	1,221	1,879
O15162-2	Phospholipid scramblase 1	PLSCR1	27,081	4	4	1,162			1,914
P29590	Protein PML	PML	92,563	9	15	0,928	0,504	1,717	1,318
Q9Y3Z3	Deoxynucleoside triphosphate triphosphohydrolase SAMHD1	SAMHD1	72,2	16	20	1,896	1,331	2,909	2,290
P42224	Signal transducer and activator of transcription 1-alpha/beta	STAT1	87,334	34	39	1,695	1,911	2,334	2,384
P52630-4	Signal transducer and activator of transcription 2	STAT2	97,701	14	22	1,449	1,018	5,360	1,598
Q8IYM9-2	E3 ubiquitin-protein ligase TRIM22	TRIM22	56,372	5	6	1,771	0,899	1,433	1,534
Q14258	E3 ubiquitin/ISG15 ligase TRIM25	TRIM25	70,973	20	21	1,062	0,692	1,238	1,369

Ubiquitin Conjugation Pathway

Protein.ID	Protein.name	Gene.name	Mass (kDa)	Experiment 2 Razor + unique peptides	Experiment 3 Razor + unique peptides	Experiment 2 log2.Ratio.DB/Contr replicate 1	Experiment 2 log2.Ratio.DB/Contr replicate 2	Experiment 3 log2.Ratio.DB/Contr replicate 1	Experiment 3 log2.Ratio.DB/Contr replicate 2
P46934-4	E3 ubiquitin-protein ligase NEDD4	NEDD4	104,16	2	5		1,112	0,587	0,233
Q63HN8	E3 ubiquitin-protein ligase RNF213	RNF213	591,4	34	60	1,207	0,630	1,973	1,751
O14933	Ubiquitin/ISG15-conjugating enzyme E2 L6	UBE2L6	17,769	6	7	1,279	0,929	2,630	2,246
P19474	E3 ubiquitin-protein ligase TRIM21	TRIM21	54,169	4	9		0,582	2,234	1,339
Q8IVU3-2	Probable E3 ubiquitin-protein ligase HERC6	HERC6	68,048	2	5	1,077			0,788
Q9UMW8	Ubl carboxyl-terminal hydrolase 18	USP18	41,351	3	5		1,530	4,550	2,783
Q8IYM9-2	E3 ubiquitin-protein ligase TRIM22	TRIM22	56,372	5	6	1,771	0,899	1,433	1,534
Q14258	E3 ubiquitin/ISG15 ligase TRIM25	TRIM25	70,973	20	21	1,062	0,692	1,238	1,369
P05161	Ubiquitin-like protein ISG15	ISG15	17,887	7	7	3,313	3,689	4,571	4,494
Q8TDB6	E3 ubiquitin-protein ligase DTX3L	DTX3L	83,553	5	12	1,531	0,961	1,515	2,321
O95155-3	Ubiquitin conjugation factor E4 B	UBE4B	121,37	3	5	-0,022	-1,033	-0,310	-1,057
Q5VTR2	E3 ubiquitin-protein ligase BRE1A	RNF20	113,66	2	4		-1,046	-0,644	-0,064

Cell Motility

Protein.ID	Protein.name	Gene.name	Mass (kDa)	Experiment 2 Razor + unique peptides	Experiment 3 Razor + unique peptides	Experiment 2 log2.Ratio.DB/Contr replicate 1	Experiment 2 log2.Ratio.DB/Contr replicate 2	Experiment 3 log2.Ratio.DB/Contr replicate 1	Experiment 3 log2.Ratio.DB/Contr replicate 2
P17301	Integrin alpha-2	ITGA2	129,29	20	24	0,627	0,490	0,612	0,528
P31689-2	DnaJ homolog subfamily A member 1	DNAJA1	37,044	5	12	1,160	0,574	0,665	0,729
P29317	Ephrin type-A receptor 2	EPHA2	73,014	3	3		0,630	0,225	1,491
P02452	Collagen alpha-1(I) chain	COL1A1	138,94	31	32	-0,922	-0,966	-0,682	-0,616
P08123	Collagen alpha-2(I) chain	COL1A2	129,15	24	29	-0,668	-0,683	-0,543	-0,650
P20908	Collagen alpha-1(V) chain	COL5A1	178,51	7	8	-0,265	-0,911	-0,802	-0,448
P09619	Platelet-derived growth factor receptor beta	PDGFRB	123,97	10	12	-0,616	-0,809	-0,649	-0,655
P14923	Junction plakoglobin	JUP	81,744	5	4	-0,916		-0,708	-1,257
Q6UVK1	Chondroitin sulfate proteoglycan 4	CSPG4	250,53	6	9	-0,965	-0,993	-0,221	-0,865
Q9Y6W5	Wiskott-Aldrich syndrome protein family member 2	WASF2	54,283	3	2		-1,109	-0,220	-0,905
P29590	Protein PML	PML	92,563	9	15	0,928	0,504	1,717	1,318
Q8IXQ6-2	Poly [ADP-ribose] polymerase 9	PARP9	92,27	9	10	1,094	0,373	1,221	1,879

Apoptosis

Protein.ID	Protein.name	Gene.name	Mass (kDa)	Experiment 2 Razor + unique peptides	Experiment 3 Razor + unique peptides	Experiment 2 log2.Ratio.DB/Contr replicate 1	Experiment 2 log2.Ratio.DB/Contr replicate 2	Experiment 3 log2.Ratio.DB/Contr replicate 1	Experiment 3 log2.Ratio.DB/Contr replicate 2
P29466-3	Caspase-1	CASP1	40,943	2	3		1,337	1,591	1,128
Q99836-2	Myeloid differentiation primary response protein MyD88	MYD88	9,4461	2	3		0,702	0,929	0,579
Q9Y3T9	Nucleolar complex protein 2 homolog	NOC2L	84,916	5	5	-1,047	-0,308	0,000	-1,249
P11388	DNA topoisomerase 2-alpha	TOP2A	174,38	36	35	1,491	1,890	1,482	1,816
O95155-3	Ubiquitin conjugation factor E4 B	UBE4B	121,37	3	5	-0,022	-1,033	-0,310	-1,057
P29317	Ephrin type-A receptor 2	EPHA2	73,014	3	3		0,630	0,225	1,491
P29590	Protein PML	PML	92,563	9	15	0,928	0,504	1,717	1,318
Q16666-3	Gamma-interferon-inducible protein 16	IFI16	82,422	16	23	0,505	0,792	1,248	1,001
P20591	Interferon-induced GTP-binding protein Mx1	MX1	75,519	38	40	3,899	2,650	9,036	4,535
Q05DN2	Interferon-induced protein with tetratricopeptide repeats 2	IFIT2	54,704	9	19	2,379	0,723	2,989	3,785
O15162-2	Phospholipid scramblase 1	PLSCR1	27,081	4	4	1,162			1,914

Antigen processing and presentation

Protein.ID	Protein.name	Gene.name	Mass (kDa)	Experiment 2 Razor + unique peptides	Experiment 3 Razor + unique peptides	Experiment 2 log2.Ratio.DB/Contr replicate 1	Experiment 2 log2.Ratio.DB/Contr replicate 2	Experiment 3 log2.Ratio.DB/Contr replicate 1	Experiment 3 log2.Ratio.DB/Contr replicate 2
P61769	Beta-2-microglobulin	B2M	13,946	3	4	1,342	1,237	1,409	1,466
Q9UL46	Proteasome activator complex subunit 2	PSME2	27,401	8	8	0,600	0,231	0,661	0,545
Q03518	Antigen peptide transporter 1	TAP1	80,964	4	5	1,011	0,675	2,009	1,936
Q03519	Antigen peptide transporter 2	TAP2	75,663	4	5	1,117	0,866	1,648	1,358
O15533-2	Tapasin	TAPBP	47,625	3	6	0,408	0,593	2,290	1,326

Cell cycle

Protein.ID	Protein.name	Gene.name	Mass (kDa)	Experiment 2 Razor + unique peptides	Experiment 3 Razor + unique peptides	Experiment 2 log2.Ratio.DB/Contr replicate 1	Experiment 2 log2.Ratio.DB/Contr replicate 2	Experiment 3 log2.Ratio.DB/Contr replicate 1	Experiment 3 log2.Ratio.DB/Contr replicate 2
P46013	Proliferation marker protein Ki-67	MKI67	358,69	16	17	1,262	0,442	0,623	0,981
Q9BXS6-7	Nucleolar and spindle-associated protein 1	NUSAP1	49,438	3	2	1,103	0,742	0,465	0,938
Q96KB5	Lymphokine-activated killer T-cell-originated protein kinase	PBK	36,085	7	7	0,467	0,620	0,490	0,807
Q9H0H5	Rac GTPase-activating protein 1	RACGAP1	70,968	4	6	1,268		1,126	0,306
Q96GD4-4	Aurora kinase B	AURKB	27,956	2	2	1,154	1,147		0,955

Protein Trafficking

Protein.ID	Protein.name	Gene.name	Mass (kDa)	Experiment 2 Razor + unique peptides	Experiment 3 Razor + unique peptides	Experiment 2 log2.Ratio.DB/Contr replicate 1	Experiment 2 log2.Ratio.DB/Contr replicate 2	Experiment 3 log2.Ratio.DB/Contr replicate 1	Experiment 3 log2.Ratio.DB/Contr replicate 2
Q9UJS0	Calcium-binding mitochondrial carrier protein Aralar2	SLC25A13	74,116	10	5	0,708	0,333	0,961	0,081
Q8N0X7	Spartin	SPART	72,831	6	6	0,656	0,024	0,383	0,628
P57737	Coronin-7	CORO7	114,16	2	3		-1,710	-1,466	
Q9BRG1	Vacuolar protein-sorting-associated protein 25	VPS25	20,747	3	2		-1,173		-1,356
Q7Z3E5-2	LisH domain-containing protein ARMC9	ARMC9	22,221	3	5		-0,697	-1,252	-0,429

RNA processing

Protein.ID	Protein.name	Gene.name	Mass (kDa)	Experiment 2 Razor + unique peptides	Experiment 3 Razor + unique peptides	Experiment 2 log2.Ratio.DB/Contr replicate 1	Experiment 2 log2.Ratio.DB/Contr replicate 2	Experiment 3 log2.Ratio.DB/Contr replicate 1	Experiment 3 log2.Ratio.DB/Contr replicate 2
Q8TCS8	Polyribonucleotide nucleotidyltransferase 1, mitochondrial	PNPT1	85,95	13	19	1,558	0,981	1,991	1,460
P09012	U1 small nuclear ribonucleoprotein A	SNRPA	31,307	4	7	1,006	0,306	0,068	0,997
Q8IZH2-2	5-3 exoribonuclease 1	XRN1	130,08	5	12	0,873	0,211	0,922	0,893
O95478	Ribosome biogenesis protein NSA2 homolog	NSA2	30,065	2	2	-0,676		-1,083	
Q8N5L8	Ribonuclease P protein subunit p25-like protein	RPP25L	17,631	3	2		-0,580	-2,088	-1,474

Transcription and Translation

Protein.ID	Protein.name	Gene.name	Mass (kDa)	Experiment 2 Razor + unique peptides	Experiment 3 Razor + unique peptides	Experiment 2 log2.Ratio.DB/Contr replicate 1	Experiment 2 log2.Ratio.DB/Contr replicate 2	Experiment 3 log2.Ratio.DB/Contr replicate 1	Experiment 3 log2.Ratio.DB/Contr replicate 2
Q460N5-1	Poly [ADP-ribose] polymerase 14	PARP14	193,75	28	30	2,855	1,238	2,230	2,097
P23497	Nuclear autoantigen Sp-100	SP100	96,548	4	4	0,688	0,627	1,586	0,869
Q9P2E3	NFX1-type zinc finger-containing protein 1	ZNFX1	146,22	4	4	0,655		1,234	0,933
P23381	Tryptophan--tRNA ligase, cytoplasmic	WARS	53,165	23	29	0,736	0,590	1,045	0,866

ER-Golgi Transport

Protein.ID	Protein.name	Gene.name	Mass (kDa)	Experiment 2 Razor + unique peptides	Experiment 3 Razor + unique peptides	Experiment 2 log2.Ratio.DB/Contr replicate 1	Experiment 2 log2.Ratio.DB/Contr replicate 2	Experiment 3 log2.Ratio.DB/Contr replicate 1	Experiment 3 log2.Ratio.DB/Contr replicate 2
P54920	Alpha-soluble NSF attachment protein	NAPA	9,8571	13	13	1,312	0,162	0,733	0,920
P83436	Conserved oligomeric Golgi complex subunit 7	COG7	68,899	3	4	0,876		1,472	
Q15006	ER membrane protein complex subunit 2	EMC2	34,761	3	4	0,361	0,637	0,974	0,584
Q7Z392	Trafficking protein particle complex subunit 11	TRAPPC11	83,018	2	2	-0,518	-0,613	-0,957	-0,301

Cell adhesion, growth and migration

Protein.ID	Protein.name	Gene.name	Mass (kDa)	Experiment 2 Razor + unique peptides	Experiment 3 Razor + unique peptides	Experiment 2 log2.Ratio.DB/Contr replicate 1	Experiment 2 log2.Ratio.DB/Contr replicate 2	Experiment 3 log2.Ratio.DB/Contr replicate 1	Experiment 3 log2.Ratio.DB/Contr replicate 2
Q8TCG1	Protein CIP2A	CIP2A	102,28	2	4	0,726		2,399	0,856
Q8WUJ3	Cell migration-inducing and hyaluronan-binding protein	CEMIP	153	3	10		-1,293	-2,075	-1,330
Q13641	Trophoblast glycoprotein	TPBG	46,031	7	7	-0,242	-0,658	-0,343	-0,884

Cytoskeleton Organization

Protein.ID	Protein.name	Gene.name	Mass (kDa)	Experiment 2 Razor + unique peptides	Experiment 3 Razor + unique peptides	Experiment 2 log2.Ratio.DB/Contr replicate 1	Experiment 2 log2.Ratio.DB/Contr replicate 2	Experiment 3 log2.Ratio.DB/Contr replicate 1	Experiment 3 log2.Ratio.DB/Contr replicate 2
P09543-2	2,3-cyclic-nucleotide 3-phosphodiesterase	CNP	20,245	8	5	1,118	0,571	1,392	1,374
Q92629-2	Delta-sarcoglycan	SGCD	32,202	4	5	-1,533	-0,078	-0,211	-0,643

Lipid Metabolism

Protein.ID	Protein.name	Gene.name	Mass (kDa)	Experiment 2 Razor + unique peptides	Experiment 3 Razor + unique peptides	Experiment 2 log2.Ratio.DB/Contr replicate 1	Experiment 2 log2.Ratio.DB/Contr replicate 2	Experiment 3 log2.Ratio.DB/Contr replicate 1	Experiment 3 log2.Ratio.DB/Contr replicate 2
O95864	Acyl-CoA 6 desaturase	FADS2	52,259	7	7	-0,628	-0,542	-0,404	-0,844
Q6P1M0	Long-chain fatty acid transport protein 4	SLC27A4	57,194	3	3	-1,803		-0,643	

Proteolysis

Protein.ID	Protein.name	Gene.name	Mass (kDa)	Experiment 2 Razor + unique peptides	Experiment 3 Razor + unique peptides	Experiment 2 log2.Ratio.DB/Contr replicate 1	Experiment 2 log2.Ratio.DB/Contr replicate 2	Experiment 3 log2.Ratio.DB/Contr replicate 1	Experiment 3 log2.Ratio.DB/Contr replicate 2
P28838-2	Cytosol aminopeptidase	LAP3	56,049	19	26	1,147	1,277	1,697	1,558
Q15113	Procollagen C-endopeptidase enhancer 1	PCOLCE	47,972	5	6	-0,190	-0,670	-0,436	-0,644

Other

Protein.ID	Protein.name	Gene.name	Mass (kDa)	Experiment 2 Razor + unique peptides	Experiment 3 Razor + unique peptides	Experiment 2 log2.Ratio.DB/Contr replicate 1	Experiment 2 log2.Ratio.DB/Contr replicate 2	Experiment 3 log2.Ratio.DB/Contr replicate 1	Experiment 3 log2.Ratio.DB/Contr replicate 2
P83916	Chromobox protein homolog 1	CBX1	20,03	2	3		0,896	0,002	0,728
Q96RS6	NudC domain-containing protein 1	NUDCD1	63,501	7	7	0,661	0,148	0,757	0,592
Q5R3I4	Tetratricopeptide repeat protein 38	TTC38	50,74	4	4	2,678	0,136	0,700	0,840
Q5EBM0	UMP-CMP kinase 2, mitochondrial	CMPK2	49,447	5	6	0,838	0,485	1,787	1,760
P30711	Glutathione S-transferase theta-1	GSTT1	24,739	3	2	3,514	0,296	1,521	
Q8TER5	Rho guanine nucleotide exchange factor 40	ARHGEF40	162,79	3	3		-0,611	-0,617	-0,590
P12277	Creatine kinase B-type	CKB	42,644	3	3	-0,840		-1,823	

S5:
Endothelial cells_Interferon regulated protein groups 24h after DBs exposure in Experiment_1

Threshold: log2Ratio 0.58 in both technical replicates
log2Ratio 0.58 = fold increase of 1.5

upregulated
downregulated
HCMV protein

Protein.ID	Protein.name	Gene.name	Mass (kDa)	Razor+ unique peptides	Experiment 1 log2.Ratio.DB/Contr replicate 1	Experiment 1 log2.Ratio.DB/Contr replicate 2
P20591	Interferon-induced GTP-binding protein MX1	MX1	75,519	27	3,479	3,193
P09914-2	Interferon-induced protein with tetratricopeptide repeats 1	IFIT1	51,713	7	2,284	1,367
Q9NWH9	SAFB-like transcription modulator	SLTM	117,15	3	1,442	2,079
P29728-2	2'-5'-oligoadenylate synthase 2	OAS2	78,816	10	1,926	1,400
P05161	Ubiquitin-like protein ISG15	ISG15	17,887	5	1,910	1,840
Q10589-2	Bone marrow stromal antigen 2	BST2	19,769	2	1,039	1,316
O95786-2	Antiviral innate immune response receptor RIG-I	DDX58	82,612	5	0,958	1,063
Q9Y6K5	2'-5'-oligoadenylate synthase 3	OAS3	121,21	15	0,978	0,739
P42224	Signal transducer and activator of transcription 1-alpha/beta	STAT1	87,334	25	0,794	0,856
Q460N5-3	Protein mono-ADP-ribosyltransferase PARP14	PARP14	160,16	6	0,717	0,799
P05120	Plasminogen activator inhibitor 2	SERPINB2	46,611	5	0,774	0,695
Q9Y3Z3	Deoxynucleoside triphosphate triphosphohydrolase SAMHD1	SAMHD1	72,2	20	0,718	0,630
P52630-4	Signal transducer and activator of transcription 2	STAT2	97,897	3	0,708	0,669
O95864	Fatty acid desaturase 2	FADS2	52,259	7	-0,589	-0,652
Q8NBQ5	Estradiol 17-beta-dehydrogenase 11	HSD17B11	28,102	3	-0,702	-0,621

Endothelial cells_Not interferon regulated protein groups 24h after DBs exposure in Experiment_1

Threshold: log2Ratio 0.58 in both technical replicates
log2Ratio 0.58 = fold increase of 1.5

upregulated
downregulated
HCMV protein

Protein.ID	Protein.name	Gene.name	Mass (kDa)	Razor+ unique peptides	Experiment 1 log2.Ratio.DB/Contr replicate 1	Experiment 1 log2.Ratio.DB/Contr replicate 2
Q7TER5	Tegument protein pp65	pp65	62,872	7	2,386	2,375
Q53FA7	Quinone oxidoreductase PIG3	TP53I3	35,536	13	0,807	1,037
O60443	Gasdermin-E	GSDME	47,735	8	0,586	0,612
P56385	ATP synthase subunit e, mitochondrial	ATP5I	7,9331	2	-0,870	-0,872

S6:

Endothelial Cells_Classification of regulated protein groups according to GO - Biological processes (UniProtKB) in Experiment_1

Threshold: log2Ratio 0.58 in both technical replicates
log2Ratio 0.58 = fold increase of 1.5

upregulated
downregulated
HCMV protein

Viral Protein

Protein.ID	Protein.name	Gene.name	Mass (kDa)	Razor+ unique peptides	Experiment 1 log2.Ratio.DB/Contr replicate 1	replicate 2
Q7TER5	Tegument protein pp65	pp65	62,872	7	2,386	2,375

Antiviral Defense

Protein.ID	Protein.name	Gene.name	Mass (kDa)	Razor+ unique peptides	Experiment 1 log2.Ratio.DB/Contr replicate 1	replicate 2
P20591	Interferon-induced GTP-binding protein Mx1	MX1	75,519	27	3,479	3,193
P05161	Ubiquitin-like protein ISG15	ISG15	17,887	5	1,910	1,840
P29728-2	2-5-oligoadenylate synthase 2	OAS2	78,816	10	1,926	1,400
P09914-2	Interferon-induced protein with tetratricopeptide repeats 1	IFIT1	51,713	7	2,284	1,367
Q10589-2	Bone marrow stromal antigen 2	BST2	19,769	2	1,039	1,316
O95786-2	Probable ATP-dependent RNA helicase DDX58	DDX58	82,612	5	0,958	1,063
P42224	Signal transducer and activator of transcription 1-alpha/beta	STAT1	87,334	25	0,794	0,856
Q9Y6K5	2-5-oligoadenylate synthase 3	OAS3	121,21	15	0,978	0,739
P52630-4	Signal transducer and activator of transcription 2	STAT2	97,897	3	0,708	0,669
Q9Y3Z3	Deoxynucleoside triphosphate triphosphohydrolase SAMHD1	SAMHD1	72,2	20	0,718	0,630

Transcription

Protein.ID	Protein.name	Gene.name	Mass (kDa)	Razor+ unique peptides	Experiment 1 log2.Ratio.DB/Contr replicate 1	replicate 2
Q9NWH9	SAFB-like transcription modulator	SLTM	117,15	3	1,442	2,079
Q460N5-3	Protein mono-ADP-ribosyltransferase PARP14	PARP14	160,16	6	0,717	0,799

Lipid Metabolism

Protein.ID	Protein.name	Gene.name	Mass (kDa)	Razor+ unique peptides	Experiment 1 log2.Ratio.DB/Contr replicate 1	replicate 2
O95864	Fatty acid desaturase 2	FADS2	52,259	7	-0,589	-0,652
Q8NBQ5	Estradiol 17-beta-dehydrogenase 11	HSD17B11	28,102	3	-0,702	-0,621

Other

Protein.ID	Protein.name	Gene.name	Mass (kDa)	Razor+ unique peptides	Experiment 1 log2.Ratio.DB/Contr replicate 1	replicate 2
Q53FA7	Quinone oxidoreductase PIG3	TP53I3	35,536	13	0,807	1,037
O60443	Gasdermin-E	GSDME	47,735	8	0,586	0,612
P05120	Plasminogen activator inhibitor 2	SERPINB2	46,611	5	0,774	0,695
P56385	ATP synthase subunit e, mitochondrial	ATP5I	7,9331	2	-0,870	-0,872

S7:
Endothelial cells_Interferon regulated protein groups 24h after DBs exposure in Experiments 2 and 3

Threshold: log2Ratio 0.58 in both technical replicates
log2Ratio 0.58 = fold increase of 1.5

upregulated
downregulated
HCMV protein

				Experiment 2	Experiment 3	Experiment 2 log2.Ratio.DB/Contr		Experiment 3 log2.Ratio.DB/Contr	
Protein.ID	Protein.name	Gene.name	Mass (kDa)	Razor + unique peptides		replicate 1	replicate 2	replicate 1	replicate 2
D9IG50	Tegument protein pp65	pp65	9	9	62,872	2,717	0,849	2,176	0,430
Q96DG6	Carboxymethylenebutenolidase homolog	CMBL	8	8	28,048	1,426	2,417	1,766	1,551
Q53FA7	Quinone oxidoreductase PIG3	TP53I3	10	10	35,536	1,049	2,202	0,821	2,222
P22570-4	NADPH:adrenodoxin oxidoreductase, mitochondrial	FDXR	14	14	48,056	1,628	1,397	2,013	1,444
Q01995	Transgelin	TAGLN	5	5	16,733	1,037	1,892	1,600	1,301
P20591	Interferon-induced GTP-binding protein Mx1	MX1	17	17	75,519	1,285	1,328	1,756	0,887
P26006	Integrin alpha-3	ITGA3	7	7	116,61	1,391	1,484	1,750	1,111
P05161	Ubiquitin-like protein ISG15	ISG15	5	5	17,887	1,321	1,404	1,499	1,492
Q14764	Major vault protein	MVP	23	23	99,326	1,348	1,099	1,495	0,989
P14209-3	CD99 antigen	CD99	2	2	17,128	1,053	1,156	0,702	1,383
P06703	Protein S100-A6	S100A6	3	3	9,681	0,860	1,301	0,905	0,744
Q9Y570	Protein phosphatase methylesterase 1	PPME1	10	10	42,315	0,759	1,265	0,892	1,163
P13598	Intercellular adhesion molecule 2	ICAM2	3	3	28,181	1,007	0,917	1,237	1,235
P02794	Ferritin heavy chain	FTH1	5	5	21,225	0,749	1,204	0,658	0,843
Q9Y617-2	Phosphoserine aminotransferase	PSAT1	8	8	35,188	0,795	1,156	0,793	0,623
P15144	Aminopeptidase N	ANPEP	5	5	109,54	0,947	0,909	1,072	0,840
O95810	Caveolae-associated protein 2	CAVIN2	11	11	47,173	1,037	0,695	0,787	0,742
P05121	Plasminogen activator inhibitor 1	SERPINE1	7	7	45,059	1,012	1,069	0,787	0,691
Q15149	Plectin	PLEC	197	197	531,78	0,955	0,820	0,950	0,891
Q09666	Neuroblast differentiation-associated protein AHNAK	AHNAK	170	170	629,09	0,943	0,628	0,875	0,854
P09525	Annexin A4	ANXA4	14	14	35,882	0,884	0,925	0,942	0,922
O00469	Procollagen-lysine,2-oxoglutarate 5-dioxygenase 2	PLOD2	13	13	81,169	0,835	0,729	0,876	0,611
P27105	Erythrocyte band 7 integral membrane protein	STOM	7	7	31,73	0,600	0,699	0,591	0,815
Q14315-2	Filamin-C	FLNC	49	49	287,28	0,804	0,783	0,736	0,725
Q9H4M9	EH domain-containing protein 1	EHD1	9	9	60,626	0,699	0,696	0,804	0,608
O75828	Carbonyl reductase [NADPH] 3	CBR3	2	2	30,85	-0,636	-0,601	-0,586	-0,642
Q9NR30	Nucleolar RNA helicase 2	DDX21	16	16	87,343	-0,582	-0,580	-0,654	-0,595
P07108	Acyl-CoA-binding protein	DBI	4	4	10,044	-0,813	-0,715	-0,785	-0,748
P16401	Histone H1.5	HIST1H1B	7	7	22,58	-0,827	-0,874	-0,833	-0,843
P62805	Histone H4	H4C1	10	10	11,367	-0,910	-0,702	-0,827	-0,840
P33992	DNA replication licensing factor MCM5	MCM5	9	9	82,285	-0,928	-0,762	-0,709	-0,641
P35659	Protein DEK	DEK	6	6	42,674	-0,936	-0,626	-0,652	-0,690
P49736	DNA replication licensing factor MCM2	MCM2	11	11	101,89	-0,845	-0,952	-0,787	-0,832
Q14566	DNA replication licensing factor MCM6	MCM6	13	13	92,888	-0,775	-0,957	-0,947	-0,639
Q14683	Structural maintenance of chromosomes protein 1A	SMC1A	8	8	140,86	-0,937	-0,964	-0,839	-0,649
P33991	DNA replication licensing factor MCM4	MCM4	9	9	91,19	-1,032	-0,921	-0,830	-0,883
Q9NTJ3	Structural maintenance of chromosomes protein 4	SMC4	8	8	144,45	-0,904	-0,976	-0,750	-1,037
P52701-3	DNA mismatch repair protein Msh6	MSH6	5	5	137,96	-0,834	-1,025	-1,050	-0,972
P16949	Stathmin	STMN1	12	12	17,302	-0,918	-0,838	-1,057	-0,813
P26583	High mobility group protein B2	HMGB2	10	10	24,033	-0,956	-0,836	-1,106	-0,837
P00352	Retinal dehydrogenase 1	ALDH1A1	11	11	54,861	-1,123	-1,211	-1,025	-1,131
Q15392-2	Delta(24)-sterol reductase	DHCR24	5	5	54,75	-1,236	-1,059	-0,617	-0,805
P41567	Eukaryotic translation initiation factor 1	EIF1	2	2	13,607	-1,265	-1,073	-1,149	-0,617
P06454-2	Prothymosin alpha	PTMA	7	7	11,758	-1,456	-1,097	-1,146	-0,855
P04637	Cellular tumor antigen p53	TP53	4	4	45,884	-1,549	-1,301	-1,640	-1,285
P06493	Cyclin-dependent kinase 1	CDK1	7	7	34,095	-1,719	-1,283	-1,682	-1,656
P11388	DNA topoisomerase 2-alpha	TOP2A	9	9	174,38	-1,745	-1,340	-1,610	-1,790
P26358	DNA (cytosine-5)-methyltransferase 1	DNMT1	2	2	183,16	-0,748	-1,340	-1,873	-1,216
P00374	Dihydrofolate reductase	DHFR	3	3	21,452	-1,934	-1,465	-1,181	-1,285
P52292	Importin subunit alpha-1	KPNA2	4	4	57,861	-1,942	-1,777	-1,905	-1,536
P31350	Ribonucleoside-diphosphate reductase subunit M2	RRM2	3	3	33,789	-3,175	-2,729	-2,915	-1,968

S8:

Endothelial Cells_Classification of regulated protein groups according to GO - Biological processes (UniProtKB) in Experiments 2 and 3

Threshold: log2Ratio 0.58 in both technical replicates
log2Ratio 0.58 = fold increase of 1.5

upregulated
downregulated
HCMV protein

Viral Protein

				Experiment 2	Experiment 3	Experiment 2		Experiment 3	
				Razor +		log2.Ratio.DB/Contr		log2.Ratio.DB/Contr	
Protein.ID	Protein.name	Gene.name	Mass (kDa)	unique peptides		replicate 1	replicate 2	replicate 1	replicate 2
D9IG50	Tegument protein pp65	pp65	9	9	62,872	2,717	0,849	2,176	0,430

Cell Cycle

				Experiment 2	Experiment 3	Experiment 2		Experiment 3	
				Razor +		log2.Ratio.DB/Contr		log2.Ratio.DB/Contr	
Protein.ID	Protein.name	Gene.name	Mass (kDa)	unique peptides		replicate 1	replicate 2	replicate 1	replicate 2
Q9Y570	Protein phosphatase methylesterase 1	PPME1	10	10	42,315	0,759	1,265	0,892	1,163
P33992	DNA replication licensing factor MCM5	MCM5	9	9	82,285	-0,928	-0,762	-0,709	-0,641
P49736	DNA replication licensing factor MCM2	MCM2	11	11	101,89	-0,845	-0,952	-0,787	-0,832
Q14566	DNA replication licensing factor MCM6	MCM6	13	13	92,888	-0,775	-0,957	-0,947	-0,639
Q14683	Structural maintenance of chromosomes protein 1A	SMC1A	8	8	140,86	-0,937	-0,964	-0,839	-0,649
P33991	DNA replication licensing factor MCM4	MCM4	9	9	91,19	-1,032	-0,921	-0,830	-0,883
Q9NTJ3	Structural maintenance of chromosomes protein 4	SMC4	8	8	144,45	-0,904	-0,976	-0,750	-1,037
P52701-3	DNA mismatch repair protein Msh6	MSH6	5	5	137,96		-1,025	-1,050	-0,972
P06493	Cyclin-dependent kinase 1	CDK1	7	7	34,095	-1,719	-1,283	-1,682	-1,656
P31350	Ribonucleoside-diphosphate reductase subunit M2	RRM2	3	3	33,789	-3,175	-2,729	-2,915	-1,968
P16949	Stathmin	STMN1	12	12	17,302	-0,918	-0,838	-1,057	-0,813
P04637	Cellular tumor antigen p53	TP53	4	4	45,884	-1,549	-1,301	-1,640	-1,285
P11388	DNA topoisomerase 2-alpha	TOP2A	9	9	174,38	-1,745	-1,340	-1,610	-1,790
P00374	Dihydrofolate reductase	DHFR	21,452	3	3	-1,934	-1,465	-1,181	-1,285
Q15392-2	Delta(24)-sterol reductase	DHCR24	54,75	5	5	-1,236	-1,059	-0,617	-0,805

Chromosome Organization

				Experiment 2	Experiment 3	Experiment 2		Experiment 3	
				Razor +		log2.Ratio.DB/Contr		log2.Ratio.DB/Contr	
Protein.ID	Protein.name	Gene.name	Mass (kDa)	unique peptides		replicate 1	replicate 2	replicate 1	replicate 2
P16401	Histone H1.5	HIST1H1B	22,58	7	7	-0,827	-0,874	-0,833	-0,843
P62805	Histone H4	H4C1	11,367	10	10	-0,910	-0,702	-0,827	-0,840
P35659	Protein DEK	DEK	42,674	6	6	-0,936	-0,626	-0,652	-0,690
P26583	High mobility group protein B2	HMGB2	10	10	24,033	-0,956	-0,836	-1,106	-0,837
P06454-2	Prothymosin alpha	PTMA	11,758	7	7	-1,456	-1,097	-1,146	-0,855
P04637	Cellular tumor antigen p53	TP53	4	4	45,884	-1,549	-1,301	-1,640	-1,285
P06493	Cyclin-dependent kinase 1	CDK1	7	7	34,095	-1,719	-1,283	-1,682	-1,656
P11388	DNA topoisomerase 2-alpha	TOP2A	9	9	174,38	-1,745	-1,340	-1,610	-1,790
Q9NTJ3	Structural maintenance of chromosomes protein 4	SMC4	8	8	144,45	-0,904	-0,976	-0,750	-1,037
P49736	DNA replication licensing factor MCM2	MCM2	11	11	101,89	-0,845	-0,952	-0,787	-0,832
Q14566	DNA replication licensing factor MCM6	MCM6	13	13	92,888	-0,775	-0,957	-0,947	-0,639
P33991	DNA replication licensing factor MCM4	MCM4	9	9	91,19	-1,032	-0,921	-0,830	-0,883
Q14683	Structural maintenance of chromosomes protein 1A	SMC1A	8	8	140,86	-0,937	-0,964	-0,839	-0,649
P26358	DNA (cytosine-5)-methyltransferase 1	DNMT1	2	2	183,16	-0,748	-1,340	-1,873	-1,216

Apoptosis

				Experiment 2	Experiment 3	Experiment 2		Experiment 3	
				Razor +		log2.Ratio.DB/Contr		log2.Ratio.DB/Contr	
Protein.ID	Protein.name	Gene.name	Mass (kDa)	unique peptides		replicate 1	replicate 2	replicate 1	replicate 2
Q53FA7	Quinone oxidoreductase PIG3	TP53I3	10	10	35,536	1,049	2,202	0,821	2,222
P09525	Annexin A4	ANXA4	14	14	35,882	0,884	0,925	0,942	0,922
P26583	High mobility group protein B2	HMGB2	10	10	24,033	-0,956	-0,836	-1,106	-0,837
P04637	Cellular tumor antigen p53	TP53	4	4	45,884	-1,549	-1,301	-1,640	-1,285
P11388	DNA topoisomerase 2-alpha	TOP2A	9	9	174,38	-1,745	-1,340	-1,610	-1,790

Antiviral Defense

				Experiment 2	Experiment 3	Experiment 2		Experiment 3	
				Razor +		log2.Ratio.DB/Contr		log2.Ratio.DB/Contr	
Protein.ID	Protein.name	Gene.name	Mass (kDa)	unique peptides		replicate 1	replicate 2	replicate 1	replicate 2
P20591	Interferon-induced GTP-binding protein Mx1	MX1	75,519	17	17	1,285	1,328	1,756	0,887
P05161	Ubiquitin-like protein ISG15	ISG15	17,887	5	5	1,321	1,404	1,499	1,492
Q9NR30	Nucleolar RNA helicase 2	DDX21	87,343	16	16	-0,582	-0,580	-0,654	-0,595

Cell adhesion

				Experiment 2	Experiment 3	Experiment 2		Experiment 3	
				Razor +		log2.Ratio.DB/Contr		log2.Ratio.DB/Contr	
Protein.ID	Protein.name	Gene.name	Mass (kDa)	unique peptides		replicate 1	replicate 2	replicate 1	replicate 2
P13598	Intercellular adhesion molecule 2	ICAM2	3	3	28,181	1,007	0,917	1,237	1,235
P26006	Integrin alpha-3	ITGA3	7	7	116,61	1,391	1,484	1,750	1,111
P14209-3	CD99 antigen	CD99	2	2	17,128	1,053	1,156	0,702	1,383

Cytoskeleton Organization

Protein.ID	Protein.name	Gene.name	Mass (kDa)	Experiment 2 Razor + unique peptides	Experiment 3 Razor + unique peptides	Experiment 2 log2.Ratio.DB/Contr replicate 1	Experiment 2 log2.Ratio.DB/Contr replicate 2	Experiment 3 log2.Ratio.DB/Contr replicate 1	Experiment 3 log2.Ratio.DB/Contr replicate 2
Q01995	Transgelin	TAGLN	5	5	16,733	1,037	1,892	1,600	1,301
P16949	Stathmin	STMN1	12	12	17,302	-0,918	-0,838	-1,057	-0,813
P06703	Protein S100-A6	S100A6	3	3	9,681	0,860	1,301	0,905	0,744
Q15149	Plectin	PLEC	531,78	197	197	0,955	0,820	0,950	0,891

Protein Transport

Protein.ID	Protein.name	Gene.name	Mass (kDa)	Experiment 2 Razor + unique peptides	Experiment 3 Razor + unique peptides	Experiment 2 log2.Ratio.DB/Contr replicate 1	Experiment 2 log2.Ratio.DB/Contr replicate 2	Experiment 3 log2.Ratio.DB/Contr replicate 1	Experiment 3 log2.Ratio.DB/Contr replicate 2
Q14764	Major vault protein	MVP	99,326	23	23	1,348	1,099	1,495	0,989
P27105	Erythrocyte band 7 integral membrane protein	STOM	31,73	7	7	0,600	0,699	0,591	0,815
P52292	Importin subunit alpha-1	KPNA2	57,861	4	4	-1,942	-1,777	-1,905	-1,536

Xenobiotic metabolic process

Protein.ID	Protein.name	Gene.name	Mass (kDa)	Experiment 2 Razor + unique peptides	Experiment 3 Razor + unique peptides	Experiment 2 log2.Ratio.DB/Contr replicate 1	Experiment 2 log2.Ratio.DB/Contr replicate 2	Experiment 3 log2.Ratio.DB/Contr replicate 1	Experiment 3 log2.Ratio.DB/Contr replicate 2
Q96DG6	Carboxymethylenebutenolidase homolog	CMBL	28,048	8	8	1,426	2,417	1,766	1,551
O75828	Carbonyl reductase [NADPH] 3	CBR3	30,85	2	2	-0,636	-0,601	-0,586	-0,642

Protein Biosynthesis

Protein.ID	Protein.name	Gene.name	Mass (kDa)	Experiment 2 Razor + unique peptides	Experiment 3 Razor + unique peptides	Experiment 2 log2.Ratio.DB/Contr replicate 1	Experiment 2 log2.Ratio.DB/Contr replicate 2	Experiment 3 log2.Ratio.DB/Contr replicate 1	Experiment 3 log2.Ratio.DB/Contr replicate 2
P41567	Eukaryotic translation initiation factor 1	EIF1	13,607	2	2	-1,265	-1,073	-1,149	-0,617
P06454-2	Prothymosin alpha	PTMA	11,758	7	7	-1,456	-1,097	-1,146	-0,855

Lipid Metabolism

Protein.ID	Protein.name	Gene.name	Mass (kDa)	Experiment 2 Razor + unique peptides	Experiment 3 Razor + unique peptides	Experiment 2 log2.Ratio.DB/Contr replicate 1	Experiment 2 log2.Ratio.DB/Contr replicate 2	Experiment 3 log2.Ratio.DB/Contr replicate 1	Experiment 3 log2.Ratio.DB/Contr replicate 2
P22570-4	NADPH:adrenodoxin oxidoreductase, mitochondrial	FDXR	48,056	14	14	1,628	1,397	2,013	1,444
Q15392-2	Delta(24)-sterol reductase	DHCR24	54,75	5	5	-1,236	-1,059	-0,617	-0,805

Other

Protein.ID	Protein.name	Gene.name	Mass (kDa)	Experiment 2 Razor + unique peptides	Experiment 3 Razor + unique peptides	Experiment 2 log2.Ratio.DB/Contr replicate 1	Experiment 2 log2.Ratio.DB/Contr replicate 2	Experiment 3 log2.Ratio.DB/Contr replicate 1	Experiment 3 log2.Ratio.DB/Contr replicate 2
P02794	Ferritin heavy chain	FTH1	21,225	5	5	0,749	1,204	0,658	0,843
Q9Y617-2	Phosphoserine aminotransferase	PSAT1	35,188	8	8	0,795	1,156	0,793	0,623
O95810	Caveolae-associated protein 2	CAVIN2	47,173	11	11	1,037	0,695	0,787	0,742
Q09666	Neuroblast differentiation-associated protein AHNAK	AHNAK	629,09	170	170	0,943	0,628	0,875	0,854
O00469	Procollagen-lysine,2-oxoglutarate 5-dioxygenase 2	PLOD2	81,169	13	13	0,835	0,729	0,876	0,611
Q14315-2	Filamin-C	FLNC	287,28	49	49	0,804	0,783	0,736	0,725
Q9H4M9	EH domain-containing protein 1	EHD1	60,626	9	9	0,699	0,696	0,804	0,608
P15144	Aminopeptidase N	ANPEP	5	5	109,54	0,947	0,909	1,072	0,840
P05121	Plasminogen activator inhibitor 1	SERPINE1	7	7	45,059	1,012	1,069	0,787	0,691
P07108	Acyl-CoA-binding protein	DBI	10,044	4	4	-0,813	-0,715	-0,785	-0,748
P00352	Retinal dehydrogenase 1	ALDH1A1	54,861	11	11	-1,123	-1,211	-1,025	-1,131

S9:

Monocytes_Interferon regulated protein groups 24h after DBs exposure

Threshold: log2Ratio 0.58 in minimum three Donors
log2Ratio 0.58 = fold increase of 1.5

upregulated
downregulated

Regulated protein groups that were regulated in both,
monocytes exosed to DBs derived from Towne-BAC or DBs derived from Towne-repΔGFP

DB_Towne-BAC

				Donor 1 log2.Ratio.DB-BAC/Contr		Donor 2 log2.Ratio.DB-BAC/Contr		Donor 3 log2.Ratio.DB-BAC/Contr		Donor 4 log2.Ratio.DB-BAC/Contr		Donor 5 log2.Ratio.DB-BAC/Contr		Donor 6 log2.Ratio.DB-BAC/Contr	
Protein.ID	Protein.name	Gene.name	Mass (kDa)	replicate 1	replicate 2	replicate 1	replicate 2	replicate 1	replicate 2	replicate 1	replicate 2	replicate 1	replicate 2	replicate 1	replicate 2
P10909-4	Clusterin	CLU	48,803	13,153	1,261							0,436	0,605	0,965	0,419
P00747	Plasminogen	PLG	90,568	3,018	3,301	2,071	2,114	1,370	1,459	1,283	0,770	1,691	2,180	1,285	1,560
P04179-4	Superoxide dismutase [Mn], mitochondrial	SOD2	23,672	1,764	1,416	1,525	1,239	1,690	1,741			0,858	1,328		
P05120	Plasminogen activator inhibitor 2	SERPINB2	46,596	1,345	1,563	1,282	1,019	1,831	1,539						
P33121-3	Long-chain-fatty-acid--CoA ligase 1	ACSL1	77,951	1,255	1,574	0,688	0,630	1,315	1,279						
P29966	Myristoylated alanine-rich C-kinase substrate	MARCKS	31,554	0,941	1,244	0,022	0,807	1,514	0,798	1,143	0,431				
A0A140T955	HLA class I histocompatibility antigen, A alpha chain	HLA-A	34,288	-0,700						0,220	1,457	0,707	0,949		
P30273	High affinity immunoglobulin epsilon receptor subunit gamma	FCER1G	9,6674	0,682		0,052	0,699					0,500	1,179		
P05362	Intercellular adhesion molecule 1	ICAM1	57,768	0,578	1,218	0,729	0,823	1,073	1,034			0,883	0,440		
P02747	Complement C1q subcomponent subunit C	C1QC	25,773	0,932	0,986	0,469	0,586			1,327		0,110	1,126	0,785	0,825
P04004	Vitronectin	VTN	54,305	1,650	1,624	0,927	0,735	-0,611	-0,576			0,401	0,652		
P00734	Prothrombin	F2	33,637	1,644	1,156	0,735	0,504	-0,670	-0,772	0,831	0,818				
P04196	Histidine-rich glycoprotein	HRG	59,512	4,754	4,909				-0,942			0,651	0,239		
P01009	Alpha-1-antitrypsin	SERPINA1	46,736	0,808	0,683					2,009	0,053			-0,617	-0,662
P07858	Cathepsin B	CTSB	37,821	-0,607	-0,340	-0,918					0,712	1,035	0,957		
P12236	ADP/ATP translocase 3	SLC25A6	32,866	-0,688	-0,114					0,908	0,119	0,099	0,593		
P34741	Syndecan-2	SDC2	14,905	-0,763		-0,802	-0,694		-1,441					0,935	0,368
P00738	Haptoglobin	HP	45,205					-0,597	-0,294	2,128	1,393			-0,403	-0,612
P01023	Alpha-2-macroglobulin	A2M	163,29	-0,834	-0,523			-0,513	-0,775	1,272	1,407			-0,654	-0,583
Q9Y336	Sialic acid-binding Ig-like lectin 9	SIGLEC9	50,081	-0,697		-0,180	-0,613		-0,839			-0,618	-0,059		
P02787	Serotransferrin	TF	77,063	-1,002	-1,305					1,865	1,102			-0,795	-0,696
Q01469	Fatty acid-binding protein 5	FABP5	15,164	-1,341	-1,346	-0,968	-1,113	-1,350	-0,835	0,152	0,820	-0,690	-0,697		
P17813-2	Endoglin	ENG	67,541	-1,303	-1,264	-0,679	-1,086	-1,212	-1,506						
Q9UI08-4	Ena/VASP-like protein	EVL	41,306	-1,127				-0,802				-1,285			
P16671	Platelet glycoprotein 4	CD36	52,062	-2,205	-1,873	-1,307	-1,266	-1,924	-2,127	0,714		-1,210	-0,585		
Q9UIB8-3	SLAM family member 5	CD84	36,87	-1,949	-2,321	-1,607			-2,259						
P38571-2	Lysosomal acid lipase/cholesteryl ester hydrolase	LIPA	32,57	-2,308	-2,192	-0,865	-1,275	-1,711	-1,883					0,713	
P15090	Fatty acid-binding protein, adipocyte	FABP4	14,719	-3,457	-5,410	-3,872	-3,003	-3,481	-2,446	1,293	0,480	-1,316	-1,371		

DB_RV-Towne-repΔGFP

				Donor 1 log2.Ratio.DB-ΔGFP/Contr		Donor 2 log2.Ratio.DB-ΔGFP/Contr		Donor 3 log2.Ratio.DB-ΔGFP/Contr		Donor 4 log2.Ratio.DB-ΔGFP/Contr		Donor 5 log2.Ratio.DB-ΔGFP/Contr		Donor 6 log2.Ratio.DB-ΔGFP/Contr	
Protein.ID	Protein.name	Gene.name	Mass (kDa)	replicate 1	replicate 2	replicate 1	replicate 2	replicate 1	replicate 2	replicate 1	replicate 2	replicate 1	replicate 2	replicate 1	replicate 2
P10909-4	Clusterin	CLU	48,803	1,076	0,865	0,750	0,542	8,960	0,138			0,531	0,831		
P00747	Plasminogen	PLG	90,568	1,995	2,602	2,557	2,186	1,631	1,410	1,705	0,650	2,079	2,518	1,100	
P04179-4	Superoxide dismutase [Mn], mitochondrial	SOD2	23,672	2,136	1,783	1,678	1,553	2,570	2,384			1,349	1,282	0,539	
P05120	Plasminogen activator inhibitor 2	SERPINB2	46,596	1,652	1,695	1,934	1,644	1,519	1,337			0,661	0,982		
P33121-3	Long-chain-fatty-acid--CoA ligase 1	ACSL1	77,951	1,549	1,743	0,583	0,512	1,687	1,351			1,196	0,817		
P29966	Myristoylated alanine-rich C-kinase substrate	MARCKS	31,554	1,291	1,603	0,494	1,569	0,856	1,328						

A0A140T955	HLA class I histocompatibility antigen, A alpha chain	HLA-A	34,288	-1,0816						0,7758	0,2963	0,5414	0,6349				
P30273	High affinity immunoglobulin epsilon receptor subunit gamma	FCER1G	9,6674	0,682		0,395	0,745	0,429	1,660			0,712	0,667				
P05362	Intercellular adhesion molecule 1	ICAM1	57,768	0,791	0,824	0,753	0,753	1,146	1,267			0,967	0,757				
P02747	Complement C1q subcomponent subunit C	C1QC	25,773	0,493	0,672	0,755	0,498	-0,447	-0,832			0,787	0,757				
P04004	Vitronectin	VTN	54,305	0,779	0,881	1,214	1,008	-0,891	-0,889								
P00734	Prothrombin	F2	33,637	0,896	0,753	1,099	0,601	-1,125	-1,253	1,125	0,983						
P04196	Histidine-rich glycoprotein	HRG	59,512	0,687	0,954	0,763	0,604		-1,950								
P01009	Alpha-1-antitrypsin	SERPINA1	46,736	0,598	0,451	0,591	0,431	1,288	0,922	1,194	0,127			-0,909			
P07858	Cathepsin B	CTSB	37,821	-1,308	-0,704	-0,606	-0,907	-0,725	-0,626			0,659	0,307				
P12236	ADP/ATP translocase 3	SLC25A6	32,866							-0,603	-0,796	0,399	0,647	0,705	0,242		
P34741	Syndecan-2	SDC2	14,905	-1,114		-1,513	-1,413		-0,771								
P00738	Haptoglobin	HP	45,205			0,622	0,432	1,070	1,423	0,736	0,937	0,028	0,592	-1,144			
P01023	Alpha-2-macroglobulin	A2M	163,29	-0,957	-0,401					0,752	0,633			-0,611	-0,644		
Q9Y336	Sialic acid-binding Ig-like lectin 9	SIGLEC9	50,081	-0,659		-0,592	-0,655		-1,574								
P02787	Serotransferrin	TF	77,063					1,288	0,888	0,769	0,255			-1,305	-1,130		
Q01469	Fatty acid-binding protein 5	FABP5	15,164	-1,650	-1,203	-1,190	-0,715	-1,815	-1,573			-0,846	-0,529	-0,380			
P17813-2	Endoglin	ENG	67,541	-1,743	-1,156	-1,892	-1,950	-1,076	-1,961			-0,850					
Q9UI08-4	Ena/VASP-like protein	EVL	41,306	-2,178				-1,405				-0,934					
P16671	Platelet glycoprotein 4	CD36	52,062	-1,486	-1,519	-2,155	-2,163	-2,255	-2,490			-0,862	-1,030				
Q9UIB8-3	SLAM family member 5	CD84	36,87	-1,686	-2,371	-2,215			-3,296								
P38571-2	Lysosomal acid lipase/cholesteryl ester hydrolase	LIPA	32,57	-1,650	-2,671	-2,560	-3,423	-2,734	-3,101								
P15090	Fatty acid-binding protein, adipocyte	FABP4	14,719	-3,120	-4,820	-3,573	-0,916	-3,880	-3,935	-0,420	-0,723	-1,369	-1,705	-0,579			

Regulated protein groups that were found in monocytes exposed to DBs of RV-Towne-BAC

DB_Towne-BAC

				Donor 1 log2.Ratio.DB-BAC/Contr		Donor 2 log2.Ratio.DB-BAC/Contr		Donor 3 log2.Ratio.DB-BAC/Contr		Donor 4 log2.Ratio.DB-BAC/Contr		Donor 5 log2.Ratio.DB-BAC/Contr		Donor 6 log2.Ratio.DB-BAC/Contr	
Protein.ID	Protein.name	Gene.name	Mass (kDa)	replicate 1	replicate 2	replicate 1	replicate 2	replicate 1	replicate 2	replicate 1	replicate 2	replicate 1	replicate 2	replicate 1	replicate 2
Q8IUE6	Histone H2A type 2-B	HIST2H2AB	13,995	-1,505	-1,903	6,460	2,160	2,795	2,581						
P62081	40S ribosomal protein S7	RPS7	22,127			3,029	0,132			2,063		-0,880	-0,076		
Q9NY25	C-type lectin domain family 5 member A	CLEC5A	18,031	2,589		0,665	0,374								0,746
P00450	Ceruloplasmin	CP	97,712							1,833		0,386	0,705	0,776	0,856
P0C0L4-2	Complement C4-A	C4A	187,67	1,001	1,375	0,759		0,202	0,735	1,771	1,501				
P26447	Protein S100-A4	S100A4	11,728	0,254	1,627			0,290	0,820			-0,637	-0,289		
P05109	Protein S100-A8	S100A8	10,834	1,553	1,606			0,122	1,446	1,110	0,722	-0,690	-0,377		
P62081	40S ribosomal protein S7	RPS7	22,127	1,565	0,848					1,534	0,501	0,550	0,689		
O00571-2	ATP-dependent RNA helicase DDX3X	DDX3X	81,476			0,608	1,549					0,453	0,595	0,489	0,588
P62249	40S ribosomal protein S16	RPS16	14,419	0,592	0,351			0,213	0,671	1,466	0,079				
P02671-2	Fibrinogen alpha chain	FGA	69,756	1,457	1,298	0,987	0,769					0,647	0,467		
P02679-2	Fibrinogen gamma chain	FGG	49,496	1,274	1,107	1,007	0,913	-0,709	-0,653			0,497	0,881		
Q16543	Hsp90 co-chaperone Cdc37	CDC37	44,468	0,827	0,179			1,159	0,352			-0,694	-0,330		
P25774	Cathepsin S	CTSS	37,495	-0,791	-0,847	-0,373	-0,624			1,143	0,842				
Q14019	Coactosin-like protein	COTL1	8,2242					0,448	0,663	1,036		-0,611	-0,570		
O00175	C-C motif chemokine 24	CCL24	13,133			1,031			0,655			-0,626	-0,220		
P02675	Fibrinogen beta chain	FGB	39,736	0,887	0,913	0,693	1,007	-1,105	-0,476			0,543	0,825		
P14780	Matrix metalloproteinase-9	MMP9	78,457	0,573	0,701	0,401	0,767	0,981	0,900						
Q9H299	SH3 domain-binding glutamic acid-rich-like protein 3	SH3BGRL3	9,3804	-0,205	-0,665	-0,466	-0,662	0,062	0,893				-0,602	0,643	0,070
P07737	Profilin-1	PFN1	15,054					0,376	0,843	0,740	0,408	-0,809	-0,321		
P02747	Complement C1q subcomponent subunit C	C1QC	25,773	0,811	0,992	0,373	0,591							0,706	0,743
P20645	Cation-dependent mannose-6-phosphate receptor	M6PR	30,993			-0,796	-0,085	-0,650	-0,004			-0,029	-0,647		
P62424	60S ribosomal protein L7a	RPL7A	21,545	0,737	0,206				-0,816					0,655	0,486
P61916	NPC intracellular cholesterol transporter 2	NPC2	16,23	-0,261	-1,181	-0,686	-0,540	-0,655	-0,157						
P16284-3	Platelet endothelial cell adhesion molecule	PECAM1	81,779	-1,235	-1,222			-0,729	-0,854					0,581	0,055
Q02818	Nucleobindin-1	NUCB1	34,773	-0,857	-1,016			-4,355				0,127	0,851		

Regulated protein groups that were found in monocytes exposed to DBs of RV-Towne-rep ΔGFP

DB_RV-Towne-repΔGFP				Donor 1		Donor 2		Donor 3		Donor 4		Donor 5		Donor 6	
				log2.Ratio.DB-ΔGFP/Contr		log2.Ratio.DB-ΔGFP/Contr		log2.Ratio.DB-ΔGFP/Contr		log2.Ratio.DB-ΔGFP/Contr		log2.Ratio.DB-ΔGFP/Contr		log2.Ratio.DB-ΔGFP/Contr	
Protein.ID	Protein.name	Gene.name	Mass (kDa)	replicate 1	replicate 2	replicate 1	replicate 2	replicate 1	replicate 2	replicate 1	replicate 2	replicate 1	replicate 2	replicate 1	replicate 2
P01583	Interleukin-1 alpha	IL1A	30,606	3,1248	1,6248	3,1063	0,3017	3,7477	3,6634						
Q9ULZ3-3	Apoptosis-associated speck-like protein containing a CARD	PYCARD	21,628	3,4618	0,3855	0,3566	0,5882	1,0101	1,0449						
P08603	Complement factor H	CFH	138,95	0,0467	2,1550	0,7473	0,4862		-1,0743						
P35542	Serum amyloid A-4 protein	SAA4	14,808	1,0188		0,6649	0,5043	-1,4092	-1,2507			0,0828	0,7506		
P60468	Protein transport protein Sec61 subunit beta	SEC61B	9,9743	1,0120		0,0144	0,6899					0,7428	0,0584		
P01008	Antithrombin-III	SERPINC1	52,602	0,7464	0,7976	0,8368	0,5076	-0,9585	-1,0911			0,6342	0,7133	-0,5879	
P01871	Immunoglobulin heavy constant mu	IGHM	49,439	0,6707	0,8410	0,8024	0,6311			0,7125	0,5733	0,6260	0,4692		
P62280	40S ribosomal protein S11	RPS11	18,431			0,8056	0,8290	0,1725	1,0816					0,3247	0,6203
P02751-10	Fibronectin	FN1	246,7	0,6978	0,5206			-0,8715	-0,9372			-0,9424	-1,2899		
P02749	Beta-2-glycoprotein 1	APOH	38,298	0,1776	0,6467					0,6848			0,7332	-0,3386	
P02649	Apolipoprotein E	APOE	36,154	0,1189	0,6222	0,6538	0,5372	-0,9624	-1,0060	0,7592	0,1193				
P01024	Complement C3	C3	187,15			0,6227	0,5611	-0,4451	-0,6239	0,7366	0,7727			-0,4453	
P46777	60S ribosomal protein L5	RPL5	28,044	-0,6571	-0,0757			-0,7277	-0,0053		-0,6680				
Q9Y4P3	Transducin beta-like protein 2	TBL2	45,935		-0,6756	-0,7910	-0,5444		-0,9926			-0,1819	-0,8885		
P11717	Cation-independent mannose-6-phosphate receptor	IGF2R	274,37		-0,6804	-0,5848	-1,1874	-0,7041	-1,3795						
Q6NVH9	Galectin	LGALS3	26,197	-0,7091	-0,7184	-0,4676	-0,7959	-1,0296	-1,1328						
Q15758	Neutral amino acid transporter B(0)	SLC1A5	56,583	-0,6715	-1,0443	-0,9744		-1,3594	-0,9093						
Q07954	Prolow-density lipoprotein receptor-related protein 1	LRP1	504,6	-1,4361	-0,2668	-0,8826	-1,7474	-1,7428	-1,7419						
P13686	Tartrate-resistant acid phosphatase type 5	ACP5	36,598	-2,1283	-0,7143	-1,5878		-2,4259	-2,8776						

S10:
Monocytes_Not interferon regulated protein groups 24h after DBs exposure

Threshold: log2Ratio 0.58 in minimum three Donors — upregulated
log2Ratio 0.58 = fold increase of 1.5 — downregulated

Regulated protein groups that were found in monocytes exposed to DBs of RV-Towne-BAC
and also in monocytes exposed to DBs of RV-Towne-repΔGFP

DB_Towne-BAC				Donor 1		Donor 2		Donor 3		Donor 4		Donor 5		Donor 6	
				log2.Ratio.DB-BAC/Contr		log2.Ratio.DB-BAC/Contr		log2.Ratio.DB-BAC/Contr		log2.Ratio.DB-BAC/Contr		log2.Ratio.DB-BAC/Contr		log2.Ratio.DB-BAC/Contr	
Protein.ID	Protein.name	Gene.name	Mass (kDa)	replicate 1	replicate 2	replicate 1	replicate 2	replicate 1	replicate 2	replicate 1	replicate 2	replicate 1	replicate 2	replicate 1	replicate 2
P15880	40S ribosomal protein S2	RPS2	21,154		0,683		0,706	0,742	0,131					0,634	0,265
Q8TD55-2	Pleckstrin homology domain-containing family O member 2	PLEKHO2	47,785			-2,928	-0,317	0,610	0,094	0,635					

DB_RV-Towne-repΔGFP				Donor 1		Donor 2		Donor 3		Donor 4		Donor 5		Donor 6	
				log2.Ratio.DB-ΔGFP/Contr		log2.Ratio.DB-ΔGFP/Contr		log2.Ratio.DB-ΔGFP/Contr		log2.Ratio.DB-ΔGFP/Contr		log2.Ratio.DB-ΔGFP/Contr		log2.Ratio.DB-ΔGFP/Contr	
Protein.ID	Protein.name	Gene.name	Mass (kDa)	replicate 1	replicate 2	replicate 1	replicate 2	replicate 1	replicate 2	replicate 1	replicate 2	replicate 1	replicate 2	replicate 1	replicate 2
P15880	40S ribosomal protein S2	RPS2	21,154		0,654			0,200	0,984					0,664	0,521
Q8TD55-2	Pleckstrin homology domain-containing family O member 2	PLEKHO2	47,785			-1,177	-0,599	-0,377	-0,661	0,664					

Regulated protein groups that were found in monocytes exposed to DBs of RV-Towne-BAC

DB_Towne-BAC				Donor 1		Donor 2		Donor 3		Donor 4		Donor 5		Donor 6	
				log2.Ratio.DB-BAC/Contr		log2.Ratio.DB-BAC/Contr		log2.Ratio.DB-BAC/Contr		log2.Ratio.DB-BAC/Contr		log2.Ratio.DB-BAC/Contr		log2.Ratio.DB-BAC/Contr	
Protein.ID	Protein.name	Gene.name	Mass (kDa)	replicate 1	replicate 2	replicate 1	replicate 2	replicate 1	replicate 2	replicate 1	replicate 2	replicate 1	replicate 2	replicate 1	replicate 2
P62851	40S ribosomal protein S25	RPS25	13,742	0,761	0,717			0,052	0,720					0,510	0,682

Regulated protein groups that were found in monocytes exposed to DBs of RV-Towne-repΔGFP

DB_RV-Towne-repΔGFP				Donor 1		Donor 2		Donor 3		Donor 4		Donor 5		Donor 6	
				log2.Ratio.DB-ΔGFP/Contr		log2.Ratio.DB-ΔGFP/Contr		log2.Ratio.DB-ΔGFP/Contr		log2.Ratio.DB-ΔGFP/Contr		log2.Ratio.DB-ΔGFP/Contr		log2.Ratio.DB-ΔGFP/Contr	
Protein.ID	Protein.name	Gene.name	Mass (kDa)	replicate 1	replicate 2	replicate 1	replicate 2	replicate 1	replicate 2	replicate 1	replicate 2	replicate 1	replicate 2	replicate 1	replicate 2
P01834	Immunoglobulin kappa constant	IGKC	24,03	0,5233	0,7654	0,6508	0,4357	1,2948	1,1081	1,0212	0,2816	0,6731	0,1441	-0,4446	-0,8026

S11:
Monocytes_Classification of regulated protein groups according to GO - Biological processes (UniProtKB)

Biological processes that were regulated in both monocytes exosed to DBs derived from Towne-BAC or DBs derived from Towne-repΔGFP

upregulated
downregulated

Exocytosis

DB_Towne-BAC

				Donor 1		Donor 2		Donor 3		Donor 4		Donor 5		Donor 6	
				log2.Ratio.DB-BAC/Contr		log2.Ratio.DB-BAC/Contr		log2.Ratio.DB-BAC/Contr		log2.Ratio.DB-BAC/Contr		log2.Ratio.DB-BAC/Contr		log2.Ratio.DB-BAC/Contr	
Protein.ID	Protein.name	Gene.name	Mass (kDa)	replicate 1	replicate 2	replicate 1	replicate 2	replicate 1	replicate 2	replicate 1	replicate 2	replicate 1	replicate 2	replicate 1	replicate 2
P02787	Serotransferrin	TF	77,063	-1,002	-1,305					1,865	1,102			-0,795	-0,696
P01009	Alpha-1-antitrypsin	SERPINA1	46,736	0,808	0,683					2,009	0,053			-0,617	-0,662
P04196	Histidine-rich glycoprotein	HRG	59,512	4,754	4,909				-0,942			0,651	0,239		
P01023	Alpha-2-macroglobulin	A2M	163,29	-0,834	-0,523			-0,513	-0,775	1,272	1,407			-0,654	-0,583
P10909-4	Clusterin	CLU	48,803	13,153	1,261							0,436	0,605	0,965	0,419
P00738	Haptoglobin	HP	45,205					-0,597	-0,294	2,128	1,393			-0,403	-0,612
P00747	Plasminogen	PLG	90,568	3,018	3,301	2,071	2,114	1,370	1,459	1,283	0,770	1,691	2,180	1,285	1,560
A0A140T955	HLA class I histocompatibility antigen, A alpha chain	HLA-A	34,288	-0,700						0,220	1,457	0,707	0,949		
Q8TD55-2	Pleckstrin homology domain-containing family O member 2	PLEKHO2	47,785			-2,928	-0,317	0,610	0,094	0,635					
Q9Y336	Sialic acid-binding Ig-like lectin 9	SIGLEC9	50,081	-0,697		-0,180	-0,613		-0,839			-0,618	-0,059		
Q01469	Fatty acid-binding protein 5	FABP5	15,164	-1,341	-1,346	-0,968	-1,113	-1,350	-0,835	0,152	0,820	-0,690	-0,697		
P16671	Platelet glycoprotein 4	CD36	52,062	-2,205	-1,873	-1,307	-1,266	-1,924	-2,127	0,714		-1,210	-0,585		
P30273	High affinity immunoglobulin epsilon receptor subunit gamma	FCER1G	9,6674	0,682		0,052	0,699					0,500	1,179		

DB_RV-Towne-repΔGFP

				Donor 1		Donor 2		Donor 3		Donor 4		Donor 5		Donor 6	
				log2.Ratio.DB-ΔGFP/Contr		log2.Ratio.DB-ΔGFP/Contr		log2.Ratio.DB-ΔGFP/Contr		log2.Ratio.DB-ΔGFP/Contr		log2.Ratio.DB-ΔGFP/Contr		log2.Ratio.DB-ΔGFP/Contr	
Protein.ID	Protein.name	Gene.name	Mass (kDa)	replicate 1	replicate 2	replicate 1	replicate 2	replicate 1	replicate 2	replicate 1	replicate 2	replicate 1	replicate 2	replicate 1	replicate 2
P02787	Serotransferrin	TF	77,063					1,288	0,888	0,769	0,255			-1,305	-1,130
P01009	Alpha-1-antitrypsin	SERPINA1	46,736	0,598	0,451	0,591	0,431	1,288	0,922	1,194	0,127			-0,909	
P04196	Histidine-rich glycoprotein	HRG	59,512	0,687	0,954	0,763	0,604		-1,950						
P01023	Alpha-2-macroglobulin	A2M	163,29	-0,957	-0,401					0,752	0,633			-0,611	-0,644
P10909-4	Clusterin	CLU	48,803	1,076	0,865	0,750	0,542	8,960	0,138			0,531	0,831		
P00738	Haptoglobin	HP	45,205			0,622	0,432	1,070	1,423	0,736	0,937	0,028	0,592	-1,144	
P00747	Plasminogen	PLG	90,568	1,995	2,602	2,557	2,186	1,631	1,410	1,705	0,650	2,079	2,518	1,100	
A0A140T955	HLA class I histocompatibility antigen, A alpha chain	HLA-A	34,288	-1,0816						0,7758	0,2963	0,5414	0,6349		
Q8TD55-2	Pleckstrin homology domain-containing family O member 2	PLEKHO2	47,785			-1,177	-0,599	-0,377	-0,661	0,664					
Q9Y336	Sialic acid-binding Ig-like lectin 9	SIGLEC9	50,081	-0,659		-0,592	-0,655		-1,574						
Q01469	Fatty acid-binding protein 5	FABP5	15,164	-1,650	-1,203	-1,190	-0,715	-1,815	-1,573			-0,846	-0,529	-0,380	
P16671	Platelet glycoprotein 4	CD36	52,062	-1,486	-1,519	-2,155	-2,163	-2,255	-2,490			-0,862	-1,030		
P30273	High affinity immunoglobulin epsilon receptor subunit gamma	FCER1G	9,6674	0,682		0,395	0,745	0,429	1,660			0,712	0,667		

Defense Response

DB_Towne-BAC

Protein.ID	Protein.name	Gene.name	Mass (kDa)	Donor 1 log2.Ratio.DB-BAC/Contr		Donor 2 log2.Ratio.DB-BAC/Contr		Donor 3 log2.Ratio.DB-BAC/Contr		Donor 4 log2.Ratio.DB-BAC/Contr		Donor 5 log2.Ratio.DB-BAC/Contr		Donor 6 log2.Ratio.DB-BAC/Contr	
				replicate 1	replicate 2	replicate 1	replicate 2	replicate 1	replicate 2	replicate 1	replicate 2	replicate 1	replicate 2	replicate 1	replicate 2
P00734	Prothrombin	F2	33,637	1,644	1,156	0,735	0,504	-0,670	-0,772	0,831	0,818				
P04196	Histidine-rich glycoprotein	HRG	59,512	4,754	4,909				-0,942			0,651	0,239		
P01009	Alpha-1-antitrypsin	SERPINA1	46,736	0,808	0,683					2,009	0,053			-0,617	-0,662
P00738	Haptoglobin	HP	45,205					-0,597	-0,294	2,128	1,393			-0,403	-0,612
P10909-4	Clusterin	CLU	48,803	13,153	1,261							0,436	0,605	0,965	0,419
A0A140T955	HLA class I histocompatibility antigen, A alpha chain	HLA-A	34,288	-0,700						0,220	1,457	0,707	0,949		
P05362	Intercellular adhesion molecule 1	ICAM1	57,768	0,578	1,218	0,729	0,823	1,073	1,034			0,883	0,440		
Q9UI08-4	Ena/VASP-like protein	EVL	41,306	-1,127				-0,802				-1,285			
P02747	Complement C1q subcomponent subunit C	C1QC	25,773	0,932	0,986	0,469	0,586			1,327		0,110	1,126	0,785	0,825
P30273	High affinity immunoglobulin epsilon receptor subunit gamma	FCER1G	9,6674	0,682		0,052	0,699					0,500	1,179		
Q9UIB8-3	SLAM family member 5	CD84	36,87	-1,949	-2,321	-1,607			-2,259						
P16671	Platelet glycoprotein 4	CD36	52,062	-2,205	-1,873	-1,307	-1,266	-1,924	-2,127	0,714		-1,210	-0,585		
P38571-2	Lysosomal acid lipase/cholesteryl ester hydrolase	LIPA	32,57	-2,308	-2,192	-0,865	-1,275	-1,711	-1,883					0,713	

DB_RV-Towne-repΔGFP

Protein.ID	Protein.name	Gene.name	Mass (kDa)	Donor 1 log2.Ratio.DB-ΔGFP/Contr		Donor 2 log2.Ratio.DB-ΔGFP/Contr		Donor 3 log2.Ratio.DB-ΔGFP/Contr		Donor 4 log2.Ratio.DB-ΔGFP/Contr		Donor 5 log2.Ratio.DB-ΔGFP/Contr		Donor 6 log2.Ratio.DB-ΔGFP/Contr	
				replicate 1	replicate 2	replicate 1	replicate 2	replicate 1	replicate 2	replicate 1	replicate 2	replicate 1	replicate 2	replicate 1	replicate 2
P00734	Prothrombin	F2	33,637	0,896	0,753	1,099	0,601	-1,125	-1,253	1,125	0,983				
P04196	Histidine-rich glycoprotein	HRG	59,512	0,687	0,954	0,763	0,604		-1,950						
P01009	Alpha-1-antitrypsin	SERPINA1	46,736	0,598	0,451	0,591	0,431	1,288	0,922	1,194	0,127			-0,909	
P00738	Haptoglobin	HP	45,205			0,622	0,432	1,070	1,423	0,736	0,937	0,028	0,592	-1,144	
P10909-4	Clusterin	CLU	48,803	1,076	0,865	0,750	0,542	8,960	0,138			0,531	0,831		
A0A140T955	HLA class I histocompatibility antigen, A alpha chain	HLA-A	34,288	-1,0816						0,7758	0,2963	0,5414	0,6349		
P05362	Intercellular adhesion molecule 1	ICAM1	57,768	0,791	0,824	0,753	0,753	1,146	1,267			0,967	0,757		
Q9UI08-4	Ena/VASP-like protein	EVL	41,306	-2,178				-1,405				-0,934			
P02747	Complement C1q subcomponent subunit C	C1QC	25,773	0,493	0,672	0,755	0,498	-0,447	-0,832			0,787	0,757		
P30273	High affinity immunoglobulin epsilon receptor subunit gamma	FCER1G	9,6674	0,682		0,395	0,745	0,429	1,660			0,712	0,667		
Q9UIB8-3	SLAM family member 5	CD84	36,87	-1,686	-2,371	-2,215			-3,296						
P16671	Platelet glycoprotein 4	CD36	52,062	-1,486	-1,519	-2,155	-2,163	-2,255	-2,490			-0,862	-1,030		
P38571-2	Lysosomal acid lipase/cholesteryl ester hydrolase	LIPA	32,57	-1,650	-2,671	-2,560	-3,423	-2,734	-3,101						

Lipid Metabolism

DB_Towne-BAC

Protein.ID	Protein.name	Gene.name	Mass (kDa)	Donor 1 log2.Ratio.DB-BAC/Contr		Donor 2 log2.Ratio.DB-BAC/Contr		Donor 3 log2.Ratio.DB-BAC/Contr		Donor 4 log2.Ratio.DB-BAC/Contr		Donor 5 log2.Ratio.DB-BAC/Contr		Donor 6 log2.Ratio.DB-BAC/Contr	
				replicate 1	replicate 2	replicate 1	replicate 2	replicate 1	replicate 2	replicate 1	replicate 2	replicate 1	replicate 2	replicate 1	replicate 2
P34741	Syndecan-2	SDC2	14,905	-0,763		-0,802	-0,694		-1,441					0,935	0,368
P10909-4	Clusterin	CLU	48,803	13,153	1,261							0,436	0,605	0,965	0,419
P38571-2	Lysosomal acid lipase/cholesteryl ester hydrolase	LIPA	32,57	-2,308	-2,192	-0,865	-1,275	-1,711	-1,883					0,713	

Q01469	Fatty acid-binding protein 5	FABP5	15,164	-1,341	-1,346	-0,968	-1,113	-1,350	-0,835	0,152	0,820	-0,690	-0,697				
P15090	Fatty acid-binding protein, adipocyte	FABP4	14,719	-3,457	-5,410	-3,872	-3,003	-3,481	-2,446	1,293	0,480	-1,316	-1,371				
P33121-3	Long-chain-fatty-acid--CoA ligase 1	ACSL1	77,951	1,255	1,574	0,688	0,630	1,315	1,279								
P16671	Platelet glycoprotein 4	CD36	52,062	-2,205	-1,873	-1,307	-1,266	-1,924	-2,127	0,714		-1,210	-0,585				

DB_RV-Towne-repΔGFP

				Donor 1		Donor 2		Donor 3		Donor 4		Donor 5		Donor 6	
				log2.Ratio.DB-ΔGFP/Contr		log2.Ratio.DB-ΔGFP/Contr		log2.Ratio.DB-ΔGFP/Contr		log2.Ratio.DB-ΔGFP/Contr		log2.Ratio.DB-ΔGFP/Contr		log2.Ratio.DB-ΔGFP/Contr	
Protein.ID	Protein.name	Gene.name	Mass (kDa)	replicate 1	replicate 2	replicate 1	replicate 2	replicate 1	replicate 2	replicate 1	replicate 2	replicate 1	replicate 2	replicate 1	replicate 2
P34741	Syndecan-2	SDC2	14,905	-1,114		-1,513	-1,413		-0,771						
P10909-4	Clusterin	CLU	48,803	1,076	0,865	0,750	0,542	8,960	0,138			0,531	0,831		
P38571-2	Lysosomal acid lipase/cholesteryl ester hydrolase	LIPA	32,57	-1,650	-2,671	-2,560	-3,423	-2,734	-3,101						
Q01469	Fatty acid-binding protein 5	FABP5	15,164	-1,650	-1,203	-1,190	-0,715	-1,815	-1,573			-0,846	-0,529	-0,380	
P15090	Fatty acid-binding protein, adipocyte	FABP4	14,719	-3,120	-4,820	-3,573	-0,916	-3,880	-3,935	-0,420	-0,723	-1,369	-1,705	-0,579	
P33121-3	Long-chain-fatty-acid--CoA ligase 1	ACSL1	77,951	1,549	1,743	0,583	0,512	1,687	1,351			1,196	0,817		
P16671	Platelet glycoprotein 4	CD36	52,062	-1,486	-1,519	-2,155	-2,163	-2,255	-2,490			-0,862	-1,030		

Regulation of Cell Death

DB_Towne-BAC

				Donor 1		Donor 2		Donor 3		Donor 4		Donor 5		Donor 6	
				log2.Ratio.DB-BAC/Contr		log2.Ratio.DB-BAC/Contr		log2.Ratio.DB-BAC/Contr		log2.Ratio.DB-BAC/Contr		log2.Ratio.DB-BAC/Contr		log2.Ratio.DB-BAC/Contr	
Protein.ID	Protein.name	Gene.name	Mass (kDa)	replicate 1	replicate 2	replicate 1	replicate 2	replicate 1	replicate 2	replicate 1	replicate 2	replicate 1	replicate 2	replicate 1	replicate 2
P05120	Plasminogen activator inhibitor 2	SERPINB2	46,596	1,345	1,563	1,282	1,019	1,831	1,539						
P10909-4	Clusterin	CLU	48,803	13,153	1,261							0,436	0,605	0,965	0,419
P04196	Histidine-rich glycoprotein	HRG	59,512	4,754	4,909				-0,942			0,651	0,239		
P00738	Haptoglobin	HP	45,205					-0,597	-0,294	2,128	1,393			-0,403	-0,612
P07858	Cathepsin B	CTSB	37,821	-0,607	-0,340	-0,918					0,712	1,035	0,957		
P05362	Intercellular adhesion molecule 1	ICAM1	57,768	0,578	1,218	0,729	0,823	1,073	1,034			0,883	0,440		
P04179-4	Superoxide dismutase [Mn], mitochondrial	SOD2	23,672	1,764	1,416	1,525	1,239	1,690	1,741			0,858	1,328		
P30273	High affinity immunoglobulin epsilon receptor subunit gamma	FCER1G	9,6674	0,682		0,052	0,699					0,500	1,179		
P16671	Platelet glycoprotein 4	CD36	52,062	-2,205	-1,873	-1,307	-1,266	-1,924	-2,127	0,714		-1,210	-0,585		
P12236	ADP/ATP translocase 3	SLC25A6	32,866	-0,688	-0,114					0,908	0,119	0,099	0,593		

DB_RV-Towne-repΔGFP

				Donor 1		Donor 2		Donor 3		Donor 4		Donor 5		Donor 6	
				log2.Ratio.DB-ΔGFP/Contr		log2.Ratio.DB-ΔGFP/Contr		log2.Ratio.DB-ΔGFP/Contr		log2.Ratio.DB-ΔGFP/Contr		log2.Ratio.DB-ΔGFP/Contr		log2.Ratio.DB-ΔGFP/Contr	
Protein.ID	Protein.name	Gene.name	Mass (kDa)	replicate 1	replicate 2	replicate 1	replicate 2	replicate 1	replicate 2	replicate 1	replicate 2	replicate 1	replicate 2	replicate 1	replicate 2
P05120	Plasminogen activator inhibitor 2	SERPINB2	46,596	1,652	1,695	1,934	1,644	1,519	1,337			0,661	0,982		
P10909-4	Clusterin	CLU	48,803	1,076	0,865	0,750	0,542	8,960	0,138			0,531	0,831		
P04196	Histidine-rich glycoprotein	HRG	59,512	0,687	0,954	0,763	0,604		-1,950						
P00738	Haptoglobin	HP	45,205			0,622	0,432	1,070	1,423	0,736	0,937	0,028	0,592	-1,144	
P07858	Cathepsin B	CTSB	37,821	-1,308	-0,704	-0,606	-0,907	-0,725	-0,626			0,659	0,307		
P05362	Intercellular adhesion molecule 1	ICAM1	57,768	0,791	0,824	0,753	0,753	1,146	1,267			0,967	0,757		
P04179-4	Superoxide dismutase [Mn], mitochondrial	SOD2	23,672	2,136	1,783	1,678	1,553	2,570	2,384			1,349	1,282	0,539	
P30273	High affinity immunoglobulin epsilon receptor subunit gamma	FCER1G	9,6674	0,682		0,395	0,745	0,429	1,660			0,712	0,667		
P16671	Platelet glycoprotein 4	CD36	52,062	-1,486	-1,519	-2,155	-2,163	-2,255	-2,490			-0,862	-1,030		
P12236	ADP/ATP translocase 3	SLC25A6	32,866							-0,603	-0,796	0,399	0,647	0,705	0,242

Cell Adhesion

DB_Towne-BAC

Protein.ID	Protein.name	Gene.name	Mass (kDa)	Donor 1 log2.Ratio.DB-BAC/Contr		Donor 2 log2.Ratio.DB-BAC/Contr		Donor 3 log2.Ratio.DB-BAC/Contr		Donor 4 log2.Ratio.DB-BAC/Contr		Donor 5 log2.Ratio.DB-BAC/Contr		Donor 6 log2.Ratio.DB-BAC/Contr	
				replicate 1	replicate 2	replicate 1	replicate 2	replicate 1	replicate 2	replicate 1	replicate 2	replicate 1	replicate 2	replicate 1	replicate 2
P17813-2	Endoglin	ENG	67,541	-1,303	-1,264	-0,679	-1,086	-1,212	-1,506						
P04004	Vitronectin	VTN	54,305	1,650	1,624	0,927	0,735	-0,611	-0,576			0,401	0,652		

DB_RV-Towne-repΔGFP

Protein.ID	Protein.name	Gene.name	Mass (kDa)	Donor 1 log2.Ratio.DB-ΔGFP/Contr		Donor 2 log2.Ratio.DB-ΔGFP/Contr		Donor 3 log2.Ratio.DB-ΔGFP/Contr		Donor 4 log2.Ratio.DB-ΔGFP/Contr		Donor 5 log2.Ratio.DB-ΔGFP/Contr		Donor 6 log2.Ratio.DB-ΔGFP/Contr	
				replicate 1	replicate 2	replicate 1	replicate 2	replicate 1	replicate 2	replicate 1	replicate 2	replicate 1	replicate 2	replicate 1	replicate 2
P17813-2	Endoglin	ENG	67,541	-1,743	-1,156	-1,892	-1,950	-1,076	-1,961			-0,850			
P04004	Vitronectin	VTN	54,305	0,779	0,881	1,214	1,008	-0,891	-0,889						

Other

DB_Towne-BAC

Protein.ID	Protein.name	Gene.name	Mass (kDa)	Donor 1 log2.Ratio.DB-BAC/Contr		Donor 2 log2.Ratio.DB-BAC/Contr		Donor 3 log2.Ratio.DB-BAC/Contr		Donor 4 log2.Ratio.DB-BAC/Contr		Donor 5 log2.Ratio.DB-BAC/Contr		Donor 6 log2.Ratio.DB-BAC/Contr	
				replicate 1	replicate 2	replicate 1	replicate 2	replicate 1	replicate 2	replicate 1	replicate 2	replicate 1	replicate 2	replicate 1	replicate 2
P29966	Myristoylated alanine-rich C-kinase substrate	MARCKS	31,554	0,941	1,244	0,022	0,807	1,514	0,798	1,143	0,431				
P15880	40S ribosomal protein S2	RPS2	21,154		0,683		0,706	0,742	0,131					0,634	0,265

DB_RV-Towne-repΔGFP

Protein.ID	Protein.name	Gene.name	Mass (kDa)	Donor 1 log2.Ratio.DB-ΔGFP/Contr		Donor 2 log2.Ratio.DB-ΔGFP/Contr		Donor 3 log2.Ratio.DB-ΔGFP/Contr		Donor 4 log2.Ratio.DB-ΔGFP/Contr		Donor 5 log2.Ratio.DB-ΔGFP/Contr		Donor 6 log2.Ratio.DB-ΔGFP/Contr	
				replicate 1	replicate 2	replicate 1	replicate 2	replicate 1	replicate 2	replicate 1	replicate 2	replicate 1	replicate 2	replicate 1	replicate 2
P29966	Myristoylated alanine-rich C-kinase substrate	MARCKS	31,554	1,291	1,603	0,494	1,569	0,856	1,328						
P15880	40S ribosomal protein S2	RPS2	21,154		0,654			0,200	0,984					0,664	0,521

S12:

Monocytes_Classification of regulated protein groups according to GO - Biological processes (UniProtKB) in monocytes exposed to DBs-Towne-BAC

upregulated
downregulated

Exocytosis

				Donor 1		Donor 2		Donor 3		Donor 4		Donor 5		Donor 6	
				log2.Ratio.DB-BAC/Contr		log2.Ratio.DB-BAC/Contr		log2.Ratio.DB-BAC/Contr		log2.Ratio.DB-BAC/Contr		log2.Ratio.DB-BAC/Contr		log2.Ratio.DB-BAC/Contr	
Protein.ID	Protein.name	Gene.name	Mass (kDa)	replicate 1	replicate 2	replicate 1	replicate 2	replicate 1	replicate 2	replicate 1	replicate 2	replicate 1	replicate 2	replicate 1	replicate 2
P02675	Fibrinogen beta chain	FGB	39,736	0,887	0,913	0,693	1,007	-1,105	-0,476			0,543	0,825		
P02671-2	Fibrinogen alpha chain	FGA	69,756	1,457	1,298	0,987	0,769					0,647	0,467		
P02679-2	Fibrinogen gamma chain	FGG	49,496	1,274	1,107	1,007	0,913	-0,709	-0,653			0,497	0,881		
Q9NY25	C-type lectin domain family 5 member A	CLEC5A	18,031	2,589		0,665	0,374								0,746
P61916	NPC intracellular cholesterol transporter 2	NPC2	16,23	-0,261	-1,181	-0,686	-0,540	-0,655	-0,157						
P25774	Cathepsin S	CTSS	37,495	-0,791	-0,847	-0,373	-0,624			1,143	0,842				
P05109	Protein S100-A8	S100A8	10,834	1,553	1,606			0,122	1,446	1,110	0,722	-0,690	-0,377		
P14780	Matrix metalloproteinase-9	MMP9	78,457	0,573	0,701	0,401	0,767	0,981	0,900						
P16284-3	Platelet endothelial cell adhesion molecule	PECAM1	81,779	-1,235	-1,222			-0,729	-0,854					0,581	0,055
O00571-2	ATP-dependent RNA helicase DDX3X	DDX3X	81,476			0,608	1,549					0,453	0,595	0,489	0,588
Q14019	Coactosin-like protein	COTL1	8,2242					0,448	0,663	1,036		-0,611	-0,570		

Defense Response

				Donor 1		Donor 2		Donor 3		Donor 4		Donor 5		Donor 6	
				log2.Ratio.DB-BAC/Contr		log2.Ratio.DB-BAC/Contr		log2.Ratio.DB-BAC/Contr		log2.Ratio.DB-BAC/Contr		log2.Ratio.DB-BAC/Contr		log2.Ratio.DB-BAC/Contr	
Protein.ID	Protein.name	Gene.name	Mass (kDa)	replicate 1	replicate 2	replicate 1	replicate 2	replicate 1	replicate 2	replicate 1	replicate 2	replicate 1	replicate 2	replicate 1	replicate 2
P02747	Complement C1q subcomponent subunit C	C1QC	25,773	0,811	0,992	0,373	0,591							0,706	0,743
P0C0L4-2	Complement C4-A	C4A	187,67	1,001	1,375	0,759		0,202	0,735	1,771	1,501				
O00175	C-C motif chemokine 24	CCL24	13,133			1,031			0,655			-0,626	-0,220		
Q16543	Hsp90 co-chaperone Cdc37	CDC37	44,468	0,827	0,179			1,159	0,352			-0,694	-0,330		
P02675	Fibrinogen beta chain	FGB	39,736	0,887	0,913	0,693	1,007	-1,105	-0,476			0,543	0,825		
P02671-2	Fibrinogen alpha chain	FGA	69,756	1,457	1,298	0,987	0,769					0,647	0,467		
P02679-2	Fibrinogen gamma chain	FGG	49,496	1,274	1,107	1,007	0,913	-0,709	-0,653			0,497	0,881		
P25774	Cathepsin S	CTSS	37,495	-0,791	-0,847	-0,373	-0,624			1,143	0,842				
P05109	Protein S100-A8	S100A8	10,834	1,553	1,606			0,122	1,446	1,110	0,722	-0,690	-0,377		

Regulation of apoptotic process

				Donor 1		Donor 2		Donor 3		Donor 4		Donor 5		Donor 6	
				log2.Ratio.DB-BAC/Contr		log2.Ratio.DB-BAC/Contr		log2.Ratio.DB-BAC/Contr		log2.Ratio.DB-BAC/Contr		log2.Ratio.DB-BAC/Contr		log2.Ratio.DB-BAC/Contr	
Protein.ID	Protein.name	Gene.name	Mass (kDa)	replicate 1	replicate 2	replicate 1	replicate 2	replicate 1	replicate 2	replicate 1	replicate 2	replicate 1	replicate 2	replicate 1	replicate 2
P02675	Fibrinogen beta chain	FGB	39,736	0,887	0,913	0,693	1,007	-1,105	-0,476			0,543	0,825		
P02671-2	Fibrinogen alpha chain	FGA	69,756	1,457	1,298	0,987	0,769					0,647	0,467		
P02679-2	Fibrinogen gamma chain	FGG	49,496	1,274	1,107	1,007	0,913	-0,709	-0,653			0,497	0,881		

Q9NY25	C-type lectin domain family 5 member A	CLEC5A	18,031	2,589		0,665	0,374									0,746
P05109	Protein S100-A8	S100A8	10,834	1,553	1,606			0,122	1,446	1,110	0,722	-0,690	-0,377			
P14780	Matrix metalloproteinase-9	MMP9	78,457	0,573	0,701	0,401	0,767	0,981	0,900							
P62081	40S ribosomal protein S7	RPS7	22,127	1,565	0,848	3,029	0,132			2,063		-0,880	-0,076			

Translation

				Donor 1		Donor 2		Donor 3		Donor 4		Donor 5		Donor 6	
				log2.Ratio.DB-BAC/Contr		log2.Ratio.DB-BAC/Contr		log2.Ratio.DB-BAC/Contr		log2.Ratio.DB-BAC/Contr		log2.Ratio.DB-BAC/Contr		log2.Ratio.DB-BAC/Contr	
Protein.ID	Protein.name	Gene.name	Mass (kDa)	replicate 1	replicate 2	replicate 1	replicate 2	replicate 1	replicate 2	replicate 1	replicate 2	replicate 1	replicate 2	replicate 1	replicate 2
O00571-2	ATP-dependent RNA helicase DDX3X	DDX3X	81,476			0,608	1,549					0,453	0,595	0,489	0,588
P62424	60S ribosomal protein L7a	RPL7A	21,545	0,737	0,206				-0,816					0,655	0,486
P62249	40S ribosomal protein S16	RPS16	14,419	0,592	0,351			0,213	0,671	1,466	0,079				
P62851	40S ribosomal protein S25	RPS25	13,742	0,761	0,717			0,052	0,720					0,510	0,682
P62081	40S ribosomal protein S7	RPS7	22,127	1,565	0,848	3,029	0,132			2,063		-0,880	-0,076		

Other

				Donor 1		Donor 2		Donor 3		Donor 4		Donor 5		Donor 6	
				log2.Ratio.DB-BAC/Contr		log2.Ratio.DB-BAC/Contr		log2.Ratio.DB-BAC/Contr		log2.Ratio.DB-BAC/Contr		log2.Ratio.DB-BAC/Contr		log2.Ratio.DB-BAC/Contr	
Protein.ID	Protein.name	Gene.name	Mass (kDa)	replicate 1	replicate 2	replicate 1	replicate 2	replicate 1	replicate 2	replicate 1	replicate 2	replicate 1	replicate 2	replicate 1	replicate 2
P00450	Ceruloplasmin	CP	97,712							1,833		0,386	0,705	0,776	0,856
Q8IUE6	Histone H2A type 2-B	HIST2H2AB	13,995	-1,505	-1,903	6,460	2,160	2,795	2,581						
P20645	Cation-dependent mannose-6-phosphate rec	M6PR	30,993			-0,796	-0,085	-0,650	-0,004			-0,029	-0,647		
Q02818	Nucleobindin-1	NUCB1	34,773	-0,857	-1,016			-4,355				0,127	0,851		
P07737	Profilin-1	PFN1	15,054					0,376	0,843	0,740	0,408	-0,809	-0,321		
P26447	Protein S100-A4	S100A4	11,728	0,254	1,627			0,290	0,820			-0,637	-0,289		
Q9H299	SH3 domain-binding glutamic acid-rich-like p	SH3BGRL3	9,3804	-0,205	-0,665	-0,466	-0,662	0,062	0,893				-0,602	0,643	0,070

S13:

Monocytes_Classification of regulated protein groups according to GO - Biological processes (UniProtKB) in monocytes exposed to DBs-Towne-repΔGFP

upregulated
downregulated

Immunity

				Donor 1		Donor 2		Donor 3		Donor 4		Donor 5		Donor 6	
				log2.Ratio.DB-ΔGFP/Contr		log2.Ratio.DB-ΔGFP/Contr		log2.Ratio.DB-ΔGFP/Contr		log2.Ratio.DB-ΔGFP/Contr		log2.Ratio.DB-ΔGFP/Contr		log2.Ratio.DB-ΔGFP/Contr	
Protein.ID	Protein.name	Gene.name	Mass (kDa)	replicate 1	replicate 2	replicate 1	replicate 2	replicate 1	replicate 2	replicate 1	replicate 2	replicate 1	replicate 2	replicate 1	replicate 2
P01871	Immunoglobulin heavy constant mu	IGHM	49,439	0,671	0,841	0,802	0,631			0,712	0,573	0,626	0,469		
P01834	Immunoglobulin kappa constant	IGKC	24,03	0,523	0,765	0,651	0,436	1,295	1,108	1,021	0,282	0,673	0,144	-0,445	-0,803

Defense Response

Protein.ID	Protein.name	Gene.name	Mass (kDa)	Donor 1 log2.Ratio.DB-ΔGFP/Contr		Donor 2 log2.Ratio.DB-ΔGFP/Contr		Donor 3 log2.Ratio.DB-ΔGFP/Contr		Donor 4 log2.Ratio.DB-ΔGFP/Contr		Donor 5 log2.Ratio.DB-ΔGFP/Contr		Donor 6 log2.Ratio.DB-ΔGFP/Contr	
				replicate 1	replicate 2	replicate 1	replicate 2	replicate 1	replicate 2	replicate 1	replicate 2	replicate 1	replicate 2	replicate 1	replicate 2
P13686	Tartrate-resistant acid phosphatase type 5	ACP5	36,598	-2,128	-0,714	-1,588		-2,426	-2,878						
P01583	Interleukin-1 alpha	IL1A	30,606	3,125	1,625	3,106	0,302	3,748	3,663						
P08603	Complement factor H	CFH	138,95	0,047	2,155	0,747	0,486		-1,074						
Q07954	Prolow-density lipoprotein receptor-related protein 1	LRP1	504,6	-1,436	-0,267	-0,883	-1,747	-1,743	-1,742						
P01024	Complement C3	C3	187,15			0,623	0,561	-0,445	-0,624	0,737	0,773			-0,445	
P02751-10	Fibronectin	FN1	246,7	0,698	0,521			-0,871	-0,937			-0,942	-1,290		
Q9ULZ3-3	Apoptosis-associated speck-like protein containing a CARD	PYCARD	21,628	3,462	0,386	0,357	0,588	1,010	1,045						
Q6NVH9	Galectin	LGALS3	26,197	-0,709	-0,718	-0,468	-0,796	-1,030	-1,133						
P35542	Serum amyloid A-4 protein	SAA4	14,808	1,019		0,665	0,504	-1,409	-1,251			0,083	0,751		
P01008	Antithrombin-III	SERPINC1	52,602	0,746	0,798	0,837	0,508	-0,958	-1,091			0,634	0,713	-0,588	

Endocytosis

Protein.ID	Protein.name	Gene.name	Mass (kDa)	Donor 1 log2.Ratio.DB-ΔGFP/Contr		Donor 2 log2.Ratio.DB-ΔGFP/Contr		Donor 3 log2.Ratio.DB-ΔGFP/Contr		Donor 4 log2.Ratio.DB-ΔGFP/Contr		Donor 5 log2.Ratio.DB-ΔGFP/Contr		Donor 6 log2.Ratio.DB-ΔGFP/Contr	
				replicate 1	replicate 2	replicate 1	replicate 2	replicate 1	replicate 2	replicate 1	replicate 2	replicate 1	replicate 2	replicate 1	replicate 2
Q07954	Prolow-density lipoprotein receptor-related protein 1	LRP1	504,6	-1,436	-0,267	-0,883	-1,747	-1,743	-1,742						
P01024	Complement C3	C3	187,15			0,623	0,561	-0,445	-0,624	0,737	0,773			-0,445	
P02649	Apolipoprotein E	APOE	36,154	0,119	0,622	0,654	0,537	-0,962	-1,006	0,759	0,119				
Q9ULZ3-3	Apoptosis-associated speck-like protein containing a CARD	PYCARD	21,628	3,462	0,386	0,357	0,588	1,010	1,045						
Q6NVH9	Galectin	LGALS3	26,197	-0,709	-0,718	-0,468	-0,796	-1,030	-1,133						

Exocytosis

Protein.ID	Protein.name	Gene.name	Mass (kDa)	Donor 1 log2.Ratio.DB-ΔGFP/Contr		Donor 2 log2.Ratio.DB-ΔGFP/Contr		Donor 3 log2.Ratio.DB-ΔGFP/Contr		Donor 4 log2.Ratio.DB-ΔGFP/Contr		Donor 5 log2.Ratio.DB-ΔGFP/Contr		Donor 6 log2.Ratio.DB-ΔGFP/Contr	
				replicate 1	replicate 2	replicate 1	replicate 2	replicate 1	replicate 2	replicate 1	replicate 2	replicate 1	replicate 2	replicate 1	replicate 2
P02751-10	Fibronectin	FN1	246,7	0,698	0,521			-0,871	-0,937			-0,942	-1,290		
Q9ULZ3-3	Apoptosis-associated speck-like protein containing a CARD	PYCARD	21,628	3,462	0,386	0,357	0,588	1,010	1,045						
Q6NVH9	Galectin	LGALS3	26,197	-0,709	-0,718	-0,468	-0,796	-1,030	-1,133						
P01024	Complement C3	C3	187,15			0,623	0,561	-0,445	-0,624	0,737	0,773			-0,445	
P02749	Beta-2-glycoprotein 1	APOH	38,298	0,178	0,647					0,685			0,733	-0,339	
P11717	Cation-independent mannose-6-phosphate receptor	IGF2R	274,37		-0,680	-0,585	-1,187	-0,704	-1,379						

ER translocation

Protein.ID	Protein.name	Gene.name	Mass (kDa)	Donor 1 log2.Ratio.DB-ΔGFP/Contr		Donor 2 log2.Ratio.DB-ΔGFP/Contr		Donor 3 log2.Ratio.DB-ΔGFP/Contr		Donor 4 log2.Ratio.DB-ΔGFP/Contr		Donor 5 log2.Ratio.DB-ΔGFP/Contr		Donor 6 log2.Ratio.DB-ΔGFP/Contr	
				replicate 1	replicate 2	replicate 1	replicate 2	replicate 1	replicate 2	replicate 1	replicate 2	replicate 1	replicate 2	replicate 1	replicate 2
P46777	60S ribosomal protein L5	RPL5	28,044	-0,657	-0,076			-0,728	-0,005		-0,668				
P62280	40S ribosomal protein S11	RPS11	18,431			0,806	0,829	0,172	1,082					0,325	0,620
P60468	Protein transport protein Sec61 subunit beta	SEC61B	9,9743	1,012		0,014	0,690					0,743	0,058		

Other

Protein.ID	Protein.name	Gene.name	Mass (kDa)	Donor 1 log2.Ratio.DB-ΔGFP/Contr		Donor 2 log2.Ratio.DB-ΔGFP/Contr		Donor 3 log2.Ratio.DB-ΔGFP/Contr		Donor 4 log2.Ratio.DB-ΔGFP/Contr		Donor 5 log2.Ratio.DB-ΔGFP/Contr		Donor 6 log2.Ratio.DB-ΔGFP/Contr	
				replicate 1	replicate 2	replicate 1	replicate 2	replicate 1	replicate 2	replicate 1	replicate 2	replicate 1	replicate 2	replicate 1	replicate 2
Q15758	Neutral amino acid transporter B(0)	SLC1A5	56,583	-0,671	-1,044	-0,974		-1,359	-0,909						
Q9Y4P3	Transducin beta-like protein 2	TBL2	45,935		-0,676	-0,791	-0,544		-0,993			-0,182	-0,888		

S14:
iDC_Interferon regulated protein groups 24h after DBs exposure

Regulated protein groups that were regulated in both,
iDCs exosed to DBs derived from Towne-BAC or DBs derived from Towne-repΔGFP

Threshold: log2Ratio 0.58 = fold increase of 1.5

upregulated
downregulated

DB_RV-Towne-BAC

			Razor + unique peptides				Donor_1 log2.Ratio DB-BAC/Contr		Donor_2 log2.Ratio DB-BAC/Contr		Donor_3 log2.Ratio DB-BAC/Contr	
Protein.ID	Protein.name	Gene.name	Donor_1	Donor_2	Donor_3	Mass (kDa)	replicate 1	replicate 2	replicate 1	replicate 2	replicate 1	replicate 2
P11717	Cation-independent mannose-6-phosphate receptor	IGF2R		9	23	274,37			2,088	0,082	1,125	0,617
Q8WZ42-3	Titin	TTN	2		3	2992,9		1,919			0,811	
P07339	Cathepsin D	CTSD	12	15		43,831	0,587	0,521	0,562	0,834		
Q9H0J9	Protein mono-ADP-ribosyltransferase PARP12	PARP12		5	3	79,063			0,772	0,067	0,163	0,832
P42766	60S ribosomal protein L35	RPL35	4		5	14,551	0,891	0,287			0,806	0,163
Q9Y6K5	2-5-oligoadenylate synthase 3	OAS3	7		11	121,17	0,725	0,286			0,677	0,273
O75558	Syntaxin-11	STX11	2		3	33,195		0,771				0,596
Q9NNX6	CD209 antigen	CD209		8	5	45,774			0,390	0,685	0,601	0,127
P04179	Superoxide dismutase [Mn], mitochondrial	SOD2		11	12	24,75			-0,739	-0,581	1,025	1,090
Q9P0J1-2	[Pyruvate dehydrogenase [acetyl-transferring]]-phosphatase 1	PDP1	4	3	3	61,053	1,167		0,872	0,050	-0,601	
P25942	Tumor necrosis factor receptor superfamily member 5	CD40	4		3	30,619	-0,198	-0,649			0,871	0,688
P55774	C-C motif chemokine 18	CCL18	3	3		9,8487	-0,244	-0,714	1,030	0,480		
Q68CZ2-2	Tensin-3	TNS3	3		8	129,06		-1,132			1,023	0,558

DB_RV-Towne-repΔGFP

Protein.ID	Protein.name	Gene.name	Razor + unique peptides Donor_1	Donor_2	Donor_3	Mass (kDa)	Donor_1 log2.Ratio DB-dGFP/Contr replicate 1	replicate 2	Donor_2 log2.Ratio DB-dGFP/Contr replicate 1	replicate 2	Donor_3 log2.Ratio DB-dGFP/Contr replicate 1	replicate 2
P11717	Cation-independent mannose-6-phosphate receptor	IGF2R	9	14	23	274,37	1,840	1,065	0,372	0,735	1,039	1,002
Q8WZ42-3	Titin	TTN		2	3	2992,9				1,347	0,994	
P07339	Cathepsin D	CTSD	15	12		43,831	0,854	1,105	0,614	0,452		
Q9H0J9	Protein mono-ADP-ribosyltransferase PARP12	PARP12	5		3	79,063	1,081	0,148			1,055	0,653
P42766	60S ribosomal protein L35	RPL35	5	4		14,551	1,053	0,198	0,577	0,710		
Q9Y6K5	2-5-oligoadenylate synthase 3	OAS3	12		11	121,17	0,717	0,992			0,918	0,521
O75558	Syntaxin-11	STX11	2	2		33,195	0,638			0,721		
Q9NNX6	CD209 antigen	CD209	8		5	45,774	0,006	0,601			0,641	0,129
P04179	Superoxide dismutase [Mn], mitochondrial	SOD2		11	12	24,75			1,313	1,284	1,343	1,438
Q9P0J1-2	[Pyruvate dehydrogenase [acetyl-transferring]]-phosphatase 1	PDP1	3	4		61,053	0,935	0,306	0,960			
P25942	Tumor necrosis factor receptor superfamily member 5	CD40		4	3	30,619			0,803	0,047	1,181	0,990
P55774	C-C motif chemokine 18	CCL18	3		4	9,8487	0,151	0,703			0,738	1,598
Q68CZ2-2	Tensin-3	TNS3		3	8	129,06				0,631	1,310	0,372

iDC_Not interferon regulated protein groups 24h after DBs exposure

DB_RV-Towne-BAC

Protein.ID	Protein.name	Gene.name	Razor + unique peptides Donor_1	Donor_2	Donor_3	Mass (kDa)	Donor_1 log2.Ratio DB-BAC/Contr replicate 1	replicate 2	Donor_2 log2.Ratio DB-BAC/Contr replicate 1	replicate 2	Donor_3 log2.Ratio DB-BAC/Contr replicate 1	replicate 2
A0A0G2T825	Tegument protein UL25	UL25	7	9	8	73,511	2,880	3,239	3,091	5,338	3,391	4,106
A0A0A7CGS9	Tegument protein pp71	pp71	5	4	4	62,102	1,912		1,278		3,029	3,756
P14927	Cytochrome b-c1 complex subunit 7	UQCRB	4	5		13,53	0,971	0,420	1,043	0,370		
O43760	Synaptogyrin-2	SYNGR2	6	5		24,81	0,741	0,892	0,991	0,323		
P63173	60S ribosomal protein L38	RPL38		3	4	8,2178			-0,745	-0,512	-0,804	-0,461
Q9C002	Normal mucosa of esophagus-specific gene 1 protein	NMES1	4	2		9,6172	-0,620	-0,325	-1,126	-1,797		

DB_RV-Towne-repΔGFP

Protein.ID	Protein.name	Gene.name	Razor + unique peptides Donor_1	Donor_2	Donor_3	Mass (kDa)	Donor_1 log2.Ratio DB-dGFP/Contr replicate 1	replicate 2	Donor_2 log2.Ratio DB-dGFP/Contr replicate 1	replicate 2	Donor_3 log2.Ratio DB-dGFP/Contr replicate 1	replicate 2
A0A0G2T825	Tegument protein UL25	UL25	7	9	8	73,511	1,347	1,473	0,482	2,161	2,283	3,362
A0A0A7CGS9	Tegument protein pp71	pp71			4	62,102					2,183	3,673
P14927	Cytochrome b-c1 complex subunit 7	UQCRB	5	4		13,53	0,983	0,126	1,133	0,175		
O43760	Synaptogyrin-2	SYNGR2	5	5		24,81	0,780	0,087	0,677	0,139		
P63173	60S ribosomal protein L38	RPL38		3	4	8,2178			0,816	0,174	0,749	0,117
Q9C002	Normal mucosa of esophagus-specific gene 1 protein	NMES1	2	4	5	9,6172	0,714	0,283	1,429	1,519	0,964	0,924

S15:
iDC_Interferon regulated protein groups 24h after DBs exposure in iDCs exposed to DBs-Towne-BAC

Threshold: log2Ratio 0.58 = fold increase of 1.5

upregulated
downregulated

			Razor + unique peptides				Donor_1 log2.Ratio DB-BAC/Contr		Donor_2 log2.Ratio DB-BAC/Contr		Donor_3 log2.Ratio DB-BAC/Contr	
Protein.ID	Protein.name	Gene.name	Donor_1	Donor_2	Donor_3	Mass (kDa)	replicate 1	replicate 2	replicate 1	replicate 2	replicate 1	replicate 2
P19525-2	Interferon-induced, double-stranded RNA-activated protein kinase	PKR	7	5	3	57,39	0,462	0,736		0,607	2,038	
P01024	Complement C3	C3	24	10	60	187,15	-0,678	-0,494	0,664	0,833	1,268	0,934
P01009	Alpha-1-antitrypsin	SERPINA1	18	5	24	46,736	-0,486	-0,643		0,582	1,224	1,193
P49589-2	Cysteine--tRNA ligase, cytoplasmic	CARS	7	8	4	82,845	0,970	0,139	-0,603	-0,197		-0,670
P28067	HLA class II histocompatibility antigen, DM alpha chain	HLA-DMA	4	2	2	32,745	-0,759	-0,072		0,856	-0,706	-0,662
Q8TDW0	Volume-regulated anion channel subunit LRRC8C	LRRC8C	3	4	4	92,448	0,617			-1,047	0,721	0,274
Q08752	Peptidyl-prolyl cis-trans isomerase D	PPID	3	4	2	40,763		-1,259		-1,029		-0,633
Q9BV40	Vesicle-associated membrane protein 8	VAMP8	4	3		11,438	0,161	0,632		-1,374	-0,619	-0,206
O00629	Importin subunit alpha-3	KPNA4	4	4	4	57,886	-0,023	-1,596		-1,286	-0,062	-1,479
P46379-3	Large proline-rich protein BAG6	BAG6	3	7	4	122,34		-0,714	-0,004	-1,643	-0,092	-1,056

iDC_Interferon regulated protein groups 24h after DBs exposure in iDCs exposed to DBs-Towne-repΔGFP

			Razor + unique peptides				Donor_1 log2.Ratio DB-dGFP/Contr		Donor_2 log2.Ratio DB-dGFP/Contr		Donor_3 log2.Ratio DB-dGFP/Contr	
Protein.ID	Protein.name	Gene.name	Donor_1	Donor_2	Donor_3	Mass (kDa)	replicate 1	replicate 2	replicate 1	replicate 2	replicate 1	replicate 2
O14879	Interferon-induced protein with tetratricopeptide repeats 3	IFIT3	6	5	6	55,984	0,536	1,882	1,192	0,962	0,635	0,726
Q14699	Raftlin	RFTN1	6	11	8	63,145	1,430	0,197	0,761	0,213	0,873	0,404
P33121-2	Long-chain-fatty-acid--CoA ligase 1	ACSL1	11	14	17	76,87	0,670	0,108	0,679	0,415	0,872	1,035
P02786	Transferrin receptor protein 1	TFRC	16	16	23	84,87	0,597	0,661	0,736	0,564	0,357	0,731

S16:
iDCs_Classification of regulated protein groups according to GO - Biological processes (UniProtKB)

upregulated
downregulated

Antiviral Defence

			DB_RV-Towne-BAC						DB_RV-Towne-repΔGFP					
			Donor_1 log2.Ratio DB-		Donor_2 log2.Ratio DB-		Donor_3 log2.Ratio DB-		Donor_1 log2.Ratio DB-		Donor_2 log2.Ratio DB-		Donor_3 log2.Ratio DB-	
Protein.ID	Protein.name	Gene.name	replicate 1	replicate 2	replicate 1	replicate 2	replicate 1	replicate 2	replicate 1	replicate 2	replicate 1	replicate 2	replicate 1	replicate 2
Q9H0J9	Protein mono-ADP-ribosyltransferase PARP12	PARP12			0,772	0,067	0,163	0,832	1,081	0,148			1,055	0,653
P55774	C-C motif chemokine 18	CCL18	-0,244	-0,714	1,030	0,480			0,151	0,703			0,738	1,598
Q9Y6K5	2-5-oligoadenylate synthase 3	OAS3	0,725	0,286			0,677	0,273	0,717	0,992			0,918	0,521
P25942	Tumor necrosis factor receptor superfamily member 5	CD40	-0,198	-0,649			0,871	0,688			0,803	0,047	1,181	0,990
P19525-2	Interferon-induced, double-stranded RNA-activated protein kinase	PKR	0,462	0,736		0,607	2,038							
O14879	Interferon-induced protein with tetratricopeptide repeats 3	IFIT3							0,536	1,882	1,192	0,962	0,635	0,726

Antigen processing and presentation

			DB_RV-Towne-BAC						DB_RV-Towne-repΔGFP					
			Donor_1 log2.Ratio DB-		Donor_2 log2.Ratio DB-		Donor_3 log2.Ratio DB-		Donor_1 log2.Ratio DB-		Donor_2 log2.Ratio DB-		Donor_3 log2.Ratio DB-	
Protein.ID	Protein.name	Gene.name	replicate 1	replicate 2	replicate 1	replicate 2	replicate 1	replicate 2	replicate 1	replicate 2	replicate 1	replicate 2	replicate 1	replicate 2
P07339	Cathepsin D	CTSD	0,587	0,521	0,562	0,834			0,854	1,105	0,614	0,452		
Q9NNX6	CD209 antigen	CD209			0,390	0,685	0,601	0,127	0,006	0,601			0,641	0,129
P28067	HLA class II histocompatibility antigen, DM alpha chain	HLA-DMA	-0,759	-0,072		0,856	-0,706	-0,662						
Q14699	Raftlin	RFTN1							1,430	0,197	0,761	0,213	0,873	0,404
Q9BV40	Vesicle-associated membrane protein 8	VAMP8	0,161	0,632		-1,374	-0,619	-0,206						

Endocytosis

			DB_RV-Towne-BAC						DB_RV-Towne-repΔGFP					
			Donor_1 log2.Ratio DB-BAC/Contr		Donor_2 log2.Ratio DB-BAC/Contr		Donor_3 log2.Ratio DB-BAC/Contr		Donor_1 log2.Ratio DB-dGFP/Contr		Donor_2 log2.Ratio DB-dGFP/Contr		Donor_3 log2.Ratio DB-dGFP/Contr	
Protein.ID	Protein.name	Gene.name	replicate 1	replicate 2	replicate 1	replicate 2	replicate 1	replicate 2	replicate 1	replicate 2	replicate 1	replicate 2	replicate 1	replicate 2
P33121-2	Long-chain-fatty-acid--CoA ligase 1	ACSL1							0,670	0,108	0,679	0,415	0,872	1,035
P02786	Transferrin receptor protein 1	TFRC							0,597	0,661	0,736	0,564	0,357	0,731

P11717	Cation-independent mannose-6-phosphate receptor	IGF2R			2,088	0,082	1,125	0,617	1,840	1,065	0,372	0,735	1,039	1,002
P01024	Complement C3	C3	-0,678	-0,494	0,664	0,833	1,268	0,934						
Q9NNX6	CD209 antigen	CD209			0,390	0,685	0,601	0,127	0,006	0,601			0,641	0,129

Exocytosis

			DB_RV-Towne-BAC						DB_RV-Towne-repΔGFP					
			Donor_1 log2.Ratio DB-		Donor_2 log2.Ratio DB-		Donor_3 log2.Ratio DB-		Donor_1 log2.Ratio DB-		Donor_2 log2.Ratio DB-		Donor_3 log2.Ratio DB-	
Protein.ID	Protein.name	Gene.name	replicate 1	replicate 2	replicate 1	replicate 2	replicate 1	replicate 2	replicate 1	replicate 2	replicate 1	replicate 2	replicate 1	replicate 2
O43760	Synaptogyrin-2	SYNGR2	0,741	0,892	0,991	0,323			0,780	0,087	0,677	0,139		
O75558	Syntaxin-11	STX11		0,771				0,596	0,638			0,721		
Q8WZ42-3	Titin	TTN		1,919			0,811					1,347	0,994	
Q9BV40	Vesicle-associated membrane protein 8	VAMP8	0,161	0,632		-1,374	-0,619	-0,206						
P11717	Cation-independent mannose-6-phosphate receptor	IGF2R			2,088	0,082	1,125	0,617	1,840	1,065	0,372	0,735	1,039	1,002
P07339	Cathepsin D	CTSD	0,587	0,521	0,562	0,834			0,854	1,105	0,614	0,452		
P01009	Alpha-1-antitrypsin	SERPINA1	-0,486	-0,643		0,582	1,224	1,193						
P01024	Complement C3	C3	-0,678	-0,494	0,664	0,833	1,268	0,934						

Protein Transport

			DB_RV-Towne-BAC						DB_RV-Towne-repΔGFP					
			Donor_1 log2.Ratio DB-		Donor_2 log2.Ratio DB-		Donor_3 log2.Ratio DB-		Donor_1 log2.Ratio DB-		Donor_2 log2.Ratio DB-		Donor_3 log2.Ratio DB-	
Protein.ID	Protein.name	Gene.name	replicate 1	replicate 2	replicate 1	replicate 2	replicate 1	replicate 2	replicate 1	replicate 2	replicate 1	replicate 2	replicate 1	replicate 2
Q08752	Peptidyl-prolyl cis-trans isomerase D	PPID		-1,259		-1,029		-0,633						
O00629	Importin subunit alpha-3	KPNA4	-0,023	-1,596		-1,286	-0,062	-1,479						
P02786	Transferrin receptor protein 1	TFRC							0,597	0,661	0,736	0,564	0,357	0,731
Q14699	Raftlin	RFTN1							1,430	0,197	0,761	0,213	0,873	0,404
Q9BV40	Vesicle-associated membrane protein 8	VAMP8	0,161	0,632		-1,374	-0,619	-0,206						
P42766	60S ribosomal protein L35	RPL35	0,891	0,287			0,806	0,163	1,053	0,198	0,577	0,710		
P63173	60S ribosomal protein L38	RPL38			-0,745	-0,512	-0,804	-0,461			0,816	0,174	0,749	0,117
O75558	Syntaxin-11	STX11		0,771				0,596	0,638			0,721		

Translation

			DB_RV-Towne-BAC						DB_RV-Towne-repΔGFP					
			Donor_1 log2.Ratio DB-		Donor_2 log2.Ratio DB-		Donor_3 log2.Ratio DB-		Donor_1 log2.Ratio DB-		Donor_2 log2.Ratio DB-		Donor_3 log2.Ratio DB-	
Protein.ID	Protein.name	Gene.name	replicate 1	replicate 2	replicate 1	replicate 2	replicate 1	replicate 2	replicate 1	replicate 2	replicate 1	replicate 2	replicate 1	replicate 2
P42766	60S ribosomal protein L35	RPL35	0,891	0,287			0,806	0,163	1,053	0,198	0,577	0,710		
P63173	60S ribosomal protein L38	RPL38			-0,745	-0,512	-0,804	-0,461			0,816	0,174	0,749	0,117
P19525-2	Interferon-induced, double-stranded RNA-activated protein kinase	PKR	0,462	0,736		0,607	2,038							
P49589-2	Cysteine--tRNA ligase, cytoplasmic	CARS	0,970	0,139	-0,603	-0,197		-0,670						

Other

			DB_RV-Towne-BAC						DB_RV-Towne-repΔGFP					
			Donor_1 log2.Ratio DB-		Donor_2 log2.Ratio DB-		Donor_3 log2.Ratio DB-		Donor_1 log2.Ratio DB-		Donor_2 log2.Ratio DB-		Donor_3 log2.Ratio DB-	
Protein.ID	Protein.name	Gene.name	replicate 1	replicate 2	replicate 1	replicate 2	replicate 1	replicate 2	replicate 1	replicate 2	replicate 1	replicate 2	replicate 1	replicate 2
P14927	Cytochrome b-c1 complex subunit 7	UQCRB	0,971	0,420	1,043	0,370			0,983	0,126	1,133	0,175		
P04179	Superoxide dismutase [Mn], mitochondrial	SOD2			-0,739	-0,581	1,025	1,090			1,313	1,284	1,343	1,438
Q9P0J1-2	[Pyruvate dehydrogenase [acetyl-transferring]]-phosphatase 1	PDP1	1,167		0,872	0,050	-0,601		0,935	0,306	0,960			
Q68CZ2-2	Tensin-3	TNS3		-1,132			1,023	0,558				0,631	1,310	0,372
Q9C002	Normal mucosa of esophagus-specific gene 1 protein	NMES1	-0,620	-0,325	-1,126	-1,797			0,714	0,283	1,429	1,519	0,964	0,924
Q8TDW0	Volume-regulated anion channel subunit LRRC8C	LRRC8C	0,617			-1,047	0,721	0,274						
P46379-3	Large proline-rich protein BAG6	BAG6		-0,714	-0,004	-1,643	-0,092	-1,056						

Acknowledgements/ Danksagung